

University of Windsor

Scholarship at UWindor

Electronic Theses and Dissertations

Theses, Dissertations, and Major Papers

2015

Generation of Model Systems for the Study of Novel Cell Cycle Regulation in Development: Implications for Spy1 in Tumour Susceptibility

Bre-Anne Fifield
University of Windsor

Follow this and additional works at: <https://scholar.uwindsor.ca/etd>



Part of the [Biology Commons](#)

Recommended Citation

Fifield, Bre-Anne, "Generation of Model Systems for the Study of Novel Cell Cycle Regulation in Development: Implications for Spy1 in Tumour Susceptibility" (2015). *Electronic Theses and Dissertations*. 5717.

<https://scholar.uwindsor.ca/etd/5717>

This online database contains the full-text of PhD dissertations and Masters' theses of University of Windsor students from 1954 forward. These documents are made available for personal study and research purposes only, in accordance with the Canadian Copyright Act and the Creative Commons license—CC BY-NC-ND (Attribution, Non-Commercial, No Derivative Works). Under this license, works must always be attributed to the copyright holder (original author), cannot be used for any commercial purposes, and may not be altered. Any other use would require the permission of the copyright holder. Students may inquire about withdrawing their dissertation and/or thesis from this database. For additional inquiries, please contact the repository administrator via email (scholarship@uwindsor.ca) or by telephone at 519-253-3000ext. 3208.

**Generation of Model Systems for the Study of Novel Cell Cycle Regulation in
Development: Implications for Spy1 in Tumour Susceptibility**

By

Bre-Anne Fifield

A Dissertation
Submitted to the Faculty of Graduate Studies
through the Department of Biological Sciences
in Partial Fulfillment of the Requirements for
the Degree of Doctor of Philosophy
at the University of Windsor

Windsor, Ontario, Canada

2014

© 2014 Bre-Anne Fifield

**Generation of Model Systems for the Study of Novel Cell Cycle Regulation in Development:
Implications for Spyl in Tumour Susceptibility**

by

Bre-Anne Fifield

APPROVED BY:

A. MacNicol, External Examiner
University of Arkansas

M. Boffa
Department of Chemistry and Biochemistry

A. Swan
Department of Biological Sciences

M. Crawford
Department of Biological Sciences

L.A. Porter, Advisor
Department of Biological Sciences

December 11, 2014

Declaration of Co-Authorship / Previous Publication

I. Co-Authorship Declaration

I hereby declare that this dissertation incorporates material that is result of joint research, as follows:

Chapter 2 incorporates the outcome of a joint research undertaken in collaboration with Espanta Jalili under the supervision of professor Porter. The collaboration is covered in Chapter 2 of the dissertation. In all cases, the key ideas, primary contributions, experimental designs, data analysis and interpretation relating to the MMTV-Spy1 mouse model were performed by the author, and the contribution of co-authors was primarily through the ideas, experimental designs and data analysis of all *in vitro* work concerning Spy1 and p53 signaling in HEK-293s, HCT116, U-2 OS, Saos2 and NIH3T3 cells.

Appendix C incorporates the outcome of a joint research undertaken in collaboration with Mohammed Al Sorkhy under the supervision of professor Porter. The collaboration is covered in Appendix C of the dissertation. In all cases, the key ideas, primary contributions, experimental designs, data analysis and interpretation were performed by Mohammed Al Sorkhy, and the contribution of co-author was primarily through all experiments pertaining to the *in vivo* mammary fat pad experiments, revisions, and editing of the manuscript.

I am aware of the University of Windsor Senate Policy on Authorship and I certify that I have properly acknowledged the contribution of other researchers to my thesis, and have obtained written permission from Mohammed Al Sorkhy and permission from Dr. Lisa Porter to include the above material(s) in my dissertation.

I certify that, with the above qualification, this dissertation, and the research to which it refers, is the product of my own work.

II. Declaration of Previous Publication

This dissertation includes 1 original paper that has been previously submitted for publication in peer reviewed journals, as follows:

Thesis Chapter	Publication title/full citation	Publication status*
<i>Appendix C</i>	Direct Interactions with p27 and Cdk2 Regulate Spy1-Induced Mammary Tumorigenesis	<i>Submitted; in revision</i>

I certify that I have obtained a written permission from the copyright owner(s) to include the above published material(s) in my dissertation. I certify that the above material describes work completed during my registration as graduate student at the University of Windsor.

I declare that, to the best of my knowledge, my dissertation does not infringe upon anyone's copyright nor violate any proprietary rights and that any ideas, techniques, quotations, or any other material from the work of other people included in my dissertation, published or otherwise, are fully acknowledged in accordance with the standard referencing practices. Furthermore, to the extent that I have included copyrighted material that surpasses the bounds of fair dealing within the meaning of the Canada Copyright Act, I certify that I have obtained a written permission from the copyright owner(s) to include such material(s) in my dissertation.

I declare that this is a true copy of my dissertation, including any final revisions, as approved by my dissertation committee and the Graduate Studies office, and that this dissertation has not been submitted for a higher degree to any other University or Institution.

Abstract

Cell cycle regulation lies at the heart of all developmental decisions, and aberrant regulation represents an important step in the onset of tumorigenesis. Alterations in cell cycle regulators are known to play a critical role in promoting tumour formation in a wide variety of tissues. The cyclin-like protein Spy1 is capable of binding and activating CDK2 and promoting progression through G1/S phase of the cell cycle. Spy1 can also target the cell cycle inhibitor p27 for degradation, and it has been shown to override cellular checkpoints and apoptotic pathways in response to DNA damage leading to enhanced cell survival. Previous data has shown that Spy1 levels are tightly regulated throughout mammary gland development, and high levels are associated with breast cancer, as well as cancer of the brain and liver. This suggests a role for Spy1 in normal mammary development as well as in the development of tumorigenesis. Transgenic and gene targeted models represent an ideal system in which to study altered protein expression on development and tumour initiation. This work describes the development of three novel model systems to study altered Spy1 expression on normal and abnormal development of the mammary gland. Using the newly generated MMTV-Spy1 mouse we have demonstrated that elevated levels of Spy1 increases mammary tumour susceptibility, and interestingly liver tumour susceptibility. We demonstrate that levels of Spy1 are downregulated in the event of DNA damage and the tumour suppressor p53 may be responsible for mediating this event. If p53 is unable to keep levels of Spy1 in check this can lead to uncontrolled cell proliferation, a hallmark of oncogenesis, and may contribute to tumour initiation. Thus for the first time, we demonstrate a role for Spy1 in mediating tumour susceptibility, highlighting the importance of maintaining proper checkpoint responses. Our work demonstrates that Spy1 could prove to be an attractive diagnostic marker and therapeutic target in the treatment of various forms of cancer, helping to eradicate this deadly disease.

Dedication

This dissertation is dedicated to my family, for their unconditional love and support, without which, this would not have been possible. Thank you for your constant understanding and motivation to keep going through every step of the way.

Acknowledgements

First and foremost, I owe my sincerest thanks to my supervisor Dr. Lisa Porter. For opening my eyes to the world of research, being a constant source of guidance, encouragement and motivation over the years and always being willing to lend your expertise -I am truly lucky to have had you as a supervisor.

To my committee members Drs A. Swan, M. Crawford and M. Boffa- thank you for your time and valuable expertise and advice throughout the course of this study. Sincere thanks to Drs M. Crawford, D. Higgs, J. Hudson, and C. Shemanko for use of equipment and providing cell lines. Thanks to Drs R. Moorehead and G.E. DiMattia for donation of the MMTV-rtTA mouse and MMTV-SV40-TRPS-1 plasmid respectively. Special thanks to Dr. C Pin and L. Drysdale from the London Regional Transgenic and Gene Targeting Facility for generation of mouse models and for technical assistance. Thanks to Dr. F Dick for assistance with design and execution of all steps pertaining to the gene targeted mouse, and P Stafford and D Passos for technical assistance.

This study would not have been possible without the help of many individuals who provided assistance in the care, handling and genotyping of mice. To our animal care technicians- Linda Sterling, Melissa Gabrieau and Elaine Rupke, for overseeing day to day maintenance. Special thanks to Dorota Lubanksa for not only assisting with genotyping but for always being willing to listen and provide guidance and advice. To Ingrid Qemo, for assistance with genotyping, being a source of motivation and making lab work enjoyable. Ellen Laurie, Mitchell Elliot and Nick Paquette- thank you for your assistance with all things mouse-for all of your time and dedication to everything from day to day maintenance, genotyping and processing tissues. A special thanks to Ellen Laurie who went above and beyond what any undergraduate has done. You made not so glamorous work enjoyable and gave me peace of mind knowing I could leave things in capable hands. To Jiamila Maimaiti for showing me the ropes when I first started, Dr. E. Fildago da Silva for technical assistance, Janice Tubman for assistance with image analysis and Agnes Malysa for assistance with statistical analysis. To Rosa Ferraiuolo, we started this journey together and I am so grateful that you have been by my side through it all. Thanks for your continued support and friendship. To Nicole Lyons, Kaitlyn Matthews, and Jessica Dare- thank you for being wonderful colleagues and friends, providing assistance and feedback, and for making lab work enjoyable. It truly was enjoyable coming into lab every day to work alongside you and all of the other Porter lab members past and present.

Table of Contents

Declaration of Co-Authorship.....	iii
Abstract.....	v
Dedication.....	vi
Acknowledgements.....	vii
List of Tables.....	xii
List of Figures.....	xiii
List of Appendices.....	xv
List of Abbreviations.....	xvi

Chapter 1: General Introduction

The Cell Cycle.....	2
Cyclins and CDKs.....	2
Cell Cycle Inhibition: Cyclin Dependent Kinase Inhibitors.....	4
DNA Damage Response.....	5
Speedy/RINGO: A Family of Cell Cycle Regulators.....	8
Speedy/RINGO: Discovery, Function and Family Members.....	8
Spy1 and Cell Cycle Regulation.....	14
Spy1 and the DNA Damage Response.....	17
The Mammary Gland.....	19
Development of the Murine Mammary Gland during Embryogenesis and Puberty.....	21
Pregnancy and Lactation.....	23
Involution.....	24
Mammary Cell Populations and Hierarchy.....	25
Breast Cancer: Incidence, Susceptibility and Subtypes.....	28
Cell Cycle Regulators and the Mammary Gland.....	29
Comparison of Murine and Human Mammary Gland Development.....	32
Spy1, Mammary Gland Development and Tumourigenesis.....	33
Liver.....	35
Murine Liver Development.....	35
Cell Cycle, Ploidy and Regeneration in the Liver.....	37
Diseases of the Liver: NAFLD and NASH.....	38
Hepatocellular Carcinoma.....	40
Spy1 and the Liver.....	43

The Mouse as a Model Organism	43
Transgenic Model Systems	44
Gene Targeted Mice.....	49
Mammary Specific Mouse Model Systems	52
Hypothesis and Objectives.....	55
References.....	56
Chapter 2: MMTV-Spy1 Mice Demonstrate Increased Susceptibility to Mammary Tumourigenesis	
Introduction.....	84
Materials and Methods.....	87
Construction of Transgene.....	87
Generation and Maintenance of MMTV-Spy1 Transgenic Mice	87
Primary Cell Harvest and Culture.....	88
Cell Culture.....	88
Plasmids	89
Transfection and Infection	89
UV Irradiation.....	90
DMBA Treatments.....	90
Histology and Immunostaining.....	90
Quantitative Real Time PCR Analysis.....	91
Protein Isolation and Immunoblotting	92
Antibodies	93
BrdU Incorporation Assay	93
Whole Mount Analysis	93
Results.....	95
Generation of MMTV-Spy1 transgenic mouse model system	95
Spy1 increases mammary tumour susceptibility	99
Spy1 expression disrupts the DDR in the presence of DMBA	103
Spy1 can override p53 in response to DNA damage	106
Levels of Spy1 are tightly regulated in the DNA damage response	106
p53 negatively regulates Spy1 protein levels	106
Spy1 overcomes UV-induced cell cycle arrest	111

Discussion.....	113
Acknowledgements.....	117
References.....	118
Chapter 3: The Role of Spy1 in Liver Steatosis and Susceptibility to Hepatocellular Carcinoma	
Introduction.....	123
Materials and Methods.....	126
Maintenance of MMTV-Spy1 Transgenic Mice	126
Plasmids	126
Cell Culture and Transfection	126
Histology and Immunostaining	127
Quantitative Real Time PCR Analysis	128
Protein Isolation and Immunoblotting	128
BrdU Incorporation Assay	129
Oil-Red O Staining	129
Results.....	130
Male MMTV-Spy1 exhibit an increase in Spy1 and increased tumourigenesis	130
Elevated levels of Spy1 lead to increased fat accumulation and increased nuclear size	130
Increased levels of Spy1 does not alter expression of known markers of HCC	134
Up-regulation of damage response pathways in MMTV-Spy1 mice	135
Alteration of Spy1 levels in a HCC cell line causes changes in proliferation and fatty acid accumulation	140
Discussion.....	143
Acknowledgements.....	147
References.....	148
Chapter 4: An Inducible Model System for Spatial and Temporal Control of Spy1 Expression	
Introduction.....	155
Materials and Methods.....	158
Construction and Generation of Spy1-pTRE Transgene	158
Generation and Maintenance of Spy1-pTRE Mice and Maintenance of MMTV-rtTA Mice	158
Quantitative Real Time PCR Analysis	159
Whole Mount Analysis	159

Histology and Immunostaining	160
Results	162
Spy1-pTRE transgenic mouse model generation and model validation	162
Prolonged expression of Spy1 does not alter gross mammary gland morphology	164
Discussion	166
Acknowledgements	169
References	170
Chapter 5: Development of a Gene Targeted Spy1 Model System	
Introduction	173
Materials and Methods	176
Plasmids	176
Gene Targeting	176
Southern Blot Analysis	176
Genotyping Procedure	178
Results	179
SpdyA conditional knockout targeting vector design	179
Identification of ES cell clone demonstrating successful homologous recombination	182
Discussion	184
Acknowledgements	189
References	190
Chapter 6: General Discussion and Future Directions	194
References	203
Appendices	207
Vita Auctoris	241

List of Tables

Table 1: Speedy/RINGO Family Members..... 13

List of Figures

Chapter 1: General Introduction

Figure 1: Schematic of Speedy/RINGO.....	13
Figure 2: Mammary Gland Development Summary.....	20
Figure 3: Structure of the Mammary Gland.....	20
Figure 4: Liver Disease Progression to Hepatocellular Carcinoma.....	42
Figure 5: Mechanism of tet-off and tet-on systems.....	48

Chapter 2: MMTV-Spy1 Mice Demonstrate Increased Susceptibility to Mammary Tumourigenesis

Figure 1: Generation of MMTV-Spy1 mouse model system.....	96
Figure 2: Spy1 overexpression leads to increased mammary tumour susceptibility.....	101
Figure 3: MMTV-Spy1 mice show alterations in DDR pathway when exposed to DMBA....	104
Figure 4: Endogenous and exogenous levels of Spy1 are controlled during DNA damage ...	108
Figure 5: Intact DDR pathway creates a negative feedback loop for Spy1.....	110
Figure 6: Spy1 overrides p53 in response to DNA damage.....	112
Figure 7: Mechanism of action.....	112
Supplementary Figure 1: Characterization of MMTV-Spy1 mouse model system.....	97
Supplementary Figure 2: Analysis of MMTV-Spy1 early development.....	98
Supplementary Figure 3: Mouse strain does not influence effects of Spy1 on normal development.....	116

Chapter 3: The Role of Spy1 in Liver Steatosis and Susceptibility to Hepatocellular Carcinoma

Figure 1: MMTV-Spy1 male mice are more susceptible to liver tumourigenesis.....	133
Figure 2: Levels of Spy1 effectors are not altered in MMTV-Spy1 mice.....	136
Figure 3: MMTV-Spy1 mice show increased inflammatory pathway signaling and apoptosis.....	137
Figure 4: Spy1 overexpression leads to increased proliferation and lipid accumulation.....	141
Figure 5: Spy1 knockdown leads to decreased proliferation and lipid accumulation.....	142
Supplementary Figure 1: qRT-PCR analysis in MMTV-Spy1 male livers.....	138
Supplementary Figure 2: MMTV-Spy1 male mice immunohistochemical analysis.....	139

Chapter 4: An Inducible Model System for Spatial and Temporal Control of Spy1 Expression

Figure 1: Generation of Spy1-pTRE transgenic mouse model.....	163
Figure 2: Long term exposure to doxycycline does not alter mammary development.....	165

Chapter 5: Development of a Gene Targeted Spy1 Model System

Figure 1: <i>Spy1</i> conditional knockout mouse targeting vector design	180
Figure 2: Screening strategy for Neo incorporation and PCR analysis.....	181
Figure 3: Southern blot analysis of ES cell clones.....	183

List of Appendices

Appendix A: List of Primers	207
Appendix B: Detailed Protocols	209
Appendix C: Direct Interactions with p27 and Cdk2 Regulate Spy1-Induced Mammary Tumorigenesis.....	214
Appendix D: Permissions.....	240

List of Abbreviations

Alb	Albumin
ATM	Ataxia telangiectasia mutated
ATR	Ataxia telangiectasia and Rad 3 related
BMP	Bone morphogenetic protein
CAK	CDK activating kinase
CDK	Cyclin dependent kinase
CKI	Cyclin dependent kinase inhibitor
Cntl	Control
DAB	3,3'-Diaminobenzidine
DDR	DNA damage response
DMBA	7,12-dimethylbenz(a)anthracene
DMEM	Dulbecco's modified Eagle's medium
EDTA	Ethylenediaminetetraacetic acid
EGF	Epidermal growth factor
EGTA	Ethylene glycol tetraacetic acid
EMEM	Eagle's Minimum Essential Medium
ER	Estrogen receptor
ESC	Embryonic stem cell
FBS	Fetal bovine serum
FGF	Fibroblast growth factor
GAPDH	Glyceraldehyde 3-phosphate dehydrogenase
H2AX	Histone H2A variant
H&E	Hematoxylin and eosin
HCC	Hepatocellular carcinoma
HGF	Hepatocyte growth factor
MAPK	Mitogen activated protein kinase
MMTV	Mouse mammary tumour virus
NAFLD	Non-alcoholic fatty liver disease
NASH	Non-alcoholic steatohepatitis
NBCS	Newborn bovine calf serum
NEDD4	Neuronal precursor cell-expressed developmentally downregulated 4
NF κ B	Nuclear factor kappa light chain enhancer of activated B cells

PAH.....	Polycyclic aromatic hydrocarbon
PBS	Phosphate buffered saline
PCR.....	Polymerase chain reaction
PBS	Phosphate buffered saline
PEI	Polyethylenimine
PI3K.....	Phosphatidylinositide 3 kinase
qRT-PCR.....	Quantitative real time PCR
RINGO.....	Rapid inducer of G2/M progression in oocytes
RPMI.....	Roswell Park Memorial Institute medium
RQ	Relative quantification
rtTA.....	Reverse tetracycline transactivator
SDS	Sodium dodecyl sulfate
shRNA.....	Small hairpin RNA
siRNA	Small interfering RNA
TBST.....	Tris buffered saline and Tween 20
TDLU.....	Terminal ductal lobular unit
TEB.....	Terminal end bud
TetO.....	Tet operator
TK	Thymidine kinase
tTa.....	Tetracycline transactivator
UTR.....	Untranslated region
UV.....	Ultraviolet
WT	Wild type

Chapter 1
General Introduction

Introduction

The Cell Cycle

The cell cycle lies at the heart of all developmental decisions and provides precise control over the balance between quiescence, proliferation, differentiation and apoptosis (Schafer, 1998; Vermeulen et al., 2003). The cell cycle is divided into 4 distinct phases, G1, S, G2 and M phase (Schafer, 1998; Vermeulen et al., 2003). During G1 phase, the cell receives cues that trigger preparation for DNA synthesis and allow cells to progress through to S phase of the cell cycle, which is characterized by DNA synthesis (Donjerkovic and Scott, 2000; Schafer, 1998; Vermeulen et al., 2003). Following S phase, cells enter into G2 where they prepare for the final stage in cell division, mitosis. After successful completion of mitosis, the cell can either terminally differentiate, re-enter the cell cycle, or enter G0, a state of quiescence characterized by reversible cell cycle arrest if the proper cues are received (Schafer, 1998; Vermeulen et al., 2003). Throughout the cell cycle, checkpoints can be activated to halt progression in unfavourable circumstances, such as in the event of DNA damage or improper DNA replication. Additionally, when the cell reaches the end of its lifespan or in response to certain stresses, cells can enter a state of irreversible cell cycle arrest known as senescence (Acosta and Gil, 2012). Progression and inhibition of the cell cycle is tightly controlled by the activity of cyclins, cyclin dependent kinases (CDKs) and cyclin dependent kinase inhibitors (CKIs) (Nakayama, 1998; Roussel, 1999; Schafer, 1998). Activation and inhibition of these regulatory proteins provides tight control over entry and exit of each stage of the cell cycle.

Cyclins and CDKs

Progression through the cell cycle is controlled by a number of regulatory proteins. Binding of cyclins to their binding partners, CDKs, and phosphorylation and de-phosphorylation of key residues on the CDK, activates the cyclin-CDK complex enabling phosphorylation of key substrates known to control cellular division. Protein levels of cyclins are transient and cycle

throughout the duration of the cell cycle, with levels increasing only when necessary (Evans et al., 1983; Pines, 1991; Vermeulen et al., 2003). CDKs are serine/threonine kinases that are expressed ubiquitously through the cell cycle and are modulated through post-transcriptional modifications such as activating and inhibitory phosphorylation (Malumbres and Barbacid, 2005; Schafer, 1998; Vermeulen et al., 2003). Different cyclin-CDK complexes are required for progression at each stage of the cell cycle. For example, Cyclin E-CDK2 plays a key role in regulating the transition from G1 to S phase of the cell cycle while Cyclin B-CDK1 initiates entry into mitosis (Schafer, 1998; Vermeulen et al., 2003). Full activation of CDKs requires binding of the appropriate cyclin binding partner and key phosphorylating and de-phosphorylating events. Binding of cyclins to CDKs is regulated by key regions located on the cyclin and CDK (Malumbres and Barbacid, 2005; Pavletich, 1999; Schafer, 1998; Vermeulen et al., 2003). Cyclins have a characteristic conserved region of approximately 150 amino acids known as the cyclin box, which plays a critical role in mediating binding with the appropriate CDK (Kobayashi et al., 1992; Noble et al., 1997). CDKs contain a PSTAIRE helix which makes contact with the cyclin box (Morgan, 1997; Pavletich, 1999). Binding of the cyclin alters the conformation of the CDK such that the T-loop phosphorylation site becomes accessible and relieves partial blocking of the catalytic cleft (Jeffrey et al., 1995; Pavletich, 1999). Further conformational changes are achieved after T-loop phosphorylation on Thr160 (CDK2)/Thr161 (CDK1) by CDK activating kinases (CAK) (Jeffrey et al., 1995; Pavletich, 1999; Russo et al., 1996; Solomon et al., 1992). For full activation of the cyclin-CDK complex, the inhibitory phosphorylation on Thr14/Tyr15 by Myt1 is removed by the phosphatase Cdc25 (Lew and Kornbluth, 1996; Nigg, 1995). Three isoforms of Cdc25 exist and function in distinct phases of the cell cycle (Donzelli and Draetta, 2003; Karlsson-Rosenthal and Millar, 2006). Cdc25A promotes entry into S phase and progression through the G2/M transition and dephosphorylates Cyclin E-CDK2, Cyclin A-CDK2 and Cyclin B-CDK1 (Donzelli and Draetta, 2003; Karlsson-Rosenthal and Millar, 2006). Cdc25B and Cdc25C however, only dephosphorylate Cyclin B-CDK1 and therefore promote entry into

mitosis (Donzelli and Draetta, 2003; Karlsson-Rosenthal and Millar, 2006). In this state, the cyclin-CDK complex is fully activated and will phosphorylate target substrates to promote progression through the cell cycle.

Cell Cycle Inhibition: Cyclin Dependent Kinase Inhibitors

In response to DNA damage or environmental stressors, cyclin dependent kinase inhibitors (CKIs) will inhibit the kinase activity of cyclin-CDK complexes to halt progression of the cell cycle (Nakayama, 1998). Two classes of CKIs exist, the INK4 family of inhibitors and Cip/Kip family. Each family of proteins inhibits cyclin-CDK activity in a unique fashion. The INK4 family consists of p15, p16, p18 and p19, and this class of inhibitors binds monomeric CDK4 or 6 effectively altering the conformation of the CDK so that Cyclin D can no longer bind (Canepa et al., 2007; Sherr and Roberts, 1995). The inability of Cyclin D to bind to its CDK binding partner renders the kinase inactive preventing progression through G1 phase of the cell cycle. Additionally, these inhibitors have been shown to play important roles in regulating senescence and alterations or mutations could contribute to the development of cancer (Canepa et al., 2007; Roussel, 1999).

The Cip/Kip family of inhibitors consists of p21^{WAF1/Cip1}, p27^{kip1}, and p57^{kip2} (Nakayama, 1998). In contrast to the INK4 family of inhibitors, Cip/Kip members inhibit a broader range of CDKs and instead bind the cyclin-CDK complex (Nakayama, 1998; Pavletich, 1999). Binding to the cyclin-CDK complex can induce conformational changes and prevent access to the catalytic cleft thereby preventing cyclin-CDK activity (Pavletich, 1999). Binding of these inhibitory proteins is mediated through the presence of a conserved hydrophobic patch on the cyclin containing the MRAIL motif, which is also responsible for substrate recognition (Chen et al., 1996; Schulman et al., 1998). Members of this family of inhibitors are known to play crucial roles in regulating normal developmental processes to prevent aberrant rates of proliferation. Levels of p27 are tightly regulated via ubiquitin-mediated proteolysis and levels rapidly decrease in late G1

and S phase (Nakayama, 1998; Pagano et al., 1995). p27 primarily inhibits the cell cycle during G1 and thus plays a critical role in mediating cellular proliferation (Donjerkovic and Scott, 2000; Nakayama, 1998). This is demonstrated by the phenotype seen in mice lacking p27; without p27, mice are significantly larger than control littermates and multiple organs exhibit significant hyperplasia, highlighting the importance of p27 in regulating cell proliferation (Fero et al., 1996; Nakayama et al., 1996). The cell cycle inhibitor p21 can be upregulated and activated through p53 dependent and independent pathways and p21 is known to play a critical role for p53 dependent cell cycle arrest in G1 in response to DNA damage (el-Deiry et al., 1994). Expression of p21 is not solely dependent on p53, although its upregulation in response to DNA damage events occurs in a p53-dependent fashion (el-Deiry et al., 1994; Gartel and Tyner, 2002; Macleod et al., 1995). In addition to its role in growth arrest in response to DNA damage, p21 may also play a role in regulating exit from the cell cycle to promote differentiation (Steinman et al., 1994). Exit from the cell cycle is a key component in terminal differentiation, thus precise control over cell cycle entry and exit is critical for the expansion and maintenance of various cell populations within the body. These regulators play a crucial role in proper development and prevent aberrant growth and proliferation, a hallmark of cancer.

DNA Damage Response

DNA within a cell is exposed to a variety of insults and can be damaged either through normal intrinsic events or from environmental stimuli such as UV irradiation or exposure to harmful chemical substances. Regardless of how the DNA has been damaged, the cell must activate pathways to repair or remove the damage, or risk accumulation of the damaged DNA which could ultimately lead to carcinogenic events. Cell cycle checkpoints during G1/S and G2/M can detect various forms of DNA damage and induce cell cycle arrest allowing the appropriate repair machinery to be activated (Sancar et al., 2004). In the event that the DNA cannot be repaired, the cell can undergo senescence to stop proliferation of the cell thereby

preventing subsequent expansion of a potentially dangerous population, or apoptotic pathways can be activated to eliminate the cell completely.

DNA damage is recognized by serine/threonine kinases ataxia telangiectasia mutated (ATM) and ataxia telangiectasia and Rad 3 related (ATR) which activate checkpoint pathways and recruit the appropriate repair machinery to the site of damage for repair to occur (Sancar et al., 2004; Smith et al., 2010). These kinases each recognize and respond to different types of DNA damage, with ATM becoming activated in response to double strand breaks and ATR responding to damage resulting from UV exposure (Hurley and Bunz, 2007; Sancar et al., 2004; Smith et al., 2010). Upon activation of ATR and ATM, protein kinases Chk1 and Chk2 are subsequently phosphorylated and activated by ATR and ATM respectively (Hurley and Bunz, 2007; Lukas et al., 2003; Smith et al., 2010). Rapid cell cycle arrest is achieved through phosphorylation of Cdc25A leading to its ubiquitin-mediated degradation (Donzelli and Draetta, 2003; Mailand et al., 2000; Mailand et al., 2002). Without active Cdc25A, cyclin-CDK complexes remain inactive allowing for cell cycle arrest and DNA repair to occur (Donzelli and Draetta, 2003; Mailand et al., 2000; Smith et al., 2010). Additionally, phosphorylation of p53 will lead to accumulation of p53 and sustained cell cycle arrest (Meek, 2004; Sakaguchi et al., 1998; Shieh et al., 1997). Under normal circumstances, levels of p53 are held in check by the E3 ubiquitin ligase Mdm2, which blocks transcriptional activity of p53 and targets it for degradation (Meek, 2004; Sakaguchi et al., 1998; Shieh et al., 1997). Phosphorylation of p53 on Ser15 and Ser20 disrupts the interaction between p53 and Mdm2 leading to stabilization of p53 (Kruse and Gu, 2009; Meek, 2004; Sakaguchi et al., 1998; Shieh et al., 1997). p53 can subsequently activate target genes such as p21, which can further inhibit the cell cycle in G1 phase, or in the event that the damage cannot be repaired, can activate apoptotic pathways (He et al., 2005; Meek, 2004). Thus, p53 serves as a master regulator of the DNA damage response, mediating activation of the appropriate repair pathways and response to damage as required by the severity of damage.

The DNA repair response is a complex set of pathways with a large number of regulators that identify the sites and types of DNA damage, recruit repair machinery, halt cell cycle progression and repair the DNA. Examining levels and phosphorylation status of many of these repair pathway proteins can indicate the level of damage and if an effective DNA repair response has occurred. Histone H2A variant (H2AX) is a reliable marker when examining activation of repair in response to DNA double stranded breaks (Dickey et al., 2009). In response to double stranded breaks, H2AX phosphorylation on Ser139 is mediated by ATM, and once phosphorylated is known as γ H2AX (Dickey et al., 2009; Paull et al., 2000; Rogakou et al., 1998). γ H2AX is found at the site of double stranded breaks and is thought to help recruit repair machinery to the site of damage by allowing the DNA to become less condensed enabling easier access for repair proteins (Dickey et al., 2009; Kinner et al., 2008; Paull et al., 2000). Studies have shown that H2AX is phosphorylated rapidly after damage, with phosphorylation evident 1 to 3 minutes after damage and levels of phosphorylation directly related to the severity of damage (Dickey et al., 2009; Paull et al., 2000; Podhorecka et al., 2010). Increased levels of γ H2AX have been found in various types of cancer cells as well as in senescent cells indicating that these cells have accumulated damage over time (Das et al., 1989; Dickey et al., 2009; Lee et al., 2008; Sedelnikova and Bonner, 2006). Rodent models in which tumours have been induced by the carcinogen 7,12-dimethylbenz(a)anthracene (DMBA) have found increased levels of γ H2AX in the tumours indicating that the development of tumours is in part due to accumulated damage (Lee et al., 2008). DMBA causes DNA adduct formation once its carcinogenic metabolite covalently binds to DNA (Das et al., 1989; Melendez-Colon et al., 1999). This triggers the DNA repair pathway activated in response to double stranded breaks (Costa et al., 2003; Dickey et al., 2009; Paull et al., 2000; Podhorecka et al., 2010). In circumstances of extensive adduct formation, such as in the case of exposure to DMBA, the repair machinery cannot keep up with the amount of damage and damage begins to accumulate. The cell continues to divide and levels of γ H2AX increase as time progresses. Ultimately, the unrepaired damage leads to deleterious mutations in

the DNA, causing tumourigenesis (Dickey et al., 2009). These findings highlight the importance of an intact and efficient DNA repair pathway in the prevention of oncogenesis.

Thus, tight regulation over the cell cycle is imperative in maintaining the genomic integrity of the cell, and in preventing unwanted, deleterious mutations from occurring. Entry and exit from each stage of the cell cycle is tightly controlled by a number of cell cycle regulators that each play a key role in ensuring the cell cycle proceeds in an effective manner. Progression through the cell cycle is required to expand or replenish cell populations, while exit from the cell cycle is needed to allow for terminal differentiation to occur. Inhibition during times of damage is critical for maintaining the health an organism, as unchecked damage can accumulate over time ultimately leading to tumourigenesis. A complete understanding of all of the regulators at play is required to fully elucidate the mechanisms which control normal growth and development and will ultimately expand understanding of the mechanisms responsible for tumour initiation and progression.

Speedy/RINGO: A Family of Cell Cycle Regulators

Speedy/RINGO: Discovery, Function and Family Members

The discovery of Speedy/RINGO, or Spy1, was initially made in a *rad1* deficient strain of *S.pombe* that typically arrest at the G2/M transition in response to DNA damage (Lenormand et al., 1999). Using this model, researchers identified and isolated *Xenopus* genes from a *Xenopus* cDNA library that were able to overcome the G2/M arrest in response to damage, thereby isolating genes involved in cell cycle regulation (Lenormand et al., 1999). Through this screen, one clone was identified to confer resistance to UV radiation, and was coined Speedy, or Spy1 (Lenormand et al., 1999). Spy1 was found to be expressed in stage IV oocytes with levels remaining fairly constant until the onset of gastrulation, where at that point, levels became undetectable (Lenormand et al., 1999). Spy1/RINGO mRNA translation is repressed by binding

of Pumilio2, an RNA binding protein, to its 3'UTR and 5'end of the cap structure until progesterone stimulation causes dissociation of Pumilio2 from Spy1/RINGO mRNA, leading to translation (Cao et al., 2010; MacNicol and MacNicol, 2010; Padmanabhan and Richter, 2006). These results show that Spy1 is present in *Xenopus* oocytes as maternal mRNA, and therefore could play a role in cell cycle regulation.

Stage IV oocytes are arrested at the G2/M boundary, and stimulation with progesterone triggers progression through this stage to allow for the completion of the first stage of meiosis (Sagata et al., 1989). Mos and mitogen activated protein kinase (MAPK) have also been shown to stimulate oocyte maturation and inhibition of either mos or MAPK resulted in a block of progesterone-induced maturation indicating the essentiality of both factors in this process (Nebreda and Hunt, 1993). To test if Spy1 was capable of regulating cell cycle dynamics, Spy1 mRNA was injected into stage IV oocytes and progression past the G2/M boundary was monitored. Injection of Spy1 mRNA not only induced release from G2 arrest and rapid oocyte maturation, but it did so approximately 2-fold faster than seen in oocytes induced with mos mRNA or progesterone (Ferby et al., 1999; Lenormand et al., 1999). To further validate the role of Spy1 in oocyte maturation, depletion of Spy1 from stage IV oocytes with antisense oligonucleotides significantly delayed oocyte maturation in response to progesterone, highlighting the importance of this protein in this process (Ferby et al., 1999). Additionally, Spy1 injection triggered cdc2 kinase activity and MAPK activation quicker than that seen in progesterone induced or mos injected oocytes (Ferby et al., 1999; Lenormand et al., 1999). When oocytes were treated with a MEK inhibitor to effectively inhibit the MAPK pathway, the ability of Spy1 to induce oocyte maturation was significantly delayed indicating a requirement for MAPK activation in Spy1 mediated oocyte maturation (Lenormand et al., 1999). The ability of Spy1 to release oocytes from the G2/M arrest established it as a cell cycle regulator. The question remained however, whether or not Spy1 was capable of interacting with other cell cycle regulatory proteins. Co-injection of Spy1 and CDK2 mRNA followed by co-immunoprecipitation

demonstrated that these two proteins were capable of directly binding to one another (Lenormand et al., 1999). CDK2 activity was also greatly up-regulated as a result of Spy1 injection as compared to mos injection or progesterone stimulation (Lenormand et al., 1999). In addition to promoting cell cycle progression, Spy1 may stimulate the translation of other mRNA important for oocyte progression by activating Musashi, a known stem cell factor which is responsible for translation of the mos mRNA required for oocyte maturation (Arumugam et al., 2012; Charlesworth et al., 2006; MacNicol and MacNicol, 2010). Thus the newly discovered Spy1 protein was shown to be capable of inducing the G2/M transition in *Xenopus* oocytes, thus establishing a new family of cell cycle proteins.

The cloning of the human homologue of Spy1 was made using a testis cDNA library identifying proteins that were homologous to *Xenopus*-Spy1 (X-Spy1) (Porter et al., 2002). The resulting match yielded 40% homology to X-Spy1 but also contained a central region with 70% homology (Porter et al., 2002). To confirm this clone was indeed the human homologue to X-Spy1, human Spy1 was injected into *Xenopus* oocytes to determine its ability to trigger oocyte maturation. Although slower than X-Spy1, human Spy1 induced oocyte maturation upon injection therefore confirming that the newly identified clone was indeed the human homologue of Spy1 (Porter et al., 2002). A panel of deletion mutants of X-Spy1 were generated to test which region of the protein was essential for its activity. It was found that the central region, the most highly conserved portion of the protein, was essential for Spy1 activity (Porter et al., 2002).

Human Spy1 is expressed in a wide variety of human tissues, with levels relatively high in the testis (Cheng et al., 2005b; Porter et al., 2002). Additionally, Spy1 is expressed in a wide variety of immortalized cell lines (Cheng et al., 2005b; Porter et al., 2002). Since X-Spy1 is an important cell cycle regulator in triggering release from the G2/M arrest, analysis of the distribution of Spy1 expression during the cell cycle was assessed. Spy1 was expressed only in G1/S phase of the cell cycle (Dinarina et al., 2009; Porter et al., 2002) and is localized to the nucleus where it is capable of binding and activating CDK2, as seen with X-Spy1 (Porter et al.,

2002). Increased levels of Spy1 led to a significant increase in the proliferative capacity of the cells, increasing cellular proliferation and shortening G1 phase of the cell cycle (Porter et al., 2002). The ability of Spy1 to enhance proliferation was dependent on CDK2, as inhibition of CDK2 inhibited the ability of Spy1 to enhance cellular proliferation (Porter et al., 2002). Spy1 is an essential player in normal cell proliferation as depletion of Spy1 from the cell significantly decreased rates of cell proliferation (Porter et al., 2002). Overall, Spy1 was established to be a critical player in the cell cycle machinery of mammalian cells.

After the discovery of human Spy1, further searches yielded new family members in the Speedy/RINGO family of proteins (Table 1) (Cheng et al., 2005b; Dinarina et al., 2005). To date, no homologues have been identified in yeast, worms, flies or plants; however, a potential homologue has been identified in *Ciona intestinalis* (Cheng et al., 2005b). The discovery of this homologue in this primitive branch of chordates suggests that homologues may exist in all vertebrates, as modern day vertebrates branched off from *Ciona intestinalis* (Cheng et al., 2005b). To date, 5 family members in total have been identified (Cheng et al., 2005b; Dinarina et al., 2005). All share homology in the central core of amino acids, the Speedy/RINGO (S/R) box, which is essential for binding to CDKs, but differ outside of this central region of similarity (Cheng et al., 2005b; Dinarina et al., 2005). Speedy/RINGO A is expressed in a wide variety of human tissues and immortalized cell lines (Cheng et al., 2005b; Dinarina et al., 2005; Porter et al., 2002). Additionally, there are 2 isoforms of Speedy/RINGO A, Spy1 A1 and Spy1 A2 which differ in their C-terminal region, with Spy1 A1 being the longer isoform (Cheng et al., 2005b). Analysis of the two isoforms demonstrated Spy1 A1 to be identical to the originally identified human Spy1, and will be referred to as Spy1 throughout (Cheng et al., 2005b). The Spy1 protein can be divided up into three basic regions (Figure 1). The central portion of the protein, the S/R box, is responsible for CDK binding, which has been previously demonstrated (Cheng et al., 2005b; Dinarina et al., 2005; Porter et al., 2002). The N terminal region was found to be responsible for regulating protein stability or degradation, while the C terminal region was noted

to be required for CDK activation (Cheng et al., 2005b; Dinarina et al., 2005). Given that the originally identified human Spy1 protein is capable of binding and activating CDK2, the CDK binding preference of Spy1A was analysed. Spy1 is capable of binding and activating both CDK2 and CDK1, consistent with previous data (Cheng et al., 2005b; Dinarina et al., 2005).

The remaining family members in the Speedy/RINGO family of proteins all possess similarities in the sequence of the S/R box, but differ in expression and binding to the CDKs (Cheng et al., 2005b; Dinarina et al., 2005). Speedy/RINGO B has been shown to be expressed solely in the testis of mice, and cannot promote oocyte maturation when injected into *Xenopus* oocytes; however it can accelerate this process in the presence of progesterone, indicating the basic function of the protein may be conserved (Cheng et al., 2005b; Dinarina et al., 2005). When binding specificity to CDK partners was analysed, Speedy/RINGO B was found to bind preferentially to Cdk1 (Cheng et al., 2005b; Dinarina et al., 2005). In contrast to Speedy/RINGO B, Speedy/Ringo C is able to bind both CDK1 and CDK2 and is expressed in a wider range of tissues (Cheng et al., 2005b; Dinarina et al., 2005). Speedy/RINGO C is found in tissues such as the liver, placenta and bone marrow, which may indicate a role in polyploidization as these tissue frequently exhibit polyploidy (Cheng and Solomon, 2008; Cheng et al., 2005b; Dinarina et al., 2005; Mouron et al.). Less is known about Speedy/RINGO D, although it is known to be expressed in mice (Cheng et al., 2005b; Dinarina et al., 2005). In contrast to the other well-known family members, Speedy/RINGO E actually impairs cell cycle progression in the *Xenopus* oocyte system despite its known ability to bind CDKs 1, 2, and 5 (Cheng et al., 2005b; Dinarina et al., 2008; Dinarina et al., 2009). Thus, the Speedy/RINGO family of proteins represents a novel class of cell cycle regulatory proteins that play a distinct role in the regulation of cell cycle progression.

Name	CDK Binding Partner	Expression
Speedy/RINGO A	CDK1, CDK2	Ubiquitous
Speedy/RINGO B	CDK1	Testis
Speedy/RINGO C	CDK1, CDK2	Liver, placenta, testis, bone marrow, small intestine, kidney
Speedy/RINGO D	Unknown	Unknown
Speedy/RINGO E	CDK1, CDK2, CDK5	Unknown

Table 1: Speedy/RINGO family members

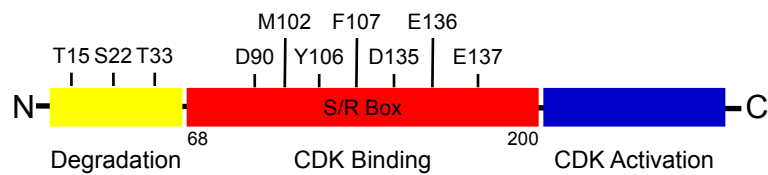


Figure 1: Schematic of Speedy/RINGO structure depicting location and function of conserved regions with important residues for degradation and CDK binding indicated.

Spy1 and Cell Cycle Regulation

Spy1 is capable of inducing oocyte maturation in *Xenopus* oocytes and stimulating cellular proliferation in mammalian cell culture systems, indicating a key role in mediating cell cycle progression (Ferby et al., 1999; Lenormand et al., 1999; Porter et al., 2002). The ability of Spy1 to bind to CDKs through a conserved stretch of amino acids known as the Speedy/RINGO (S/R) box is at least in part responsible for cell cycle progression (Cheng et al., 2005b; Dinarina et al., 2009; Porter et al., 2002). Mutation of three key amino acid residues within this region abolished binding of Spy1 to CDK2 highlighting the importance of this region in mediating the Spy1-CDK2 interaction (Dinarina et al., 2009). While Spy1 can bind and activate CDKs, it is able to do so in a unique manner. Spy1 is capable of binding and activating CDK2 in the absence of the activating T loop phosphorylation demonstrated by Spy1's ability to activate mutants of CDKs that are unable to be phosphorylated on Thr161 and Thr160 (Cheng et al., 2005a; Karaïskou et al., 2001). Spy1 is also less sensitive to inhibitory phosphorylation on Thr14/Tyr15 (Karaïskou et al., 2001). Addition of Myt1 kinase, which is known to phosphorylate the Thr14 residue, was shown to have a reduced inhibitory effect on Spy1-CDK activity, demonstrating that Spy1 is less sensitive to the inhibitory effects of these phosphorylation sites (Karaïskou et al., 2001). Thus, Spy1 is capable of activating CDKs in a manner that does not rely on the classical phosphorylating and de-phosphorylating events required for cyclin activation of CDKs. Despite this, the manner in which Spy1 and CDK binding occurs may be similar to that of cyclin-CDK binding. Mutation of amino acid residues Ile⁴⁹ and Arg⁵⁰ in the PSTAIRE region of CDK2 prevented Spy1 binding to CDK2 (Dinarina et al., 2005). These residues are also important for mediating Cyclin A binding to CDK2 indicating that Spy1 may in fact be binding in a similar manner as the classical cyclins (Dinarina et al., 2005; Karaïskou et al., 2001). The ability of Spy1 to activate CDKs in the absence of the CDK classical phosphorylation status may, however, be due in part to the ability of Spy1 to alter CDK conformation to a state that is normally induced by

T loop phosphorylation, negating the requirement of this phosphorylation event (Karaiskou et al., 2001).

CDK-cyclin complexes are known to phosphorylate canonical substrates consisting of the sequence (S/T)PX(K/R) (Errico et al., 2010). Classic CDK-cyclin complexes prefer a basic residue such as lysine or arginine to be located at the +3 position in relation to the phosphorylation site (Holmes and Solomon, 1996). In contrast, Spy1-CDK complexes can tolerate a wide variety of residues located at the +3 position and can phosphorylate non-canonical substrates of CDKs (Cheng et al., 2005a). Since the Thr160 residue makes contact with the +3 residue, it is possible that the ability of Spy1 to induce activation in the absence of Thr160 phosphorylation may alter substrate specificity (Cheng et al., 2005a). It is also conceivable that the binding of Spy1 to CDK2 may induce a different conformation than CDK-cyclin complexes, which may also contribute to its ability to phosphorylate non canonical substrates well (Cheng et al., 2005a). Taken together, the ability of Spy1 to uniquely activate CDKs and phosphorylate both canonical and non-canonical substrates contributes to its functionality in regulating cell cycle progression.

Cyclin dependent kinase inhibitors, CKIs, play a crucial role in regulating cell cycle progression, negatively affecting progression by inhibiting cyclin-CDK complexes. This may be required in the event of DNA damage whereby the cell needs to halt cell cycle progression to allow for the appropriate repair pathways to occur. The CKI p21 works to inhibit cell cycle progression at the G1/S phase of the cell cycle by binding and inhibiting cyclin-CDK complexes (Bartek and Lukas, 2001; He et al., 2005). Addition of p21 inhibits CDK2-Cyclin A activity but CDK2-Spy1 activity is not inhibited, indicating that Spy1 is less susceptible to inhibition by p21 (Karaiskou et al., 2001). The decreased sensitivity to p21 inhibition may be due in part to Spy1 lacking the hydrophobic patch of the MRAIL motif found on cyclins that allows for p21 inhibition of CDKs (Karaiskou et al., 2001). In support of this theory, it was demonstrated that addition of Spy1 with CDK1 and p21 led to a significant reduction in the amount of p21 bound to

CDK1 as compared to the addition of Cyclin B1 (Karaïskou et al., 2001). This data supports that Spy1 is less sensitive to inhibition by p21 which may be due in part to decreased binding affinity.

While Spy1 has been shown to have reduced binding affinity to p21, it has been shown to bind directly to another CKI, p27 (Porter et al., 2003). The CKI p27 is a member of the Cip/Kip family and binds CDK2-Cyclin E, and CDK4-Cyclin D complexes to inhibit their activity, thus halting cell cycle progression. In a yeast two-hybrid screen, Spy1 was shown to bind to p27; further analysis revealed that Spy1 interacts with the CDK binding region on p27 (Porter et al., 2003). Together, Spy1, CDK2 and p27 are able to form a complex; Spy1 is capable of overcoming a p27-induced cell cycle arrest and increasing turnover of p27 in G1/S phase of the cell cycle (McAndrew et al., 2007; Porter et al., 2003). Increased p27 turnover in the presence of Spy1 is due to the ability of Spy1/CDK2 to phosphorylate p27 on Thr187, targeting p27 for degradation (McAndrew et al., 2007). This phosphorylation event is dependent on the ability of Spy1 to both bind and activate CDK2, and requires the C terminal region of Spy1 for CDK2 activation (Cheng et al., 2005b; McAndrew et al., 2007). In addition to its ability to target p27 for degradation, addition of Spy1 protects CDK2-Cyclin E complexes from p27 inhibition (McAndrew et al., 2007). Thus, Spy1 could further drive cell cycle progression in part due to its ability to overcome p27-induced cell cycle arrest, target p27 for degradation, and protect CDK2-Cyclin E complexes from inhibition (McAndrew et al., 2007; Porter et al., 2003). This could provide a unique mechanism whereby Spy1 facilitates cell cycle progression and overcomes checkpoints in the event of DNA damage, an event which could have drastic consequences in the context of cancer initiation and progression.

Cyclins are subject to tight regulation of expression levels during the cell cycle. Similar to cyclins, Spy1 expression has also been shown to be regulated in a cell cycle specific manner and the presence of PEST sequences suggests it may have a short half-life (Al Sorkhy et al., 2009; Dinarina et al., 2009; Lenormand et al., 1999; Porter et al., 2002). Levels of Spy1 were shown to be higher in G1 phase of the cell cycle and were down regulated during G2/M (Al Sorkhy et al.,

2009; Dinarina et al., 2009). A panel of Spy1 deletion mutants were studied to determine the regions of Spy1 responsible for mediating its degradation. Loss of the first 57 amino acids prevented Spy1 degradation, indicating that the N terminus is required for mediating Spy1 degradation (Al Sorkhy et al., 2009). Further analysis of the N terminal region identified three key amino acid residues responsible for mediating Spy1 degradation (Al Sorkhy et al., 2009). Mutation of Thr15, Ser22, and Thr33 prevented the ubiquitination and subsequent degradation of Spy1 (Al Sorkhy et al., 2009). This mutant also showed decreased levels of phosphorylation and was capable of enhancing proliferation, even above that seen with wild-type Spy1 (Al Sorkhy et al., 2009). Additionally, Spy1 degradation has been shown to be regulated via two different E3 ubiquitin ligases, namely the SCF-Skp2 complex and Nedd4 (Al Sorkhy et al., 2009; Dinarina et al., 2009). Expression of Skp2 is inversely correlated with that of Spy1, and reduction of Skp2 levels leads to an increase in Spy1 levels, suggesting that the SCF-Skp2 complex could be involved in degradation of Spy1 (Dinarina et al., 2009). An alternative mechanism of degradation was shown to be through Nedd4 (Al Sorkhy et al., 2009). Addition of MG132 led to an increase in Spy1 protein levels and a decrease in ubiquitination indicating a ubiquitin proteasome system was responsible for Spy1 degradation (Al Sorkhy et al., 2009; Dinarina et al., 2009). A search of possible E3 ubiquitin ligases yielded Nedd4 (Al Sorkhy et al., 2009). Co-immunoprecipitation experiments showed direct binding of Spy1 to Nedd4 and increased Nedd4 led to a reduction in Spy1 protein levels (Al Sorkhy et al., 2009). Spy1 protein levels are controlled by a variety of cellular mechanisms and are tightly controlled during the cell cycle. This likely serves to prevent early activation and prevent cell cycle progression under unwanted circumstances.

Spy1 and the DNA Damage Response

In the event of DNA damage, cell cycle checkpoints are activated, halting cell cycle progression allowing for the damage to be repaired. If the damage cannot be repaired, apoptotic pathways can be activated leading the cell death. Spy1 was initially isolated in a strain of rad1

deficient yeast and was able to confer resistance to UV damage allowing for progression through the cell cycle (Lenormand et al., 1999). This initial discovery demonstrated that in addition to its ability to promote cell cycle progression, Spy1 may also override cell cycle checkpoints in the event of DNA damage. Indeed, it was shown that in the case of exposure to DNA damaging agents or after exposure to UV, cells with elevated levels of Spy1 showed increased cell survival (Barnes et al., 2003; Gastwirt et al., 2006). The ability of Spy1 to promote cell survival is dependent on both its interaction and activation of CDK2 and is p53-dependent (Barnes et al., 2003; Gastwirt et al., 2006; McAndrew et al., 2009). Upon DNA damage, increased interaction between Spy1 and CDK2, as well as increased CDK2 activity, is essential for Spy1 mediated increases in cell survival (Barnes et al., 2003; Gastwirt et al., 2006). Cell cycle checkpoint activation at both S and the G2/M phase of the cell cycle was also inhibited as no changes were observed in either DNA synthesis or in the levels of phosphorylated histone 3 (Gastwirt et al., 2006). Overexpression of Spy1 results in decreased phosphorylation of key mediators of DNA damage signaling, such as H2AX, RPA32 and Chk1 indicating impaired DNA damage signaling (Gastwirt et al., 2006). Knockdown of Spy1 levels decreases cell survival in the presence of DNA damage, indicating a potential role for Spy1 in the normal repair process (Barnes et al., 2003; McAndrew et al., 2009). Thus, given Spy1's ability to promote cell cycle progression, Spy1 may serve as a mediator between cell cycle progression and checkpoint activation (McAndrew et al., 2009). In the event of damage, elevated levels of Spy1 could continue to promote cellular proliferation allowing for the accumulation of deleterious mutations, thereby playing a role in cancer initiation and progression.

Indeed, elevated levels of Spy1 have been found in breast, brain and liver cancers, among others, highlighting the importance of this protein in maintaining the balance between cell cycle progression and inhibition (Al Sorkhy et al., 2012; Ke et al., 2009; Lubanska et al., 2014; Zucchi et al., 2004). Elucidating the mechanism by which Spy1 regulates growth and development in

normal developmental systems will provide further insight into the role it may play in the initiation and progression of tumourigenesis.

The Mammary Gland

The mammary gland is an excellent study system as the majority of development occurs post-natally allowing for investigators to study normal developmental processes that regulate growth and development of the gland (Figure 2) (Howlin et al., 2006; Richert et al., 2000). The gross structure of the murine mammary gland is composed of an extensive ductal network composed of primary ducts as well as lateral branching which fills the fat pad (Hinck and Silberstein, 2005; Richert et al., 2000). The hollow lumen of each duct is lined by luminal epithelial cells which are surrounded by myoepithelial cells, the contractile cells within the gland (Figure 3B) (Richert et al., 2000). During pregnancy, alveoli form and fill the fat pad, producing and secreting milk proteins during lactation (Oakes et al., 2006; Richert et al., 2000). Once lactation is complete, the gland involutes returning to its post-pubertal state where it awaits the next round of pregnancy (Richert et al., 2000; Watson, 2006).

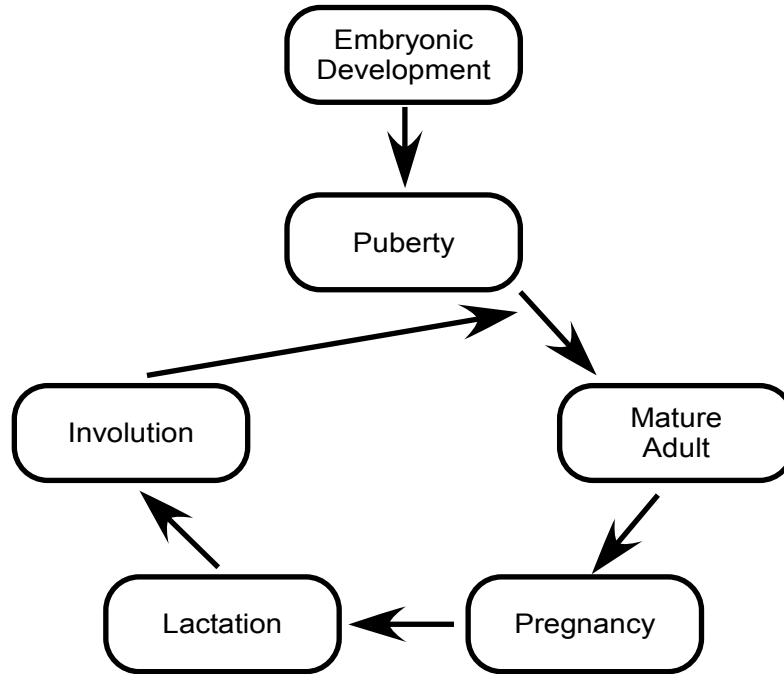


Figure 2: The majority of mammary gland development occurs postnatal in a cyclic fashion with repeated cycles of proliferation, differentiation, apoptosis and regeneration.

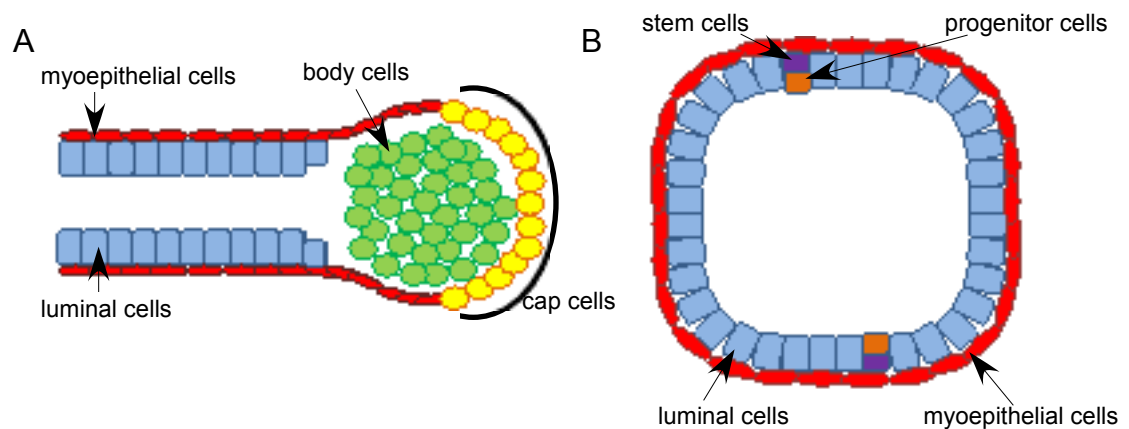


Figure 3: Schematic representation of the structures of the mammary gland, A) the terminal end bud and **B)** a mature duct. Yellow represents the highly proliferative cap cells, green represents body cells, purple are the stem cells which reside in the mature duct and orange represents progenitor cells. Mature luminal and myoepithelial cells are indicated in blue and red respectively.

Development of the Murine Mammary Gland during Embryogenesis and Puberty

Development of the murine mammary gland begins mid-gestation and sets the stage for rapid outgrowth of the rudimentary ductal tree formed during post-natal development. Embryonic development of the murine mammary gland begins at embryonic day 10.5 with the formation of mammary lines. Ectodermal cells migrate along this line and aggregate together to form mammary placodes which dictate the location of the 5 pairs of mammary glands (Cowin and Wysolmerski, 2010; Hens and Wysolmerski, 2005). At embryonic day 14.5, the placodes begin to invaginate into the underlying mesenchyme to form mammary buds (Cowin and Wysolmerski, 2010; Hens and Wysolmerski, 2005; Richert et al., 2000). Ductal branching morphogenesis generates a small number of ducts with a small number of side branches, and this process is arrested at embryonic day 18.5 where the gland then remains developmentally arrested until the onset of puberty (Cowin and Wysolmerski, 2010; Hens and Wysolmerski, 2005; Richert et al., 2000). At the onset of puberty, the gland undergoes a period of development characterized by rapid outgrowth of the ductal network, which is regulated in a hormone dependent manner, in contrast to embryonic development which is regulated in a hormone independent manner (Briskin and O'Malley, 2010; Richert et al., 2000). The driving force behind ductal elongation during this period of development is the steroid hormone estrogen (Briskin and O'Malley, 2010; Richert et al., 2000; Sternlicht, 2006). Estrogen signaling stimulates elongation of the rudimentary ductal network formed during embryonic development allowing the duct to elongate to fill the mammary fat pad (Briskin and O'Malley, 2010; Richert et al., 2000; Sternlicht, 2006). Mice lacking estrogen receptor α are unable to respond to estrogen stimulation, fail to undergo ductal morphogenesis, and the primitive ductal network remains in this form (Mallepell et al., 2006). While estrogen may stimulate ductal morphogenesis and is essential for this process, the driving force behind ductal elongation and bifurcation of the ducts are terminal end buds (TEBs) (Hinck and Silberstein, 2005; Richert et al., 2000; Sternlicht, 2006). TEBs are bulbous structures located on the ends of the elongating ducts and are known to be the site of the highest rates of

proliferation within the mammary gland (Figure 3A) (Williams and Daniel, 1983). At approximately 3 weeks of age at the onset of puberty, TEBs first appear and begin to drive elongation of the ductal network (Hinck and Silberstein, 2005; Richert et al., 2000). At the leading edge of TEBs are a population of undifferentiated pluripotent stem cells called the cap cells, with the highest proliferative capacity of any cell population within the mammary gland (Hinck and Silberstein, 2005; Richert et al., 2000; Williams and Daniel, 1983). Cap cells will eventually give rise to the myoepithelial cells of the ducts but can also migrate into the inner epithelial layer to give rise to luminal epithelial cells (Hinck and Silberstein, 2005; Richert et al., 2000; Williams and Daniel, 1983). Beneath the cap cells are multiple layers of epithelial cells which proliferate to help drive ductal elongation (Hinck and Silberstein, 2005; Richert et al., 2000). As the TEBs progress through the fat pad, the innermost layer of epithelial cells undergo apoptosis to produce a hollowed out lumen characteristic of the mammary ductal structure (Hinck and Silberstein, 2005; Humphreys et al., 1996; Richert et al., 2000). Along the trailing edge of the TEBs, cells differentiate, and myoepithelial cells help to produce the basement membrane known to surround the ductal structures (Hinck and Silberstein, 2005; Richert et al., 2000; Williams and Daniel, 1983). In addition to driving ductal elongation, TEBs are also capable of bifurcating to produce additional branches on the ductal tree (Hinck and Silberstein, 2005; Richert et al., 2000). This process produces the complex ductal structure characteristic of the mature mammary gland. The TEBs guide and direct elongation of the ductal network through the fat pad; when they reach connective tissue that has been generated by another epithelial structure, or once the edge of the fat pad is detected, TEBs regress and terminal ducts are generated (Hinck and Silberstein, 2005; Richert et al., 2000; Sternlicht, 2006). The filling of the fat pad signals the end of this phase of development, which is usually completed between 10 and 12 weeks of age (Richert et al., 2000; Sternlicht, 2006). Cyclic secretion of hormones during the estrous cycle, such as progesterone, continues to stimulate lateral side branching and alveolar buds during post-pubertal development

(Briskin and O'Malley, 2010; Richert et al., 2000; Robinson et al., 1995). The mammary gland will remain in this state until the next stage of development, pregnancy, occurs.

Pregnancy and Lactation

The mammary gland exists in a highly dynamic state, ready to respond to changes in hormone stimulation that occur with the onset of pregnancy (Oakes et al., 2006; Richert et al., 2000). This stage of mammary development is characterized by an initial burst in proliferation, followed by functional differentiation to generate the functional milk producing units of the mammary gland, the alveoli (Anderson et al., 2007; Oakes et al., 2006; Richert et al., 2000; Sternlicht, 2006). The initial stage of pregnancy consists of rapid expansion of the ductal network leading to increased side branching and development of alveolar buds (Briskin, 2002; Oakes et al., 2006; Richert et al., 2000). The steroid hormone progesterone is responsible for inducing proliferation that leads to increased side branching as well as for inducing the formation of alveoli (Briskin, 2002; Briskin and O'Malley, 2010). Mice lacking the progesterone receptor show significant defects in pregnancy induced side branching as well as lobuloalveolar development (Briskin et al., 1998; Humphreys et al., 1997). As pregnancy progresses, the epithelial to adipocyte ratio increases and the number of lipid droplets is greatly diminished allowing for expansion of the epithelial population to generate the functional units of the gland, the alveoli (Anderson et al., 2007; Oakes et al., 2006; Richert et al., 2000). While the early stages of pregnancy are characterized by proliferation, at mid-pregnancy the gland shifts to a state predominated by differentiation. While progesterone plays a critical role in side branching, the hormone prolactin plays a key role in differentiation and milk production through activation of the Jak2-Stat5 pathway (Anderson et al., 2007; Briskin, 2002; Briskin et al., 1999; Briskin and O'Malley, 2010; Gouilleux et al., 1994; Ormandy et al., 1997). Mice with loss of the prolactin receptor in a gene knockout model display normal outgrowth and side branching, however, show defects in differentiation and production of alveoli (Ormandy et al., 1997). The alveolar buds

begin to progressively cleave and differentiate, generating individual alveoli that will acquire the capacity to produce and secrete milk proteins (Anderson et al., 2007; Oakes et al., 2006; Richert et al., 2000). Alveoli are composed of an inner layer of alveolar cells which line the hollow cavity and are capable of secreting milk proteins (Anderson et al., 2007; Oakes et al., 2006; Richert et al., 2000). Surrounding the alveolar cells is a discontinuous single cell layer of myoepithelial cells which allow the inner alveolar cells to make contacts with the basement membrane which is required for full differentiation to occur (Adams and Watt, 1993; Howlett and Bissell, 1993; Richert et al., 2000). While the alveolar cells are responsible for milk production, the myoepithelial cells are responsible for contracting to push the milk out of the alveoli into the ducts (Richert et al., 2000). At the end of pregnancy and throughout lactation, the gland is filled entirely with alveoli, and continues to produce and secrete milk proteins until the suckling stimulus is removed. The gland then reverts back to its post-pubertal state.

Involution

During involution, remodelling of the gland reverts the gland back to its pre-pregnancy state with the removal of alveolar cells and the reappearance of adipocytes (Richert et al., 2000; Watson, 2006). This stage of development is characterized by apoptosis and can be divided into two distinct phases (Richert et al., 2000; Watson, 2006). The first phase is initially reversible and is characterized by flattening and shedding of the alveolar cells into the lumen and activation of apoptotic pathways (Li et al., 1997; Richert et al., 2000; Watson, 2006). During this 48 hour stage of development, no remodeling of the gland occurs; however at the onset of the second phase of development while apoptosis is still occurring, remodelling of the gland begins to occur and this process is now irreversible (Richert et al., 2000; Watson, 2006). The peak of apoptosis occurs at approximately day 4 of involution when alveolar cells are detached from the alveolar structure and have undergone programmed cell death (Quarrie et al., 1995; Richert et al., 2000). These cells are cleared away by surrounding epithelial cells or macrophages that have invaded the area

(Fadok, 1999; Richert et al., 2000). By day 4, the alveoli have collapsed, and are being cleared away. At the same time adipocytes begin to refill to restore the original ratio of epithelial cells to adipocytes that was altered during pregnancy and lactation (Richert et al., 2000; Watson, 2006). Matrix metalloproteinases play a key role in the remodelling process by breaking down the extracellular matrix to allow for detachment of the cells serving to trigger the apoptotic response required for this stage of development (Green and Lund, 2005; Richert et al., 2000; Watson, 2006). By day 6 of involution, the alveoli have collapsed and the focus shifts to remodelling the epithelium and stroma back to its pre-pregnant state (Richert et al., 2000; Strange et al., 1992). Although massive remodelling of the gland needs to occur and apoptosis is extensive, systemic hormones act as survival signals for the extracellular matrix and basement membrane structures ensuring that the integrity of the gland is not fully disrupted (Li et al., 1997; Richert et al., 2000; Watson, 2006). The entire gland is fully remodelled by day 21 and resembles its pre-pregnant state; however it is known that the post-pregnant gland appears to be more differentiated when compared to a nulliparous gland and may retain some alveoli that were generated during pregnancy and lactation (Richert et al., 2000).

The mammary gland possesses the unique ability to undergo cyclic development throughout life, and can completely remodel and regenerate itself after involution. This implies the existence of stem or progenitor cell populations within the mammary gland that have the capacity to reconstitute the various cell types within the gland.

Mammary Cell Populations and Hierarchy

The mammary gland retains a tremendous capacity for regeneration throughout the duration of development due to populations of stem and progenitor cells that harness the potential to reconstitute the gland during stages of remodelling. The entire mammary gland can be reconstituted from the implantation of tissue fragments taken from any portion of the developed mammary gland (Deome et al., 1959). Further work using flow cytometry analysis to isolate

specific cell populations within the mammary gland demonstrated that the mammary gland can be reconstituted in its entirety from the implantation of one stem cell into the cleared fat pad (Kordon and Smith, 1998; Shackleton et al., 2006; Stingl et al., 2006). The stem cell population known to have the ability to reconstitute a functional murine gland can be identified by the cell surface markers CD49^{hi}CD29^{hi}CD24^{+/med}Sca1^{low} (Shackleton et al., 2006; Shehata et al., 2012; Sleeman et al., 2007; Stingl et al., 2006). The stem cell population can undergo symmetric division to replenish itself or asymmetric division to generate an identical daughter cell and a more committed progenitor cell (Visvader and Lindeman, 2006; Visvader and Stingl, 2014). This balance between symmetric and asymmetric division helps to maintain the correct number of cells within the gland and allows for the massive expansion of epithelial cells seen during puberty and pregnancy, as well as aids in remodelling of the gland during involution (Visvader and Lindeman, 2006; Visvader and Stingl, 2014). The mammary gland is thought to possess a hierarchy of cells which arise from a common multipotent fetal mammary stem cell (Makarem et al., 2013; Spike et al., 2012; Visvader and Stingl, 2014). The stem cell compartment in the mammary gland is not a homogenous one, instead being comprised of both long and short term repopulating cells, with the short term repopulating cells potentially playing a role in the transient but dramatic increase in cell numbers associated with pregnancy (Asselin-Labat et al., 2010; Visvader and Lindeman, 2006; Visvader and Stingl, 2014). It is also thought that there may be a population of basal and luminal stem cells that give rise to the progenitor cell populations, but further investigation is required (Visvader and Lindeman, 2006; Visvader and Stingl, 2014). The number and type of progenitors that exists within the mammary gland is also controversial; however, it is known that progenitors of both the luminal and myoepithelial lineage exist (Visvader and Lindeman, 2006; Visvader and Stingl, 2014). Myoepithelial progenitors give rise to mature myoepithelial cells. The myoepithelial cells constitute the basal layer of ducts and alveoli. During puberty, myoepithelial cells help to produce the basement membrane which surrounds the structures of the gland; during pregnancy, these contractile cells respond to hormone stimulation to help expel

milk from the alveoli into the ducts (Richert et al., 2000; Visvader and Lindeman, 2006; Visvader and Stingl, 2014). Myoepithelial cells can be identified and extracted from the mammary cell population based on surface marker expression of $CD29^{hi}CD49f^{hi}CD24^{+}EpCAM^{lo/med}$ (Visvader and Lindeman, 2006; Visvader and Stingl, 2014). In addition to myoepithelial cells, the gland is also composed of cells of a luminal lineage which can be isolated based on the cell surface expression of $CD49f^{lo}CD29^{lo}CD24^{+}CD14^{-}EpCAM^{hi}c-kit^{-}Sca1^{+}CD61^{-}CD49b^{-}$ and mature ductal and alveolar cells can be isolated based on $CD49f^{lo}CD29^{lo}CD24^{+}CD14^{-}EpCAM^{hi}c-kit^{-}Sca1^{+}CD61^{-}CD49b^{-}$ and $CD49f^{lo}CD29^{lo}CD24^{+}CD14^{-}EpCAM^{hi}c-kit^{-}Sca1^{low}CD61^{-}$ respectively (Shehata et al., 2012; Sleeman et al., 2007; Visvader and Lindeman, 2006; Visvader and Stingl, 2014). Ductal epithelial cells line the lumen of the ducts, while alveolar cells line the inside of the alveoli and are capable of producing and secreting milk proteins during pregnancy. The hierarchy may not be as straightforward as it seems. Luminal progenitors implanted into a cleared fat pad can reconstitute the gland suggesting that luminal progenitors may retain a certain degree of plasticity, and may have the potential to revert back to a more stem like state (Visvader and Stingl, 2014). Injecting this population with certain basement membrane substrates may enhance this phenotype, thus demonstrating the importance of the microenvironment on mammary cell status (Shehata et al., 2012; Sleeman et al., 2007; Vaillant et al., 2011; Visvader and Stingl, 2014). Additionally, a population of parity-induced mammary epithelial cells was identified (Chang et al., 2014; Visvader and Stingl, 2014; Wagner et al., 2002). This population of cells is located within the luminal cell layer of the ducts and arises during pregnancy (Chang et al., 2014; Visvader and Stingl, 2014; Wagner et al., 2002). They can survive the process of involution, and can continue to reside within the ducts, lying dormant until a subsequent round of pregnancy to give rise to alveoli (Chang et al., 2014; Visvader and Stingl, 2014; Wagner et al., 2002). Although much remains to be learned about the hierarchy of cells within the gland, these cells demonstrate a remarkable capacity for self-renewal and contribute to regenerative processes that allow the

mammary gland to exist in a highly dynamic state, perpetuating multiple rounds of proliferation, differentiation and self-renewal.

Breast Cancer: Incidence, Susceptibility and Subtypes

Breast cancer remains the leading cancer diagnosis in women with 1 in 9 Canadian women expected to develop breast cancer in their lifetime (Canadian Cancer Society, 2014). Despite recent improvements in screening procedures and treatment options, 1 in 30 women will ultimately succumb to the disease making it the second most common cause of cancer related deaths in women (Canadian Cancer Society, 2014). A number of factors can contribute to a woman's risk of developing breast cancer. For instance, it is known that late onset of menstruation, early age at first full term pregnancy, breast feeding and early onset of menopause can all help to decrease the risk of developing breast cancer (2002; Byers et al., 1985; Hsieh et al., 1990; Kelsey et al., 1993; MacMahon et al., 1970; Russo et al., 2005). This is presumably because these events decrease a woman's exposure to cycling hormones. Additionally, the cellular changes that occur during pregnancy and lactation result in a more differentiated population of cells which may be less susceptible to transformation events that would ultimately lead to the development of breast cancer (Britt et al., 2007). In contrast, puberty represents a period of development characterized by rapid proliferation and represents a period of increased susceptibility when exposed to harmful stimuli such as ionizing radiation (Preston et al., 2002). Irradiated adult mice were less susceptible to the development of aggressive estrogen receptor negative (ER-) tumours while juvenile mice that were irradiated developed tumours at a much higher frequency, presumably due to an expansion in the mammary stem cell population (Tang et al., 2014). Thus, environmental factors and lifestyle can contribute to a woman's susceptibility of developing breast cancer by potentially altering the population of cells that reside within the mammary gland.

Complicating treatment of this disease are the various known subtypes of breast cancer. At least five major subtypes of breast cancer have been identified and distinct cell types are thought to serve as the cell of origin for each (Perou et al., 2000; Sorlie et al., 2001). Claudin-low breast cancers are thought to arise from the mammary stem cells that sit at the top of the cellular hierarchy within the mammary gland based on a similar gene expression profile (Prat et al., 2010). Basal-like breast cancer is associated with a poor clinical outcome due in part to its common status as a triple negative breast cancer, meaning it lacks estrogen, progesterone and Her2 receptors (Liedtke et al., 2008; Rakha et al., 2008). Carriers for the BRCA1 mutation have an increased tendency to develop breast cancer of this subtype, and while the cells display a basal like phenotype, the cell of origin has been demonstrated to be the luminal progenitor (Lim et al., 2009; Turner and Reis-Filho, 2006). The cell of origin for the remaining subtypes, luminal A, luminal B and Her2-positive, have not been conclusively demonstrated. There is some evidence to suggest that luminal A may arise from a mature luminal cell while luminal B and Her2-positive may arise from cells higher up the cell hierarchy as the cell transitions from luminal progenitor to mature luminal cell (Visvader and Stingl, 2014). A complete understanding of the populations and cycling dynamics of cells within the mammary gland must be fully understood in order to fully elucidate the cell of origin for all breast cancer subtypes and better target and treat the disease.

Cell Cycle Regulators and the Mammary Gland

The mammary gland exists in a highly dynamic state, characterized by cyclic stages of development requiring cells to be able to exert tight control over proliferation, differentiation and apoptosis. Misregulation at any stage of development could lead to aberrant growth and ultimately tumour initiation. Cell cycle regulators play a key role in regulating each stage of development and transgenic model systems have elucidated and highlighted the importance of tight control of the cell cycle during mammary gland development (Hennighausen and Robinson,

2001). Knockout studies in mice have demonstrated the importance of cyclins and CDKs in regulating both normal development and promoting tumorigenesis. Ablation of CDK2 leads to decreased branching and proliferation during puberty, indicating a requirement for this CDK in pubertal development (Ray et al., 2011). Study of the role of CDK2 in other stages of mammary development has proven difficult given that the CDK2 null mouse is sterile and thus the female is unable to go through the stages of pregnancy, lactation and involution (Berthet et al., 2003). It was additionally shown through crosses with the MMTV-neu mouse model, which drives expression of the transgene specifically within the mammary gland, that CDK2 is required for ErbB2 induced tumorigenesis (Ray et al., 2011). Ablation of CDK2 resulted in a significant decrease in tumour incidence as well as an increase in tumour latency (Ray et al., 2011). Similarly, loss of Cyclin D1-CDK activity also exerted a protective effect from MMTV-neu induced mammary tumours (Landis et al., 2006). Although loss of Cyclin D1-CDK kinase activity proved to be detrimental for tumour development, it did not have any significant effects on mammary development (Landis et al., 2006). Complete loss of Cyclin D1 causes severe defects in pregnancy and lactation, with mothers unable to nurse their pups due to a reduction in acinar development during pregnancy (Fantl et al., 1995). The reduction in acinar development may be in part due to significant defects in the ability of the gland to undergo the proliferative changes necessary for pregnancy and lactation (Sicinski et al., 1995). To further validate the key role Cyclin D1 may play in regulating proliferation within the mammary gland mice were engineered to overexpress Cyclin D1 specifically in the mammary gland. MMTV-Cyclin D1 mice display increased rates of proliferation with increased lobuloalveolar development and ductal side branching (Wang et al., 1994). MMTV-Cyclin D1 mice also develop mammary adenocarcinomas at a significantly higher rate than control littermates, indicating that Cyclin D1 plays an important role in regulating proliferative events in the mammary gland and misregulation of these processes could lead to tumorigenesis (Wang et al., 1994). Thus, data from these models further highlight

the importance of appropriate control of the cell cycle in mammary development and tumorigenesis.

The transcription factor c-Myc is a master regulator of many cellular processes such as proliferation and apoptosis and is elevated in a large number of breast cancer cases (Dang, 1999; Escot et al., 1986). The MMTV-Myc mouse was developed to study the effects of aberrant Myc expression in the mammary gland. Mice containing the transgene displayed significantly more mammary adenocarcinomas and this was associated with multiple rounds of pregnancy (Stewart et al., 1984). MMTV-Myc mice are unable to lactate due to tumour onset and burden. Thus, an inducible overexpression model was generated to allow expression of c-Myc to be turned on in the mammary gland under the control of doxycycline during specific periods of development. Utilization of this model identified a 72 hour period of time during pregnancy that was responsible for the lactation defect observed in these mice (Blakely et al., 2005). Aberrant expression of c-Myc from day 12.5 to 15.5 of pregnancy induces precocious development of the gland leading to accelerated differentiation, and early onset of lactation (Blakely et al., 2005). Since the gland prematurely lactates, milk stasis triggers involution prior to the birth of the pups, leaving the mother unable to nurse her young (Blakely et al., 2005). Thus c-Myc contributes to the control of many developmental events that occur during mammary gland development.

Positive cell cycle regulation is crucial to the proper development of the mammary gland; however, tumour suppressors must be activated during specific times of development and in cases of aberrant growth to prevent the onset of tumorigenesis. The tumour suppressor p53 is mutated in approximately half of all human breast cancers. Patients with germline mutations in p53 are predisposed to developing cancer, with breast cancer being one of the leading forms (Akashi and Koeffler, 1998; Coles et al., 1992). Deletion of p53 in mice leads to significant tumorigenesis, with mice succumbing to tumour formation between 4 and 6 months of age, and lymphomas being the primary cause of death (Jacks et al., 1994). Due to early mortality from lymphomas, breast tumour development is not seen at high levels in these mice. To study the effects of loss of

p53 on tumour development, p53 null epithelium was transplanted into the cleared fat pad of wild-type hosts and mice were treated with hormone stimulation or carcinogens (Jerry et al., 2000). Mice lacking p53 developed significantly more tumours highlighting the importance of this tumour suppressor on preventing tumour initiation (Jerry et al., 2000). Developmentally, p53 has also been shown to regulate symmetric versus asymmetric division of the mammary stem cell population, with loss of p53 promoting symmetric division (Cicalese et al., 2009). Therefore, loss of p53 could promote expansion of a population of tumour initiating cells promoting the initiation and progression of breast cancer. Tight control of p53 levels and activity is required to allow for proper function and to prevent the onset of tumorigenesis.

Thus, cell cycle regulators play a critical role in regulating the developmental decisions of the mammary gland and help to promote proper growth and development. Disruption of these pathways can lead to aberrant growth and onset of tumorigenesis further highlighting the importance of fully elucidating the mechanisms regulating growth and development of the mammary gland.

Comparison of Murine and Human Mammary Gland Development

Development of the murine and human mammary gland is regulated by the same developmental processes but the gross morphological structure contains important differences. The mammary fat pad of the mouse contains far more adipocytes and less fibrous material than that found in the human breast indicating that while the cellular hierarchy between species is highly similar, they may require different environmental stimuli for proper development (Hovey et al., 1999; Visvader, 2009). In addition to differences in the fat pad, gross morphological differences also exist between mouse and human. In humans, the network of ducts is highly segmented and ducts terminate into the functional units of the gland the terminal ductal lobular units (TDLU) (Cardiff and Wellings, 1999; Visvader, 2009). In contrast, the ductal network of the murine mammary gland is not segmented and grows in a more linear fashion (Cardiff and

Wellings, 1999). Mice lack TDLUs but instead possess lobuloalveolar units which form during each estrous cycle (Cardiff and Wellings, 1999; Visvader, 2009). Despite these differences, the cellular composition of the structures remains the same and they are able to carry out the same functions.

While the cellular hierarchy is similar, differences do exist in the expression profiles of surface markers used to identify key lineages within the mammary cell hierarchy. For instance, CD24 is used to identify cells strictly of a luminal lineage in humans but in mice, is used as a pan-epithelial marker (Shackleton et al., 2006; Stingl et al., 2006; Visvader, 2009). In humans, increased activity of the enzyme aldehyde dehydrogenase (ALDH) can be used to identify populations of cells with increased stem/progenitor properties but is not used to identify stem/progenitor populations of the mouse mammary gland (Ginestier et al., 2007; Visvader, 2009). Tumourigenesis in transgenic mouse models can recapitulate phenotypes seen in human breast cancer samples indicating that the proposed cell of origin remains the same (Cardiff and Wellings, 1999). Thus, while differences may exist in gross morphological structure between the murine and human mammary gland, the cellular composition remains unchanged. Both normal and abnormal development of the gland are controlled by the same driving factors, making the murine mammary gland an ideal study system for comparison of the events occurring in the human breast.

Spy1, Mammary Gland Development and Tumourigenesis

Levels of Spy1 protein were analyzed during mammary gland development to determine if expression changed depending on the stage of development. Spy1 protein levels were found to be high during proliferative phases of development such as during puberty and early pregnancy, and were drastically downregulated during late pregnancy and lactation, a period of development characterized by differentiation (Golipour et al., 2008). Interestingly, levels of Spy1 were elevated at the onset of involution, a developmental stage characterized by apoptosis (Golipour et

al., 2008). Downregulation of Spy1 levels during differentiation was confirmed using the HC11 model system, a mammary epithelial cell system that responds to the same differentiation stimuli they would be exposed to *in vivo* and are capable of forming spheroid structures which mimic the morphology seen *in vivo* (Ball et al., 1988). A differentiation time course also showed a decrease in Spy1 levels at the onset of differentiation. Overexpression of Spy1 during differentiation of HC11 cells accelerated the expression of β -casein, a milk protein commonly used as an indicator of differentiation during mammary pregnancy and lactation (Golipour et al., 2008). Additionally, cells with elevated levels of Spy1 displayed disorganized piles of cells and were unable to form the organized spherical structures typically formed by mammary epithelial cells (Golipour et al., 2008). *In vivo* overexpression of Spy1 via mammary fat pad transplantation of Spy1 expressing HC11 cells caused increased ductal branching and PCNA staining, a marker of proliferation (Golipour et al., 2008). Additionally, increased rates of tumorigenesis were found with increased levels of Spy1 (Golipour et al., 2008); however, the HC11 cells utilized contain a mutated p53, therefore one can only conclude that Spy1 may accelerate or help to promote tumour initiation (Golipour et al., 2008). Using the non-degradable mutant of Spy1, Spy1-TST, it was demonstrated that losing the ability to degrade Spy1 leads to increased onset of tumorigenesis and an increased tumour volume as compared to wild-type Spy1, indicating that losing the ability to degrade Spy1 at the G2/M checkpoint may contribute to the onset of tumorigenesis (Al Sorkhy et al.). To further highlight the importance of Spy1 in breast cancer initiation and progression, analysis of Spy1 levels in various forms of human breast cancer revealed significantly higher levels of Spy1 in all forms analyzed over that of pair matched adjacent or normal tissue (Al Sorkhy et al.). Spy1 levels were also found to be elevated in more aggressive lines of human breast cancer cells and Spy1 was found to be one of the fifty most upregulated genes in invasive ductal carcinoma of the breast (Al Sorkhy et al.; Zucchi et al., 2004). Given the tight regulation of Spy1 protein levels during mammary gland development, the ability to accelerate mammary tumorigenesis *in vivo*, and the high levels of Spy1 noted in breast cancer

samples, it appears that *Spy1* plays a key role in regulating normal mammary gland development. Misregulation of *Spy1* could lead to the onset of tumorigenesis, highlighting the importance of further elucidating the role *Spy1* plays during mammary gland development.

Liver

The liver is a vital organ comprising 2 to 5% of a person's total body weight and plays a wide variety of roles ranging from protein secretion, detoxification and cholesterol metabolism among others (Bisteau et al., 2014; Si-Tayeb et al., 2010). The large number of functions the liver performs means it is essential for survival, thus loss of function resulting from chronic injury or hepatocellular carcinoma is devastating. Those diagnosed with primary liver cancer face a survival rate of only 5 years and death due to liver cancer remains the second most common cause of cancer related death worldwide (Canadian Cancer Society, 2014; World Health Organization, 2014). In addition to the devastating effects of hepatocellular carcinoma, non-alcoholic fatty liver disease (NAFLD) and non-alcoholic steatohepatitis (NASH), diseases of the liver characterized by increased fat, inflammation and damage have been on the rise in recent years (Dowman et al., 2010; Takahashi et al., 2012; The National Digestive Diseases Information Clearinghouse, 2014). To better treat these debilitating, and sometimes life threatening conditions, a more thorough understanding of the molecular mechanisms regulating growth and development are required.

Murine Liver Development

The majority of liver development takes place embryonically, with specification of the liver starting at approximately embryonic day 9 (Kung et al., 2010; Si-Tayeb et al., 2010; Zorn, 2008). The liver arises in the ventral foregut from the lateral domains of the endoderm (Tremblay and Zaret, 2005). During foregut closure, the medial and lateral domains become fused; the endoderm becomes specified to a hepatic fate due to FGF signaling from the cardiac mesoderm and BMP signaling arising from the septum transverse mesenchyme (Gualdi et al., 1996;

Houssaint, 1980; Rossi et al., 2001; Serls et al., 2005; Si-Tayeb et al., 2010; Zorn, 2008). Wnt signaling is crucial for proper differentiation of the specified tissue generating the hepatoblasts, or bipotential cells within the foregut (Monga et al., 2003; Suksaweang et al., 2004; Tan et al., 2008; Zorn, 2008). Wnt signaling also promotes the formation of the liver bud at approximately day 9.5 when the hepatoblasts form a columnar shape and invade into the septum transversum mesenchyme (Si-Tayeb et al., 2010; Zorn, 2008). Once the liver bud has been formed, the hepatoblasts continue to proliferate, and differentiation commences at embryonic day 13, continuing even after birth until all cells have become mature differentiated cells (Kung et al., 2010; Si-Tayeb et al., 2010; Zhao and Duncan, 2005). During this period of differentiation, the liver also separates into separate lobes, and sinusoids and bile canaliculi appear (Si-Tayeb et al., 2010). Hepatoblasts in contact with the portal vein will differentiate to form a bi-layer of biliary precursors that will ultimately give rise to cholangiocytes which are characterized by expression of cytokeratin 19 (CK19) (Germain et al., 1988; Lemaigre, 2003; Zorn, 2008). Hepatoblasts not in contact with the portal vein will give rise to hepatocytes, characterized by expression of α -fetoprotein (AFP) during fetal development and albumin (Alb) (Germain et al., 1988; Shiojiri, 1981; Zorn, 2008). Hepatocytes constitute approximately 70% of the liver and thus perform the vast majority of all liver functions (Blouin et al., 1977; Si-Tayeb et al., 2010). By embryonic day 17, hepatocytes are arranged in their characteristic morphology arranged into hepatic chords with their apical surface in contact with bile canaliculi (Zorn, 2008). The process of differentiation continues after birth until most of the cells are unipotent and committed to either a mature cholangiocyte or hepatocyte. Thus, the liver remains in a relatively quiescent state throughout life, unless injury to the liver occurs, in which case proliferation can once again be activated to reconstitute the liver tissues; additionally a reservoir of adult liver stem cells known as oval cells can be stimulated to divide and differentiate into the various cells that constitute the liver.

Cell Cycle, Ploidy and Regeneration in the Liver

Hepatocytes of the liver remain in a state of quiescence throughout much of adult life; however, it retains a remarkable capacity to regenerate itself in the event of liver injury. Proliferation and differentiation of hepatocytes continues after birth up until approximately 4 weeks of age, in the case of mice (Celton-Morizur et al., 2009; Viola-Magni, 1972). Until 3 weeks of age, all of the hepatocytes within the liver are diploid (Gentric et al., 2012). At 3 weeks of age when weaning occurs, the hepatocyte population switches from a mostly diploid population to a mostly tetraploid population, with 70% of mouse hepatocytes being tetraploid (Gentric et al., 2012; Severin et al., 1984). The switch in ploidy results from the activation of altered cell division which leads to incomplete cytokinesis. In essence, the cleavage furrow is not formed and the cell does not divide, leading to generation of bi-nucleated tetraploid cells (Gentric et al., 2012). This process is regulated through insulin signaling regulation of the PI3-K/Akt pathway, as inhibition of Akt at this stage of development increased the number of diploid hepatocytes seen in the post-natal liver (Celton-Morizur et al., 2009). Thus, hepatocyte polyploidization is a naturally occurring process which may serve important roles in maintaining the function and integrity of the liver (Gentric et al., 2012). Polyploidy may serve as a protective mechanism for hepatocytes as one of their primary functions is detoxification of harmful substances (Gentric et al., 2012). Having increased DNA content may serve as a back-up in the event of damage or mutation (Gentric et al., 2012). Additionally, polyploidy may also decrease the energy demands on hepatocytes, especially in the case of regeneration when hepatocytes not only need to divide but also maintain liver function during this process (Gentric et al., 2012).

Although hepatocytes rarely divide, in the event of regeneration they are capable of re-entering the cell cycle to regenerate the entire mass of the liver through compensatory growth mechanisms (Fausto and Campbell, 2003). Exit from G_0 is a highly coordinated process composed of priming of the hepatocytes to respond to growth factor signaling and coordination of DNA replication and cellular division (Bisteau et al., 2014; Ehrenfried et al., 1997; Fausto and

Campbell, 2003). Tumour necrosis factor signaling primes hepatocytes to exit from quiescence and enables them to respond to growth factor signaling such as hepatocyte growth factor (HGF) and epidermal growth factor (EGF) (Fausto and Campbell, 2003; Webber et al., 1998; Webber et al., 1994). Once hepatocytes are capable of responding to mitogenic stimuli, Cyclin D1 levels are upregulated, leading to activation of CDK4-Cyclin D complexes (Bisteau et al., 2014; Ehrenfried et al., 1997). This triggers activation of the cell cycle which proceeds in the usual manner with activation of the CDK2-Cyclin E complex followed by CDK2-Cyclin A and finally CDK1-Cyclin B (Bisteau et al., 2014; Ehrenfried et al., 1997). Regeneration of the liver occurs with 2 highly synchronized rounds of cellular proliferation, the first peak in DNA synthesis occurring approximately 36 hours after initiation of the process, and the next occurring approximately 60 hours after regeneration commences (Bisteau et al., 2014; Ehrenfried et al., 1997; Fausto and Campbell, 2003; Grisham, 1962). Within a week, the liver mass is restored to its original size (Ehrenfried et al., 1997; Fausto and Campbell, 2003). While hepatocytes may be a differentiated cell type typically held in a state of quiescence, they retain a remarkable capacity for proliferation, highlighting the importance of understanding cell cycle regulation in liver development and regeneration.

Diseases of the Liver: NAFLD and NASH

Non-alcoholic fatty liver disease (NAFLD) and non-alcoholic steatohepatitis (NASH) are conditions characterized by excess fat accumulation in the liver (Dowman et al., 2010; Jou et al., 2008; Takahashi et al., 2012). They differ from each other in that NASH is also characterized by increased inflammation and damage in the liver, representing the more severe disease (Dowman et al., 2010; Jou et al., 2008; Takahashi et al., 2012). Both NAFLD and NASH resemble alcoholic disease but are found in people with little to no alcohol intake (Dowman et al., 2010; Jou et al., 2008; Takahashi et al., 2012). The incidence of fatty liver disease is currently on the rise presumably due to the increased prevalence of obesity and type 2 diabetes (Farrell et al., 2009;

Takahashi et al., 2012). There are currently no specific therapies to treat NAFLD/NASH and its exact causes are still unclear, making it an important area of research.

Accumulation of fat within the liver can occur by a variety of mechanisms such as increased fat synthesis, decreased fat export, decreased fat oxidation or increased fat delivery (Bradbury and Berk, 2004; Dowman et al., 2010; Takahashi et al., 2012). All mechanisms contribute to fat accumulation within the liver, constituting the first hit in development of NAFLD/NASH (Dowman et al., 2010; Takahashi et al., 2012). Fat accumulation within the liver can then activate inflammatory response pathways such as NF κ B, leading to elevated expression of inflammatory cytokines resulting in increased injury to the liver (Cai et al., 2005). The proliferative capacity of mature hepatocytes begins to decline over time as a by-product of the increased inflammatory response and oxidative stress that is a direct result of the increase in free fatty acids (Dowman et al., 2010; Feldstein et al., 2004; Takahashi et al., 2012). Loss of proliferative hepatocytes over time leads to increased amounts of apoptosis, significantly damaging the liver and decreasing its ability to regenerate (Dowman et al., 2010; Jou et al., 2008; Roskams et al., 2003). Additionally, fibrosis of the liver becomes apparent as the disease progresses (Dowman et al., 2010; Jou et al., 2008). Fibrosis results in cases of severe injury when the liver's response is to deposit fibrous material, such as collagen, to repair the damage (Bataller and Brenner, 2005; Friedman et al., 1985). In severe cases, the architecture of the liver is compromised after decreases in blood flow and liver function lead to the development of cirrhosis of the liver (Bataller and Brenner, 2005). Once the disease has progressed to this stage, the risk of liver failure and hepatocellular carcinoma (HCC) rises greatly (Figure 4) (Bataller and Brenner, 2005; Dowman et al., 2010).

NASH is characterized by increased inflammation, fibrosis and increased rates of apoptosis (Dowman et al., 2010; Takahashi et al., 2012). Given these characteristic changes, expression of apoptotic regulators may be altered in this disease. Expression of p53 is upregulated in fatty liver diseases with increased levels correlating with increased degrees of inflammation

and fibrosis (Kodama et al., 2011; Panasiuk et al., 2006; Yahagi et al., 2004). Additionally, the downstream target p21 is also upregulated indicating increased activity of p53 (Farrell et al., 2009). p53 may be involved with progression of the disease by activating apoptotic pathways leading to increased hepatocyte death (Farrell et al., 2009; Panasiuk et al., 2006). Levels of the anti-apoptotic protein Bcl-XL were found to be downregulated in response to p53 expression in cases of fatty liver disease indicating that elevation and activation of p53 may contribute to further inflammation and injury to the liver thus playing a key role in progression of this disease (Farrell et al., 2009; Panasiuk et al., 2006).

Although the molecular mechanisms that cause NAFLD and NASH are still poorly understood, these findings highlight the importance of dissecting the molecular mechanisms that regulate damage responses and apoptotic pathways to treat and prevent the progression of this disease.

Hepatocellular Carcinoma

Hepatocellular carcinoma (HCC) is one of the leading diagnoses of cancer worldwide and is the second leading cause of death due to cancer (Canadian Cancer Society, 2014). Diagnosis with HCC has a very poor prognosis with a 5 year survival rate of only 20%. Incidences of HCC are on the rise possibly due to an increase in the incidence of obesity, which is a known risk factor for the development of HCC (Kant and Hull, 2011; Venook et al., 2010). Infection with hepatitis B or C and chronic alcohol abuse can all lead to cirrhosis of the liver, which can progress to HCC over time (Fattovich et al., 2004). Additionally, rates of HCC are higher in males than females. Although the exact cause of this predisposition is unknown, it is hypothesized that an increased inflammatory response specifically in males may lead to increased inflammation and therefore, increased incidences of HCC (Naugler et al., 2007). Deregulation of the cell cycle is also known to contribute to the onset of HCC (Aravalli et al., 2008; Pascale et al., 2002). Cyclin D1 amplification is seen in 11 to 20% of HCC cases (Bisteau et al., 2014; Wang et

al., 2013). Overexpression of Cyclin D leads to aneuploidy in hepatocytes, which can persist and ultimately contribute to HCC initiation and overexpression of Cyclin D alone can initiate HCC although with a long latency (Deane et al., 2001; Nelsen et al., 2005). Thus it appears that additional genetic alterations are necessary to fully progress to HCC. The CKI p27 is known to inhibit cell cycle re-entry in quiescent hepatocytes, preventing cell cycle entry until required (Albrecht et al., 1998; Ilyin et al., 2003). Loss of p27 leads to acceleration of DNA replication but only promotes tumour formation when livers have been chronically injured (Bisteau et al., 2014; Hayashi et al., 2003; Sun et al., 2007a). Decreased levels of p27 are more often seen in advanced or aggressive stages of disease and correlate with poor patient prognosis, indicating a critical role for p27 in maintaining the quiescent state of hepatocytes (Ito et al., 1999; Matsuda et al., 2013; Tannapfel et al., 2000). The transcription factor c-Myc is also known to contribute to HCC, as mice expressing elevated levels develop tumours after a long latency (Beer et al., 2004; Heindryckx et al., 2009; Thorgeirsson and Santoni-Rugiu, 1996). Additionally, inactivation of Myc results in regression of the tumour and differentiation of tumour cells into hepatocytes and biliary forming cells (Shachaf et al., 2004). Increased expression and activity of Myc may play a key role in initiating tumour onset as well as help to sustain its growth throughout tumour progression. These studies highlight the importance of regulated cell proliferation in preventing the onset of liver tumourigenesis, emphasizing the tight control over proliferation that must be exerted on hepatocytes to prevent oncogenesis.

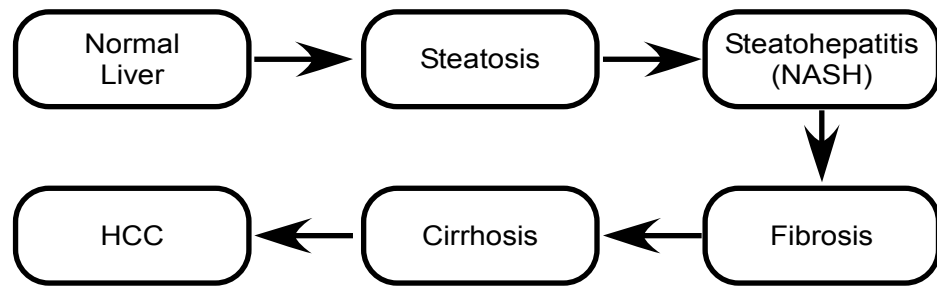


Figure 4: Liver disease progression from simple steatosis to hepatocellular carcinoma (HCC).

Spy1 and the Liver

Cell cycle regulation has proven to play a key role in regulating normal liver development, regenerative processes and tumour initiation and progression. High levels of the cyclin-like protein Spy1 have been found in HCC samples compared to pair matched normal or adjacent tissue and correlate with increased levels of the proliferation marker ki67 (Ke et al., 2009). Additionally, levels of Spy1 were found to correlate with levels of α -fetoprotein, a protein expressed during fetal development of the liver, which is known to be re-expressed in HCC (Ke et al., 2009). Patients with increased levels of Spy1 also correlated with poorer prognosis. Thus Spy1 may play an important role in cell cycle regulation in the liver and may contribute to tumourigenesis in this system (Ke et al., 2009).

The Mouse as a Model Organism

Studies utilizing *in vitro* cell systems and transplantation of cell systems back into an *in vivo* setting have shed great insight on a vast amount of regulatory mechanisms in normal and abnormal tissue development. Although these approaches are valuable, a more realistic setting to study the effects of altered protein expression would provide an even greater depth of knowledge as the multitude of factors that influence and regulate growth and development would be present in their natural state. The mouse represents an ideal model system to study the effects of altered protein expression on either the organism as a whole or through targeted tissue approaches. Humans and mice share approximately 99% of their genes, and have similar numbers of protein coding genes, making the mouse an ideal system of study which can then be translated back to humans (Guenet, 2005). Additionally, the ease of model generation and relatively quick generation time makes the mouse an excellent candidate for the study of growth and development. Furthermore, the genetics and physiology of the mouse are well characterized, enabling detailed analysis of complex phenotypes that may arise from altering gene expression. Mice can be generated through a targeted approach by knocking down or introducing mutations

within a specific gene, or can be generated by introducing foreign DNA, called a transgene, directly into the oocyte. Using either approach will result in a genetically modified animal that can be used to assess phenotypic changes resulting from the alteration or addition of gene expression.

Transgenic Model Systems

Each year hundreds of results are published which utilize transgenic model systems, highlighting the importance of this approach in the study of development and oncogenesis. Development of this approach began in the 1970s when experiments were conducted to generate chimeric mice either through direct embryo aggregation or blastocyst injection (Brinster, 1974). It wasn't until 1980 that the first successful transgenic mouse was generated through pronuclear injections (Gordon et al., 1980). Although this mouse did not express the transgene because the sequence had become rearranged, it was the first demonstration of the pronuclear injection technique which is the most successful, widely used technique today (Gordon et al., 1980). Just one year later, the first transgenic mice capable of transgene expression were produced, and in 1982, the first mouse with a visible phenotype due to transgene expression was created (Brinster et al., 1981; Palmiter et al., 1982). These seminal discoveries paved the way for researchers as transgenic mouse models have become a staple of many studies involving development, cancer initiation and progression and in the study of new drugs developed to target disease. Pronuclear injection of a segment of double stranded DNA is the most widely used approach in the generation of transgenic mouse models (Haruyama et al., 2009). In this approach, the gene of interest is cloned into an expression vector containing a promoter that can drive expression of the transgene in a tissue and sometimes, temporal specific manner (Hanahan et al., 2007; Haruyama et al., 2009). The expression cassette must also contain an enhancer region and poly adenylation sequence to ensure proper RNA transcription and translation (Haruyama et al., 2009). The generated transgenic vector can be tested for expression in an *in vitro* setting before being

digested to isolate the transgene fragment. The transgene is injected into a fertilized oocyte during the pronuclear period (Brinster et al., 1985; Si-Hoe et al., 2001). This is the period immediately following fertilization when the male and female pronuclei are both still visible (Brinster et al., 1985; Si-Hoe et al., 2001). This ensures that the transgene integrates into the chromosome prior to the first doubling of genetic material that occurs before the first cleavage event (Brinster et al., 1985; Si-Hoe et al., 2001). If integration occurs after this point, a mosaic animal will be generated in which many of the cells may not express the transgene (Brinster et al., 1985; Si-Hoe et al., 2001). Integration of the transgene is a random event, thus it is highly unlikely that two founder mice, mice resulting from pronuclear injection, will contain the same integration event (Bishop and Smith, 1989). Additionally, it is difficult to determine how many copies of the transgene integrate although many times, the transgene will integrate in a linear array called a concatamer (Bishop and Smith, 1989). Although the number of copies of a transgene that integrate into the genome cannot be controlled, transgene expression does not correlate with the number of transgene copies inserted. Since integration is a random event, it is important to have multiple founders to assess the phenotype of transgene expression in the early stages of analysis to rule out the possibility of insertional mutagenesis (Woychik et al., 1985). Insertional mutagenesis occurs when the phenotype seen is not due to the transgene itself, but rather that the transgene has inserted within a functional endogenous gene and interrupted the function of this gene (Woychik et al., 1985). Thus, it is imperative that multiple founders are analyzed to ensure that the phenotype observed is due to the transgene itself, and not modification of endogenous gene expression due to transgene insertion site. Once generated, transgenic mice can be utilized for a wide range of applications making them an attractive model system for research.

From the date of injection of the transgene, generation and identification of transgenic mice takes a minimum of 7 weeks, making it a relatively quick process. Using this approach, investigators can generate mice in which a gene of interest is overexpressed in its endogenous form and can introduce transgenes containing mutations or modification of their gene of interest.

Recent advances allow the production of transgenic mice in which knockdown of a gene can be achieved through the use of shRNA (Premisrut et al.; Yahagi et al., 2004). Expression of these transgenes, whether overexpression or knockdown, can be constitutive utilizing only the promoter found within the transgene or transgene expression can be inducible through the use of tetracycline transactivator (tTA) or reverse tetracycline transactivator (rtTA) systems (Furth et al., 1994; Gossen and Bujard, 1992; Gossen et al., 1995; Hennighausen et al., 1995; Sun et al., 2007b; Zhu et al., 2002). Both systems require a regulatory unit called a responsive element, and an induction agent to work; this allows the generation of transgenic models in which expression of a transgene can be rapidly shut off or induced enabling the study of transgenes during specified times of development (Furth et al., 1994; Gossen and Bujard, 1992; Gossen et al., 1995; Hennighausen et al., 1995; Sun et al., 2007b; Zhu et al., 2002). In both systems, the TetO promoter is the responsive element that is bound by either tTA or rtTA, both of which are fusion proteins of tetracycline (Furth et al., 1994; Gossen and Bujard, 1992; Gossen et al., 1995; Hennighausen et al., 1995; Sun et al., 2007b; Zhu et al., 2002). Both systems make use of the antibiotic tetracycline or its derivative doxycycline to either repress or induce expression (Furth et al., 1994; Gossen and Bujard, 1992; Gossen et al., 1995; Hennighausen et al., 1995; Sun et al., 2007b; Zhu et al., 2002). The difference lies in how the tTA or rtTA binds the TetO responsive element. The tTA system is referred to as a tet-off system as addition of doxycycline causes a conformational change in tTA leading to dissociation of tTA from the TetO responsive element thereby repressing expression of the transgene (Furth et al., 1994). Thus in the absence of doxycycline, the transgene is expressed in the tTA system (Figure 5A). The rtTA system works in an opposite fashion. In the absence of doxycycline, the rtTA protein cannot bind to the TetO responsive element; however, upon addition of doxycycline, rtTA now binds and induces rapid expression of the transgene (Gossen et al., 1995). Removal of doxycycline leads to dissociation of rtTA from the responsive element and the transgene is no longer expressed (Figure 5 B). Use of either the tet-off or tet-on system allows for tighter control of transgene expression and for rapid

induction or suppression of expression during specified periods of time (Furth et al., 1994; Sun et al., 2007b; Zhu et al., 2002). Additionally, this system can be combined with tissue specific promoters driving expression of tTA or rtTA allowing for both temporal and spatial control of transgene expression (Gunther et al., 2002; Zhang et al., 2010). Thus, transgenic model systems represent a powerful tool in which expression can be controlled both spatially and temporally to study altered gene expression in a natural *in vivo* setting.

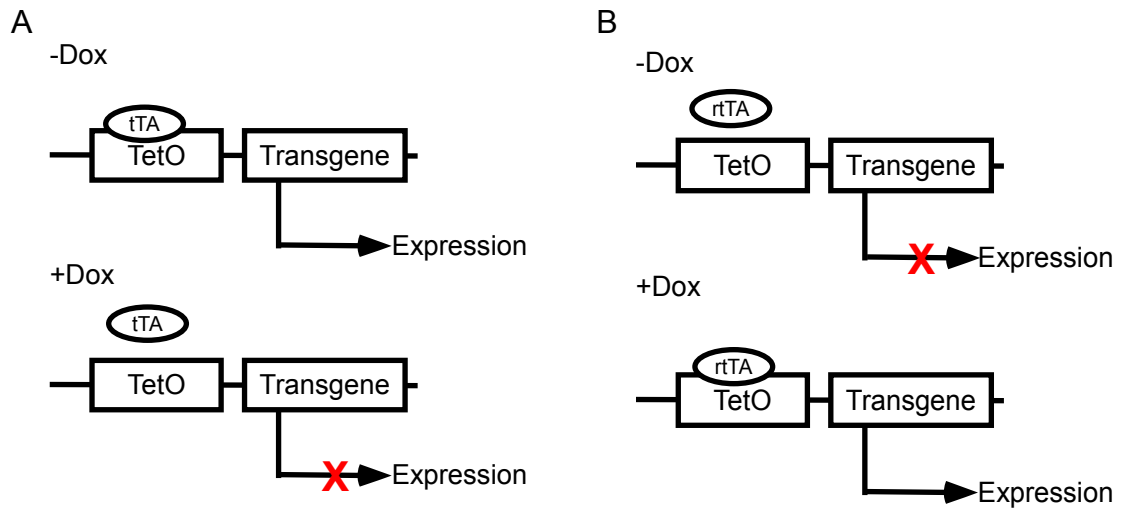


Figure 5: Mechanism of **A)** tet-off and **B)** tet-on systems. In the tet-off system, the presence of doxycycline (Dox) prevents binding of the tetracycline transactivator (tTA) to the Tet operator (TetO) therefore preventing transgene expression. In the tet-on system, doxycycline is required for binding of the reverse tetracycline transactivator (rtTA) to TetO and transgene expression.

Gene Targeted Mice

The 2007 Nobel Prize in Physiology or Medicine was awarded to Mario Capecchi, Oliver Smithies and Martin Evans, all of whom pioneered technology now commonly used for the generation of gene targeted mouse models (Abbott, 2007). Capecchi and Smithies independently discovered that a new section of DNA could be introduced into the genome by flanking the segment with matching regions of DNA from the region to be targeted (Smithies et al., 1985; Thomas and Capecchi, 1986). This early work was conducted in mammalian cell culture where it proved to be highly successful. It wasn't until Evans demonstrated how to isolate embryonic stem (ES) cells from 3.5 day old mouse blastocysts and inject them back into a blastocyst of a different strain that the true potential of this technique could be realized (Evans and Kaufman, 1981). Evans' work demonstrated that injection of ES cells into a recipient blastocyst could incorporate and become established into the germline creating a chimeric mouse (Bradley et al., 1984; Hall et al., 2009). Using ES cells, alterations at the level of the genome could now be introduced directly into ES cells and subsequently be used in blastocyst injections establishing gene targeted mice (Doetschman et al., 1987; Thomas and Capecchi, 1987). This technique takes advantage of the cell's own DNA repair machinery. Although rates of successful recombination are much lower than seen with successful random integration in the generation of transgenic mice, this technique harnesses greater power in its ability to completely ablate gene function and introduce mutations at the level of the genome. This eliminates the possibility of insertional mutagenesis that can be seen with random integration (Hall et al., 2009; Muller, 1999). Gene targeting can be used in a variety of applications to study the effects of altered gene expression. It is commonly used to study the effects of loss of gene function through the direct inactivation of a gene. This can be accomplished directly through the generation of one mouse, or can be accomplished in a conditional fashion such as in the study of genes which can cause embryonic lethality, or to study loss of function during specified times of development (Nagy, 2000; Wagner et al., 1997). In addition to loss of function studies, targeted approaches can also be utilized to introduce

mutations directly into the genome to study the effects of these mutations on development and disease processes, which aid in our understanding of identified mutations in human disease (Hall et al., 2009; Muller, 1999).

While this technique can be utilized in a number of different ways, generation of gene targeted mice follows the same basic approach. Homologous recombination lies at the basis of this system. A segment of linear DNA containing regions of homology, known as homologous arms, on both the 5' and 3' end is electroporated into ES cells typically from a substrain of 129/SV mice (Hall et al., 2009; Muller, 1999). The homologous arms direct recombination to the appropriate location in the genome and allow for introduction of a modified gene segment which lies between the regions of homology. To increase rates of successful recombination, a total of 6 to 14kb of homology is typically required in a targeting vector made up of a one longer arm of homology and one short arm (Deng and Capecchi, 1992; Hasty et al., 1991; Muller, 1999). Since hundreds of cells are electroporated, a method of negative and positive selection is employed to better detect cells which may have undergone proper homologous recombination (Mansour et al., 1988; Muller, 1999). Placed next to one of the homologous arms outside of the regions of homology, is the HSV thymidine kinase gene (TK) (Hall et al., 2009; Muller, 1999). This acts as a negative selection marker, since only random integration events will have the TK cassette (Hall et al., 2009; Muller, 1999). Those cells which have undergone proper homologous recombination will survive when grown in the presence of the antiviral medication gancyclovir, while any cells which have undergone random integration will die in its presence due to inhibition of DNA synthesis by the TK gene (Daher et al., 1990; Hall et al., 2009; Muller, 1999). A neomycin selectable marker is used as a means of positive selection, as cells containing the neo marker will survive when grown in the presence of neomycin (Hall et al., 2009; Mansour et al., 1993; Muller, 1999; Schwartzberg et al., 1989). The neo marker is placed between the arms of homology and thus is part of the modified gene segment that is introduced during homologous recombination (Hall et al., 2009; Muller, 1999). In some cases, the neo marker is introduced into a critical exon,

interrupting expression and consequently generates a loss of function model (Hall et al., 2009; Muller, 1999). In cases of knock in models where mutations are introduced or when conditional models are being generated, care must be taken to ensure the neo marker is inserted into an intronic region that will not interrupt endogenous gene function prior to the gene being knocked out (Hall et al., 2009; Muller, 1999). Additionally, the neo marker is typically inserted in the opposite orientation of the gene of interest to eliminate the possibility that its promoter will influence expression of any downstream genes or to avoid transcription of exons located downstream of the neo marker (Hall et al., 2009; Muller, 1999). Thus, addition of positive and negative selection markers greatly aids in the screening process when searching for cells which have undergone successful homologous recombination.

The modified gene segment between the homologous arms can either introduce a gene mutation via a mutated version of the endogenous gene, completely disrupt gene function by interrupting a critical exon or deleting a segment of the gene, or a conditional approach can be utilized whereby loxP sites are placed flanking a critical exon of the gene (Hall et al., 2009; Muller, 1999; Nagy, 2000). In a complete knockout, the open reading frame of the gene is completely disrupted eliminating function during embryogenesis. At times, this can be deleterious to the growth of the organism leading to embryonic lethality. To circumvent this, conditional approaches can be utilized to shut off gene function at later stages of development (Hall et al., 2009; Muller, 1999; Nagy, 2000). Additionally, conditional approaches offer a further level of spatial and temporal control. Most conditionally targeted mice make use of the Cre/loxP system (Hall et al., 2009; Muller, 1999; Nagy, 2000; Sauer, 1998; Wagner et al., 1997). Cre recombinase is from the P1 bacteriophage that will excise a segment of DNA flanked on either side by loxP sites, 34bp sequences composed of 13bp inverted repeats which flank an 8bp asymmetric sequence of DNA (Hamilton and Abremski, 1984; Nagy, 2000). These sequences are placed in the same direction around an essential exon such that when Cre recombinase is expressed, the flanked area of DNA is removed, leaving behind one loxP site, thereby disrupting gene function

(Hall et al., 2009; Nagy, 2000; Voziyanov et al., 1999). Care must be taken to place the loxP sites in introns so that endogenous function is not interrupted prior to the expression of Cre recombinase, allowing the gene to maintain its endogenous expression and function up until that point (Hall et al., 2009; Nagy, 2000). Using this approach, a floxed mouse containing the loxP sites is generated. To ablate gene function, this mouse must be crossed with a transgenic mouse expressing Cre recombinase, typically under the control of a tissue specific promoter (Hall et al., 2009; Nagy, 2000; Wagner et al., 1997). Mice resulting from this cross containing both the floxed allele and the Cre transgene will undergo Cre mediated excision of the gene of interest generating the conditional knockout mouse.

Development of gene targeted mice typically takes one year from the date of electroporation until homozygous mice are generated. Although this time frame is considerably longer than that required for the generation of transgenic mice, the advantages this system provides over transgenic approaches outweigh the length of time required for model development. Gene targeted mice are an excellent tool for studying known mutations, and loss of function in human disease to enhance our understanding of the developmental processes that cause disease, as well as to generate more effective therapies in the treatment of human disease.

Mammary Specific Mouse Model Systems

The study of mammary development and tumour biology was revolutionized by the advent of transgenic model systems which drive specific expression within the mammary gland (Callahan and Smith, 2000; Cardiff and Kenney, 2011; Hutchinson and Muller, 2000). Studies in the 1930s identified a factor present in a mother's milk that could be transmitted to their offspring and ultimately cause breast tumourigenesis (Callahan and Smith, 2000; Cardiff and Kenney, 2011; Hutchinson and Muller, 2000). The 'milk factor' was later named the mouse mammary tumour virus (MMTV), and was found to cause mammary tumours through insertional mutagenesis, whereby insertion of MMTV caused activation of oncogenes (Callahan and Smith,

2000; Cardiff and Kenney, 2011; Nusse and Varmus, 1982). These activated genes were later identified as Wnt1, Fgf3 and Notch (Cardiff and Kenney, 2011; Dickson et al., 1990; Jhappan et al., 1992; Nusse and Varmus, 1982). Although other tissues within the mouse become infected with MMTV, tumours are only seen in mammary tissue, suggesting that the cyclic nature of the gland may contribute to tumourigenesis (Cardiff and Kenney, 2011). A seminal discovery in breast cancer research came in 1984 when the first transgenic mouse model utilizing the MMTV promoter was described (Callahan and Smith, 2000; Cardiff and Kenney, 2011; Stewart et al., 1984). The transcription factor c-Myc was placed under the control of the MMTV promoter and transgenic mice were generated through established protocols (Stewart et al., 1984). Mice containing the MMTV-Myc transgene developed mammary tumours by 10 to 19 months of age demonstrating the oncogenic properties of Myc (Stewart et al., 1984). Utilization of the MMTV promoter expanded this area of research and currently, the MMTV promoter remains the most widely used promoter in the study of breast development and tumourigenesis.

The MMTV promoter contains a hormone responsive element, directing expression mainly to mammary epithelium, although there has been documented expression in other tissues such as the salivary gland; this suggests either activation during embryonic development or low levels of activity in other tissues (Callahan and Smith, 2000; Cardiff and Kenney, 2011). The MMTV promoter is active throughout mammary development with increased expression during pregnancy, when surges of hormones further stimulate activity of the promoter (Callahan and Smith, 2000; Cardiff and Kenney, 2011). Thus the MMTV promoter represents a useful tool in the study of altered gene expression on normal and abnormal development of the mammary gland.

Transgenic systems in which genes are placed under the control of the MMTV promoter to drive increased expression are widely utilized. Since the generation of the MMTV-Myc mouse, this system has been used extensively to study the effects of increased expression on breast tumour initiation. MMTV driven expression of Cyclin D1 has demonstrated its involvement in

regulating proliferative stages of development as MMTV-Cyclin D1 mice exhibit proliferative abnormalities and display increased lobuloalveolar development during puberty (Wang et al., 1994). In addition to its role in driving increased protein expression, the MMTV promoter has been utilized to generate conditional knockouts to enable the study of loss of function on mammary development and tumorigenesis (Hutchinson and Muller, 2000). Brca1 null mice are embryonic lethal preventing the study of this gene on breast cancer initiation (Hakem et al., 1996). Since Brca1 has been implicated in breast cancer patients demonstrating germline mutations in this gene, studying the effects of loss of function are essential to understanding this subset of breast cancer. Using the MMTV-Cre mouse, a floxed Brca1 mouse was generated and was used to study its role in tumour initiation (Xu et al., 1999). Using this approach, loss of Brca1 was found to lead to the development of genetically unstable mammary tumours with a long latency period, highlighting the significance of this tumour suppressor in maintaining genomic integrity (Xu et al., 1999).

The MMTV promoter represents an excellent system to drive gene expression specifically to the mammary epithelium. Use of this mammary specific promoter has revolutionized our understanding of important regulators in mammary development and tumorigenesis and proves to be a reliable tool to study breast cancer initiation and progression.

Hypothesis and Objectives

Mouse model systems to address the role of Spy1 in development and tumour initiation and progression do not currently exist. This work will describe the generation of transgenic and gene targeted mouse models to address the effects of altered protein expression on development and tumourigenesis, specifically within the mammary gland.

We hypothesize that *tight regulation of Spy1 protein levels is essential for proper mammary gland development and aberrant regulation is an important step for breast cancer initiation.*

This hypothesis will be addressed through the following objectives:

- Generate and characterize transgenic mouse model systems to overexpress Spy1 specifically within the mammary gland
- Elucidate the role of Spy1 in breast cancer susceptibility and tumour initiation
- Generate a gene targeted mouse model for the conditional knockout of Spy1 within the mammary gland

This work will provide new study systems that will aid and enhance our understanding of the role Spy1 plays in development and tumourigenesis. Data obtained from this study may ultimately contribute to our understanding of the molecular factors influencing breast cancer initiation and progression. This work offers promise for the development of novel diagnostic and therapeutic targets that will contribute to the eradication of this disease.

References

- (2002). Breast cancer and breastfeeding: collaborative reanalysis of individual data from 47 epidemiological studies in 30 countries, including 50302 women with breast cancer and 96973 women without the disease. *Lancet* *360*, 187-195.
- Abbott, A. (2007). Biologists claim Nobel prize with a knock-out. *Nature* *449*, 642.
- Acosta, J. C., and Gil, J. (2012). Senescence: a new weapon for cancer therapy. *Trends Cell Biol* *22*, 211-219.
- Adams, J. C., and Watt, F. M. (1993). Regulation of development and differentiation by the extracellular matrix. *Development* *117*, 1183-1198.
- Akashi, M., and Koeffler, H. P. (1998). Li-Fraumeni syndrome and the role of the p53 tumor suppressor gene in cancer susceptibility. *Clin Obstet Gynecol* *41*, 172-199.
- Al Sorkhy, M., Craig, R., Market, B., Ard, R., and Porter, L. A. (2009). The cyclin-dependent kinase activator, Spy1A, is targeted for degradation by the ubiquitin ligase NEDD4. *J Biol Chem* *284*, 2617-2627.
- Al Sorkhy, M., Ferraiuolo, R. M., Jalili, E., Malysa, A., Fratiloiu, A. R., Sloane, B. F., and Porter, L. A. The cyclin-like protein Spy1/RINGO promotes mammary transformation and is elevated in human breast cancer. *BMC Cancer* *12*, 45.
- Al Sorkhy, M., Ferraiuolo, R. M., Jalili, E., Malysa, A., Fratiloiu, A. R., Sloane, B. F., and Porter, L. A. (2012). The cyclin-like protein Spy1/RINGO promotes mammary transformation and is elevated in human breast cancer. *BMC Cancer* *12*, 45.
- Albrecht, J. H., Poon, R. Y., Ahonen, C. L., Rieland, B. M., Deng, C., and Crary, G. S. (1998). Involvement of p21 and p27 in the regulation of CDK activity and cell cycle progression in the regenerating liver. *Oncogene* *16*, 2141-2150.
- Anderson, S. M., Rudolph, M. C., McManaman, J. L., and Neville, M. C. (2007). Key stages in mammary gland development. Secretory activation in the mammary gland: it's not just about milk protein synthesis! *Breast Cancer Res* *9*, 204.

Aravalli, R. N., Steer, C. J., and Cressman, E. N. (2008). Molecular mechanisms of hepatocellular carcinoma. *Hepatology* 48, 2047-2063.

Arumugam, K., MacNicol, M. C., Wang, Y., Cragle, C. E., Tackett, A. J., Hardy, L. L., and MacNicol, A. M. (2012). Ringo/cyclin-dependent kinase and mitogen-activated protein kinase signaling pathways regulate the activity of the cell fate determinant Musashi to promote cell cycle re-entry in *Xenopus* oocytes. *J Biol Chem* 287, 10639-10649.

Asselin-Labat, M. L., Vaillant, F., Sheridan, J. M., Pal, B., Wu, D., Simpson, E. R., Yasuda, H., Smyth, G. K., Martin, T. J., Lindeman, G. J., and Visvader, J. E. (2010). Control of mammary stem cell function by steroid hormone signalling. *Nature* 465, 798-802.

Ball, R. K., Friis, R. R., Schoenenberger, C. A., Doppler, W., and Groner, B. (1988). Prolactin regulation of beta-casein gene expression and of a cytosolic 120-kd protein in a cloned mouse mammary epithelial cell line. *EMBO J* 7, 2089-2095.

Barnes, E. A., Porter, L. A., Lenormand, J. L., Dellinger, R. W., and Donoghue, D. J. (2003). Human Spyl promotes survival of mammalian cells following DNA damage. *Cancer Res* 63, 3701-3707.

Bartek, J., and Lukas, J. (2001). Pathways governing G1/S transition and their response to DNA damage. *FEBS Lett* 490, 117-122.

Bataller, R., and Brenner, D. A. (2005). Liver fibrosis. *J Clin Invest* 115, 209-218.

Beer, S., Zetterberg, A., Ihrie, R. A., McTaggart, R. A., Yang, Q., Bradon, N., Arvanitis, C., Attardi, L. D., Feng, S., Ruebner, B., *et al.* (2004). Developmental context determines latency of MYC-induced tumorigenesis. *PLoS Biol* 2, e332.

Berthet, C., Aleem, E., Coppola, V., Tessarollo, L., and Kaldis, P. (2003). Cdk2 knockout mice are viable. *Curr Biol* 13, 1775-1785.

Bishop, J. O., and Smith, P. (1989). Mechanism of chromosomal integration of microinjected DNA. *Mol Biol Med* 6, 283-298.

Bisteau, X., Caldez, M. J., and Kaldis, P. (2014). The Complex Relationship between Liver Cancer and the Cell Cycle: A Story of Multiple Regulations. *Cancers (Basel)* 6, 79-111.

Blakely, C. M., Sintasath, L., D'Cruz, C. M., Hahn, K. T., Dugan, K. D., Belka, G. K., and Chodosh, L. A. (2005). Developmental stage determines the effects of MYC in the mammary epithelium. *Development* 132, 1147-1160.

Blouin, A., Bolender, R. P., and Weibel, E. R. (1977). Distribution of organelles and membranes between hepatocytes and nonhepatocytes in the rat liver parenchyma. A stereological study. *J Cell Biol* 72, 441-455.

Bradbury, M. W., and Berk, P. D. (2004). Lipid metabolism in hepatic steatosis. *Clin Liver Dis* 8, 639-671, xi.

Bradley, A., Evans, M., Kaufman, M. H., and Robertson, E. (1984). Formation of germ-line chimaeras from embryo-derived teratocarcinoma cell lines. *Nature* 309, 255-256.

Brinster, R. L. (1974). The effect of cells transferred into the mouse blastocyst on subsequent development. *J Exp Med* 140, 1049-1056.

Brinster, R. L., Chen, H. Y., Trumbauer, M., Senear, A. W., Warren, R., and Palmiter, R. D. (1981). Somatic expression of herpes thymidine kinase in mice following injection of a fusion gene into eggs. *Cell* 27, 223-231.

Brinster, R. L., Chen, H. Y., Trumbauer, M. E., Yagle, M. K., and Palmiter, R. D. (1985). Factors affecting the efficiency of introducing foreign DNA into mice by microinjecting eggs. *Proc Natl Acad Sci U S A* 82, 4438-4442.

Briskin, C. (2002). Hormonal control of alveolar development and its implications for breast carcinogenesis. *J Mammary Gland Biol Neoplasia* 7, 39-48.

Briskin, C., Kaur, S., Chavarria, T. E., Binart, N., Sutherland, R. L., Weinberg, R. A., Kelly, P. A., and Ormandy, C. J. (1999). Prolactin controls mammary gland development via direct and indirect mechanisms. *Dev Biol* 210, 96-106.

Briskin, C., and O'Malley, B. (2010). Hormone action in the mammary gland. *Cold Spring Harb Perspect Biol* 2, a003178.

Briskin, C., Park, S., Vass, T., Lydon, J. P., O'Malley, B. W., and Weinberg, R. A. (1998). A paracrine role for the epithelial progesterone receptor in mammary gland development. *Proc Natl Acad Sci U S A* 95, 5076-5081.

Britt, K., Ashworth, A., and Smalley, M. (2007). Pregnancy and the risk of breast cancer. *Endocr Relat Cancer* 14, 907-933.

Byers, T., Graham, S., Rzepka, T., and Marshall, J. (1985). Lactation and breast cancer. Evidence for a negative association in premenopausal women. *Am J Epidemiol* 121, 664-674.

Cai, D., Yuan, M., Frantz, D. F., Melendez, P. A., Hansen, L., Lee, J., and Shoelson, S. E. (2005). Local and systemic insulin resistance resulting from hepatic activation of IKK-beta and NF-kappaB. *Nat Med* 11, 183-190.

Callahan, R., and Smith, G. H. (2000). MMTV-induced mammary tumorigenesis: gene discovery, progression to malignancy and cellular pathways. *Oncogene* 19, 992-1001.

Canadian Cancer Society (2014). Canadian Cancer Society Statistics. In.

Canepa, E. T., Scassa, M. E., Ceruti, J. M., Marazita, M. C., Carcagno, A. L., Sirkin, P. F., and Ogara, M. F. (2007). INK4 proteins, a family of mammalian CDK inhibitors with novel biological functions. *IUBMB Life* 59, 419-426.

Cao, Q., Padmanabhan, K., and Richter, J. D. (2010). Pumilio 2 controls translation by competing with eIF4E for 7-methyl guanosine cap recognition. *RNA* 16, 221-227.

Cardiff, R. D., and Kenney, N. (2011). A compendium of the mouse mammary tumor biologist: from the initial observations in the house mouse to the development of genetically engineered mice. *Cold Spring Harb Perspect Biol* 3.

Cardiff, R. D., and Wellings, S. R. (1999). The comparative pathology of human and mouse mammary glands. *J Mammary Gland Biol Neoplasia* 4, 105-122.

Celton-Morizur, S., Merlen, G., Couton, D., Margall-Ducos, G., and Desdouets, C. (2009). The insulin/Akt pathway controls a specific cell division program that leads to generation of binucleated tetraploid liver cells in rodents. *J Clin Invest* *119*, 1880-1887.

Chang, T. H., Kunasegaran, K., Tarulli, G. A., De Silva, D., Voorhoeve, P. M., and Pietersen, A. M. (2014). New insights into lineage restriction of mammary gland epithelium using parity-identified mammary epithelial cells. *Breast Cancer Res* *16*, R1.

Charlesworth, A., Wilczynska, A., Thampi, P., Cox, L. L., and MacNicol, A. M. (2006). Musashi regulates the temporal order of mRNA translation during *Xenopus* oocyte maturation. *Embo J* *25*, 2792-2801.

Chen, J., Saha, P., Kornbluth, S., Dynlacht, B. D., and Dutta, A. (1996). Cyclin-binding motifs are essential for the function of p21CIP1. *Mol Cell Biol* *16*, 4673-4682.

Cheng, A., Gerry, S., Kaldis, P., and Solomon, M. J. (2005a). Biochemical characterization of Cdk2-Speedy/Ringo A2. *BMC Biochem* *6*, 19.

Cheng, A., and Solomon, M. J. (2008). Speedy/Ringo C regulates S and G2 phase progression in human cells. *Cell Cycle* *7*, 3037-3047.

Cheng, A., Xiong, W., Ferrell, J. E., Jr., and Solomon, M. J. (2005b). Identification and comparative analysis of multiple mammalian Speedy/Ringo proteins. *Cell Cycle* *4*, 155-165.

Cicalese, A., Bonizzi, G., Pasi, C. E., Faretta, M., Ronzoni, S., Giulini, B., Brisken, C., Minucci, S., Di Fiore, P. P., and Pelicci, P. G. (2009). The tumor suppressor p53 regulates polarity of self-renewing divisions in mammary stem cells. *Cell* *138*, 1083-1095.

Coles, C., Condie, A., Chetty, U., Steel, C. M., Evans, H. J., and Prosser, J. (1992). p53 mutations in breast cancer. *Cancer Res* *52*, 5291-5298.

Costa, R. M., Chigancas, V., Galhardo Rda, S., Carvalho, H., and Menck, C. F. (2003). The eukaryotic nucleotide excision repair pathway. *Biochimie* *85*, 1083-1099.

Cowin, P., and Wysolmerski, J. (2010). Molecular mechanisms guiding embryonic mammary gland development. *Cold Spring Harb Perspect Biol* *2*, a003251.

- Daher, G. C., Harris, B. E., and Diasio, R. B. (1990). Metabolism of pyrimidine analogues and their nucleosides. *Pharmacol Ther* 48, 189-222.
- Dang, C. V. (1999). c-Myc target genes involved in cell growth, apoptosis, and metabolism. *Mol Cell Biol* 19, 1-11.
- Das, S. K., Delp, C. R., Bandyopadhyay, A. M., Mathiesen, M., Baird, W. M., and Banerjee, M. R. (1989). Fate of 7,12-dimethylbenz(a)anthracene in the mouse mammary gland during initiation and promotion stages of carcinogenesis in vitro. *Cancer Res* 49, 920-924.
- Deane, N. G., Parker, M. A., Aramandla, R., Diehl, L., Lee, W. J., Washington, M. K., Nanney, L. B., Shyr, Y., and Beauchamp, R. D. (2001). Hepatocellular carcinoma results from chronic cyclin D1 overexpression in transgenic mice. *Cancer Res* 61, 5389-5395.
- Deng, C., and Capecchi, M. R. (1992). Reexamination of gene targeting frequency as a function of the extent of homology between the targeting vector and the target locus. *Mol Cell Biol* 12, 3365-3371.
- Deome, K. B., Faulkin, L. J., Jr., Bern, H. A., and Blair, P. B. (1959). Development of mammary tumors from hyperplastic alveolar nodules transplanted into gland-free mammary fat pads of female C3H mice. *Cancer Res* 19, 515-520.
- Dickey, J. S., Redon, C. E., Nakamura, A. J., Baird, B. J., Sedelnikova, O. A., and Bonner, W. M. (2009). H2AX: functional roles and potential applications. *Chromosoma* 118, 683-692.
- Dickson, C., Acland, P., Smith, R., Dixon, M., Deed, R., MacAllan, D., Walther, W., Fuller-Pace, F., Kiefer, P., and Peters, G. (1990). Characterization of int-2: a member of the fibroblast growth factor family. *J Cell Sci Suppl* 13, 87-96.
- Dinarina, A., Perez, L. H., Davila, A., Schwab, M., Hunt, T., and Nebreda, A. R. (2005). Characterization of a new family of cyclin-dependent kinase activators. *Biochem J* 386, 349-355.
- Dinarina, A., Ruiz, E. J., O'Loughlen, A., Mouron, S., Perez, L., and Nebreda, A. R. (2008). Negative regulation of cell-cycle progression by RINGO/Speedy E. *Biochem J* 410, 535-542.

Dinarina, A., Santamaria, P. G., and Nebreda, A. R. (2009). Cell cycle regulation of the mammalian CDK activator RINGO/Speedy A. *FEBS Lett* 583, 2772-2778.

Doetschman, T., Gregg, R. G., Maeda, N., Hooper, M. L., Melton, D. W., Thompson, S., and Smithies, O. (1987). Targetted correction of a mutant HPRT gene in mouse embryonic stem cells. *Nature* 330, 576-578.

Donjerkovic, D., and Scott, D. W. (2000). Regulation of the G1 phase of the mammalian cell cycle. *Cell Res* 10, 1-16.

Donzelli, M., and Draetta, G. F. (2003). Regulating mammalian checkpoints through Cdc25 inactivation. *EMBO Rep* 4, 671-677.

Dowman, J. K., Tomlinson, J. W., and Newsome, P. N. (2010). Pathogenesis of non-alcoholic fatty liver disease. *QJM* 103, 71-83.

Ehrenfried, J. A., Ko, T. C., Thompson, E. A., and Evers, B. M. (1997). Cell cycle-mediated regulation of hepatic regeneration. *Surgery* 122, 927-935.

el-Deiry, W. S., Harper, J. W., O'Connor, P. M., Velculescu, V. E., Canman, C. E., Jackman, J., Pietenpol, J. A., Burrell, M., Hill, D. E., Wang, Y., and et al. (1994). WAF1/CIP1 is induced in p53-mediated G1 arrest and apoptosis. *Cancer Res* 54, 1169-1174.

Errico, A., Deshmukh, K., Tanaka, Y., Pozniakovsky, A., and Hunt, T. (2010). Identification of substrates for cyclin dependent kinases. *Adv Enzyme Regul* 50, 375-399.

Escot, C., Theillet, C., Lidereau, R., Spyrtos, F., Champeme, M. H., Gest, J., and Callahan, R. (1986). Genetic alteration of the c-myc protooncogene (MYC) in human primary breast carcinomas. *Proc Natl Acad Sci U S A* 83, 4834-4838.

Evans, M. J., and Kaufman, M. H. (1981). Establishment in culture of pluripotential cells from mouse embryos. *Nature* 292, 154-156.

Evans, T., Rosenthal, E. T., Youngblom, J., Distel, D., and Hunt, T. (1983). Cyclin: a protein specified by maternal mRNA in sea urchin eggs that is destroyed at each cleavage division. *Cell* 33, 389-396.

Fadok, V. A. (1999). Clearance: the last and often forgotten stage of apoptosis. *J Mammary Gland Biol Neoplasia* 4, 203-211.

Fantl, V., Stamp, G., Andrews, A., Rosewell, I., and Dickson, C. (1995). Mice lacking cyclin D1 are small and show defects in eye and mammary gland development. *Genes Dev* 9, 2364-2372.

Farrell, G. C., Larter, C. Z., Hou, J. Y., Zhang, R. H., Yeh, M. M., Williams, J., dela Pena, A., Francisco, R., Osvath, S. R., Brooling, J., *et al.* (2009). Apoptosis in experimental NASH is associated with p53 activation and TRAIL receptor expression. *J Gastroenterol Hepatol* 24, 443-452.

Fattovich, G., Stroffolini, T., Zagni, I., and Donato, F. (2004). Hepatocellular carcinoma in cirrhosis: incidence and risk factors. *Gastroenterology* 127, S35-50.

Fausto, N., and Campbell, J. S. (2003). The role of hepatocytes and oval cells in liver regeneration and repopulation. *Mech Dev* 120, 117-130.

Feldstein, A. E., Werneburg, N. W., Canbay, A., Guicciardi, M. E., Bronk, S. F., Rydzewski, R., Burgart, L. J., and Gores, G. J. (2004). Free fatty acids promote hepatic lipotoxicity by stimulating TNF- α expression via a lysosomal pathway. *Hepatology* 40, 185-194.

Ferby, I., Blazquez, M., Palmer, A., Eritja, R., and Nebreda, A. R. (1999). A novel p34(cdc2)-binding and activating protein that is necessary and sufficient to trigger G(2)/M progression in *Xenopus* oocytes. *Genes Dev* 13, 2177-2189.

Fero, M. L., Rivkin, M., Tasch, M., Porter, P., Carow, C. E., Firpo, E., Polyak, K., Tsai, L. H., Broudy, V., Perlmutter, R. M., *et al.* (1996). A syndrome of multiorgan hyperplasia with features of gigantism, tumorigenesis, and female sterility in p27(Kip1)-deficient mice. *Cell* 85, 733-744.

Friedman, S. L., Roll, F. J., Boyles, J., and Bissell, D. M. (1985). Hepatic lipocytes: the principal collagen-producing cells of normal rat liver. *Proc Natl Acad Sci U S A* 82, 8681-8685.

Furth, P. A., St Onge, L., Boger, H., Gruss, P., Gossen, M., Kistner, A., Bujard, H., and Hennighausen, L. (1994). Temporal control of gene expression in transgenic mice by a tetracycline-responsive promoter. *Proc Natl Acad Sci U S A* 91, 9302-9306.

Gartel, A. L., and Tyner, A. L. (2002). The role of the cyclin-dependent kinase inhibitor p21 in apoptosis. *Mol Cancer Ther* 1, 639-649.

Gastwirt, R. F., Slavin, D. A., McAndrew, C. W., and Donoghue, D. J. (2006). Spy1 expression prevents normal cellular responses to DNA damage: inhibition of apoptosis and checkpoint activation. *J Biol Chem* 281, 35425-35435.

Gentric, G., Desdouets, C., and Celton-Morizur, S. (2012). Hepatocytes polyploidization and cell cycle control in liver physiopathology. *Int J Hepatol* 2012, 282430.

Germain, L., Blouin, M. J., and Marceau, N. (1988). Biliary epithelial and hepatocytic cell lineage relationships in embryonic rat liver as determined by the differential expression of cytokeratins, alpha-fetoprotein, albumin, and cell surface-exposed components. *Cancer Res* 48, 4909-4918.

Ginestier, C., Hur, M. H., Charafe-Jauffret, E., Monville, F., Dutcher, J., Brown, M., Jacquemier, J., Viens, P., Kleer, C. G., Liu, S., *et al.* (2007). ALDH1 is a marker of normal and malignant human mammary stem cells and a predictor of poor clinical outcome. *Cell Stem Cell* 1, 555-567.

Golipour, A., Myers, D., Seagroves, T., Murphy, D., Evan, G. I., Donoghue, D. J., Moorehead, R. A., and Porter, L. A. (2008). The Spy1/RINGO family represents a novel mechanism regulating mammary growth and tumorigenesis. *Cancer Res* 68, 3591-3600.

Gordon, J. W., Scangos, G. A., Plotkin, D. J., Barbosa, J. A., and Ruddle, F. H. (1980). Genetic transformation of mouse embryos by microinjection of purified DNA. *Proc Natl Acad Sci U S A* 77, 7380-7384.

Gossen, M., and Bujard, H. (1992). Tight control of gene expression in mammalian cells by tetracycline-responsive promoters. *Proc Natl Acad Sci U S A* 89, 5547-5551.

Gossen, M., Freundlieb, S., Bender, G., Muller, G., Hillen, W., and Bujard, H. (1995). Transcriptional activation by tetracyclines in mammalian cells. *Science* 268, 1766-1769.

Gouilleux, F., Wakao, H., Mundt, M., and Groner, B. (1994). Prolactin induces phosphorylation of Tyr694 of Stat5 (MGF), a prerequisite for DNA binding and induction of transcription. *EMBO J* 13, 4361-4369.

Green, K. A., and Lund, L. R. (2005). ECM degrading proteases and tissue remodelling in the mammary gland. *Bioessays* 27, 894-903.

Grisham, J. W. (1962). A morphologic study of deoxyribonucleic acid synthesis and cell proliferation in regenerating rat liver; autoradiography with thymidine-H3. *Cancer Res* 22, 842-849.

Gualdi, R., Bossard, P., Zheng, M., Hamada, Y., Coleman, J. R., and Zaret, K. S. (1996). Hepatic specification of the gut endoderm in vitro: cell signaling and transcriptional control. *Genes Dev* 10, 1670-1682.

Guenet, J. L. (2005). The mouse genome. *Genome Res* 15, 1729-1740.

Gunther, E. J., Belka, G. K., Wertheim, G. B., Wang, J., Hartman, J. L., Boxer, R. B., and Chodosh, L. A. (2002). A novel doxycycline-inducible system for the transgenic analysis of mammary gland biology. *FASEB J* 16, 283-292.

Hakem, R., de la Pompa, J. L., Sirard, C., Mo, R., Woo, M., Hakem, A., Wakeham, A., Potter, J., Reitmair, A., Billia, F., *et al.* (1996). The tumor suppressor gene *Brcal* is required for embryonic cellular proliferation in the mouse. *Cell* 85, 1009-1023.

Hall, B., Limaye, A., and Kulkarni, A. B. (2009). Overview: generation of gene knockout mice. *Curr Protoc Cell Biol Chapter 19*, Unit 19 12 19 12 11-17.

Hamilton, D. L., and Abremski, K. (1984). Site-specific recombination by the bacteriophage P1 lox-Cre system. Cre-mediated synapsis of two lox sites. *J Mol Biol* 178, 481-486.

Hanahan, D., Wagner, E. F., and Palmiter, R. D. (2007). The origins of oncomice: a history of the first transgenic mice genetically engineered to develop cancer. *Genes Dev* 21, 2258-2270.

Haruyama, N., Cho, A., and Kulkarni, A. B. (2009). Overview: engineering transgenic constructs and mice. *Curr Protoc Cell Biol Chapter 19*, Unit 19 10.

Hasty, P., Rivera-Perez, J., and Bradley, A. (1991). The length of homology required for gene targeting in embryonic stem cells. *Mol Cell Biol* *11*, 5586-5591.

Hayashi, E., Yasui, A., Oda, K., Nagino, M., Nimura, Y., Nakanishi, M., Motoyama, N., Ikeda, K., and Matsuura, A. (2003). Loss of p27(Kip1) accelerates DNA replication after partial hepatectomy in mice. *J Surg Res* *111*, 196-202.

He, G., Siddik, Z. H., Huang, Z., Wang, R., Koomen, J., Kobayashi, R., Khokhar, A. R., and Kuang, J. (2005). Induction of p21 by p53 following DNA damage inhibits both Cdk4 and Cdk2 activities. *Oncogene* *24*, 2929-2943.

Heindryckx, F., Colle, I., and Van Vlierberghe, H. (2009). Experimental mouse models for hepatocellular carcinoma research. *Int J Exp Pathol* *90*, 367-386.

Hennighausen, L., and Robinson, G. W. (2001). Signaling pathways in mammary gland development. *Dev Cell* *1*, 467-475.

Hennighausen, L., Wall, R. J., Tillmann, U., Li, M., and Furth, P. A. (1995). Conditional gene expression in secretory tissues and skin of transgenic mice using the MMTV-LTR and the tetracycline responsive system. *J Cell Biochem* *59*, 463-472.

Hens, J. R., and Wysolmerski, J. J. (2005). Key stages of mammary gland development: molecular mechanisms involved in the formation of the embryonic mammary gland. *Breast Cancer Res* *7*, 220-224.

Hinck, L., and Silberstein, G. B. (2005). Key stages in mammary gland development: the mammary end bud as a motile organ. *Breast Cancer Res* *7*, 245-251.

Holmes, J. K., and Solomon, M. J. (1996). A predictive scale for evaluating cyclin-dependent kinase substrates. A comparison of p34cdc2 and p33cdk2. *J Biol Chem* *271*, 25240-25246.

Houssaint, E. (1980). Differentiation of the mouse hepatic primordium. I. An analysis of tissue interactions in hepatocyte differentiation. *Cell Differ* *9*, 269-279.

Hovey, R. C., McFadden, T. B., and Akers, R. M. (1999). Regulation of mammary gland growth and morphogenesis by the mammary fat pad: a species comparison. *J Mammary Gland Biol Neoplasia* *4*, 53-68.

Howlett, A. R., and Bissell, M. J. (1993). The influence of tissue microenvironment (stroma and extracellular matrix) on the development and function of mammary epithelium. *Epithelial Cell Biol* *2*, 79-89.

Howlin, J., McBryan, J., and Martin, F. (2006). Pubertal mammary gland development: insights from mouse models. *J Mammary Gland Biol Neoplasia* *11*, 283-297.

Hsieh, C. C., Trichopoulos, D., Katsouyanni, K., and Yuasa, S. (1990). Age at menarche, age at menopause, height and obesity as risk factors for breast cancer: associations and interactions in an international case-control study. *Int J Cancer* *46*, 796-800.

Humphreys, R. C., Krajewska, M., Krnacik, S., Jaeger, R., Weiher, H., Krajewski, S., Reed, J. C., and Rosen, J. M. (1996). Apoptosis in the terminal endbud of the murine mammary gland: a mechanism of ductal morphogenesis. *Development* *122*, 4013-4022.

Humphreys, R. C., Lydon, J., O'Malley, B. W., and Rosen, J. M. (1997). Mammary gland development is mediated by both stromal and epithelial progesterone receptors. *Mol Endocrinol* *11*, 801-811.

Hurley, P. J., and Bunz, F. (2007). ATM and ATR: components of an integrated circuit. *Cell Cycle* *6*, 414-417.

Hutchinson, J. N., and Muller, W. J. (2000). Transgenic mouse models of human breast cancer. *Oncogene* *19*, 6130-6137.

Ilyin, G. P., Glaise, D., Gilot, D., Baffet, G., and Guguen-Guillouzo, C. (2003). Regulation and role of p21 and p27 cyclin-dependent kinase inhibitors during hepatocyte differentiation and growth. *Am J Physiol Gastrointest Liver Physiol* *285*, G115-127.

Ito, Y., Matsuura, N., Sakon, M., Miyoshi, E., Noda, K., Takeda, T., Umeshita, K., Nagano, H., Nakamori, S., Dono, K., *et al.* (1999). Expression and prognostic roles of the G1-S modulators in hepatocellular carcinoma: p27 independently predicts the recurrence. *Hepatology* 30, 90-99.

Jacks, T., Remington, L., Williams, B. O., Schmitt, E. M., Halachmi, S., Bronson, R. T., and Weinberg, R. A. (1994). Tumor spectrum analysis in p53-mutant mice. *Curr Biol* 4, 1-7.

Jeffrey, P. D., Russo, A. A., Polyak, K., Gibbs, E., Hurwitz, J., Massague, J., and Pavletich, N. P. (1995). Mechanism of CDK activation revealed by the structure of a cyclinA-CDK2 complex. *Nature* 376, 313-320.

Jerry, D. J., Kittrell, F. S., Kuperwasser, C., Laucirica, R., Dickinson, E. S., Bonilla, P. J., Butel, J. S., and Medina, D. (2000). A mammary-specific model demonstrates the role of the p53 tumor suppressor gene in tumor development. *Oncogene* 19, 1052-1058.

Jhappan, C., Gallahan, D., Stahle, C., Chu, E., Smith, G. H., Merlino, G., and Callahan, R. (1992). Expression of an activated Notch-related int-3 transgene interferes with cell differentiation and induces neoplastic transformation in mammary and salivary glands. *Genes Dev* 6, 345-355.

Jou, J., Choi, S. S., and Diehl, A. M. (2008). Mechanisms of disease progression in nonalcoholic fatty liver disease. *Semin Liver Dis* 28, 370-379.

Kant, P., and Hull, M. A. (2011). Excess body weight and obesity--the link with gastrointestinal and hepatobiliary cancer. *Nat Rev Gastroenterol Hepatol* 8, 224-238.

Karaiskou, A., Perez, L. H., Ferby, I., Ozon, R., Jesus, C., and Nebreda, A. R. (2001). Differential regulation of Cdc2 and Cdk2 by RINGO and cyclins. *J Biol Chem* 276, 36028-36034.

Karlsson-Rosenthal, C., and Millar, J. B. (2006). Cdc25: mechanisms of checkpoint inhibition and recovery. *Trends Cell Biol* 16, 285-292.

Ke, Q., Ji, J., Cheng, C., Zhang, Y., Lu, M., Wang, Y., Zhang, L., Li, P., Cui, X., Chen, L., *et al.* (2009). Expression and prognostic role of Spyl as a novel cell cycle protein in hepatocellular carcinoma. *Exp Mol Pathol* 87, 167-172.

Kelsey, J. L., Gammon, M. D., and John, E. M. (1993). Reproductive factors and breast cancer. *Epidemiol Rev* 15, 36-47.

Kinner, A., Wu, W., Staudt, C., and Iliakis, G. (2008). Gamma-H2AX in recognition and signaling of DNA double-strand breaks in the context of chromatin. *Nucleic Acids Res* 36, 5678-5694.

Kobayashi, H., Stewart, E., Poon, R., Adamczewski, J. P., Gannon, J., and Hunt, T. (1992). Identification of the domains in cyclin A required for binding to, and activation of, p34cdc2 and p32cdk2 protein kinase subunits. *Mol Biol Cell* 3, 1279-1294.

Kodama, T., Takehara, T., Hikita, H., Shimizu, S., Shigekawa, M., Tsunematsu, H., Li, W., Miyagi, T., Hosui, A., Tatsumi, T., *et al.* (2011). Increases in p53 expression induce CTGF synthesis by mouse and human hepatocytes and result in liver fibrosis in mice. *J Clin Invest* 121, 3343-3356.

Kordon, E. C., and Smith, G. H. (1998). An entire functional mammary gland may comprise the progeny from a single cell. *Development* 125, 1921-1930.

Kruse, J. P., and Gu, W. (2009). Modes of p53 regulation. *Cell* 137, 609-622.

Kung, J. W., Currie, I. S., Forbes, S. J., and Ross, J. A. (2010). Liver development, regeneration, and carcinogenesis. *J Biomed Biotechnol* 2010, 984248.

Landis, M. W., Pawlyk, B. S., Li, T., Sicinski, P., and Hinds, P. W. (2006). Cyclin D1-dependent kinase activity in murine development and mammary tumorigenesis. *Cancer Cell* 9, 13-22.

Lee, H. J., Lee, Y. J., Kang, C. M., Bae, S., Jeoung, D., Jang, J. J., Lee, S. S., Cho, C. K., and Lee, Y. S. (2008). Differential gene signatures in rat mammary tumors induced by DMBA and those induced by fractionated gamma radiation. *Radiat Res* 170, 579-590.

Lemaigre, F. P. (2003). Development of the biliary tract. *Mech Dev* 120, 81-87.

Lenormand, J. L., Dellinger, R. W., Knudsen, K. E., Subramani, S., and Donoghue, D. J. (1999). Speedy: a novel cell cycle regulator of the G2/M transition. *Embo J* 18, 1869-1877.

Lew, D. J., and Kornbluth, S. (1996). Regulatory roles of cyclin dependent kinase phosphorylation in cell cycle control. *Curr Opin Cell Biol* 8, 795-804.

Li, M., Liu, X., Robinson, G., Bar-Peled, U., Wagner, K. U., Young, W. S., Hennighausen, L., and Furth, P. A. (1997). Mammary-derived signals activate programmed cell death during the first stage of mammary gland involution. *Proc Natl Acad Sci U S A* 94, 3425-3430.

Liedtke, C., Mazouni, C., Hess, K. R., Andre, F., Tordai, A., Mejia, J. A., Symmans, W. F., Gonzalez-Angulo, A. M., Hennessy, B., Green, M., *et al.* (2008). Response to neoadjuvant therapy and long-term survival in patients with triple-negative breast cancer. *J Clin Oncol* 26, 1275-1281.

Lim, E., Vaillant, F., Wu, D., Forrest, N. C., Pal, B., Hart, A. H., Asselin-Labat, M. L., Gyorki, D. E., Ward, T., Partanen, A., *et al.* (2009). Aberrant luminal progenitors as the candidate target population for basal tumor development in BRCA1 mutation carriers. *Nat Med* 15, 907-913.

Lubanska, D., Market-Velker, B. A., deCarvalho, A. C., Mikkelsen, T., Fidalgo da Silva, E., and Porter, L. A. (2014). The cyclin-like protein Spyl1 regulates growth and division characteristics of the CD133+ population in human glioma. *Cancer Cell* 25, 64-76.

Lukas, C., Falck, J., Bartkova, J., Bartek, J., and Lukas, J. (2003). Distinct spatiotemporal dynamics of mammalian checkpoint regulators induced by DNA damage. *Nat Cell Biol* 5, 255-260.

Macleod, K. F., Sherry, N., Hannon, G., Beach, D., Tokino, T., Kinzler, K., Vogelstein, B., and Jacks, T. (1995). p53-dependent and independent expression of p21 during cell growth, differentiation, and DNA damage. *Genes Dev* 9, 935-944.

MacMahon, B., Cole, P., Lin, T. M., Lowe, C. R., Mirra, A. P., Ravnihar, B., Salber, E. J., Valaoras, V. G., and Yuasa, S. (1970). Age at first birth and breast cancer risk. *Bull World Health Organ* 43, 209-221.

MacNicol, M. C., and MacNicol, A. M. (2010). Developmental timing of mRNA translation--integration of distinct regulatory elements. *Mol Reprod Dev* 77, 662-669.

Mailand, N., Falck, J., Lukas, C., Syljuasen, R. G., Welcker, M., Bartek, J., and Lukas, J. (2000). Rapid destruction of human Cdc25A in response to DNA damage. *Science* 288, 1425-1429.

Mailand, N., Podtelejnikov, A. V., Groth, A., Mann, M., Bartek, J., and Lukas, J. (2002). Regulation of G(2)/M events by Cdc25A through phosphorylation-dependent modulation of its stability. *EMBO J* 21, 5911-5920.

Makarem, M., Spike, B. T., Dravis, C., Kannan, N., Wahl, G. M., and Eaves, C. J. (2013). Stem cells and the developing mammary gland. *J Mammary Gland Biol Neoplasia* 18, 209-219.

Mallepell, S., Krust, A., Chambon, P., and Brisken, C. (2006). Paracrine signaling through the epithelial estrogen receptor alpha is required for proliferation and morphogenesis in the mammary gland. *Proc Natl Acad Sci U S A* 103, 2196-2201.

Malumbres, M., and Barbacid, M. (2005). Mammalian cyclin-dependent kinases. *Trends Biochem Sci* 30, 630-641.

Mansour, S. L., Goddard, J. M., and Capecchi, M. R. (1993). Mice homozygous for a targeted disruption of the proto-oncogene int-2 have developmental defects in the tail and inner ear. *Development* 117, 13-28.

Mansour, S. L., Thomas, K. R., and Capecchi, M. R. (1988). Disruption of the proto-oncogene int-2 in mouse embryo-derived stem cells: a general strategy for targeting mutations to non-selectable genes. *Nature* 336, 348-352.

Matsuda, Y., Wakai, T., Kubota, M., Takamura, M., Yamagiwa, S., Aoyagi, Y., Osawa, M., Fujimaki, S., Sanpei, A., Genda, T., and Ichida, T. (2013). Clinical significance of cell cycle inhibitors in hepatocellular carcinoma. *Med Mol Morphol* 46, 185-192.

McAndrew, C. W., Gastwirt, R. F., and Donoghue, D. J. (2009). The atypical CDK activator Spy1 regulates the intrinsic DNA damage response and is dependent upon p53 to inhibit apoptosis. *Cell Cycle* 8, 66-75.

McAndrew, C. W., Gastwirt, R. F., Meyer, A. N., Porter, L. A., and Donoghue, D. J. (2007). Spy1 enhances phosphorylation and degradation of the cell cycle inhibitor p27. *Cell Cycle* 6, 1937-1945.

Meek, D. W. (2004). The p53 response to DNA damage. *DNA Repair (Amst)* 3, 1049-1056.

Melendez-Colon, V. J., Luch, A., Seidel, A., and Baird, W. M. (1999). Cancer initiation by polycyclic aromatic hydrocarbons results from formation of stable DNA adducts rather than apurinic sites. *Carcinogenesis* 20, 1885-1891.

Monga, S. P., Monga, H. K., Tan, X., Mule, K., Pediaditakis, P., and Michalopoulos, G. K. (2003). Beta-catenin antisense studies in embryonic liver cultures: role in proliferation, apoptosis, and lineage specification. *Gastroenterology* 124, 202-216.

Morgan, D. O. (1997). Cyclin-dependent kinases: engines, clocks, and microprocessors. *Annu Rev Cell Dev Biol* 13, 261-291.

Mouron, S., de Carcer, G., Seco, E., Fernandez-Miranda, G., Malumbres, M., and Nebreda, A. R. RINGO C is required to sustain the spindle-assembly checkpoint. *J Cell Sci* 123, 2586-2595.

Muller, U. (1999). Ten years of gene targeting: targeted mouse mutants, from vector design to phenotype analysis. *Mech Dev* 82, 3-21.

Nagy, A. (2000). Cre recombinase: the universal reagent for genome tailoring. *Genesis* 26, 99-109.

Nakayama, K. (1998). Cip/Kip cyclin-dependent kinase inhibitors: brakes of the cell cycle engine during development. *Bioessays* 20, 1020-1029.

Nakayama, K., Ishida, N., Shirane, M., Inomata, A., Inoue, T., Shishido, N., Horii, I., and Loh, D. Y. (1996). Mice lacking p27(Kip1) display increased body size, multiple organ hyperplasia, retinal dysplasia, and pituitary tumors. *Cell* 85, 707-720.

Naugler, W. E., Sakurai, T., Kim, S., Maeda, S., Kim, K., Elsharkawy, A. M., and Karin, M. (2007). Gender disparity in liver cancer due to sex differences in MyD88-dependent IL-6 production. *Science* 317, 121-124.

Nebreda, A. R., and Hunt, T. (1993). The c-mos proto-oncogene protein kinase turns on and maintains the activity of MAP kinase, but not MPF, in cell-free extracts of *Xenopus* oocytes and eggs. *Embo J* 12, 1979-1986.

Nelsen, C. J., Kuriyama, R., Hirsch, B., Negron, V. C., Lingle, W. L., Goggin, M. M., Stanley, M. W., and Albrecht, J. H. (2005). Short term cyclin D1 overexpression induces centrosome amplification, mitotic spindle abnormalities, and aneuploidy. *J Biol Chem* 280, 768-776.

Nigg, E. A. (1995). Cyclin-dependent protein kinases: key regulators of the eukaryotic cell cycle. *Bioessays* 17, 471-480.

Noble, M. E., Endicott, J. A., Brown, N. R., and Johnson, L. N. (1997). The cyclin box fold: protein recognition in cell-cycle and transcription control. *Trends Biochem Sci* 22, 482-487.

Nusse, R., and Varmus, H. E. (1982). Many tumors induced by the mouse mammary tumor virus contain a provirus integrated in the same region of the host genome. *Cell* 31, 99-109.

Oakes, S. R., Hilton, H. N., and Ormandy, C. J. (2006). The alveolar switch: coordinating the proliferative cues and cell fate decisions that drive the formation of lobuloalveoli from ductal epithelium. *Breast Cancer Res* 8, 207.

Ormandy, C. J., Binart, N., and Kelly, P. A. (1997). Mammary gland development in prolactin receptor knockout mice. *J Mammary Gland Biol Neoplasia* 2, 355-364.

Padmanabhan, K., and Richter, J. D. (2006). Regulated Pumilio-2 binding controls RINGO/Spy mRNA translation and CPEB activation. *Genes Dev* 20, 199-209.

Pagano, M., Tam, S. W., Theodoras, A. M., Beer-Romero, P., Del Sal, G., Chau, V., Yew, P. R., Draetta, G. F., and Rolfe, M. (1995). Role of the ubiquitin-proteasome pathway in regulating abundance of the cyclin-dependent kinase inhibitor p27. *Science* 269, 682-685.

Palmiter, R. D., Brinster, R. L., Hammer, R. E., Trumbauer, M. E., Rosenfeld, M. G., Birnberg, N. C., and Evans, R. M. (1982). Dramatic growth of mice that develop from eggs microinjected with metallothionein-growth hormone fusion genes. *Nature* 300, 611-615.

Panasiuk, A., Dzieciol, J., Panasiuk, B., and Prokopowicz, D. (2006). Expression of p53, Bax and Bcl-2 proteins in hepatocytes in non-alcoholic fatty liver disease. *World J Gastroenterol* *12*, 6198-6202.

Pascale, R. M., Simile, M. M., De Miglio, M. R., Muroi, M. R., Calvisi, D. F., Asara, G., Casabona, D., Frau, M., Seddaiu, M. A., and Feo, F. (2002). Cell cycle deregulation in liver lesions of rats with and without genetic predisposition to hepatocarcinogenesis. *Hepatology* *35*, 1341-1350.

Paull, T. T., Rogakou, E. P., Yamazaki, V., Kirchgessner, C. U., Gellert, M., and Bonner, W. M. (2000). A critical role for histone H2AX in recruitment of repair factors to nuclear foci after DNA damage. *Curr Biol* *10*, 886-895.

Pavletich, N. P. (1999). Mechanisms of cyclin-dependent kinase regulation: structures of Cdks, their cyclin activators, and Cip and INK4 inhibitors. *J Mol Biol* *287*, 821-828.

Perou, C. M., Sorlie, T., Eisen, M. B., van de Rijn, M., Jeffrey, S. S., Rees, C. A., Pollack, J. R., Ross, D. T., Johnsen, H., Akslen, L. A., *et al.* (2000). Molecular portraits of human breast tumours. *Nature* *406*, 747-752.

Pines, J. (1991). Cyclins: wheels within wheels. *Cell Growth Differ* *2*, 305-310.

Podhorecka, M., Skladanowski, A., and Bozko, P. (2010). H2AX Phosphorylation: Its Role in DNA Damage Response and Cancer Therapy. *J Nucleic Acids* *2010*.

Porter, L. A., Dellinger, R. W., Tynan, J. A., Barnes, E. A., Kong, M., Lenormand, J. L., and Donoghue, D. J. (2002). Human Speedy: a novel cell cycle regulator that enhances proliferation through activation of Cdk2. *J Cell Biol* *157*, 357-366.

Porter, L. A., Kong-Beltran, M., and Donoghue, D. J. (2003). Spyl1 interacts with p27Kip1 to allow G1/S progression. *Mol Biol Cell* *14*, 3664-3674.

Prat, A., Parker, J. S., Karginova, O., Fan, C., Livasy, C., Herschkowitz, J. I., He, X., and Perou, C. M. (2010). Phenotypic and molecular characterization of the claudin-low intrinsic subtype of breast cancer. *Breast Cancer Res* *12*, R68.

Premisrirut, P. K., Dow, L. E., Kim, S. Y., Camiolo, M., Malone, C. D., Miething, C., Scuoppo, C., Zuber, J., Dickins, R. A., Kogan, S. C., *et al.* A rapid and scalable system for studying gene function in mice using conditional RNA interference. *Cell* *145*, 145-158.

Preston, D. L., Mattsson, A., Holmberg, E., Shore, R., Hildreth, N. G., and Boice, J. D., Jr. (2002). Radiation effects on breast cancer risk: a pooled analysis of eight cohorts. *Radiat Res* *158*, 220-235.

Quarrie, L. H., Addey, C. V., and Wilde, C. J. (1995). Apoptosis in lactating and involuting mouse mammary tissue demonstrated by nick-end DNA labelling. *Cell Tissue Res* *281*, 413-419.

Rakha, E. A., Reis-Filho, J. S., and Ellis, I. O. (2008). Basal-like breast cancer: a critical review. *J Clin Oncol* *26*, 2568-2581.

Ray, D., Terao, Y., Christov, K., Kaldis, P., and Kiyokawa, H. (2011). Cdk2-null mice are resistant to ErbB-2-induced mammary tumorigenesis. *Neoplasia* *13*, 439-444.

Richert, M. M., Schwertfeger, K. L., Ryder, J. W., and Anderson, S. M. (2000). An atlas of mouse mammary gland development. *J Mammary Gland Biol Neoplasia* *5*, 227-241.

Robinson, G. W., McKnight, R. A., Smith, G. H., and Hennighausen, L. (1995). Mammary epithelial cells undergo secretory differentiation in cycling virgins but require pregnancy for the establishment of terminal differentiation. *Development* *121*, 2079-2090.

Rogakou, E. P., Pilch, D. R., Orr, A. H., Ivanova, V. S., and Bonner, W. M. (1998). DNA double-stranded breaks induce histone H2AX phosphorylation on serine 139. *J Biol Chem* *273*, 5858-5868.

Roskams, T., Yang, S. Q., Koteish, A., Durnez, A., DeVos, R., Huang, X., Achten, R., Verslype, C., and Diehl, A. M. (2003). Oxidative stress and oval cell accumulation in mice and humans with alcoholic and nonalcoholic fatty liver disease. *Am J Pathol* *163*, 1301-1311.

Rossi, J. M., Dunn, N. R., Hogan, B. L., and Zaret, K. S. (2001). Distinct mesodermal signals, including BMPs from the septum transversum mesenchyme, are required in combination for hepatogenesis from the endoderm. *Genes Dev* *15*, 1998-2009.

- Roussel, M. F. (1999). The INK4 family of cell cycle inhibitors in cancer. *Oncogene* 18, 5311-5317.
- Russo, A. A., Jeffrey, P. D., and Pavletich, N. P. (1996). Structural basis of cyclin-dependent kinase activation by phosphorylation. *Nat Struct Biol* 3, 696-700.
- Russo, J., Moral, R., Balogh, G. A., Mailo, D., and Russo, I. H. (2005). The protective role of pregnancy in breast cancer. *Breast Cancer Res* 7, 131-142.
- Sagata, N., Watanabe, N., Vande Woude, G. F., and Ikawa, Y. (1989). The c-mos proto-oncogene product is a cytostatic factor responsible for meiotic arrest in vertebrate eggs. *Nature* 342, 512-518.
- Sakaguchi, K., Herrera, J. E., Saito, S., Miki, T., Bustin, M., Vassilev, A., Anderson, C. W., and Appella, E. (1998). DNA damage activates p53 through a phosphorylation-acetylation cascade. *Genes Dev* 12, 2831-2841.
- Sancar, A., Lindsey-Boltz, L. A., Unsal-Kacmaz, K., and Linn, S. (2004). Molecular mechanisms of mammalian DNA repair and the DNA damage checkpoints. *Annu Rev Biochem* 73, 39-85.
- Sauer, B. (1998). Inducible gene targeting in mice using the Cre/lox system. *Methods* 14, 381-392.
- Schafer, K. A. (1998). The cell cycle: a review. *Vet Pathol* 35, 461-478.
- Schulman, B. A., Lindstrom, D. L., and Harlow, E. (1998). Substrate recruitment to cyclin-dependent kinase 2 by a multipurpose docking site on cyclin A. *Proc Natl Acad Sci U S A* 95, 10453-10458.
- Schwartzberg, P. L., Goff, S. P., and Robertson, E. J. (1989). Germ-line transmission of a c-abl mutation produced by targeted gene disruption in ES cells. *Science* 246, 799-803.
- Sedelnikova, O. A., and Bonner, W. M. (2006). GammaH2AX in cancer cells: a potential biomarker for cancer diagnostics, prediction and recurrence. *Cell Cycle* 5, 2909-2913.

Serls, A. E., Doherty, S., Parvatiyar, P., Wells, J. M., and Deutsch, G. H. (2005). Different thresholds of fibroblast growth factors pattern the ventral foregut into liver and lung. *Development* *132*, 35-47.

Severin, E., Willers, R., and Bettecken, T. (1984). Flow cytometric analysis of mouse hepatocyte ploidy. II. The development of polyploidy pattern in four mice strains with different life spans. *Cell Tissue Res* *238*, 649-652.

Shachaf, C. M., Kopelman, A. M., Arvanitis, C., Karlsson, A., Beer, S., Mandl, S., Bachmann, M. H., Borowsky, A. D., Ruebner, B., Cardiff, R. D., *et al.* (2004). MYC inactivation uncovers pluripotent differentiation and tumour dormancy in hepatocellular cancer. *Nature* *431*, 1112-1117.

Shackleton, M., Vaillant, F., Simpson, K. J., Stingl, J., Smyth, G. K., Asselin-Labat, M. L., Wu, L., Lindeman, G. J., and Visvader, J. E. (2006). Generation of a functional mammary gland from a single stem cell. *Nature* *439*, 84-88.

Shehata, M., Teschendorff, A., Sharp, G., Novcic, N., Russell, I. A., Avril, S., Prater, M., Eirew, P., Caldas, C., Watson, C. J., and Stingl, J. (2012). Phenotypic and functional characterisation of the luminal cell hierarchy of the mammary gland. *Breast Cancer Res* *14*, R134.

Sherr, C. J., and Roberts, J. M. (1995). Inhibitors of mammalian G1 cyclin-dependent kinases. *Genes Dev* *9*, 1149-1163.

Shieh, S. Y., Ikeda, M., Taya, Y., and Prives, C. (1997). DNA damage-induced phosphorylation of p53 alleviates inhibition by MDM2. *Cell* *91*, 325-334.

Shiojiri, N. (1981). Enzymo- and immunocytochemical analyses of the differentiation of liver cells in the prenatal mouse. *J Embryol Exp Morphol* *62*, 139-152.

Si-Hoe, S. L., Wells, S., and Murphy, D. (2001). Production of transgenic rodents by the microinjection of cloned DNA into fertilized one-cell eggs. *Mol Biotechnol* *17*, 151-182.

Si-Tayeb, K., Lemaigre, F. P., and Duncan, S. A. (2010). Organogenesis and development of the liver. *Dev Cell* *18*, 175-189.

Sicinski, P., Donaher, J. L., Parker, S. B., Li, T., Fazeli, A., Gardner, H., Haslam, S. Z., Bronson, R. T., Elledge, S. J., and Weinberg, R. A. (1995). Cyclin D1 provides a link between development and oncogenesis in the retina and breast. *Cell* 82, 621-630.

Sleeman, K. E., Kendrick, H., Robertson, D., Isacke, C. M., Ashworth, A., and Smalley, M. J. (2007). Dissociation of estrogen receptor expression and in vivo stem cell activity in the mammary gland. *J Cell Biol* 176, 19-26.

Smith, J., Tho, L. M., Xu, N., and Gillespie, D. A. (2010). The ATM-Chk2 and ATR-Chk1 pathways in DNA damage signaling and cancer. *Adv Cancer Res* 108, 73-112.

Smithies, O., Gregg, R. G., Boggs, S. S., Koralewski, M. A., and Kucherlapati, R. S. (1985). Insertion of DNA sequences into the human chromosomal beta-globin locus by homologous recombination. *Nature* 317, 230-234.

Solomon, M. J., Lee, T., and Kirschner, M. W. (1992). Role of phosphorylation in p34cdc2 activation: identification of an activating kinase. *Mol Biol Cell* 3, 13-27.

Sorlie, T., Perou, C. M., Tibshirani, R., Aas, T., Geisler, S., Johnsen, H., Hastie, T., Eisen, M. B., van de Rijn, M., Jeffrey, S. S., *et al.* (2001). Gene expression patterns of breast carcinomas distinguish tumor subclasses with clinical implications. *Proc Natl Acad Sci U S A* 98, 10869-10874.

Spike, B. T., Engle, D. D., Lin, J. C., Cheung, S. K., La, J., and Wahl, G. M. (2012). A mammary stem cell population identified and characterized in late embryogenesis reveals similarities to human breast cancer. *Cell Stem Cell* 10, 183-197.

Steinman, R. A., Hoffman, B., Iro, A., Guillouf, C., Liebermann, D. A., and el-Houseini, M. E. (1994). Induction of p21 (WAF-1/CIP1) during differentiation. *Oncogene* 9, 3389-3396.

Sternlicht, M. D. (2006). Key stages in mammary gland development: the cues that regulate ductal branching morphogenesis. *Breast Cancer Res* 8, 201.

Stewart, T. A., Pattengale, P. K., and Leder, P. (1984). Spontaneous mammary adenocarcinomas in transgenic mice that carry and express MTV/myc fusion genes. *Cell* 38, 627-637.

Stingl, J., Eirew, P., Ricketson, I., Shackleton, M., Vaillant, F., Choi, D., Li, H. I., and Eaves, C. J. (2006). Purification and unique properties of mammary epithelial stem cells. *Nature* 439, 993-997.

Strange, R., Li, F., Saurer, S., Burkhardt, A., and Friis, R. R. (1992). Apoptotic cell death and tissue remodelling during mouse mammary gland involution. *Development* 115, 49-58.

Suksaweang, S., Lin, C. M., Jiang, T. X., Hughes, M. W., Widelitz, R. B., and Chuong, C. M. (2004). Morphogenesis of chicken liver: identification of localized growth zones and the role of beta-catenin/Wnt in size regulation. *Dev Biol* 266, 109-122.

Sun, D., Ren, H., Oertel, M., Sellers, R. S., and Zhu, L. (2007a). Loss of p27Kip1 enhances tumor progression in chronic hepatocyte injury-induced liver tumorigenesis with widely ranging effects on Cdk2 or Cdc2 activation. *Carcinogenesis* 28, 1859-1866.

Sun, Y., Chen, X., and Xiao, D. (2007b). Tetracycline-inducible expression systems: new strategies and practices in the transgenic mouse modeling. *Acta Biochim Biophys Sin (Shanghai)* 39, 235-246.

Takahashi, Y., Soejima, Y., and Fukusato, T. (2012). Animal models of nonalcoholic fatty liver disease/nonalcoholic steatohepatitis. *World J Gastroenterol* 18, 2300-2308.

Tan, X., Yuan, Y., Zeng, G., Apte, U., Thompson, M. D., Cieply, B., Stolz, D. B., Michalopoulos, G. K., Kaestner, K. H., and Monga, S. P. (2008). Beta-catenin deletion in hepatoblasts disrupts hepatic morphogenesis and survival during mouse development. *Hepatology* 47, 1667-1679.

Tang, J., Fernandez-Garcia, I., Vijayakumar, S., Martinez-Ruis, H., Illa-Bochaca, I., Nguyen, D. H., Mao, J. H., Costes, S. V., and Barcellos-Hoff, M. H. (2014). Irradiation of juvenile, but not adult, mammary gland increases stem cell self-renewal and estrogen receptor negative tumors. *Stem Cells* 32, 649-661.

Tannapfel, A., Grund, D., Katalinic, A., Uhlmann, D., Kockerling, F., Haugwitz, U., Wasner, M., Hauss, J., Engeland, K., and Wittekind, C. (2000). Decreased expression of p27 protein is associated with advanced tumor stage in hepatocellular carcinoma. *Int J Cancer* 89, 350-355.

The National Digestive Diseases Information Clearinghouse (2014). Nonalcoholic Steatohepatitis. In.

Thomas, K. R., and Capecchi, M. R. (1986). Introduction of homologous DNA sequences into mammalian cells induces mutations in the cognate gene. *Nature* 324, 34-38.

Thomas, K. R., and Capecchi, M. R. (1987). Site-directed mutagenesis by gene targeting in mouse embryo-derived stem cells. *Cell* 51, 503-512.

Thorgeirsson, S. S., and Santoni-Rugiu, E. (1996). Transgenic mouse models in carcinogenesis: interaction of c-myc with transforming growth factor alpha and hepatocyte growth factor in hepatocarcinogenesis. *Br J Clin Pharmacol* 42, 43-52.

Tremblay, K. D., and Zaret, K. S. (2005). Distinct populations of endoderm cells converge to generate the embryonic liver bud and ventral foregut tissues. *Dev Biol* 280, 87-99.

Turner, N. C., and Reis-Filho, J. S. (2006). Basal-like breast cancer and the BRCA1 phenotype. *Oncogene* 25, 5846-5853.

Vaillant, F., Lindeman, G. J., and Visvader, J. E. (2011). Jekyll or Hyde: does Matrigel provide a more or less physiological environment in mammary repopulating assays? *Breast Cancer Res* 13, 108.

Venook, A. P., Papandreou, C., Furuse, J., and de Guevara, L. L. (2010). The incidence and epidemiology of hepatocellular carcinoma: a global and regional perspective. *Oncologist* 15 Suppl 4, 5-13.

Vermeulen, K., Van Bockstaele, D. R., and Berneman, Z. N. (2003). The cell cycle: a review of regulation, deregulation and therapeutic targets in cancer. *Cell Prolif* 36, 131-149.

Viola-Magni, M. P. (1972). Synthesis and turnover of DNA in hepatocytes of neonatal rats. *J Microsc* 96, 191-203.

Visvader, J. E. (2009). Keeping abreast of the mammary epithelial hierarchy and breast tumorigenesis. *Genes Dev* 23, 2563-2577.

- Visvader, J. E., and Lindeman, G. J. (2006). Mammary stem cells and mammapoiesis. *Cancer Res* 66, 9798-9801.
- Visvader, J. E., and Stingl, J. (2014). Mammary stem cells and the differentiation hierarchy: current status and perspectives. *Genes Dev* 28, 1143-1158.
- Voziyanov, Y., Pathania, S., and Jayaram, M. (1999). A general model for site-specific recombination by the integrase family recombinases. *Nucleic Acids Res* 27, 930-941.
- Wagner, K. U., Boulanger, C. A., Henry, M. D., Sgagias, M., Hennighausen, L., and Smith, G. H. (2002). An adjunct mammary epithelial cell population in parous females: its role in functional adaptation and tissue renewal. *Development* 129, 1377-1386.
- Wagner, K. U., Wall, R. J., St-Onge, L., Gruss, P., Wynshaw-Boris, A., Garrett, L., Li, M., Furth, P. A., and Hennighausen, L. (1997). Cre-mediated gene deletion in the mammary gland. *Nucleic Acids Res* 25, 4323-4330.
- Wang, K., Lim, H. Y., Shi, S., Lee, J., Deng, S., Xie, T., Zhu, Z., Wang, Y., Pocalyko, D., Yang, W. J., *et al.* (2013). Genomic landscape of copy number aberrations enables the identification of oncogenic drivers in hepatocellular carcinoma. *Hepatology* 58, 706-717.
- Wang, T. C., Cardiff, R. D., Zukerberg, L., Lees, E., Arnold, A., and Schmidt, E. V. (1994). Mammary hyperplasia and carcinoma in MMTV-cyclin D1 transgenic mice. *Nature* 369, 669-671.
- Watson, C. J. (2006). Involution: apoptosis and tissue remodelling that convert the mammary gland from milk factory to a quiescent organ. *Breast Cancer Res* 8, 203.
- Webber, E. M., Bruix, J., Pierce, R. H., and Fausto, N. (1998). Tumor necrosis factor primes hepatocytes for DNA replication in the rat. *Hepatology* 28, 1226-1234.
- Webber, E. M., Godowski, P. J., and Fausto, N. (1994). In vivo response of hepatocytes to growth factors requires an initial priming stimulus. *Hepatology* 19, 489-497.
- Williams, J. M., and Daniel, C. W. (1983). Mammary ductal elongation: differentiation of myoepithelium and basal lamina during branching morphogenesis. *Dev Biol* 97, 274-290.

World Health Organization (2014). Cancer. In.

Woychik, R. P., Stewart, T. A., Davis, L. G., D'Eustachio, P., and Leder, P. (1985). An inherited limb deformity created by insertional mutagenesis in a transgenic mouse. *Nature* 318, 36-40.

Xu, X., Wagner, K. U., Larson, D., Weaver, Z., Li, C., Ried, T., Hennighausen, L., Wynshaw-Boris, A., and Deng, C. X. (1999). Conditional mutation of *Brcal* in mammary epithelial cells results in blunted ductal morphogenesis and tumour formation. *Nat Genet* 22, 37-43.

Yahagi, N., Shimano, H., Matsuzaka, T., Sekiya, M., Najima, Y., Okazaki, S., Okazaki, H., Tamura, Y., Iizuka, Y., Inoue, N., *et al.* (2004). p53 involvement in the pathogenesis of fatty liver disease. *J Biol Chem* 279, 20571-20575.

Zhang, Q., Triplett, A. A., Harms, D. W., Lin, W. C., Creamer, B. A., Rizzino, A., and Wagner, K. U. (2010). Temporally and spatially controlled expression of transgenes in embryonic and adult tissues. *Transgenic Res* 19, 499-509.

Zhao, R., and Duncan, S. A. (2005). Embryonic development of the liver. *Hepatology* 41, 956-967.

Zhu, Z., Zheng, T., Lee, C. G., Homer, R. J., and Elias, J. A. (2002). Tetracycline-controlled transcriptional regulation systems: advances and application in transgenic animal modeling. *Semin Cell Dev Biol* 13, 121-128.

Zorn, A. M. (2008). Liver development.

Zucchi, I., Mento, E., Kuznetsov, V. A., Scotti, M., Valsecchi, V., Simionati, B., Vicinanza, E., Valle, G., Pilotti, S., Reinbold, R., *et al.* (2004). Gene expression profiles of epithelial cells microscopically isolated from a breast-invasive ductal carcinoma and a nodal metastasis. *Proc Natl Acad Sci U S A* 101, 18147-18152.

Chapter 2

MMTV-Spy1 Mice Demonstrate Increased Susceptibility to Mammary Tumourigenesis

Introduction

The ability of a cell to sense and repair DNA damage is crucial to prevent the accumulation of DNA damage, deleterious mutations, and progression to carcinogenesis. The DNA damage response pathway is a large network of signaling cascades that trigger cell cycle arrest once damage is detected (Sancar et al., 2004). Upon cell cycle arrest, the appropriate repair mechanism is activated, and once damage is repaired, the cell is allowed to re-enter the cell cycle. If the damage is extensive, the cell has the option to trigger apoptosis, removing the cell from the population and thereby eliminating the deleterious mutation. The tumour suppressor p53 lies at the heart of this process and plays a critical role in regulating cell growth and repair (Bartek and Lukas, 2001; Meek, 2004; Sakaguchi et al., 1998). In the event of DNA damage, levels of p53 begin to accumulate within the cell leading to cell cycle arrest and DNA repair (Meek, 2004; Sakaguchi et al., 1998; Shieh et al., 1997). In cases of irreparable damage, p53 can trigger apoptosis, leading to removal of the cell thereby preventing the accumulation of damaged cells which could ultimately lead to carcinogenesis (Meek, 2004; Sancar et al., 2004). Thus p53 plays a crucial role as a cell cycle regulator. This is highlighted by the observation that over 50% of human cancers contain a mutation of p53, indicating that loss or abrogation of p53 function may confer an advantage to cancerous cells (Soussi et al., 2006). Additionally, individuals with Li-Fraumeni syndrome, a disease characterized by germline mutations in p53, are at an increased risk of developing cancer, with the most common types including bone, breast and cancers of soft tissue (Akashi and Koeffler, 1998). Mouse models with germline knockout of p53 develop normally however develop spontaneous tumours at an increased rate (Donehower et al., 1992; Hutchinson and Muller, 2000; Jacks et al., 1994; Purdie et al., 1994). Taken together, this highlights the importance of the proper function of all proteins which mediate cell cycle progression, arrest and DNA repair in preventing the onset of tumorigenesis.

Spy1 is an atypical cyclin-like protein capable of promoting progression through G1/S phase of the cell cycle by binding and activating Cdk2 independent of the canonical

phosphorylation status (Cheng et al., 2005; Karaïskou et al., 2001; Porter et al., 2002). Spy1 was initially discovered in a screen for genes that would confer resistance to UV radiation in a rad1 deficient strain of *S.pombe*, indicating a critical role for Spy1 in the DNA damage response (Lenormand et al., 1999). Upon exposure to DNA damaging agents, Spy1 has been shown to increase cell survival, and this effect is dependent on its ability to bind and activate CDK2 (Barnes et al., 2003; Gastwirt et al., 2006). Endogenously, Spy1 levels increase following damage and knockdown of Spy1 decreases cell survival after exposure to DNA damaging agents (Barnes et al., 2003; Gastwirt et al., 2006; McAndrew et al., 2009). Proper activation of checkpoint signaling is crucial for both repair and apoptotic events following damage. Overexpression of Spy1 inhibits both S and G2/M phase checkpoint activation, allowing for continued cell division in the presence of damage (Gastwirt et al., 2006). Spy1 prevents phosphorylation of key mediators of the DNA damage response (DDR) such as H2AX, Chk1 and RPA32 thereby inhibiting the activity of proper checkpoint responses (Gastwirt et al., 2006; McAndrew et al., 2009). Spy also overrides apoptosis, and its ability to do so is dependent on p53 (McAndrew et al., 2009). Thus, Spy1 serves as an important mediator of the DDR in maintaining the proper balance of cellular proliferation and may play a crucial role in the transition from precancerous to cancerous cell.

Previous data have demonstrated that Spy1 protein levels are tightly regulated through the course of mammary gland development (Golipour et al., 2008). Levels are high during proliferative stages of development and are drastically downregulated at the onset of differentiation (Golipour et al., 2008). Interestingly, levels once again rise at the onset of involution, a period of development characterized by apoptosis (Golipour et al., 2008). Overexpression of Spy1 leads to precocious development of the mammary gland and disrupts normal morphogenesis (Golipour et al., 2008). When overexpressed in an *in vivo* setting, Spy1 accelerates mammary tumorigenesis (Golipour et al., 2008). To further highlight this finding, Spy1 has been found to be one of the 50 most upregulated genes in invasive ductal carcinoma of

the breast, and is elevated in human breast cancer samples (Al Sorkhy et al., 2012; Zucchi et al., 2004). In addition to breast cancer, elevated levels of Spy1 have been implicated in cancer of the brain, liver, and lymphoma (Hang et al., 2012; Ke et al., 2009; Lubanska et al., 2014). Although these data point to a critical role for Spy1 in regulating normal mammary development as well as tumour initiation, it is still not known what effects increased levels of Spy1 have on normal development of the mammary gland in an *in vivo* setting, or if Spy1 on its own is sufficient to drive tumorigenesis.

Herein, we describe the development of the first transgenic mouse model for Spy1 whereby we direct overexpression specifically to the mammary gland using the MMTV promoter. Using this model, we can study for the first time, the effects of altered Spy1 expression on normal and abnormal development of the mammary gland in a natural *in vivo* setting. Using a mouse strain resistant to mammary tumorigenesis, we show that the MMTV-Spy1 mice develop normally and show no gross alterations in mammary development. Treatment with 7,12-dimethylbenz(a)anthracene (DMBA) demonstrates that the MMTV-Spy1 mice are significantly more susceptible to mammary tumour formation and exhibit alterations in their DDR pathways. Increased susceptibility to tumorigenesis may in part be due to the interaction of Spy1 with the tumour suppressor p53 and its ability to overcome checkpoint responses in the event of DNA damage. Thus this data demonstrates that Spy1 is an important factor in breast cancer susceptibility and may play a key role in tumour initiation, due in part to its ability to override the DNA damage response.

Materials and Methods

Construction of Transgene

The MMTV-Spy1 transgene was prepared as follows. Site directed mutagenesis was utilized to create an additional EcoRI site in Flag-Spy1A-pLXSN (Porter et al., 2003) to allow for subsequent removal of the Spy1 coding sequence using EcoRI digestion. The MMTV-SV40-TRPS-1 vector (kind gift from Dr Gabriel E DiMattia) was digested with EcoRI to remove the TRPS-1 coding sequence to allow for subsequent ligation of the Spy1 coding sequence into the MMTV-SV40 backbone.

Generation and Maintenance of MMTV-Spy1 Transgenic Mice

The MMTV-Spy1 vector was digested with XhoI and SpeI to isolate the MMTV-Spy1 transgene fragment and remove the remainder of the vector backbone. The transgene was sent to the London Regional Transgenic and Gene Targeting Facility where pronuclear injections were performed in B6CBAF1/J hybrid embryos. Identification of founders and subsequent identification of positive pups was performed by PCR analysis. PCR was performed by adding 50ng of genomic tail DNA to a 25µL reaction (1x PCR buffer, 2mM MgSO₄, 0.2mM dNTP, 0.04U/µL UBI Taq Polymerase, 0.4µM forward primer [5'CCCAAGGCTTAAGTAAGTTTTTGG 3'], 0.4µM reverse primer [5'GGGCATAAGCACAGATAAAACACT 3'], 1% DMSO) (NCI Mouse Repository). Cycling conditions were as follows: 94°C for 3 minutes, 40 cycles of 94°C for 1 minute, 55°C for 2 minutes, and 72°C for 1 minute, and a final extension of 72°C for 3 minutes. Mice were maintained following the Canadian Council on Animal Care Guidelines under the animal utilization protocol 10-16 approved by the University of Windsor.

Primary Cell Harvest and Culture

Mammary tissue of the inguinal gland was dissected and primary cells were isolated as described (Mroue and Bissell, 2013). Briefly, tissue was digested in a collagenase solution, and the resulting suspension was spun at 1500rpm for 10 minutes. To ensure a clean epithelial culture, a series of 4 to 10 pulses were performed at 1500rpm while the resulting pellet from each pulse was monitored for the presence of organoids and single cells. For mammosphere formation assays, cells were seeded in ultra-low attachment 6 well plates at a plating density of 20,000 cells per mL in media containing 20ng/mL bFGF, 20ng/ μ L EGF, 100 μ g/mL gentamycin, 1% P/S in DMEM-F12. Mammospheres were allowed to form for 7 days before quantification. Cells were also seeded on attachment plates in media containing 5% fetal bovine serum, 5ng/mL EGF, 5 μ g/mL insulin, 50 μ g/mL gentamycin, 1% P/S in DMEM-F12 for BrdU incorporation assays conducted 1 week after isolation of the cells.

Cell Culture

Human embryonic kidney cells, HEK-293 (CRL-1573; ATCC) and NIH/3T3 cells, were cultured in Dulbecco's Modified Eagle's Medium (DMEM; D5796; Sigma Aldrich) supplemented with 10% fetal bovine serum (FBS; F1051; Sigma Aldrich) and 10% calf serum (C8056; Sigma Aldrich) respectively, and 1% penicillin/streptomycin. U-2 OS and Saos-2, human osteosarcoma cells (provided by Dr. J. Hudson, University of Windsor) and human colon carcinoma cell lines, HCT116 p21^{+/+}, p21^{-/-}, p53^{-/-}, and Chk2^{-/-} (provided by Dr. B. Vogelstein, Johns Hopkins) were maintained in McCoy's 5A 1X medium (10-050-CV; Cellgro-Mediatech) with 10% FBS and 1% penicillin/streptomycin. Mouse mammary epithelial cells, HC11 (provided by Dr. C. Shemanko) were maintained in RPMI supplemented with 10% newborn calf serum, 5 μ g/mL insulin, 10ng/mL EGF and 1% penicillin/streptomycin. All cell lines were maintained at 5% CO₂ at 37°C. A BioRad TC10 Automated Cell Counter was used to assess cell viability via trypan blue exclusion.

Plasmids

The pEIZ plasmid was a kind gift from Dr B. Welm, and the pEIZ-Flag-Spy1 vector was generated as previously described (Lubanska et al., 2014). pCS3 and Myc-Spy1-pCS3 plasmids were generated as previously described (Porter et al., 2002), and the p53-GFP backbone was purchased from Add-Gene (11770) and was utilized in p53 overexpression experiments in mammary cell lines. The Flag-p53-pcDNA3 construct was purchased from Addgene (#10838) and was used in p53 overexpression experiments in all other cell lines.

Transfection and Infection

Transfection of all mammary cell lines was performed as follows. Plasmids were transiently transfected using 25µg of polyethylenimine (PEI) and 12ug of plasmid DNA. PEI and DNA were allowed to incubate at room temperature for 10 minutes in base media before being added to the plate. Transfection reagent was left on for 16-18 hours before being removed. HC11 cells were transfected in serum and antibiotic free media.

For transfection of NIH3T3, U-2 OS, Saos2 and HCT116 cell lines, jetPRIME transfection reagent (CA89129-922; VWR) was utilized. Briefly, 4µg DNA was added to 200µl of jetPRIME buffer and subsequently vortexed. 4µl jetPRIME was then added and the mixture was vortexed again and incubated at room temperature for 10 minutes. Following incubation, the mixture was added to the plate in a drop wise fashion and cells were incubated at 37⁰C for at least 24 hours.

Transfection of primary mouse cell lines with sip53 and siRNA control (Santa Cruz) was performed using siRNA Transfection Reagent (Santa Cruz) as per manufacturer's instructions.

UV Irradiation

Media was removed from exponentially growing cells and cells were washed once with 1X PBS and subjected to ultraviolet (UV) radiation using a GS Gene Linker (Bio Rad). Immediately following irradiation, fresh medium was added to the cells.

DMBA Treatments

Mice were given 1mg of DMBA (Sigma Aldrich) in 100 μ L of a sesame:corn oil mixture (4:1 ratio) via oral gavage once per week. Treatment began when mice reached 8 weeks of age and were continued for 6 consecutive weeks. After completion of the treatment, mice were monitored on a weekly basis for the presence of tumours via palpitations. Mice were humanely sacrificed when tumours were noted, and all mice were sacrificed by 8 months of age regardless of tumour formation. Tissues were collected from sacrificed mice and were flash frozen for immunoblotting and qRT-PCR analysis, or were fixed in formalin for immunohistochemistry.

Histology and Immunostaining

Tissue was collected and fixed in 10% neutral buffered formalin. Tissue was dehydrated through a series of ascending ethanol concentrations and was subsequently cleared in xylene. Following clearing in xylene, samples were embedded in paraffin wax and sectioned into 5 μ m thick sections using Leica RM2125RT. Prior to staining, sections were rehydrated through a series of descending ethanol concentrations and heat mediated antigen retrieval was performed using 10mM sodium citrate buffer pH 6.0. Endogenous peroxidase activity was blocked with a 3% H₂O₂ solution diluted in methanol, and sections were blocked for 1 hour at room temperature in a humidified chamber with Mouse on Mouse (MOM) blocker (Biocare Medical) or 3% BSA-0.1% Tween-20 in 1x PBS for antibodies with mouse or rabbit secondary antibodies respectively. Sections were incubated in primary antibody diluted in blocking solution overnight at 4°C, followed by 3 washes with 1x PBS. Secondary antibody at a concentration of 1:750 was diluted

in blocking solution and sections were incubated in secondary antibody for 1 hour at room temperature in a humidified chamber. Sections were washed and subsequently incubated with ABC reagent as per manufacturer's instructions (Vectastain ABC Kit; 30 min in ABC reagent). Following addition of the ABC reagent, sections were stained with DAB following manufacturer's instructions (DAB Peroxidase Substrate Kit, Vector Laboratories), and were counterstained with haematoxylin (Vector Laboratories). Sections were dehydrated through a series of descending ethanol concentrations and were coverslipped using Permount toluene solution (Fisher Scientific), and imaged using the LEICA DMI6000 inverted microscope with LAS 3.6 software.

Quantitative Real Time PCR Analysis

RNA was isolated using Qiagen RNeasy Plus Mini Kit as per manufacturer's instructions. cDNA was synthesized using Superscript II (Invitrogen) as per manufacturer's instructions. SYBR Green detection (Applied Biosystems) was used to perform real time PCR and was performed and analyzed using Viia7 Real Time PCR System (Life Technologies) and software. Primers used were as follows:

Flag-Spy1 Forward: 5'TGACAAGAGGCACAATCAGATGT 3'

Flag-Spy1 Reverse: 5' CAAATAGGACGCTTCAGAGTAATGG3'

Human p53 Forward: 5' CCTGAGGTTGGCTCTGACTGTAC 3'

Human p53 Reverse: 5' TGGAGTCTTCCAGTGTGATGATG 3'

Human Spy1 Forward: 5' TTGTGAGGAGGTTATGGCCATT 3'

Human Spy1 Reverse: 5' GCAGCTGAACTTCATCTCTGTTGTAG 3'

Mouse GAPDH Forward: 5' GATGCCCCCATGTTTGTGAT 3'

Mouse GAPDH Reverse: 5' GTGGTCATGAGCCCTTCCA 3'

Protein Isolation and Immunoblotting

Flash frozen tissue was thawed and cut into small pieces. An appropriate amount of tissue lysis buffer (50mM Tris-HCl pH 7.5, 1% NP-40, 0.25% Na-deoxycholate, 1mM EGTA, 0.2% SDS, 150mM NaCl) with protease inhibitors (leupeptin 2µg/mL, aprotinin 5µg/mL, PMSF 100µg/mL) was added to the tissue. Tissue and lysis buffer were homogenized on ice using a Fisher Scientific Sonic Dismembrator 50. Homogenized tissue was flash frozen in liquid nitrogen and subsequently thawed on ice. Samples were centrifuged at 13000rpm for 20 minutes at 4°C. Supernatant was collected and centrifuged again at 13000rpm for 20 minutes at 4°C to remove any excess fat from the lysate. Supernatant was collected and stored at -20°C until future use. Cells were lysed with TNE buffer (50mM Tris, 150mM NaCl, 5mM EDTA) with protease inhibitors (leupeptin 2µg/mL, aprotinin 5µg/mL, PMSF 100µg/mL). Cells were lysed for 20 minutes on ice, vortexing every 5 minutes. Cells were centrifuged at 4°C at 10,000rpm for 10 minutes, and supernatant was collected and stored at -20°C until further use.

Protein concentrations were assessed using the Bradford assay as per manufacturer's instructions, and equal amounts of protein were prepared for loading. Equal amounts of protein were loaded on a 10%-SDS polyacrylamide gel and were transferred to PVDF membranes at 30V for 2 hours using wet transfer method. Membranes were blocked for 1 hour at room temperature in 1% BSA and were incubated in primary antibody overnight at 4°C. Membranes were washed three times in tris-buffered saline-tween 20 (TBST), 10 minutes each, following primary antibody incubation. Secondary antibody, at a concentration of 1:10,000, was used for 1 hour at room temperature and membranes were washed three times in TBST for 5 minutes each following secondary antibody incubation. Visualization was conducted using chemiluminescent peroxidase substrate (Pierce) as per manufacturer's instructions, and images were captured on Alpha Innotech HD 2 using AlphaEase FC software.

Antibodies

For western blot analysis, all primary antibodies were used at a concentration of 1:1000. Antibodies include Actin (Millipore), Spy1 (Abcam), and p53 (Abcam). Mouse IgG (Sigma Aldrich) and Rabbit IgG (Sigma Aldrich) were used at a concentration of 1:10,000. For immunohistochemical analysis, all primary antibodies were used at a concentration of 1:200 and were as follows, γ H2AX (Millipore), Spy1 (Abcam), and ki67 (Abcam). Biotinylated anti-mouse (Vector Laboratories) and biotinylated anti-rabbit (Vector Laboratories) were used at a concentration of 1:750.

BrdU Incorporation Assay

15,000 cells per well were seeded in a 96 well plate. BrdU (BD Pharmingen) was added 24 hours later to a final concentration of 10 μ M and cells were incubated in media containing BrdU for 24 hour at 37°C, 5% CO₂. Media containing BrdU was removed and cells were washed three times with 1x PBS. Cells were fixed in 4% PFA for 15 minutes and were washed twice with 1xPBS. Cells were incubated for 20 minutes at 37°C in 2M HCl and subsequently washed once with 1x PBS. Cells were incubated for 45 minutes with Anti-BrdU (BD Biosciences) in 0.2% Tween in 1x PBS. Cells were washed with 1x PBS and incubated with anti-mouse IgG and hoescht at a 1:1000 dilution in 1x PBS for 1 hour at room temperature. Cells were washed one time with 1x PBS followed by a wash with distilled water. Cells were stored at 4°C in 50% glycerol until ready to image using the LEICA DMI6000 inverted microscope.

Whole Mount Analysis

Briefly, the inguinal gland was spread onto a positively charged slide and left in Clarke's Fluid (75% ethyl alcohol, 25% acetic acid) overnight. The following day, glands were placed in 70% ethyl alcohol for 30 minutes before being stained in carmine alum (0.2% carmine, 0.5% potassium sulphate) overnight. Glands were destained for 4 to 6 hours with destaining solution

(1% HCl, 70% ethyl alcohol) and were subsequently dehydrated in ascending concentrations of alcohol (15 minutes each 70, 95, 100% ethyl alcohol) before being cleared in xylene overnight. Slides were mounted with Permount toluene solution (Fisher Scientific) before being examined on a Leica MZFLIII dissecting microscope (University of Windsor) and images were captured using Northern Eclipse software.

Results

Generation of MMTV-Spy1 transgenic mouse model system.

To study the effects of increased Spy1 expression within the mammary gland, a transgenic mouse model expressing Spy1 under the control of the MMTV-LTR promoter was generated. The Flag-Spy1 coding sequence was extracted from the previously described Flag-Spy1-pLXSN vector and was cloned into an MMTV-SV40 backbone (Figure 1A). Founder mice of the B6CBAF1/J background were identified via PCR analysis. Of the mice screened, three were identified as founders through the presence of an 825bp fragment, and all three were able to successfully transmit the transgene to their progeny (Supplemental Figure 1A). To determine if the MMTV-Spy1 mice expressed increased levels of Spy1 within the mammary gland, tissue was collected from 6 week old mice MMTV-Spy1 mice and their control littermates. Analysis of both mRNA and protein levels revealed that the MMTV-Spy1 mice contained significantly higher levels of Spy1 as compared to control littermates (Figure 1 B, C). Western blot analysis of other tissues did not show elevated levels of Spy1 in MMTV-Spy1 mice (Supplemental Figure 1B, C).

Previous data demonstrated that increased levels of Spy1 can disrupt the normal morphology of the mammary gland as well as promote accelerated development *in vivo* through the use of mammary fat pad transplantation (Golipour et al., 2008). To assess if the MMTV-Spy1 mice displayed any developmental abnormalities, whole mount and immunohistochemical analysis was conducted during puberty. Although immunohistochemical analysis revealed expression of Spy1 within the mammary gland, histopathological analysis only revealed slight phenotypic changes in the gland such as slight thickening of the ductal walls (Figure 1 D, E). Gross morphology of the gland was not altered in whole mount analysis (Supplemental Figure 2A, B) and through histological analysis. Additionally, all MMTV-Spy1 female mice successfully nursed their litters, even following multiple rounds of pregnancy, indicating that the overexpression of Spy1 does not significantly alter normal mammary gland development.

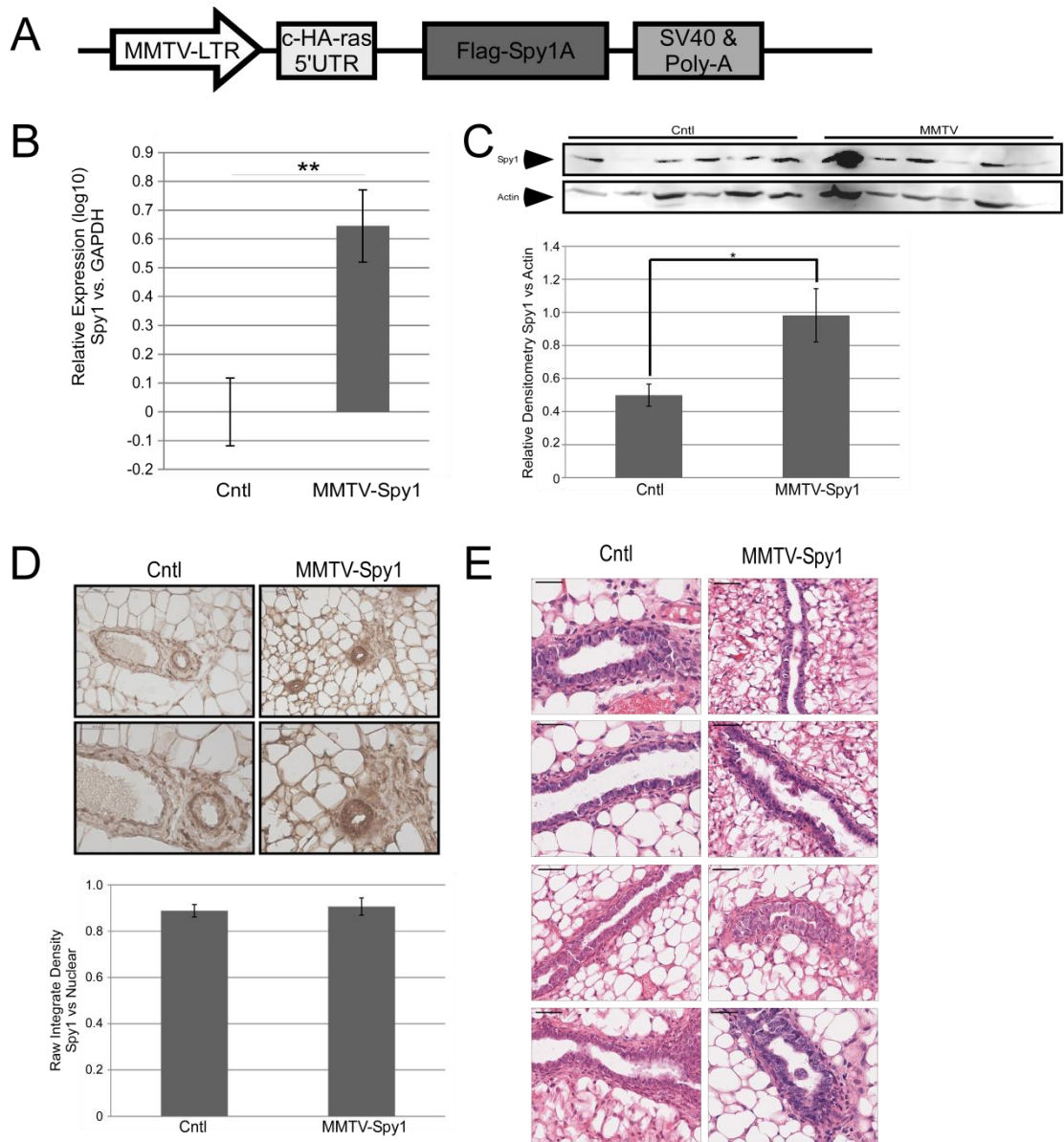
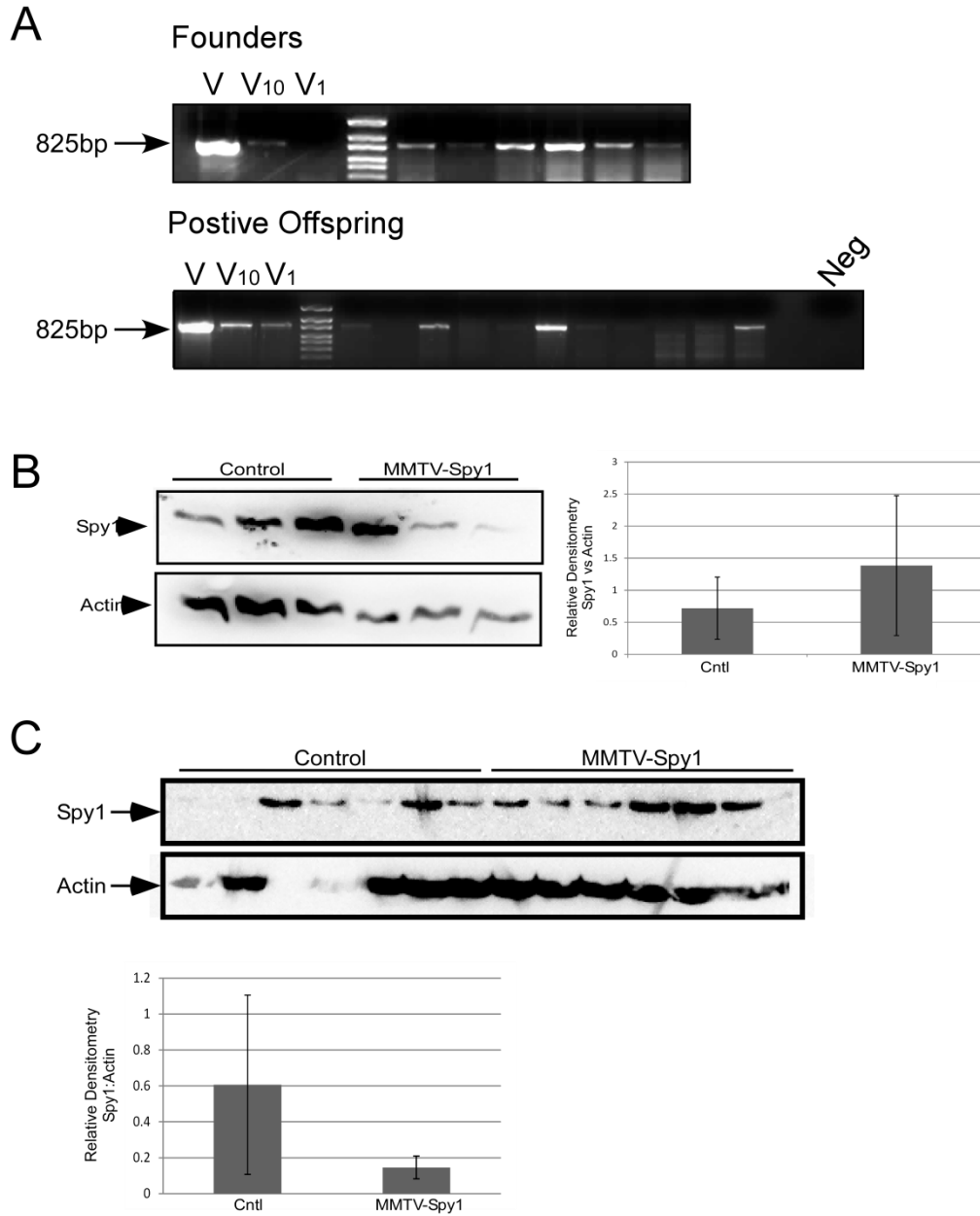
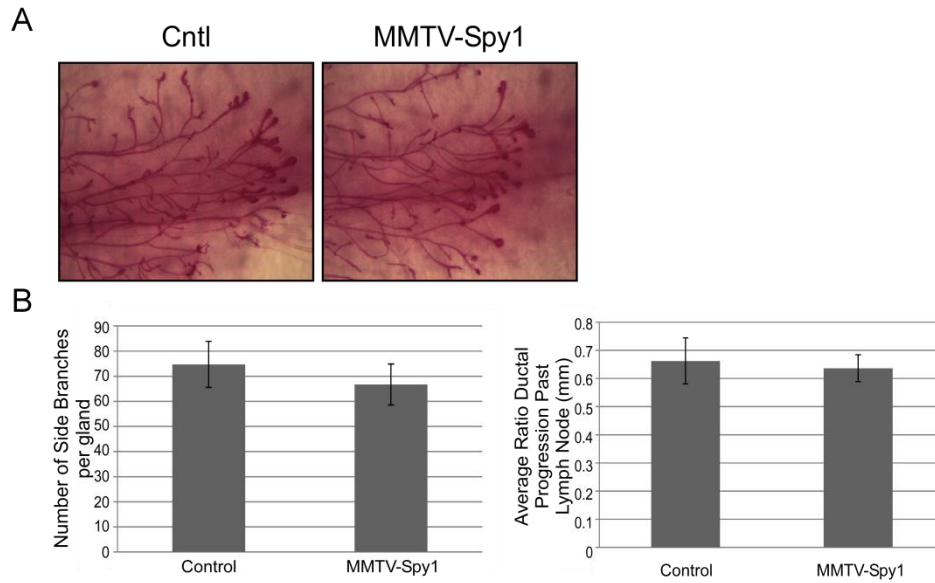


Figure 1: Generation of MMTV-Spy1 mouse model system. **A)** Schematic representation of the MMTV-Spy1 transgenic vector used in pronuclear injections for the generation of the MMTV-Spy1 mouse. **B)** qRT-PCR analysis of MMTV-Spy1 and littermate control (cntl) inguinal gland samples for Spy1 levels corrected for total levels of GAPDH. (n=8). **C)** Representative western blot of 6 week old MMTV-Spy1 inguinal glands for Spy1 levels (top panel). Levels of Spy1 protein were quantified and corrected for total Actin protein levels (bottom panel) (n=8). **D)** Representative Spy1 expression in 6 week old MMTV-Spy1 and control littermate (cntl) inguinal glands, where blue stain is haematoxylin and brown stain represents Spy1 expression. Representative images in upper panels with quantification of Spy1 levels using ImageJ software analysis shown in lower panel. Upper panels scale bar= 100 uM, lower panels scale bar= 50uM. **E)** Representative H&E stain of inguinal glands from 6 week old MMTV-Spy1 mice and control littermates (cntl). Scale bar= 50 uM Error bars reflect SE, Student's T-test *p=0.021015, **p=0.00164



Supplementary Figure 1: Characterization of MMTV-Spy1 mouse model system.

A) Blots showing PCR analysis to confirm presence of transgene in founder mice (upper blot) and in offspring from founders (lower blot) where V represents vector control, V₁₀ represents 10 copy vector control and V₁ represents 1 copy vector control. **B)** Representative western blot of 6 week old MMTV-Spy1 and littermate control (cntl) salivary glands for Spy1 levels (left panel). Quantification of densitometry analysis of Spy1 protein levels corrected for total Actin levels (right panel). (n=3) **C)** Representative western blot of 6 week old MMTV-Spy1 and littermate control (cntl) spleen for Spy1 levels (upper panel). Densitometry analysis of Spy1 protein levels corrected for total Actin levels is depicted in lower panel. (n=6). Error bars reflect SE.



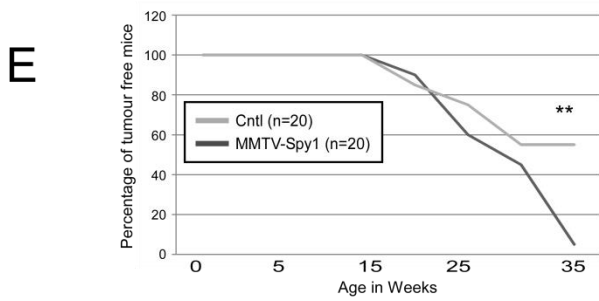
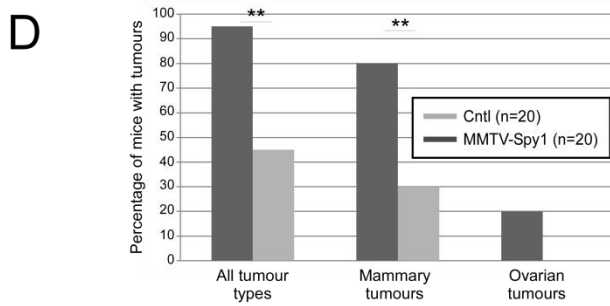
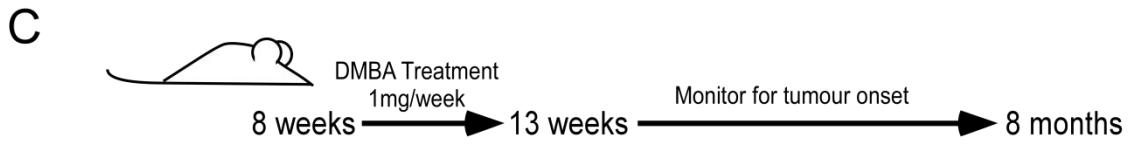
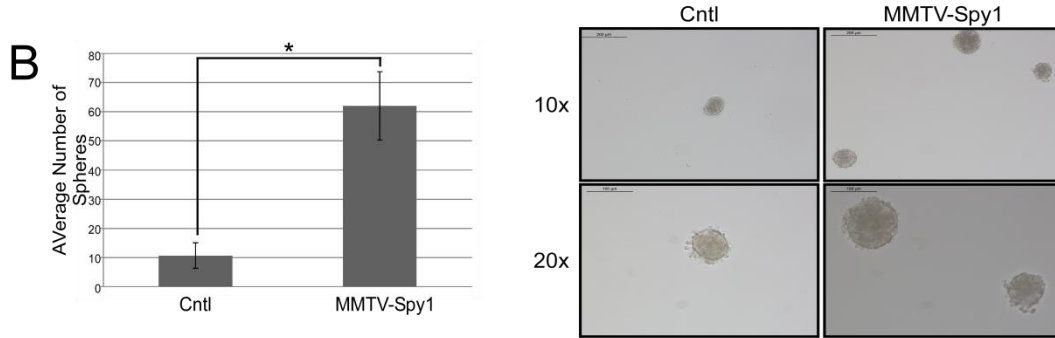
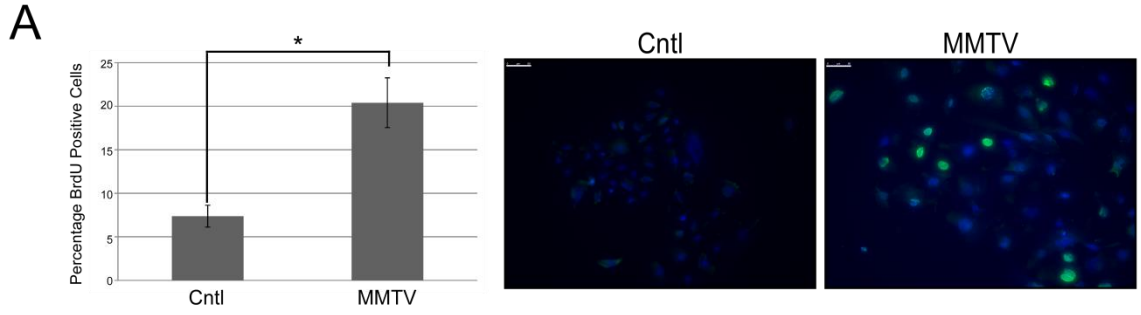
Supplementary Figure 2: Analysis of MMTV-Spy1 early development. **A)** Representative images of whole mount analysis from 6 week old MMTV-Spy1 and littermate control (cntl) B6CBAF1/J mice (Cntl n=4, MMTV-Spy1 n=4). **B)** Graphical representation of analysis of whole mount images from B6CBAF1/J inguinal glands from MMTV-Spy1 and littermate controls. Number of side branches per gland was quantified and the average number of side branches per gland was calculated (left panel). Ratio of ductal progression of ductal network past the lymph node was measured for each gland, and the average rate of ductal progression is shown in the right panel. Error bars represent SE.

Spy1 increases mammary tumour susceptibility.

Spy1 has been shown to increase cell proliferation in a variety of cell types when exogenously expressed (Al Sorkhy et al., 2012; Porter et al., 2002). To determine if Spy1 alters the proliferative characteristics of mammary epithelial cells in the MMTV-Spy1 mice, primary mammary epithelial cells were isolated from the inguinal glands of control and MMTV-Spy1 mice and were treated with BrdU. Cells extracted from MMTV-Spy1 mice displayed a significantly higher percentage of BrdU positive cells indicating increased proliferation (Figure 2A). In addition to its ability to enhance proliferation, Spy1 has also been demonstrated to alter stem cell characteristics in primary neural cells (Lubanska et al., 2014). Spy1 overexpression causes increased neurosphere formation in primary neural cells, as well, it has been demonstrated to promote stem cell self-renewal and tip the balance towards symmetric division in brain tumour cells (Lubanska et al., 2014). To determine if Spy1 alters the stem cell population within a mammary system, primary mammary epithelial cells were once again isolated from the inguinal glands of control and MMTV-Spy1 mice and were plated to select for mammosphere formation. MMTV-Spy1 mammary cells formed significantly more mammospheres than control cells indicating a potential role for Spy1 in regulating the mammary stem cell population (Figure 2B). Although elevated levels of Spy1 do not promote gross morphological changes in mammary development, they are capable of altering the characteristics of the cells within the gland.

Although cells extracted from MMTV-Spy1 mammary glands exhibit significant changes in both proliferative capacity and their ability to self-renew, MMTV-Spy1 mice develop normally and do not develop spontaneous tumours. Previous data has demonstrated that exogenous expression of Spy1 via mammary fat pad transplantation promotes mammary tumour formation, and increased levels of Spy1 have been implicated in breast cancer in addition to liver and brain (Al Sorkhy et al., 2012; Golipour et al., 2008; Ke et al., 2009; Lubanska et al., 2014). To assess whether or not elevated levels of Spy1 may affect tumour susceptibility, MMTV-Spy1 mice were treated with the known carcinogen 7,12-dimethylbenz(a)anthracene (DMBA). DMBA is

commonly used in rodent models to study the onset and timing of mammary tumour formation (Hoshino et al., 2007; Lee et al., 2008). MMTV-Spy1 mice and their control littermates were treated with DMBA once per week for 6 consecutive weeks during puberty (Figure 2C). Mice were monitored on a weekly basis for tumour formation. Over 90% of MMTV-Spy1 mice developed tumours as compared to only 50% of control mice (Figure 2D). Additionally, over 80% of MMTV-Spy1 mice developed mammary tumours, significantly more than the approximately 30% of control mice which developed mammary tumours (Figure 2D). Interestingly, although not significant, ovarian tumours were noted only in MMTV-Spy1 mice (Figure 2D). While not significant, it was noted that MMTV-Spy1 mice began to develop tumours earlier than their control littermates (Figure 2E). Tumour tissue was sent for pathological analysis, and a wide range of tumour sub-types were noted (Figure 2F). When tumour subtype was further analysed, MMTV-Spy1 mice had significantly more malignant mammary tumours over littermate controls (Figure 2G). Overall, this data demonstrates that elevated levels of Spy1 increases susceptibility to mammary tumour formation.



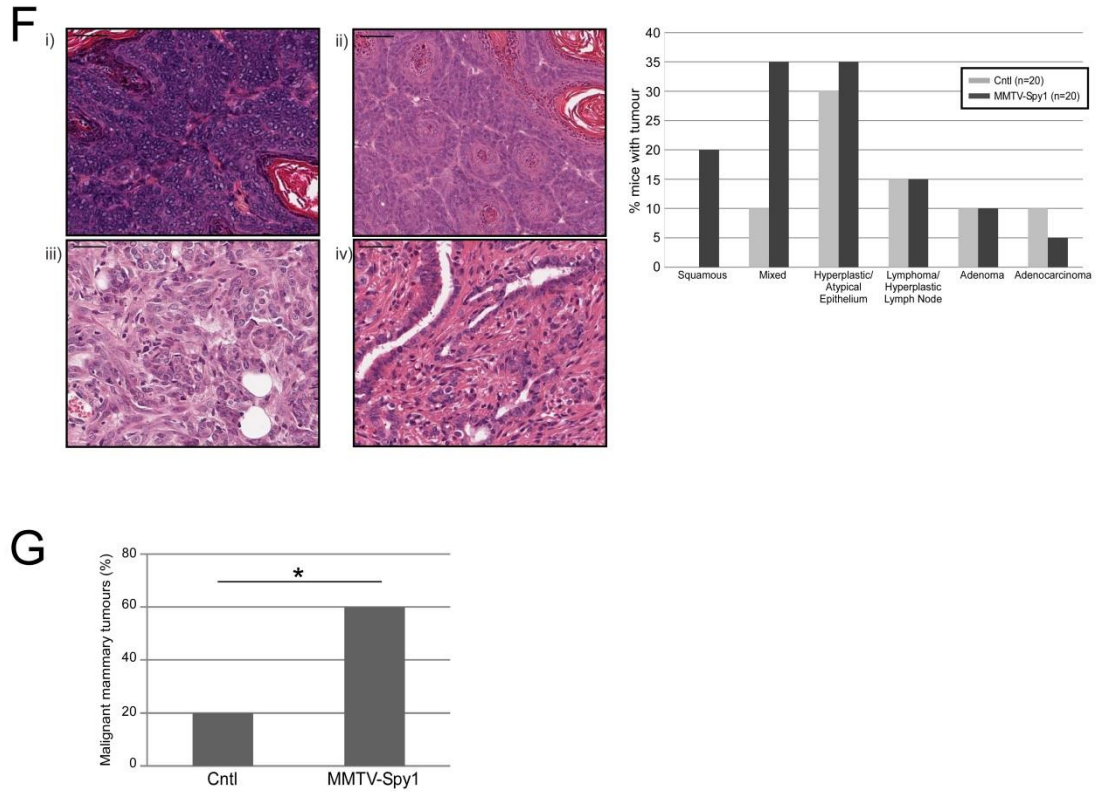


Figure 2: Spy1 overexpression leads to increased mammary tumour susceptibility
A) Representative images (right panel) and quantification of BrdU incorporation (left panel) of primary mammary epithelial cells isolated from MMTV-Spy1 mice and their control littermates (cntl) (n=4 separate isolations). Scale bar= 50 uM. **B)** Mammosphere formation assay using primary mammary epithelial cells from MMTV-Spy1 mice and their control littermates (cntl). Number of mammospheres formed was counted and average number of mammospheres was quantified (left panel). Representative images of mammosphere formation is depicted in right panel. (n=3 separate isolations) Upper panel scale bar= 200 uM, lower panel scale bar= 100uM. **C)** Schematic of DMBA treatment. **D)** Graphical representation of percentage of mice with tumours. **E)** Graphical representation of timing of tumour onset. **F)** Representative images of tumour pathology from DMBA induced mammary tumours (left panel; i) adenosquamous carcinoma, ii) pilar branching squamous cell carcinoma, iii) adenomyoepithelioma iv) adenofibromas and focal squamous pearls) and graphical representation of pathology results (right panel). Scale bar= 50 uM. **G)** Graphical representation of the number of mice with malignant mammary tumours. Error bars represent SE; **A & B**= Student's T-test, **D, E & F**= Mann-Whitney* $p < 0.05$, ** $p = 0.00714$

Spy1 expression disrupts the DDR in the presence of DMBA.

Spy1 was initially discovered in a screen for genes that could confer resistance to ultraviolet (UV) radiation in a rad-1 deficient strain of yeast (Lenormand et al., 1999). Given that DMBA is known to damage DNA, we sought to determine if the increased susceptibility observed was due to Spy1's ability to overcome the DDR and apoptosis (Barnes et al., 2003; Gastwirt et al., 2006; McAndrew et al., 2009). Mice were treated with DMBA at the time when the tumour treatment protocol would begin, and tissue was collected 48 hours later and analysed for alterations in known DNA damage response proteins. We observed that Spy1 was indeed significantly overexpressed in 8 week old MMTV-Spy1 mice with and without DMBA (Figure 3A). Levels of p53 were examined as p53 is a potent tumour suppressor and plays a key role in regulating many of the cellular processes involved in the DNA damage response (Meek, 2004). MMTV-Spy1 mice were found to have significantly increased levels of p53 in response to DMBA as compared to control littermates (Figure 3B). To determine if there was lingering DNA damage or a delay in the repair of damage, immunohistochemical analysis was performed to look for the presence of γ H2AX, a well-established marker of DNA damage (Dickey et al., 2009; Paull et al., 2000; Sedelnikova and Bonner, 2006). Significantly more γ H2AX positive cells were noted in MMTV-Spy1 mice indicating a lack of repair in response to DMBA (Figure 3C). Since Spy1 accelerates proliferation in mammary epithelial cells, expression of ki67, a known marker of proliferation, was determined in glands of MMTV-Spy1 mice and their control littermates to see if Spy1 induced accelerated proliferation in response to DMBA. Immunohistochemical analysis did not show any significant difference in the proliferative capacity of the cells (Figure 3D). This data demonstrates that elevated levels of Spy1 are capable of overriding DNA repair pathways leading to accumulation of DNA damage.

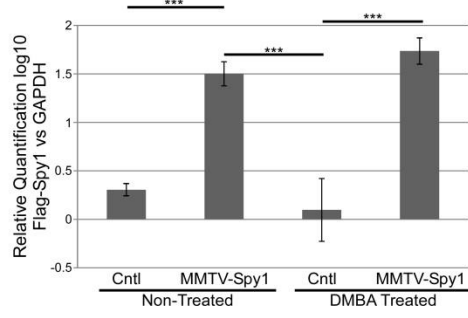
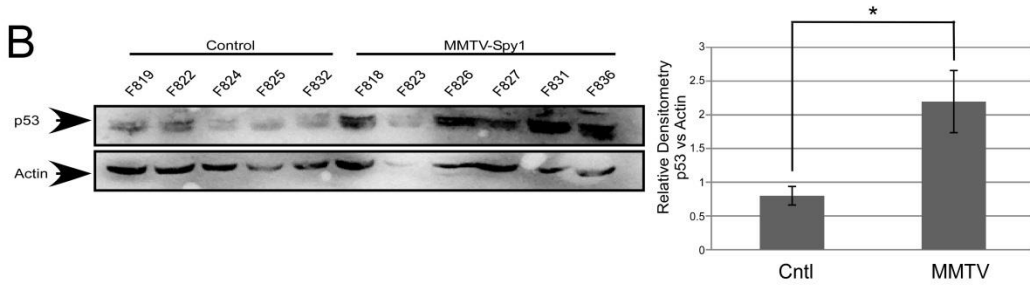
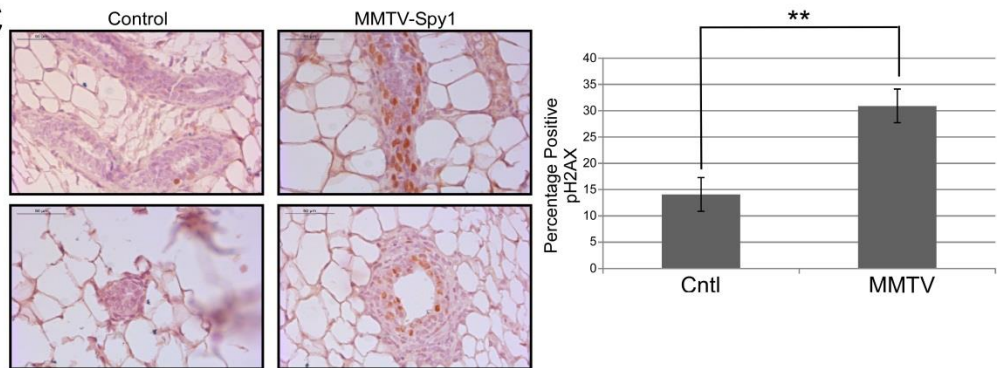
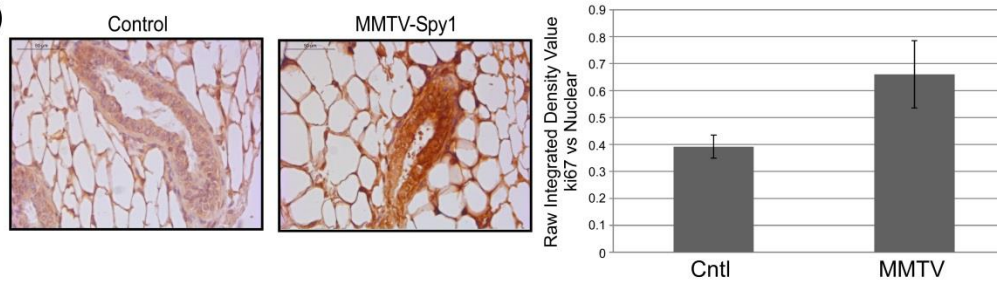
A**B****C****D**

Figure 3: MMTV-Spy1 mice show alterations in DDR pathway when exposed to DMBA. **A)** qRT-PCR analysis of Spy1 levels in 8 week old MMTV-Spy1 mice and their control littermates (cntl) 48 hours after DMBA treatment in mice with and without DMBA. Levels of Flag-Spy1 are corrected for total levels of GAPDH. **B)** Western blot for p53 levels in 8 week old mice 48 hours following DMBA exposure (left panel). Densitometry analysis is depicted in right panel with total p53 levels corrected for total levels of Actin. **C)** Representative images of immunohistochemical analysis of P-H2AX in inguinal glands of 8 week old MMTV-Spy1 and littermate control (cntl) mice after exposure to DMBA (left panel), where brown stain is P-H2AX and blue stain is haematoxylin. Number of P-H2AX positive cells were counted and quantified as percentage of P-H2AX cells (right panel). **D)** Representative images of immunohistochemical analysis of ki67 levels in inguinal glands of MMTV-Spy1 and littermate control (cntl) mice after exposure to DMBA (left panel), where brown stain is ki67 and blue stain is haematoxylin. Levels of ki67 were quantified using ImageJ analysis software correcting with haematoxylin stain (right panel). Scale bars= 50 μ M. Errors bars represent SE; Student's T-test. * $p=0.027785$, ** $p=0.00584$, *** $p<0.004$

Spy1 can override p53 in response to DNA damage.

The observed increase in p53 in response to DMBA in MMTV-Spy1 mice suggests a relationship between Spy1 and p53 in the DNA damage response. To further investigate this relationship, HC11 and NIH/3T3 cells, containing mutated p53 and wild-type p53 respectively, were transfected with Spy1, p53 or a combination of both and proliferation was assessed via trypan blue analysis (Figure 4A). Even in the presence of p53, Spy1 was still able to increase cell proliferation, although this was only significant in NIH/3T3 cells. Thus, the ability of Spy1 to enhance proliferation in the presence of p53 supports that Spy1 can overcome p53 induced cell cycle arrest.

Levels of Spy1 are tightly regulated in the DNA damage response.

To examine the endogenous regulation of Spy1 in response to DNA damage, U-2 OS cells, which have wild-type p53, were exposed to 30J/m² or 50J/m² of UV and levels of Spy1 and p53 protein were analysed (Figure 4B). In response to DNA damage, levels of Spy1 decreased, and further quantification revealed reciprocal expression of Spy1 and p53 protein levels. When Spy1 was exogenously expressed in multiple cells lines (U-2 OS, NIH/3T3, HCT116 parental and HCT116 p21^{-/-}) with varying alterations in repair pathways, downregulation of Spy1 was also observed in response to UV (Figure 4C), although this effect was not significant in HCT116 parental or p21^{-/-} cell line this downregulation is consistent with what was observed for endogenous Spy1 levels. These results support that Spy1 levels are downregulated in many cell types following DNA damage.

p53 negatively regulates Spy1 protein levels.

Levels of Spy1 and p53 demonstrate a reciprocal relationship in response to DNA damage. To assess if p53 is capable of triggering the downregulation of Spy1 protein levels, U-2 OS, HEK293, and NIH/3T3 were transfected with Spy1, p53 or Spy1 and p53 and levels of Spy1

protein were quantified (Figure 5). In every cell system studied, expression of p53 was sufficient to trigger downregulation of Spy1 protein levels, indicating that Spy1 downregulation in response to DNA damage may in part be mediated by p53.

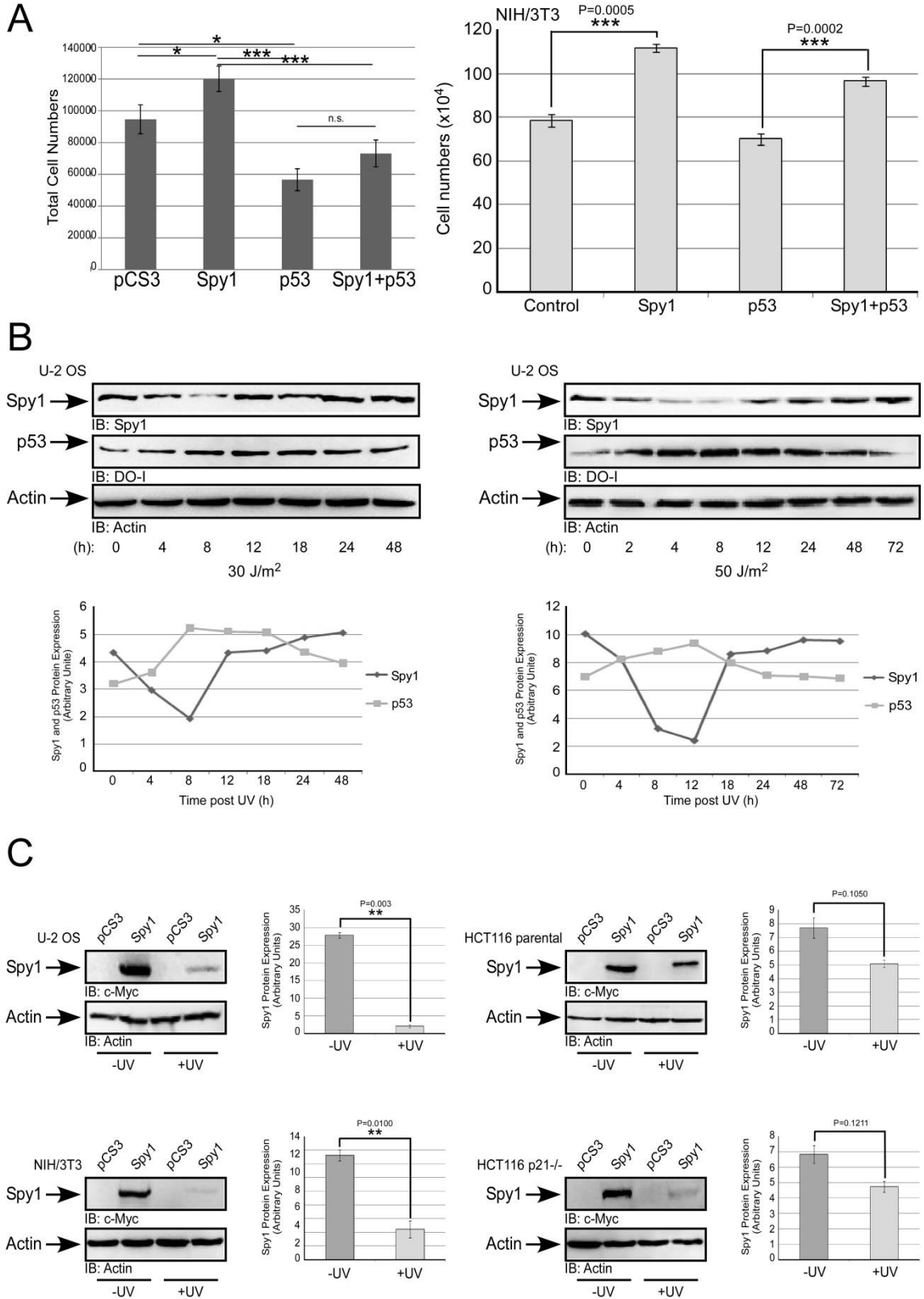


Figure 4: Endogenous and exogenous levels of Spy1 are controlled during DNA damage. A) HC11 (left) and NIH/3T3 (right) cells were transfected with vector control, Myc-Spy1-pCS3, Flag-p53 or Myc-Spy1-pCS3 and p53. Growth of cells following transfection was assessed via trypan blue analysis (n=3) **B)** Levels of endogenous Spy1 protein was assessed in U-2 OS cells following UV irradiation with either 30J/m² (left) or 50J/m². Western blot analysis was conducted for analysis of levels at the indicated time points in hours (h), and Spy1 and p53 protein levels were normalized to total Actin protein (lower panels). n>3. **C)** Levels of exogenous Spy1 was examined in U-2 OS, NIH/3T3, HCT116 parental or p21^{-/-} transfected with pCS3 or Myc-Spy1-pCS3. Cells were either untreated (left lanes) or UV irradiated with 50J/m² (right lanes), and collected after 24 hours for Western blot analysis. Densitometry analysis of Spy1 protein levels was corrected for total Actin levels (right panel) n=3. Error bars represent SE; Student's T-test. *p<0.05, **p≤0.01, ***p≤0.001.

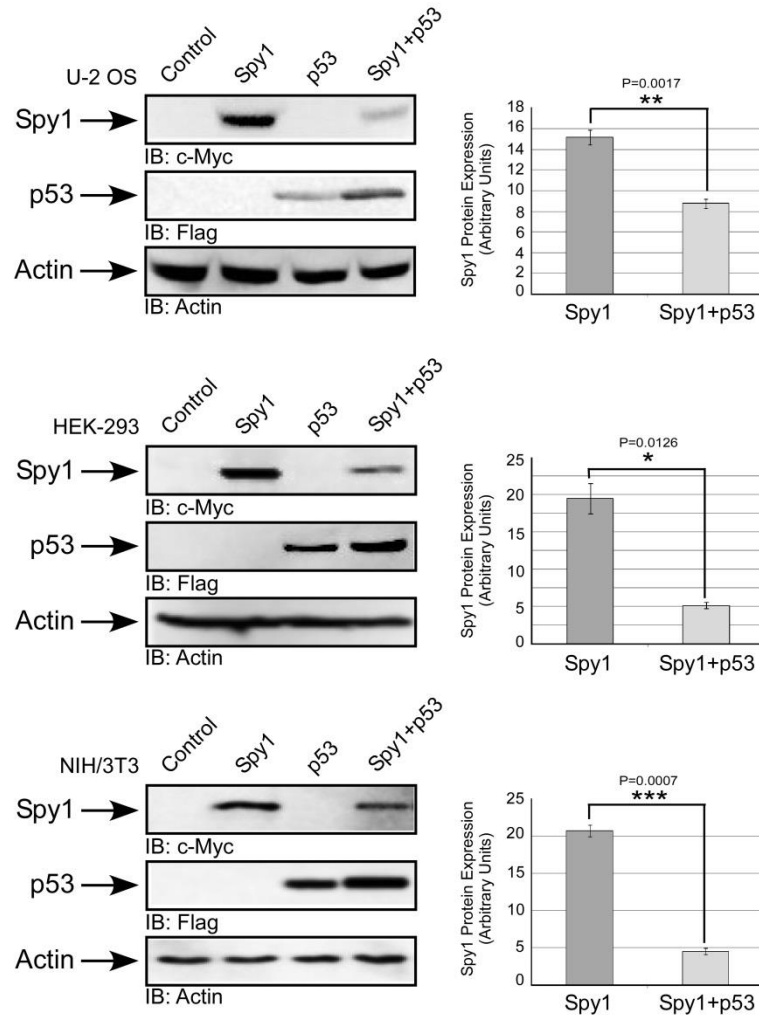


Figure 5. Intact DDR pathway creates a negative feedback loop for Spy1. Levels of Spy1 protein were assessed in U-2 OS, HEK-293 and NIH/3T3 cells after transfection with control vectors Myc-pCS3 and pcDNA3, and Myc-Spy1-pCS3, Flag-p53 or with both Myc-Spy1-pCS3 and Flag-p53. Cells were collected and subjected to Western blot analysis 24 hours after transfection (left panels). Densitometry analysis was conducted for total Spy1 protein levels which was corrected for total Actin levels (right panels). n=3; Error bars represent SE; Student's T-test. *p<0.05, **p≤0.01, ***p≤0.001.

Spy1 overcomes UV- induced cell cycle arrest.

To further investigate the relationship between Spy1 and p53, primary cells were isolated from MMTV-Spy1 mice and their control littermates. Levels of p53 were decreased using siRNA (Figure 6A) and cells were treated with UV to determine the effects of Spy1 mediated proliferation in the presence or absence of both p53 and UV. MMTV-Spy1 cells lacking p53 had a significantly higher number of BrdU positive cells (Figure 6B). This indicates that in the absence of p53 and the presence of damage, Spy1 is capable of promoting cellular proliferation.

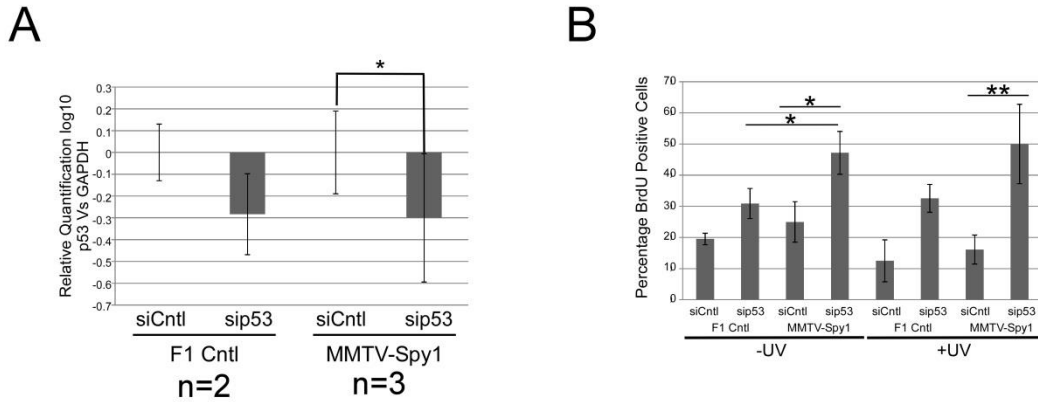


Figure 6: Spy1 does not require p53 to override the DDR. A) qRT-PCR analysis of p53 levels in littermate control (F1 Cntl) and MMTV-Spy1 primary cells corrected for total GAPDH. **B)** Quantification of BrdU positive cells with and without UV irradiation with (siCntl) and without p53 (sip53). F1 Cntl n=2, MMTV-Spy1 n=3. Error bars represent SE; Student's T-test. *p<0.05, **p<0.03, ***p<0.009 (n=3)

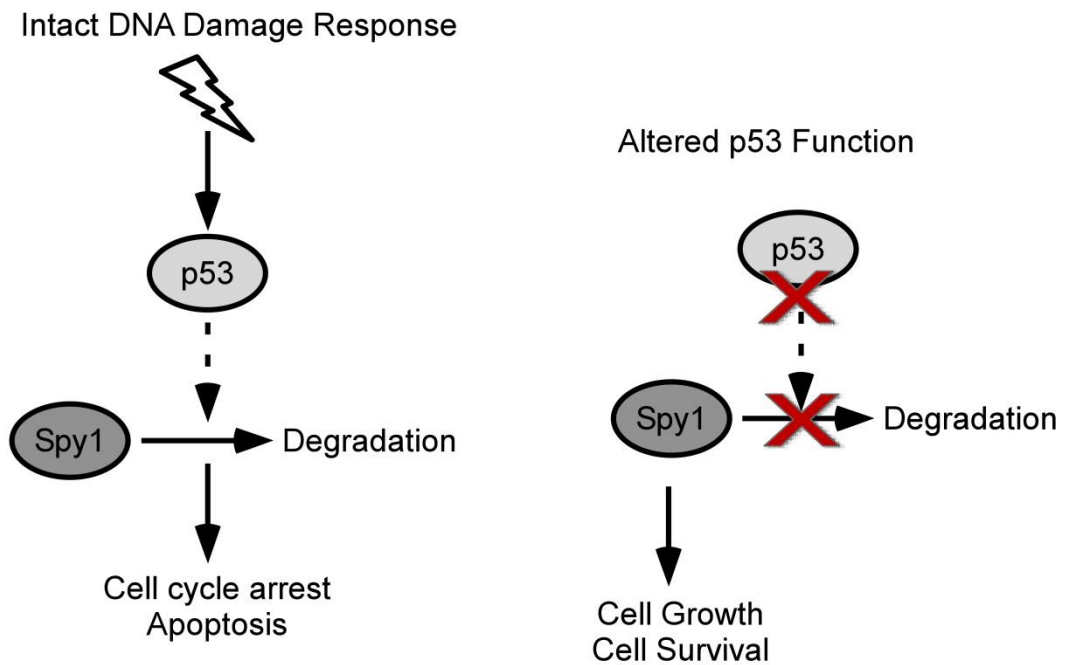


Figure 7: Mechanism of action. In the presence of wild-type p53, damage induces p53 expression which in turn downregulates Spy1 allowing for the DNA damage response to work unhindered. In cases of altered p53 function, Spy1 levels are no longer suppressed leading to enhanced cell growth and survival in the face of DNA damage.

Discussion

Development of the transgenic MMTV-Spy1 mouse has yielded new insight into the role Spy1 may have in tumour initiation and susceptibility. The MMTV-Spy1 mouse on the B6CBAF1/J background develops normally, showing no overt phenotypic differences when compared to control mice. Contrary to data in the HC11 cell line showing disrupted two-dimensional acinar development suggesting a defect in functional differentiation (Golipour et al., 2008), MMTV-Spy1 mice are capable of successfully nursing their young even through multiple rounds of pregnancy. Mammary development appears to occur normally in these mice, even with increased levels of Spy1. When primary cells are extracted from the mammary glands of control and MMTV-Spy1 mice, Spy1 expressing cells exhibit increased rates of proliferation and formed significantly more mammospheres than control cells. This indicates that although morphologically there does not appear to be any difference in mammary development, Spy1 alters characteristics of mammary epithelial cells which could trigger subtle changes in the gland.

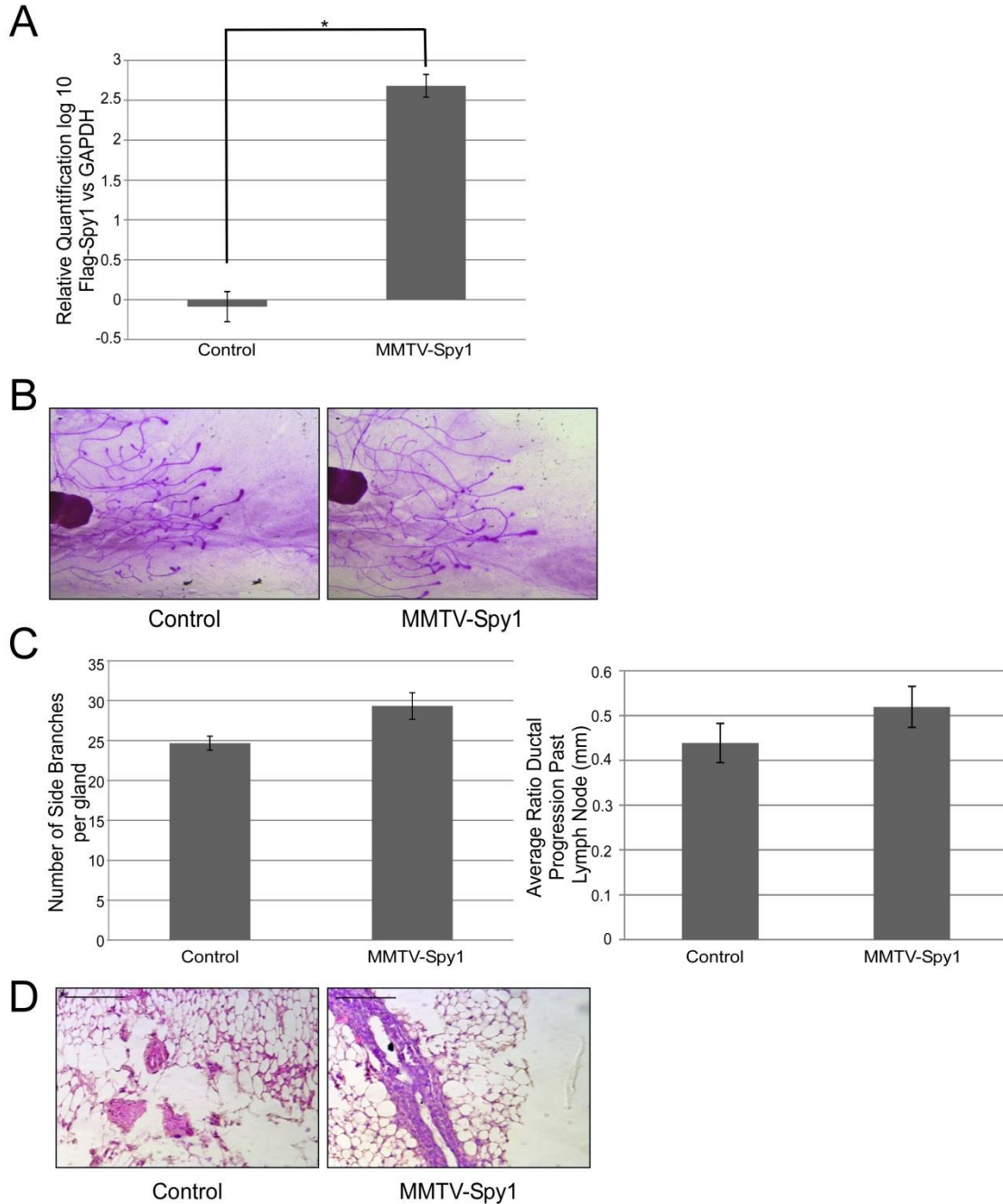
Previous data demonstrated that overexpression of Spy1 through mammary fat pad transplantation led to accelerated ductal development, and increased tumourigenesis (Golipour et al., 2008). MMTV-Spy1 mice do not display any significant changes in ductal development and do not develop spontaneous mammary tumours, even after multiple rounds of pregnancy. The reason for this phenotypic difference may lie in the p53 status of the cell line utilized in the fat pad transplantation experiment. HC11 cells contain a mutated p53 which would abrogate its function, and thus from those early experiments, it can only be said that Spy1 may increase susceptibility to tumourigenesis, and does not necessarily initiate it on its own (Merlo et al., 1993). Data from the MMTV-Spy1 mouse suggests that this is in fact the case as treatment of MMTV-Spy1 mice with the known carcinogen DMBA leads to significant formation of mammary tumours over control littermates, indicating that Spy1 increases susceptibility to mammary tumour formation.

Mouse strain is also known to play a large role in mammary tumour susceptibility. The MMTV-Spy1 mouse was generated on a resistant background of mouse, the B6CBAF1/J. C57BL6/J mice are highly resistant to various forms of tumourigenesis and are known to be resistant to MMTV infection (Beutner et al., 1996; Davie et al., 2007). Lack of developmental phenotype and spontaneous tumour formation could be due to mouse strain. To confirm this, the MMTV-Spy1 mouse has been backcrossed on the more susceptible FVB background to test the effects of aberrant Spy1 expression on spontaneous tumour formation in a susceptible genetic background (Supplemental Figure 3). This background did however allow us to truly test a susceptibility phenotype as the B6CBAF1/J strain of mouse is resistant to mammary tumour formation.

Spy1 is known to override the DNA damage response, and can override apoptosis in a p53 dependent manner (Barnes et al., 2003; Gastwirt et al., 2006; McAndrew et al., 2009). Levels of p53 were examined in mice treated with DMBA and were found to be significantly increased in MMTV-Spy1 mice treated with DMBA, along with a significant increase in the number of γ H2AX cells. Increased levels of γ H2AX can signify latent unrepaired damage, or perhaps a delay in the repair response to DNA damage. To examine the relationship between Spy1 and p53 more closely, we turned our attention to *in vitro* cell systems, using a variety of cell lines which were of varying p53 statuses and contained differences in various DNA repair pathways. We found that Spy1 overcomes a p53-mediated cell cycle arrest. During the DDR, levels of Spy1 are decreased in opposition to p53 levels, and overexpression of p53 was shown to decrease Spy1 protein levels. Lack of significance for various cell lines may be due in part to the p53 status of the cell line, or defects in repair mechanisms which could alter the cellular response to increased levels of Spy1. This data highlights a role for p53 mediation of Spy1 levels in the normal DDR. In the event of damage, p53 levels rise, and by a yet unknown mechanism, are able to trigger the downregulation of Spy1 protein levels, allowing for the DDR to work unhindered. Once the repair is completed, Spy1 levels once again rise and can trigger cell cycle progression, allowing

the cell to resume proliferation. Thus Spy1 may be a key player in mediating the DDR and triggering cell cycle re-entry.

In the event of DNA damage, wild-type p53 levels would increase and become activated to keep Spy1 levels in check to allow for the appropriate repair. In the fat pad transplant model, overexpression of Spy1 is sufficient to trigger tumourigenesis (Golipour et al., 2008). This may be due to inactivated p53, which would prevent Spy1 degradation and allow for sustained levels of Spy1 and continued proliferation in the presence of DNA damage, genomic instability, or detrimental mutations, leading to the development of tumourigenesis. Following treatment with DMBA in the MMTV-Spy1 model, Spy1 itself may act as a stressor in addition to the damage caused from the DMBA. Initially, wild-type p53 would be present and would keep Spy1 levels in check to allow for repair of damage. Over time, p53 may become mutated or inactivated, preventing its wild-type function, rendering it incapable of downregulating Spy1 levels. In this case, Spy1 would lead to continued proliferation in the presence of deleterious damage and mutations and could continue to promote cell survival in the absence of p53 (Figure 7). Thus the ability of Spy1 to initiate tumourigenesis may be dependent on loss of p53 function, highlighting a key role for Spy1 in promoting tumour initiation and progression in breast cancer subtypes which frequently display loss of p53 activity.



Supplementary Figure 3: Mouse strain does not influence effects of Spy1 overexpression on normal development. **A**) qRT-PCR analysis of Spy1 mRNA levels in the inguinal glands of control (n=3) and MMTV-Spy1 (n=3) mice. **B**) Whole mount images of the inguinal glands from 6 week old littermate control and MMTV-Spy1 FVB mice (n=3). **C**) Graphical analysis of whole mount images. Graphs depict number of side branches per gland (left panel) and ductal progression past lymph node (right panel) (n=3). Number of side branches per gland was quantified and average number of branches per gland is illustrated. **D**) Representative images of H&E stains from 6 week old MMTV-Spy1 FVB mice and their control littermates (n=2). Scale bars= 0.1 mm. Error bars represent SE; Students t-test *p=0.001967.

Acknowledgements

We thank Dr. Christopher Pin and Lindsay Drysdale from the London Regional Transgenic and Gene Targeting Facility for the development of the MMTV-Spy1 mouse, Dr. Robert Cardiff and the Mutant Mouse Pathology Lab at the University of California, Davis for pathology, and Drs Michael Crawford and Dennis Higgs for use of equipment. Special thanks to Dr. Gabriel E DiMattia for the MMTV-SV40-TRPS-1 vector, Dr. Carrie Shemanko for donation of HC11 cell line, Dr. John Hudson for U-2 OS and Saos2 cells and Dr. Bert Vogelstein for HCT116 cell lines. Thanks to Agnes Malysa for assistance with statistical analysis and Dr. Dorota Lubanska, Ingrid Qemo, Ellen Laurie and Nick Paquette for assistance with genotyping. We also thank Ellen Laurie and Mitchell Elliot for technical assistance. B.F. acknowledges support from the University of Windsor, the Ontario Graduate Scholarship Program and the Canadian Breast Cancer Foundation.

References

- Akashi, M., and Koeffler, H. P. (1998). Li-Fraumeni syndrome and the role of the p53 tumor suppressor gene in cancer susceptibility. *Clin Obstet Gynecol* 41, 172-199.
- Al Sorkhy, M., Ferraiuolo, R. M., Jalili, E., Malysa, A., Fratiloiu, A. R., Sloane, B. F., and Porter, L. A. (2012). The cyclin-like protein Spy1/RINGO promotes mammary transformation and is elevated in human breast cancer. *BMC Cancer* 12, 45.
- Barnes, E. A., Porter, L. A., Lenormand, J. L., Dellinger, R. W., and Donoghue, D. J. (2003). Human Spy1 promotes survival of mammalian cells following DNA damage. *Cancer Res* 63, 3701-3707.
- Bartek, J., and Lukas, J. (2001). Pathways governing G1/S transition and their response to DNA damage. *FEBS Lett* 490, 117-122.
- Beutner, U., McLellan, B., Kraus, E., and Huber, B. T. (1996). Lack of MMTV superantigen presentation in MHC class II-deficient mice. *Cell Immunol* 168, 141-147.
- Cheng, A., Gerry, S., Kaldis, P., and Solomon, M. J. (2005). Biochemical characterization of Cdk2-Speedy/Ringo A2. *BMC Biochem* 6, 19.
- Davie, S. A., Maglione, J. E., Manner, C. K., Young, D., Cardiff, R. D., MacLeod, C. L., and Ellies, L. G. (2007). Effects of FVB/NJ and C57Bl/6J strain backgrounds on mammary tumor phenotype in inducible nitric oxide synthase deficient mice. *Transgenic Res* 16, 193-201.
- Dickey, J. S., Redon, C. E., Nakamura, A. J., Baird, B. J., Sedelnikova, O. A., and Bonner, W. M. (2009). H2AX: functional roles and potential applications. *Chromosoma* 118, 683-692.
- Donehower, L. A., Harvey, M., Slagle, B. L., McArthur, M. J., Montgomery, C. A., Jr., Butel, J. S., and Bradley, A. (1992). Mice deficient for p53 are developmentally normal but susceptible to spontaneous tumours. *Nature* 356, 215-221.
- Gastwirt, R. F., Slavin, D. A., McAndrew, C. W., and Donoghue, D. J. (2006). Spy1 expression prevents normal cellular responses to DNA damage: inhibition of apoptosis and checkpoint activation. *J Biol Chem* 281, 35425-35435.

Golipour, A., Myers, D., Seagroves, T., Murphy, D., Evan, G. I., Donoghue, D. J., Moorehead, R. A., and Porter, L. A. (2008). The Spy1/RINGO family represents a novel mechanism regulating mammary growth and tumorigenesis. *Cancer Res* 68, 3591-3600.

Hang, Q., Fei, M., Hou, S., Ni, Q., Lu, C., Zhang, G., Gong, P., Guan, C., Huang, X., and He, S. (2012). Expression of Spy1 protein in human non-Hodgkin's lymphomas is correlated with phosphorylation of p27 Kip1 on Thr187 and cell proliferation. *Med Oncol* 29, 3504-3514.

Hoshino, A., Yee, C. J., Campbell, M., Woltjer, R. L., Townsend, R. L., van der Meer, R., Shyr, Y., Holt, J. T., Moses, H. L., and Jensen, R. A. (2007). Effects of BRCA1 transgene expression on murine mammary gland development and mutagen-induced mammary neoplasia. *Int J Biol Sci* 3, 281-291.

Hutchinson, J. N., and Muller, W. J. (2000). Transgenic mouse models of human breast cancer. *Oncogene* 19, 6130-6137.

Jacks, T., Remington, L., Williams, B. O., Schmitt, E. M., Halachmi, S., Bronson, R. T., and Weinberg, R. A. (1994). Tumor spectrum analysis in p53-mutant mice. *Curr Biol* 4, 1-7.

Karaiskou, A., Perez, L. H., Ferby, I., Ozon, R., Jesus, C., and Nebreda, A. R. (2001). Differential regulation of Cdc2 and Cdk2 by RINGO and cyclins. *J Biol Chem* 276, 36028-36034.

Ke, Q., Ji, J., Cheng, C., Zhang, Y., Lu, M., Wang, Y., Zhang, L., Li, P., Cui, X., Chen, L., *et al.* (2009). Expression and prognostic role of Spy1 as a novel cell cycle protein in hepatocellular carcinoma. *Exp Mol Pathol* 87, 167-172.

Lee, H. J., Lee, Y. J., Kang, C. M., Bae, S., Jeoung, D., Jang, J. J., Lee, S. S., Cho, C. K., and Lee, Y. S. (2008). Differential gene signatures in rat mammary tumors induced by DMBA and those induced by fractionated gamma radiation. *Radiat Res* 170, 579-590.

Lenormand, J. L., Dellinger, R. W., Knudsen, K. E., Subramani, S., and Donoghue, D. J. (1999). Speedy: a novel cell cycle regulator of the G2/M transition. *Embo J* 18, 1869-1877.

Lubanska, D., Market-Velker, B. A., deCarvalho, A. C., Mikkelsen, T., Fidalgo da Silva, E., and Porter, L. A. (2014). The cyclin-like protein Spy1 regulates growth and division characteristics of the CD133+ population in human glioma. *Cancer Cell* 25, 64-76.

McAndrew, C. W., Gastwirt, R. F., and Donoghue, D. J. (2009). The atypical CDK activator Spy1 regulates the intrinsic DNA damage response and is dependent upon p53 to inhibit apoptosis. *Cell Cycle* 8, 66-75.

Meek, D. W. (2004). The p53 response to DNA damage. *DNA Repair (Amst)* 3, 1049-1056.

Merlo, G. R., Venesio, T., Taverna, D., Callahan, R., and Hynes, N. E. (1993). Growth suppression of normal mammary epithelial cells by wild-type p53. *Ann N Y Acad Sci* 698, 108-113.

Mroue, R., and Bissell, M. J. (2013). Three-dimensional cultures of mouse mammary epithelial cells. *Methods Mol Biol* 945, 221-250.

Paull, T. T., Rogakou, E. P., Yamazaki, V., Kirchgessner, C. U., Gellert, M., and Bonner, W. M. (2000). A critical role for histone H2AX in recruitment of repair factors to nuclear foci after DNA damage. *Curr Biol* 10, 886-895.

Porter, L. A., Dellinger, R. W., Tynan, J. A., Barnes, E. A., Kong, M., Lenormand, J. L., and Donoghue, D. J. (2002). Human Speedy: a novel cell cycle regulator that enhances proliferation through activation of Cdk2. *J Cell Biol* 157, 357-366.

Porter, L. A., Kong-Beltran, M., and Donoghue, D. J. (2003). Spy1 interacts with p27Kip1 to allow G1/S progression. *Mol Biol Cell* 14, 3664-3674.

Purdie, C. A., Harrison, D. J., Peter, A., Dobbie, L., White, S., Howie, S. E., Salter, D. M., Bird, C. C., Wyllie, A. H., Hooper, M. L., and et al. (1994). Tumour incidence, spectrum and ploidy in mice with a large deletion in the p53 gene. *Oncogene* 9, 603-609.

Sakaguchi, K., Herrera, J. E., Saito, S., Miki, T., Bustin, M., Vassilev, A., Anderson, C. W., and Appella, E. (1998). DNA damage activates p53 through a phosphorylation-acetylation cascade. *Genes Dev* 12, 2831-2841.

Sancar, A., Lindsey-Boltz, L. A., Unsal-Kacmaz, K., and Linn, S. (2004). Molecular mechanisms of mammalian DNA repair and the DNA damage checkpoints. *Annu Rev Biochem* 73, 39-85.

Sedelnikova, O. A., and Bonner, W. M. (2006). GammaH2AX in cancer cells: a potential biomarker for cancer diagnostics, prediction and recurrence. *Cell Cycle* 5, 2909-2913.

Shieh, S. Y., Ikeda, M., Taya, Y., and Prives, C. (1997). DNA damage-induced phosphorylation of p53 alleviates inhibition by MDM2. *Cell* 91, 325-334.

Soussi, T., Ishioka, C., Clautres, M., and Beroud, C. (2006). Locus-specific mutation databases: pitfalls and good practice based on the p53 experience. *Nat Rev Cancer* 6, 83-90.

Zucchi, I., Mento, E., Kuznetsov, V. A., Scotti, M., Valsecchi, V., Simionati, B., Vicinanza, E., Valle, G., Pilotti, S., Reinbold, R., *et al.* (2004). Gene expression profiles of epithelial cells microscopically isolated from a breast-invasive ductal carcinoma and a nodal metastasis. *Proc Natl Acad Sci U S A* 101, 18147-18152.

Chapter 3

The Role of Spy1 in Liver Steatosis and Susceptibility to Hepatocellular Carcinoma

Introduction

Hepatocellular carcinoma, HCC, is one of the leading causes of cancer related death worldwide, with a five year survival rate of only 20% (Canadian Cancer Society, 2014; World Health Organization, 2014). Prognosis is poor mainly due to the limited treatment options and the central role the liver plays in basic human functions such as detoxification and cholesterol metabolism. A variety of factors contribute to susceptibility to HCC including hepatitis B or C infection, chronic alcoholism and cirrhosis of the liver (Fattovich et al., 2004). Cirrhosis of the liver can be caused by long term alcohol abuse triggering accumulation of lipid droplets within the liver leading to increased inflammation and fibrosis (Bataller and Brenner, 2005). Manifestation of this condition can also occur through progression of non-alcoholic fatty liver disease (NAFLD) to non-alcoholic steatohepatitis (NASH), which occur in the absence of alcoholism (Dowman et al., 2010; Takahashi et al., 2012; The National Digestive Diseases Information Clearinghouse, 2014). Incidence of HCC is currently on the rise and may be attributed to increased rates of obesity which play a contributing factor in the onset of NASH (The National Digestive Diseases Information Clearinghouse, 2014). A more thorough understanding of this disease would help to elucidate the molecular mechanism underlying the onset and initiation of HCC.

NAFLD is characterized by increased fat accumulation in the liver (The National Digestive Diseases Information Clearinghouse, 2014). In and of itself, this condition is not typically harmful, and symptoms may be absent. Changes in diet, and increased weight loss can help to reverse this condition (Dowman et al., 2010; Jou et al., 2008; Takahashi et al., 2012; The National Digestive Diseases Information Clearinghouse, 2014). Fat accumulation in the liver becomes more dangerous when it begins to trigger inflammatory response pathways leading to injury and damage to the liver (Cai et al., 2005; Dowman et al., 2010; Jou et al., 2008). Over time, the level of damage sustained by the hepatocytes diminishes their capacity to proliferate, leaving them unable to regenerate the injured and damaged areas of the liver, and increasing rates

of apoptosis (Dowman et al., 2010; Feldstein et al., 2004; Takahashi et al., 2012). When the ability to regenerate damaged areas is lost, injury is sustained and the liver begins to deposit fibrous material such as collagen, further perpetuating the condition (Bataller and Brenner, 2005; Dowman et al., 2010; Friedman et al., 1985; Jou et al., 2008). Over time, fibrosis of the liver leads to severely compromised liver blood flow and function, which increases the risk of liver failure and developing HCC (Bataller and Brenner, 2005; Dowman et al., 2010).

In normal circumstances, hepatocytes possess a remarkable capacity for regeneration (Fausto and Campbell, 2003). In the event of injury or loss of tissue, the quiescent hepatocyte population is primed to respond to mitogenic signals to stimulate re-entry into the cell cycle (Bisteau et al., 2014; Ehrenfried et al., 1997; Fausto and Campbell, 2003; Webber et al., 1998; Webber et al., 1994). The hepatocytes undergo two rounds of highly synchronized DNA replication and division to reconstitute the injured area or to compensate for lost tissue (Bisteau et al., 2014; Ehrenfried et al., 1997; Fausto and Campbell, 2003; Grisham, 1962). In models of partial hepatectomy, the liver is capable of sustaining loss of two-thirds of the overall tissue mass and can regenerate this mass within a week demonstrating the remarkable proliferative capacity of hepatocytes (Bisteau et al., 2014; Fausto and Campbell, 2003; Michalopoulos, 2007). With NASH and severe cases of injury, the hepatocytes lose their ability to proliferate and regenerate the injured tissue, eventually succumbing to apoptosis further increasing the amount of damaged tissue (Dowman et al., 2010; Farrell et al., 2009; Panasiuk et al., 2006). One regulator of activation of the apoptotic pathway is the tumour suppressor p53 (Meek, 2004). p53 acts as a master regulator of the DNA damage response and apoptosis in response to damage and inflammation (Meek, 2004; Sakaguchi et al., 1998; Sancar et al., 2004). Fatty liver diseases have been found to have increased levels of p53 which correlate positively with the amount of inflammation present, thus indicating that increased inflammation in NASH could trigger up-regulation and activation of p53 leading to increased rates of apoptosis (Farrell et al., 2009; Kodama et al., 2011; Panasiuk et al., 2006; Yahagi et al., 2004). Furthermore, p21, a target

protein of p53, was found to be up-regulated in fatty liver disease along with p53 indicating activation of p53 signaling pathways (Farrell et al., 2009). Levels of anti-apoptotic proteins, such as Bcl-XL were found to be decreased, further indicating that inflammation can trigger up-regulation of p53 leading to increased rates of apoptosis, and further perpetuating disease progression (Panasiuk et al., 2006).

Damage response pathways and cell cycle regulation play a critical role in hepatocyte proliferation in response to injury and inflammation. The cyclin-like protein Spy1 is capable of binding and activating CDK2 in the absence of canonical phosphorylation, leading to increased CDK2 activity and enhanced progression through the cell cycle (Cheng et al., 2005; Karaïskou et al., 2001; Lenormand et al., 1999; Porter et al., 2002). Additionally, Spy1 overrides DNA damage response checkpoints, promoting cell cycle progression in the presence of damage (Barnes et al., 2003; Gastwirt et al., 2006; McAndrew et al., 2009). Spy1 also overrides apoptosis in a p53-dependent manner (Gastwirt et al., 2006; McAndrew et al., 2009). Thus, Spy1 plays a critical role in regulating cell cycle progression and response to damage. Previous reports have found Spy1 levels to be high in HCC when compared to pair matched normal tissue, and increasing levels correlated with increasing severity of disease and poor prognosis (Ke et al., 2009). Levels of Spy1 also correlated positively with the proliferation marker ki67, highlighting the importance of this protein in promoting cell cycle progression (Ke et al., 2009). Thus it appears that Spy1 may play a critical role in tumour initiation and progression in the liver.

Herein we describe a surprising phenotype in the previously described MMTV-Spy1 mice. Male mice containing the transgene were found to develop tumours in the liver at a significantly higher rate than their control littermates. Additionally, histological analysis revealed the presence of increased fat accumulation in livers of male MMTV-Spy1 mice. We describe a potential role for Spy1 in increasing liver cancer susceptibility, potentially by triggering the onset of NAFLD/NASH, leading to increased damage and inflammatory response signaling, and continued cellular proliferation in the presence of damage.

Materials and Methods

Maintenance of MMTV-Spy1 Transgenic Mice

MMTV-Spy1 mice were generated as described in Chapter 2. Briefly, the Spy1 coding sequence was cloned in the MMTV-SV40 vector backbone and sent to the London Regional Transgenic and Gene Targeting Facility for pronuclear injections into B6CBAF1/J hybrid embryos. Mice were maintained on a B6CBAF1/J background. Genotyping was performed via PCR analysis. PCR was performed by adding 50ng of genomic tail DNA to a 25 μ L reaction (1x PCR buffer, 2mM MgSO₄, 0.2mM dNTP, 0.04U/ μ L UBI Taq Polymerase, 0.4 μ M forward primer [5'CCCAAGGCTTAAGTAAGTTTTTGG 3'], 0.4 μ M reverse primer [5'GGGCATAAGCACAGATAAAAACACT 3'], 1% DMSO) (NCI Mouse Repository). Cycling conditions were as follows: 94°C for 3 minutes, 40 cycles of 94°C for 1 minute, 55°C for 2 minutes, and 72°C for 1 minute, and a final extension of 72°C for 3 minutes. Mice were maintained following the Canadian Council on Animal Care Guidelines under the animal utilization protocol 10-16 approved by the University of Windsor.

Plasmids

The pCS3 and Myc-Spy1 pCS3 plasmids were utilized in overexpression experiments and were generated as previously described (Porter et al., 2002). For knockdown experiments, pLKO.1 (Addgene) and pLKO.shSpy1.2 were utilized and were generated as described (Porter et al., 2002).

Cell Culture and Transfection

HepG2 cells (a kind gift from Dr. Hudson, University of Windsor) were maintained in Eagle's Minimum Essential Medium (EMEM) supplemented with 10% FBS and 1% penicillin/streptomycin at 37°C, 5% CO₂. HepG2 cells were transfected using polyethylenimine

(PEI) branched reagent (Sigma). Briefly, 40µg of PEI and 10µg of plasmid were incubated together for 10 minutes before adding to a 10cm plate.

Histology and Immunostaining

Tissue was collected and fixed in 10% neutral buffered formalin. Tissue was dehydrated in ascending concentrations of ethanol, and cleared in xylene prior to embedding in paraffin wax. Samples were sectioned at 5 µm using the Leica RM2125RT. For haematoxylin and eosin stain, sections were rehydrated in descending concentrations of ethanol, washed in distilled water and stained with haematoxylin (Vector Laboratories). Sections were washed using running tap water, and were subsequently stained with eosin (Sigma Aldrich) before being dehydrated through ascending concentrations of ethanol. For immunohistochemistry, slides were deparaffinized in xylene, rehydrated through a descending series of ethanol concentrations and heat mediated antigen retrieval was performed with 10mM sodium citrate buffer pH 6.0. Following this, endogenous peroxidase activity was blocked using 3% H₂O₂ diluted in methanol. Sections were blocked in Mouse on Mouse (MOM) blocker (Biocare Medical) or 3% BSA-0.1% Tween-20 in 1x PBS for mouse and rabbit secondary antibodies respectively. Sections were incubated overnight at 4°C in primary antibody diluted in the appropriate blocker. Following 3 10 minute washes with 1xPBS, sections were incubated with secondary antibody (1:750) for 1 hour in a humidified chamber. Sections were subsequently incubated with ABC reagent as per manufacturer's instructions (Vectastain ABC Kit). Next, sections were stained with 3,3'-diaminobenzidine (DAB) following manufacturer's instructions (DAB Peroxidase Substrate Kit, Vector Laboratories), and were counterstained with haematoxylin (Vector Laboratories). Sections were then dehydrated in a series of ascending ethanol concentrations, coverslipped with Permount toluene solution (Fisher Scientific) and visualized using the LEICA DMI6000 inverted microscope with LAS 3.6 software.

Quantitative Real Time PCR Analysis

RNA was isolated from flash frozen tissue using TRIzol reagent (Life Technologies) as per manufacturer's instructions, while RNA isolation from cell pellets was conducted using the Qiagen RNeasy Plus Mini Kit as per manufacturer's instructions. Superscript II (Invitrogen) was used to synthesize cDNA from the obtained RNA samples as per manufacturer's instructions. Real Time PCR was performed using Sybr Green Detection (Applied Biosystems) on the Vii7 Real Time PCR System (Life Technologies) and software. Primer sequences were as follows:

Flag-Spy1 Forward: 5'TGACAAGAGGCACAATCAGATGT 3'

Flag-Spy1 Reverse: 5' CAAATAGGACGCTTCAGAGTAATGG3'

Human GAPDH Forward: 5' GCACCGTCAAGGCTGAGAAC 3'

Human GAPDH Reverse: 5' GGATCTCGCTCCTGGAAGATG 3'

Human Spy1 Forward: 5' TTGTGAGGAGGTTATGGCCATT 3'

Human Spy1 Reverse: 5' GCAGCTGAACTTCATCTCTGTTGTAG 3'

Mouse GAPDH Forward: 5' GATGCCCCCATGTTTGTGAT 3'

Mouse GAPDH Reverse: 5' GTGGTCATGAGCCCTTCCA 3'

Protein Isolation and Immunoblotting

Flash frozen tissue was thawed and an appropriate amount of tissue lysis buffer (50mM Tris-HCl pH 7.5, 1% NP-40, 0.25% Na-deoxycholate, 1mM EGTA, 0.2% SDS, 150mM NaCl) with protease inhibitors (leupeptin 2µg/mL, aprotinin 5µg/mL, PMSF 100µg/mL) was added to the tissue. Tissue was then homogenized on ice in the tissue lysis buffer with the Fisher Scientific Sonic Dismembrator 50. The homogenized tissue was flash frozen in liquid nitrogen and thawed on ice before being spun at 13,000rpm for 20 minutes at 4°C. Supernatant was isolated and spun again at 13,000rpm for 20 minutes at 4°C. To ensure equal protein loading, Bradford analysis was performed as per manufacturer's instructions to assess protein concentration. Equal amounts of protein were prepared for loading in a 10% SDS-polyacrylamide gel and were transferred to a

PVDF membrane at 30 volts for 2 hours using the wet transfer method. Membranes were subsequently blocked in 2% milk for 1 hour at room temperature before incubation with primary antibody overnight at 4°C. Following incubation with primary antibody, membranes were washed with TBST 3 times for 10 minutes each followed by incubation with secondary antibody (1:10000) for 1 hour at room temperature. Membranes were washed again with TBST 3 times, 5 minutes each and visualization of the signal was conducted using chemiluminescent peroxidase substrate (Pierce) as per manufacturer's instructions. Images were captured on Alpha Innotech HD 2 using AlphaEase FC software.

BrdU Incorporation Assay

Cells were seeded in a 96 well plate at a seeding density of 10,000 cells per well and were allowed to adhere overnight. Following adherence to the plate, cells were incubated in media containing 10µM BrdU (BD Pharmingen) for 16-18 hours. Media was removed and cells were washed with 1X PBS. Cells were subsequently fixed with 4% paraformaldehyde for 15 minutes and were washed with 1X PBS before incubation at 37°C in 2M HCl for 20 minutes. Cells were washed with 1X PBS and incubated with Anti-BrdU (BD Biosciences) in 0.2% Tween in 1X PBS for 45 minutes. After incubation, cells were washed with 1x PBS and incubated with anti-mouse IgG and hoescht at a 1:1000 dilution in 1X PBS for 1 hour at room temperature. Cells were then washed with 1X PBS followed by distilled water and were stored in 50% glycerol at 4°C until imaging and analysis.

Oil-Red O Staining

HepG2 cells were seeded at a density of 10,000 cells per well in a 96 well plate and left to adhere to the plate overnight. Cells were washed with 1X PBS and were subsequently fixed using 10% neutral buffered formalin for 30 minutes at room temperature. Following fixation, cells were washed with distilled water and were incubated in 60% isopropanol for 5 minutes.

Cells were subsequently stained with a 60% working solution of Oil-Red O (Sigma Aldrich) for 10 minutes and were washed with distilled water until water was clear. Images were obtained using the Leica DMI6000B Inverted Microscope and were analyzed using ImageJ software.

Results

Male MMTV-Spy1 exhibit an increase in Spy1 and increased tumourigenesis.

MMTV-Spy1 mice were generated on a B6CBAF1/J background to study the effects of increased Spy1 protein levels on mammary development and tumourigenesis. Given that the MMTV promoter can show residual activity in other tissue types, as well as in males, non-productive MMTV-Spy1 male breeders and their control littermates were sacrificed once they reached one year of age. Upon sacrifice, it was noted that MMTV-Spy1 males over one year of age displayed a significant increase in liver tumour formation as compared to control littermates of the same age (Figure 1A). Liver tissue was extracted from aged males and Spy1 expression levels were found to be significantly increased in liver tissue from MMTV-Spy1 males (Figure 1B). When levels of Spy1 were examined in aged female mice, the same trend was not noted (Figure 1C), indicating that expression of Spy1 and tumour onset is specific to male MMTV-Spy1 mice.

Elevated levels of Spy1 lead to increased fat accumulation and increased nuclear size.

Progression to HCC can be attributed to a number of factors such as hepatitis B or C infection or NAFLD/NASH (Fattovich et al., 2004). Both NAFLD and NASH are characterized by increased lipid accumulation within the liver which ultimately leads to increased inflammation and fibrosis, contributing to the development of HCC (Bataller and Brenner, 2005; Cai et al., 2005; Dowman et al., 2010; Takahashi et al., 2012; The National Digestive Diseases Information Clearinghouse, 2014). To determine if elevated levels of Spy1 leads to morphological changes in the liver of aged mice, liver tissue was collected, fixed and stained to assess the pathology of the livers (Figure 1D). It was found that MMTV-Spy1 mice displayed increased fat accumulation that although not significant, could play a contributing role in the initiation of liver tumourigenesis (Figure 1D, E). Additionally, the area of hepatocyte nuclei was measured and found to be significantly increased in the livers of MMTV-Spy1 mice (Figure 1F). Enlargement of hepatocyte

nuclei could signify a number of molecular mechanisms, such as cellular senescence or polyploidy, that could contribute to tumour onset in MMTV-Spy1 mice (Gonzalez-Reimers et al., 1987; Nakajima et al., 2010). Thus, MMTV-Spy1 male mice display elevated levels of Spy1 which correlates with a significant increase in nuclear area, and although not, significant, increased fat accumulation.

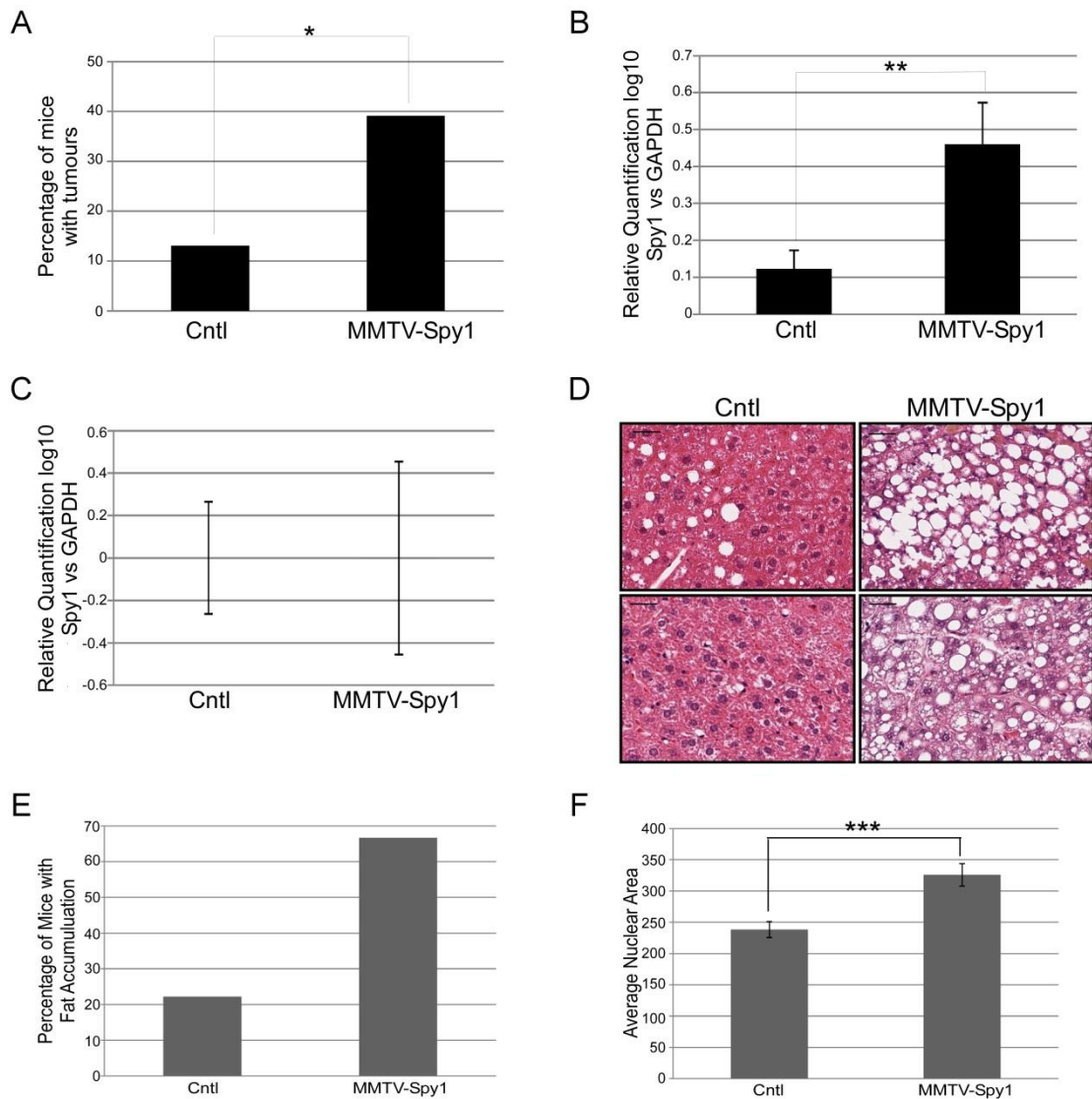


Figure 1: MMTV-Spy1 male mice are more susceptible to liver tumourigenesis.

A) Graphical representation of percentage of mice with liver tumourigenesis (MMTV-Spy1 n=23, Cntl n=23). **B) & C)** qRT-PCR analysis of MMTV-Spy1 and littermate control liver samples for Spy1 levels in males (MMTV-Spy1 n=14, Cntl n=10) and females (MMTV-Spy1 n=7, Cntl n=7) respectively corrected for total GAPDH levels. **D)** Representative H&E stain of liver tissue collected from male mice over the age of 1 year. Scale bar= 50 uM. **E)** Graphical depiction of percentage of mice with increased fat accumulation (n=9; p=0.06). **F)** Average size of nuclear area in control and MMTV-Spy1 hepatocytes (MMTV-Spy1 n=3, Cntl n=3). Error bars reflect SE, Mann-Whitney (A) and Student's T-test (B,C,E,F) *p=0.046302, **p=0.001, ***p=0.000186

Increased levels of Spy1 does not alter expression of known markers of HCC.

Spy1 accelerates cell cycle progression both by binding and activating CDK2, as well as triggering degradation of the cell cycle inhibitor p27, thereby relieving inhibition on G1/S phase of the cell cycle (Cheng et al., 2005; McAndrew et al., 2007; Porter et al., 2002; Porter et al., 2003). Given the tight relationship between Spy1 and p27 we sought to determine if p27 levels were reduced in the livers of MMTV-Spy1 mice. Analysis of protein expression revealed that although the trend of p27 protein demonstrated reduced levels in MMTV-Spy1 livers, these differences were not statistically significant (Figure 2A). We next looked further into other known cell cycle regulators and examined expression levels of c-Myc in livers of MMTV-Spy1 mice to determine if altered Myc expression levels could be contributing to tumourigenesis. Myc is known to play crucial roles in cell cycle regulation and can stimulate tumourigenesis in livers of Myc transgenic mouse models (Beer et al., 2004; Shachaf et al., 2004). Additionally, previous data has shown that Spy1 lies downstream of Myc, making it an ideal candidate for disruption of expression levels and suggesting a unique interaction between Spy1 and Myc (Golipour et al., 2008). We found no significant difference in the expression of Myc between control littermates and MMTV-Spy1 mice, indicating that altered Spy1 protein levels do not affect cell cycle mediators which are known effectors of Spy1 (Figure 2B).

Albumin is expressed in mature hepatocytes and is commonly used as marker to delineate the population of mature hepatocytes within the liver (Germain et al., 1988; Zorn, 2008). Cases of HCC are known to have decreased levels of albumin indicating a possible step back in differentiation or alterations in the hepatocyte population during tumour progression (Ljubimova et al., 1997). Spy1 has been shown to affect differentiation of mammary epithelial cells, causing disrupted morphology and early expression of differentiation markers indicating a potential failure of these cells to functionally differentiate (Golipour et al., 2008). Albumin levels were examined to determine if Spy1 was capable of altering the differentiation status of hepatocytes within the liver. No significant difference in albumin expression was noted between control and

MMTV-Spy1 aged mice (Figure 2C). Spy1 expression does not alter expression of a subset of known cell cycle mediators and proteins known to influence tumour onset and status.

Up-regulation of damage response pathways in MMTV-Spy1 mice.

Fatty liver diseases such as NASH can lead to up-regulation of inflammatory and damage pathways in response to increased damage and injury the liver sustains due to increased fat accumulation (Dowman et al., 2010; Takahashi et al., 2012; The National Digestive Diseases Information Clearinghouse, 2014). Studies have shown that levels of the tumour suppressor p53 are increased in cases of NASH positively correlating with the degree of inflammation (Kodama et al., 2011; Panasiuk et al., 2006; Yahagi et al., 2004). Given that Spy1 is known to play a role in the DNA damage response, and the relationship between NASH and p53, we sought to determine if elevated levels of p53 correlate with changes in this response pathway. Analysis of p53 levels via immunohistochemistry revealed a significant increase in the levels of p53 protein in MMTV-Spy1 male livers as compared to control (Figure 3A). Next, levels of p21, a known downstream target of p53, were analysed. Once again, MMTV-Spy1 livers showed a significant increase in p21 protein levels indicating that p53 expression was not only elevated, but its activity could also be increased (Figure 3B). A side effect of increased inflammation and damage is increased levels of apoptosis to remove severely damaged cells from the population. Levels of anti-apoptotic proteins are known to be decreased in cases of NASH, and p53 is capable of activating apoptotic pathways, therefore we next examined the rate of apoptosis in MMTV-Spy1 livers (Panasiuk et al., 2006). Through immunohistochemistry, we showed a significant increase in the levels of active caspase 3, a central player in the apoptotic pathway commonly used to indicate increased amounts of apoptosis (Figure 3C). Thus, MMTV-Spy1 mice show significantly elevated levels of proteins known to be involved in inflammatory and apoptotic pathways in response to NASH.

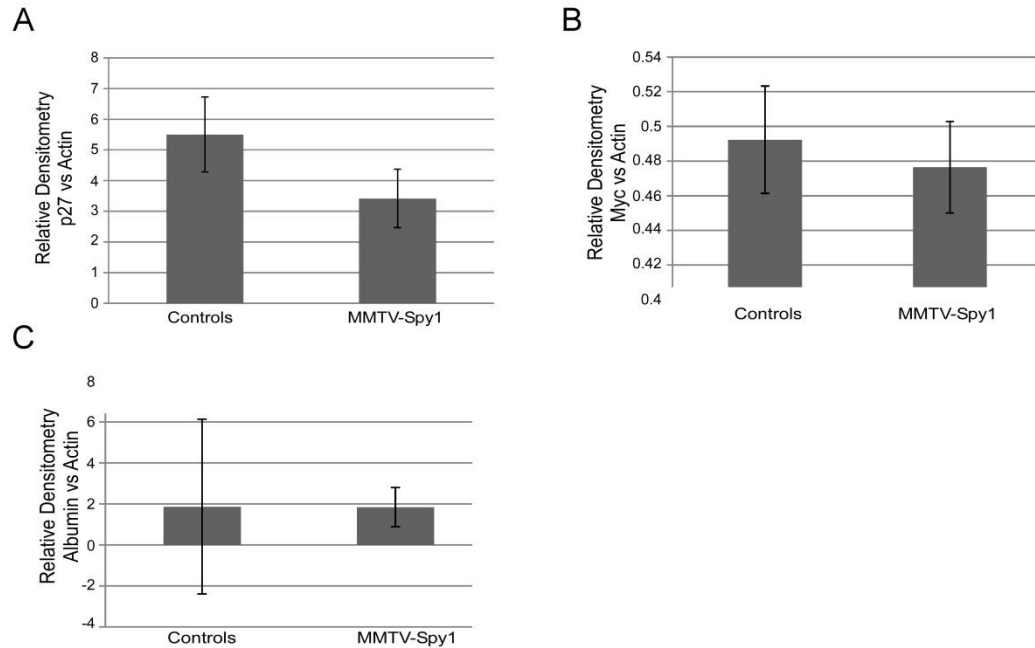


Figure 2: Levels of Spy1 effectors are not altered in MMTV-Spy1 mice. Quantification of western blot data in MMTV-Spy1 mice and littermate controls (controls). Data was corrected for equal loading using Actin. **A)** Quantification of western blot of p27 in livers of male mice over 1 year of age. **B)** Quantification of western blot of Myc in livers of male mice over 1 year of age. **C)** Quantification of western blot of albumin in livers of male mice over 1 year of age. Cntl n=15, MMTV-Spy1 n=19; Error bars reflect SE, Student's T-test

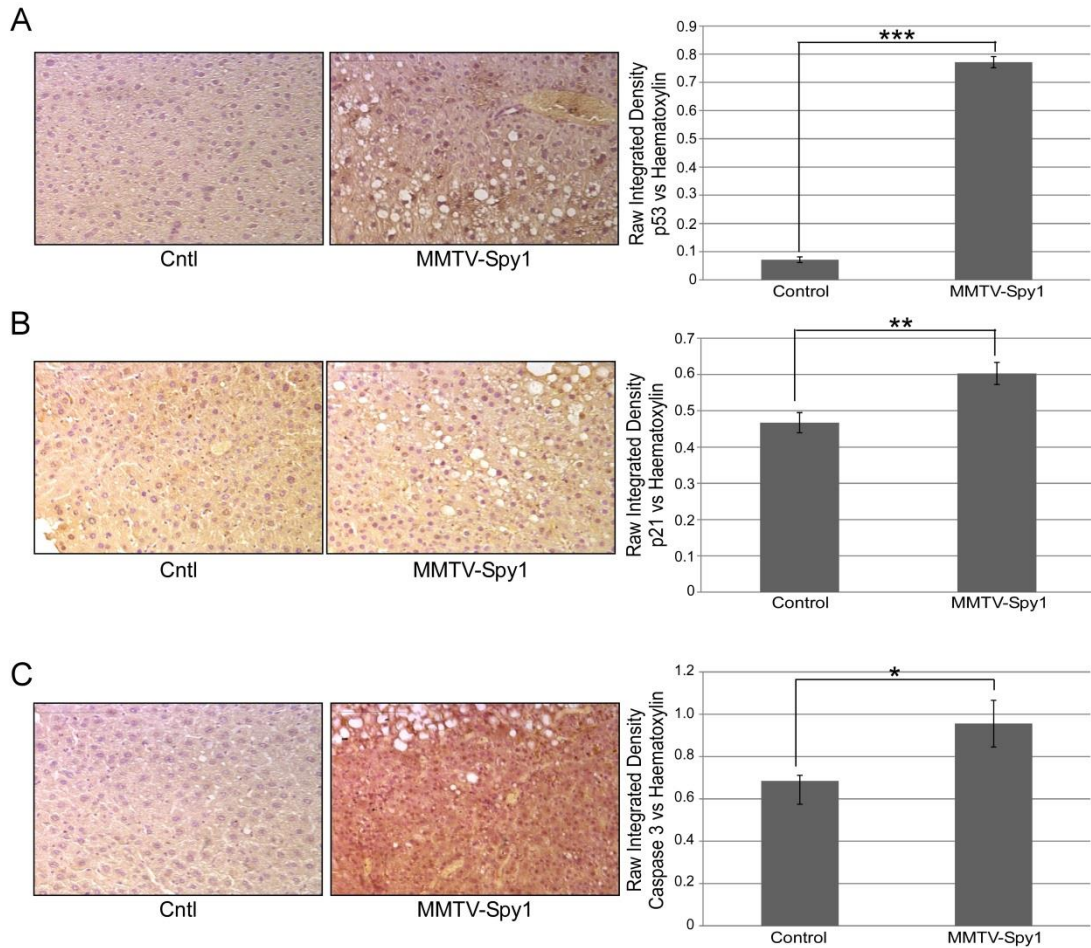
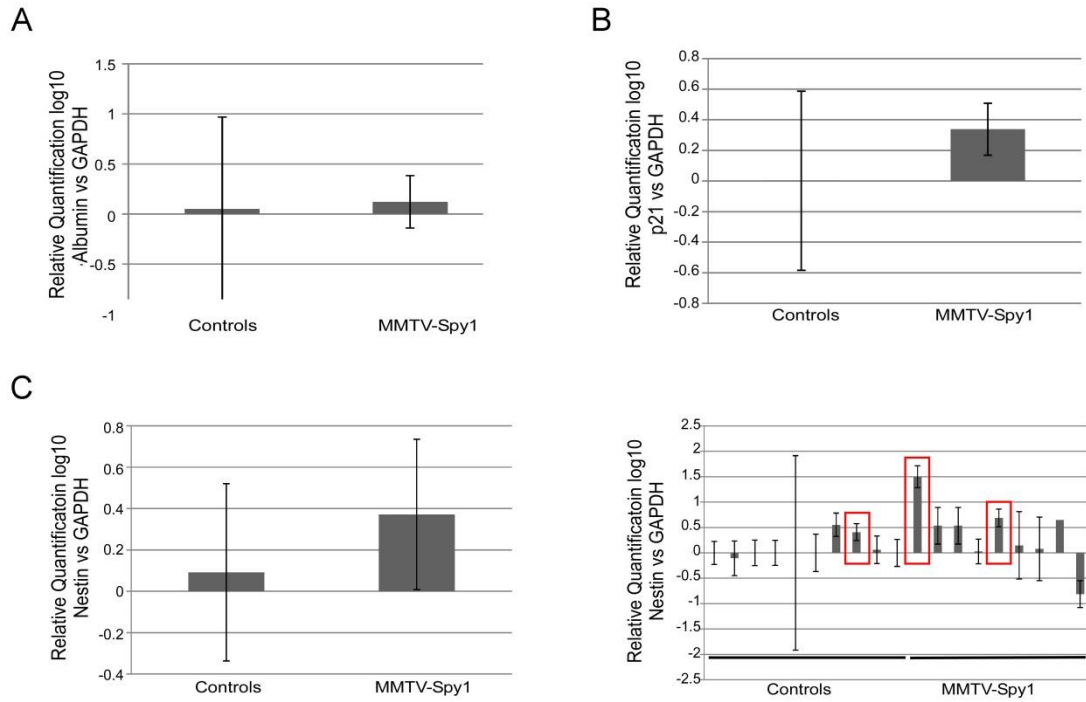
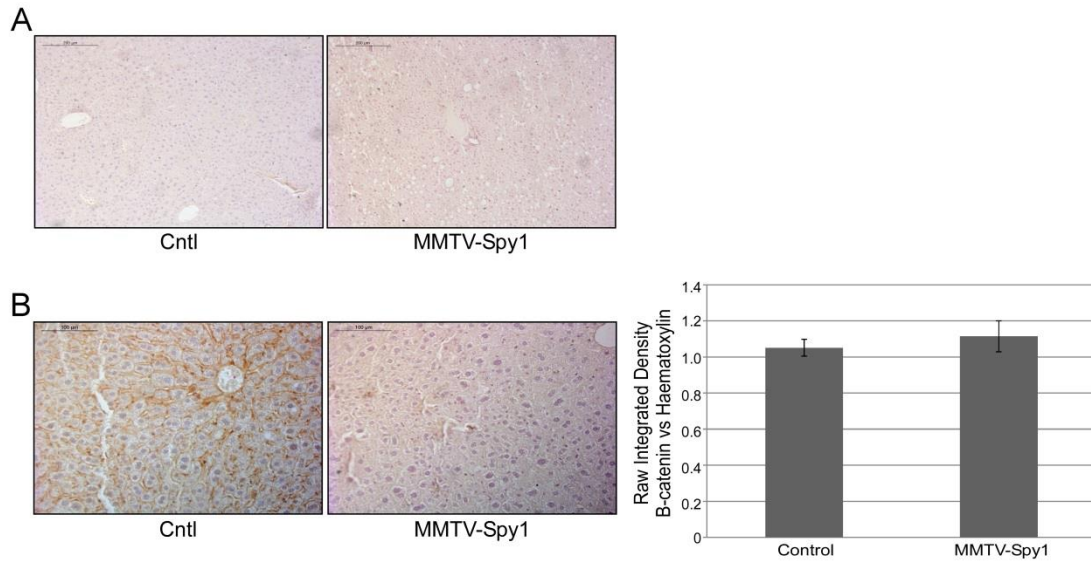


Figure 3: MMTV-Spy1 mice show increased inflammatory pathway signaling and apoptosis. Immunohistochemical analysis of MMTV-Spy1 or littermate controls (cntl). Male livers were analysed over a minimum of 4 fields of view per sample and levels were quantified using ImageJ analysis software correcting for number of cells present per field of view. Representative images are shown in left panels, and quantification of expression is depicted in right panels. **A**) Analysis of p53 levels (MMTV-Spy1 n=4, Cntl n=3). **B**) Analysis of p21 levels (MMTV-Spy1 n=4, Cntl n=3). **C**) Analysis of active caspase 3 (MMTV-Spy1 n=2, Cntl n=2) where blue stain is haematoxylin and brown stain is p53 (A), p21 (B) or active caspase 3 (C). Scale bar=0.1 mm. Error bars reflect SE; Students T-test *p=0.041105, **p=0.003244, ***p=8.56x10⁻¹⁶



Supplementary Figure 1: qRT-PCR analysis in MMTV-Spy1 male livers. qRT-PCR analysis of MMTV-Spy1 mice and littermate controls over one year of age for **A)** albumin **B)** p21 and **C)** Nestin (left panel depicts average levels, while right panel depicts Nestin levels in individual mice where red boxes indicate tumour tissue) all corrected for total GAPDH levels. Error bars reflect SE, Student's T-test



Supplementary Figure 2: MMTV-Spy1 male mice immunohistochemical analysis. Immunohistochemical analysis of MMTV-Spy1 and control (cntl) liver samples where blue stain represents haematoxylin and brown stain represents P-H2AX (A) or B-catenin (B). Quantification was conducted using ImageJ analysis software. **A)** Analysis of P-H2AX levels (right panel) and representative images (left panel). Scale bar= 200 μ M. **B)** Analysis of B-catenin levels (right panel) and representative images (left panel). Scale bar= 100 μ M. Error bars reflect SE.

Alteration of Spy1 levels in a HCC cell line causes changes in proliferation and fatty acid accumulation.

MMTV-Spy1 mice exhibit increased incidence of HCC, increased fat accumulation, and up-regulation of key mediators in the apoptotic response pathway. To determine the direct effects of increased Spy1 levels on characteristics of HCC, we utilized the well characterized HepG2 HCC cell line. Using these cells, we overexpressed Spy1 (Figure 4A) and examined the effects of elevated Spy1 on accumulation of fat within hepatocytes and proliferative capacity of the cells. Using Oil Red O staining, a technique commonly used for the staining of accumulated lipid droplets, we show that overexpression of Spy1 increases lipid accumulation in HepG2 cells (Figure 4B). Additionally, through BrdU staining, we show that elevated levels of Spy1 significantly increases the percentage of BrdU positive cells (Figure 4C). In contrast, knockdown of Spy1 (Figure 5A) leads to a significant decline in Oil Red O staining (Figure 5B), and a decrease in the percentage of BrdU positive cells (Figure 5C). Thus, Spy1 appears to play a pivotal role in maintaining elevated rates of proliferation and promoting and maintaining lipid accumulation.

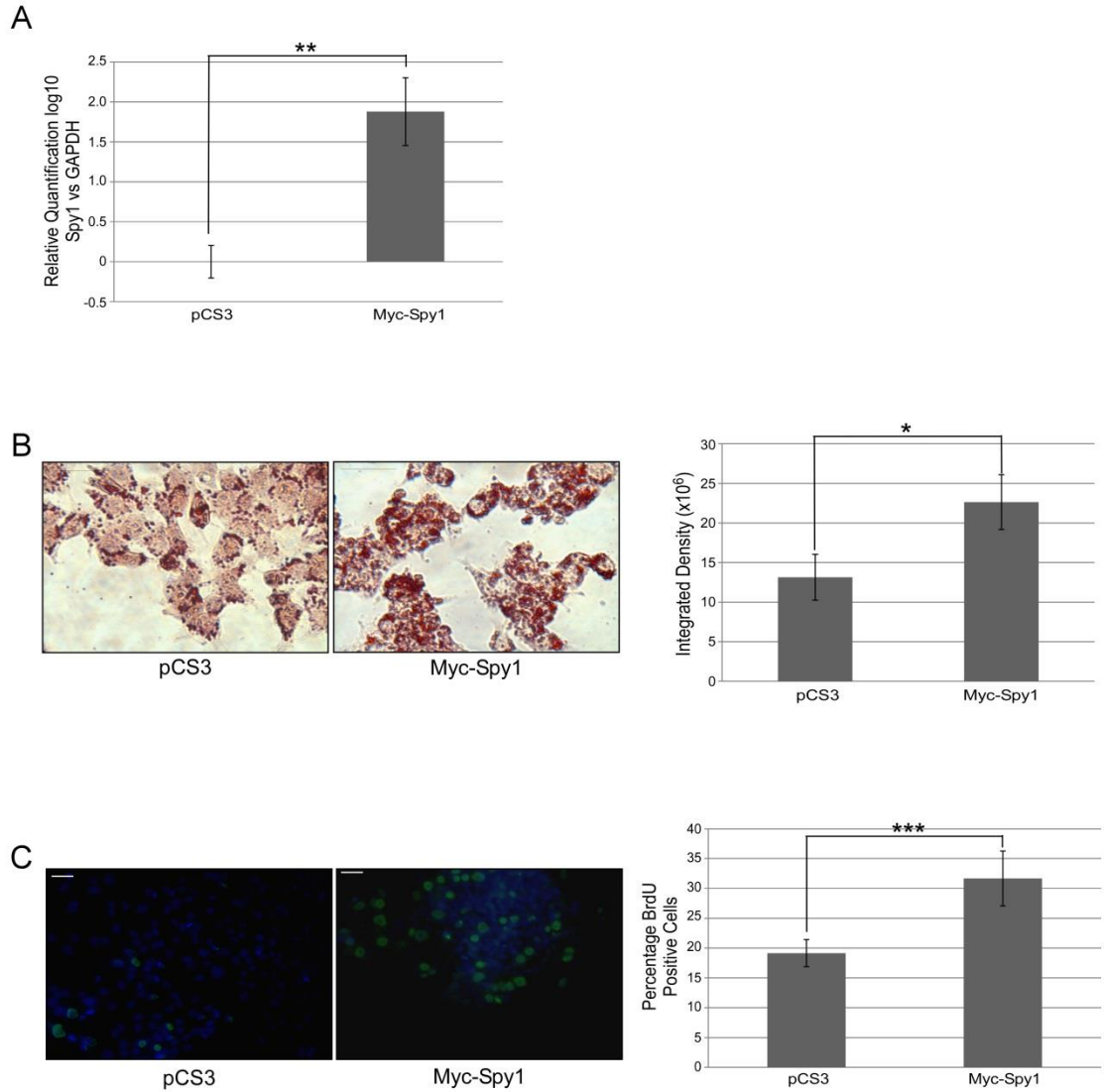


Figure 4: Spy1 overexpression leads to increased proliferation and lipid accumulation. HepG2 cells were transfected with Myc-Spy1-pCS3 (Myc-Spy1) or control vector (pCS3). **A**) qRT-PCR analysis of Spy1 levels in HepG2 cells to confirm successful transfection (n=3). **B**) Representative brightfield images of Oil Red staining of HepG2 cells (left panel) where red stain is Oil Red stain, and graphical representation of staining intensity (right panel) (n=3). Staining intensity was measured and quantified using ImageJ analysis software. **C**) Representative images of BrdU analysis of HepG2 cells (left panel), and graphical quantification (right panel) (n=3). Number of BrdU positive and total number of cells was quantified, and percentage of BrdU positive cells was calculated. Scale bar= 50 μ m. Error bars reflect SE; Student's T-test. *p=0.049282, **p=0.010626, ***p=0.005768

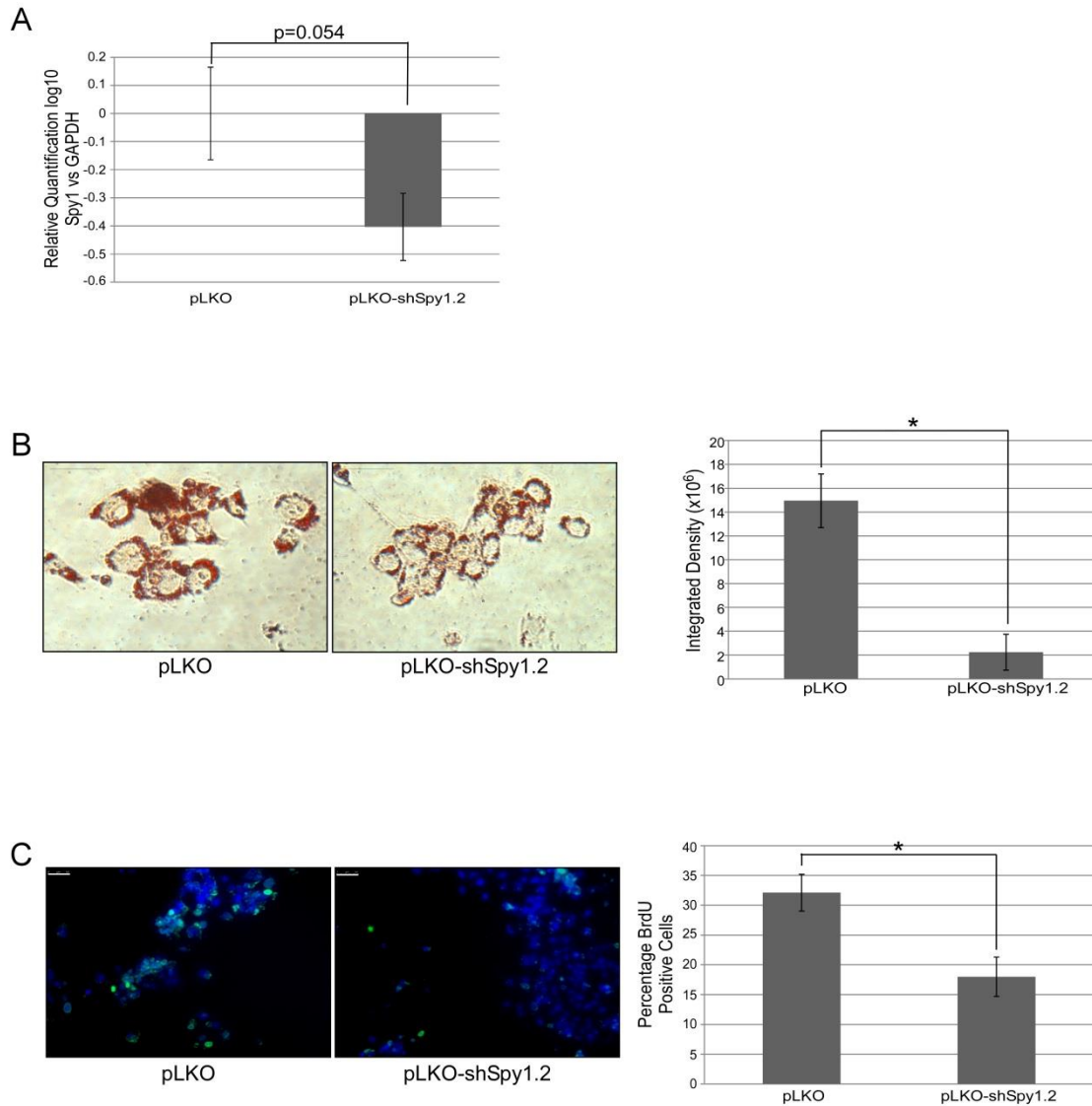


Figure 5: Spy1 knockdown leads to decreased proliferation and lipid accumulation. HepG2 cells were transfected with pLKOshSpy1.2 and vector control (pLKO). **A)** qRT-PCR analysis of Spy1 levels in HepG2 cells to confirm successful transfection (n=3). **B)** Representative brightfield images of Oil Red staining of HepG2 cells (left panel) where red stain is Oil Red stain, and graphical representation of staining intensity(right panel)(n=3). Stain intensity was measured and quantified using ImageJ analysis software. **C)** Representative images of BrdU analysis of HepG2 cells (left panel), and graphical quantification (right panel)(n=3). Number of BrdU positive and total number of cells was counted and percentage of BrdU positive cells was calculated. Scale bar=50 μ M. Error bars reflect SE; Student's T-test. *p<0.05

Discussion

The MMTV-Spy1 transgenic mouse model was initially generated to study the effects of aberrant Spy1 expression on mammary gland development and tumorigenesis. The MMTV promoter is well documented and has been shown to induce expression of the transgene in various tissue types with the most common organs affected being secretory organs such as the salivary gland (Callahan and Smith, 2000; Cardiff and Kenney, 2011). There have been however, documented cases of transgene expression in the liver (Wagner et al., 2001). Surprisingly, we find a significant increase in rates of liver tumour formation in MMTV-Spy1 male mice. Indeed, increased levels of Spy1 were found in aged MMTV-Spy1 male livers and interestingly, transgene expression was not noted in livers of aged females, further indicating male specific transgene expression within the liver. MMTV driven transgene expression has been found in other male tissues, such as male reproductive organs (Parker et al., 1987; Rollini et al., 1992). Androgen responsive elements have been noted within the MMTV promoter thus indicating the possibility that androgen stimulation could lead to male specific liver expression of the transgene (Parker et al., 1987; Rollini et al., 1992). Although MMTV-Spy1 males did develop significantly more tumours than control mice, tumours were still found in controls. CBA mice are known to have increased susceptibility to HCC, and since the MMTV-Spy1 mouse is maintained on a B6CBAF1/J background, we would expect to see tumour formation in wild-type animals as well (Bilger et al., 2004; Smith et al., 1973). Our data supports that overexpression of Spy1 is enhancing the susceptibility phenotype of this genetic background of mice.

Histological analysis revealed key differences in MMTV-Spy1 and control liver tissue. Nuclear area in livers of MMTV-Spy1 mice was found to be significantly larger than those of control livers. Increased nuclear area could be caused by either increased ploidy in hepatocytes or senescence (Gonzalez-Reimers et al., 1987; Nakajima et al., 2010). To determine if nuclear size is increased due to increased ploidy of hepatocytes, primary cells from the livers of MMTV-Spy1 and control mice could be extracted and analyzed via flow cytometry to assess DNA content.

Additionally, immunohistochemical analysis could be utilized through the use of a Feulgen stain, which directly stains DNA. The amount of stain colour and intensity of the stain is directly proportional to the amount of DNA present, therefore, if increased staining was observed this would indicate increased DNA content and ploidy. Since Spy1 is capable of promoting cell cycle progression, it is plausible that increased amounts of Spy1 could in fact be triggering elevated rates of DNA replication leading to increased DNA content in hepatocytes. In addition to increased ploidy, increased nuclear size is also known to occur during senescence (Mitsui and Schneider, 1976; Rodier and Campisi, 2011). In cases of NAFLD/NASH, increases in nuclear size correlate with elevated expression of p21, which is seen in the MMTV-Spy1 mice (Nakajima et al., 2010). Senescent cells have been shown to increase in size, and studies have proven that senescent cells are capable of promoting malignancy in premalignant epithelial cells *in vivo* indicating that the potential presence of senescent cells could in fact contribute to tumour onset (Krtolica et al., 2001). Determining the precise cause of the observed increase in nuclear size would shed light on how Spy1 may be causing enhanced tumourigenesis in MMTV-Spy1 mice.

Livers of MMTV-Spy1 mice also displayed increased levels of fat. Although the difference was not statistically significant, this manifestation could have profound consequences on the development of HCC and play a key role in its progression. NASH is characterized by increased fat droplets in the liver, and is known to be a risk factor for tumour development (The National Digestive Diseases Information Clearinghouse, 2014). Thus, even though the increase in number of mice with fatty liver is not significant, small changes in fat accumulation could play a key role in the significant increase in liver tumours seen. The predominating factor in progression from NASH to HCC is the damage inflammation causes in the liver as a result of fat accumulation. Fatty acids trigger an inflammatory response, leading to increased injury to the liver that hepatocytes would typically be able to repair (Dowman et al., 2010; Feldstein et al., 2004; Jou et al., 2008). In cases of severe injury, hepatocytes ultimately senesce or undergo apoptosis diminishing the ability of the liver to repair injured areas of tissue (Dowman et al.,

2010; Takahashi et al., 2012). Elevated levels of p53 have been found in cases of NASH and positively correlate with increasing degrees of inflammation (Farrell et al., 2009; Kodama et al., 2011; Panasiuk et al., 2006; Yahagi et al., 2004). Activation of p53 triggers up-regulation of its downstream target p21, which arrests the cell cycle, and ultimately, p53 will lead to apoptosis of damaged hepatocytes (Farrell et al., 2009; Yahagi et al., 2004). MMTV-Spy1 mice display characteristics of a severely diseased liver. We see increased levels of p53 and p21 as well as increased amounts of active caspase-3 indicating significant injury and inflammation, and a decline in the regenerative potential of the liver due to apoptosis. To confirm progression of the disease to fibrosis of the liver, trichrome staining would need to be completed to verify the presence of collagen which is deposited by stellate cells in response to inflammation.

Since Spy1 causes enhanced cell cycle progression, it could act as a stressor in and of itself, triggering and enhancing activation of p53 which would halt cell cycle progression and return the hepatocytes to a normal state of quiescence. In an already transformed cell line, we show that overexpression of Spy1 significantly increases levels of proliferation and lipid droplet accumulation, while knockdown of Spy1 has the opposite effect, leading to both decreased BrdU incorporation and Oil Red O staining. This provides further support for the theory that Spy1 could be acting as a stressor, leading to activation of stress response pathways and triggering inflammatory response pathways that would lead to development and progression of NASH. Severe cases of NASH would ultimately lead to a decline in liver function, and ultimately liver failure or HCC.

Spy1 has been demonstrated to mediate mammary tumour susceptibility using the MMTV-Spy1 transgenic model and treatment with known carcinogens. Here we describe a potential role for Spy1 in mediating susceptibility to liver tumour formation and promoting severe liver disease. Elevated levels of Spy1 increase proliferation, and trigger lipid accumulation in established HCC cells. *In vivo*, although not significant we see lipid accumulation in addition to significant up-regulation of markers associated with severe cases of NASH which can lead to the

development of HCC. Thus it appears that Spy1 plays a pivotal role in mediating liver tumour initiation and could prove to be an attractive therapeutic target in treatment of this devastating disease.

Acknowledgements

We thank Dr. Christopher Pin and Linsay Drysdale from the London Regional Transgenic and Gene Targeting Facility for generation of the MMTV-Spy1 mouse, and the Mutant Mouse Pathology Lab, Center for Comparative Medicine, University of California, Davis and Dr. Robert Cardiff for pathology. Thanks to Dr. John Hudson for donation of HepG2 cells, and Dr. Dennis Higgs for use of equipment. Special thanks to Dr. Dorota Lubanska, Ingrid Qemo, Ellen Laurie and Nick Paquette for assistance with genotyping and Mitchell Elliot for technical assistance. B.F. acknowledges support from the University of Windsor, the Ontario Graduate Scholarship Program and Canadian Breast Cancer Foundation.

References

- Barnes, E. A., Porter, L. A., Lenormand, J. L., Dellinger, R. W., and Donoghue, D. J. (2003). Human Spyl1 promotes survival of mammalian cells following DNA damage. *Cancer Res* 63, 3701-3707.
- Bataller, R., and Brenner, D. A. (2005). Liver fibrosis. *J Clin Invest* 115, 209-218.
- Beer, S., Zetterberg, A., Ihrle, R. A., McTaggart, R. A., Yang, Q., Bradon, N., Arvanitis, C., Attardi, L. D., Feng, S., Ruebner, B., *et al.* (2004). Developmental context determines latency of MYC-induced tumorigenesis. *PLoS Biol* 2, e332.
- Bilger, A., Bennett, L. M., Carabeo, R. A., Chiaverotti, T. A., Dvorak, C., Liss, K. M., Schadewald, S. A., Pitot, H. C., and Drinkwater, N. R. (2004). A potent modifier of liver cancer risk on distal mouse chromosome 1: linkage analysis and characterization of congenic lines. *Genetics* 167, 859-866.
- Bisteau, X., Caldez, M. J., and Kaldis, P. (2014). The Complex Relationship between Liver Cancer and the Cell Cycle: A Story of Multiple Regulations. *Cancers (Basel)* 6, 79-111.
- Cai, D., Yuan, M., Frantz, D. F., Melendez, P. A., Hansen, L., Lee, J., and Shoelson, S. E. (2005). Local and systemic insulin resistance resulting from hepatic activation of IKK-beta and NF-kappaB. *Nat Med* 11, 183-190.
- Callahan, R., and Smith, G. H. (2000). MMTV-induced mammary tumorigenesis: gene discovery, progression to malignancy and cellular pathways. *Oncogene* 19, 992-1001.
- Canadian Cancer Society (2014). Canadian Cancer Society Statistics. In.
- Cardiff, R. D., and Kenney, N. (2011). A compendium of the mouse mammary tumor biologist: from the initial observations in the house mouse to the development of genetically engineered mice. *Cold Spring Harb Perspect Biol* 3.
- Cheng, A., Gerry, S., Kaldis, P., and Solomon, M. J. (2005). Biochemical characterization of Cdk2-Speedy/Ringo A2. *BMC Biochem* 6, 19.

Dowman, J. K., Tomlinson, J. W., and Newsome, P. N. (2010). Pathogenesis of non-alcoholic fatty liver disease. *QJM* 103, 71-83.

Ehrenfried, J. A., Ko, T. C., Thompson, E. A., and Evers, B. M. (1997). Cell cycle-mediated regulation of hepatic regeneration. *Surgery* 122, 927-935.

Farrell, G. C., Larter, C. Z., Hou, J. Y., Zhang, R. H., Yeh, M. M., Williams, J., dela Pena, A., Francisco, R., Osvath, S. R., Brooling, J., *et al.* (2009). Apoptosis in experimental NASH is associated with p53 activation and TRAIL receptor expression. *J Gastroenterol Hepatol* 24, 443-452.

Fattovich, G., Stroffolini, T., Zagni, I., and Donato, F. (2004). Hepatocellular carcinoma in cirrhosis: incidence and risk factors. *Gastroenterology* 127, S35-50.

Fausto, N., and Campbell, J. S. (2003). The role of hepatocytes and oval cells in liver regeneration and repopulation. *Mech Dev* 120, 117-130.

Feldstein, A. E., Werneburg, N. W., Canbay, A., Guicciardi, M. E., Bronk, S. F., Rydzewski, R., Burgart, L. J., and Gores, G. J. (2004). Free fatty acids promote hepatic lipotoxicity by stimulating TNF- α expression via a lysosomal pathway. *Hepatology* 40, 185-194.

Friedman, S. L., Roll, F. J., Boyles, J., and Bissell, D. M. (1985). Hepatic lipocytes: the principal collagen-producing cells of normal rat liver. *Proc Natl Acad Sci U S A* 82, 8681-8685.

Gastwirt, R. F., Slavin, D. A., McAndrew, C. W., and Donoghue, D. J. (2006). Spyl expression prevents normal cellular responses to DNA damage: inhibition of apoptosis and checkpoint activation. *J Biol Chem* 281, 35425-35435.

Germain, L., Blouin, M. J., and Marceau, N. (1988). Biliary epithelial and hepatocytic cell lineage relationships in embryonic rat liver as determined by the differential expression of cytokeratins, alpha-fetoprotein, albumin, and cell surface-exposed components. *Cancer Res* 48, 4909-4918.

Golipour, A., Myers, D., Seagroves, T., Murphy, D., Evan, G. I., Donoghue, D. J., Moorehead, R. A., and Porter, L. A. (2008). The Spy1/RINGO family represents a novel mechanism regulating mammary growth and tumorigenesis. *Cancer Res* 68, 3591-3600.

Gonzalez-Reimers, C. E., Santolaria-Fernandez, F. J., Castaneyra-Perdomo, A., Jorge-Hernandez, J. A., Martin-Herrera, A., and Hernandez-Nieto, L. (1987). Hepatocyte and nuclear areas in alcoholic liver cirrhosis: their relationship with the size of the nodules and the degree of fibrosis. *Drug Alcohol Depend* 19, 357-362.

Grisham, J. W. (1962). A morphologic study of deoxyribonucleic acid synthesis and cell proliferation in regenerating rat liver; autoradiography with thymidine-H3. *Cancer Res* 22, 842-849.

Jou, J., Choi, S. S., and Diehl, A. M. (2008). Mechanisms of disease progression in nonalcoholic fatty liver disease. *Semin Liver Dis* 28, 370-379.

Karaiskou, A., Perez, L. H., Ferby, I., Ozon, R., Jesus, C., and Nebreda, A. R. (2001). Differential regulation of Cdc2 and Cdk2 by RINGO and cyclins. *J Biol Chem* 276, 36028-36034.

Ke, Q., Ji, J., Cheng, C., Zhang, Y., Lu, M., Wang, Y., Zhang, L., Li, P., Cui, X., Chen, L., *et al.* (2009). Expression and prognostic role of Spy1 as a novel cell cycle protein in hepatocellular carcinoma. *Exp Mol Pathol* 87, 167-172.

Kodama, T., Takehara, T., Hikita, H., Shimizu, S., Shigekawa, M., Tsunematsu, H., Li, W., Miyagi, T., Hosui, A., Tatsumi, T., *et al.* (2011). Increases in p53 expression induce CTGF synthesis by mouse and human hepatocytes and result in liver fibrosis in mice. *J Clin Invest* 121, 3343-3356.

Krtolica, A., Parrinello, S., Lockett, S., Desprez, P. Y., and Campisi, J. (2001). Senescent fibroblasts promote epithelial cell growth and tumorigenesis: a link between cancer and aging. *Proc Natl Acad Sci U S A* 98, 12072-12077.

- Lenormand, J. L., Dellinger, R. W., Knudsen, K. E., Subramani, S., and Donoghue, D. J. (1999). Speedy: a novel cell cycle regulator of the G2/M transition. *Embo J* 18, 1869-1877.
- Ljubimova, J. Y., Petrovic, L. M., Wilson, S. E., Geller, S. A., and Demetriou, A. A. (1997). Expression of HGF, its receptor c-met, c-myc, and albumin in cirrhotic and neoplastic human liver tissue. *J Histochem Cytochem* 45, 79-87.
- McAndrew, C. W., Gastwirt, R. F., and Donoghue, D. J. (2009). The atypical CDK activator Spy1 regulates the intrinsic DNA damage response and is dependent upon p53 to inhibit apoptosis. *Cell Cycle* 8, 66-75.
- McAndrew, C. W., Gastwirt, R. F., Meyer, A. N., Porter, L. A., and Donoghue, D. J. (2007). Spy1 enhances phosphorylation and degradation of the cell cycle inhibitor p27. *Cell Cycle* 6, 1937-1945.
- Meek, D. W. (2004). The p53 response to DNA damage. *DNA Repair (Amst)* 3, 1049-1056.
- Michalopoulos, G. K. (2007). Liver regeneration. *J Cell Physiol* 213, 286-300.
- Mitsui, Y., and Schneider, E. L. (1976). Increased nuclear sizes in senescent human diploid fibroblast cultures. *Exp Cell Res* 100, 147-152.
- Nakajima, T., Nakashima, T., Okada, Y., Jo, M., Nishikawa, T., Mitsumoto, Y., Katagishi, T., Kimura, H., Itoh, Y., Kagawa, K., and Yoshikawa, T. (2010). Nuclear size measurement is a simple method for the assessment of hepatocellular aging in non-alcoholic fatty liver disease: Comparison with telomere-specific quantitative FISH and p21 immunohistochemistry. *Pathol Int* 60, 175-183.
- Panasiuk, A., Dzieciol, J., Panasiuk, B., and Prokopowicz, D. (2006). Expression of p53, Bax and Bcl-2 proteins in hepatocytes in non-alcoholic fatty liver disease. *World J Gastroenterol* 12, 6198-6202.
- Parker, M. G., Webb, P., Needham, M., White, R., and Ham, J. (1987). Identification of androgen response elements in mouse mammary tumour virus and the rat prostate C3 gene. *J Cell Biochem* 35, 285-292.

Porter, L. A., Dellinger, R. W., Tynan, J. A., Barnes, E. A., Kong, M., Lenormand, J. L., and Donoghue, D. J. (2002). Human Speedy: a novel cell cycle regulator that enhances proliferation through activation of Cdk2. *J Cell Biol* *157*, 357-366.

Porter, L. A., Kong-Beltran, M., and Donoghue, D. J. (2003). Spy1 interacts with p27Kip1 to allow G1/S progression. *Mol Biol Cell* *14*, 3664-3674.

Rodier, F., and Campisi, J. (2011). Four faces of cellular senescence. *J Cell Biol* *192*, 547-556.

Rollini, P., Billotte, J., Kolb, E., and Diggelmann, H. (1992). Expression pattern of mouse mammary tumor virus in transgenic mice carrying exogenous proviruses of different origins. *J Virol* *66*, 4580-4586.

Sakaguchi, K., Herrera, J. E., Saito, S., Miki, T., Bustin, M., Vassilev, A., Anderson, C. W., and Appella, E. (1998). DNA damage activates p53 through a phosphorylation-acetylation cascade. *Genes Dev* *12*, 2831-2841.

Sancar, A., Lindsey-Boltz, L. A., Unsal-Kacmaz, K., and Linn, S. (2004). Molecular mechanisms of mammalian DNA repair and the DNA damage checkpoints. *Annu Rev Biochem* *73*, 39-85.

Shachaf, C. M., Kopelman, A. M., Arvanitis, C., Karlsson, A., Beer, S., Mandl, S., Bachmann, M. H., Borowsky, A. D., Ruebner, B., Cardiff, R. D., *et al.* (2004). MYC inactivation uncovers pluripotent differentiation and tumour dormancy in hepatocellular cancer. *Nature* *431*, 1112-1117.

Smith, G. S., Walford, R. L., and Mickey, M. R. (1973). Lifespan and incidence of cancer and other diseases in selected long-lived inbred mice and their F 1 hybrids. *J Natl Cancer Inst* *50*, 1195-1213.

Takahashi, Y., Soejima, Y., and Fukusato, T. (2012). Animal models of nonalcoholic fatty liver disease/nonalcoholic steatohepatitis. *World J Gastroenterol* *18*, 2300-2308.

The National Digestive Diseases Information Clearinghouse (2014). Nonalcoholic Steatohepatitis. In.

Wagner, K. U., McAllister, K., Ward, T., Davis, B., Wiseman, R., and Hennighausen, L. (2001). Spatial and temporal expression of the Cre gene under the control of the MMTV-LTR in different lines of transgenic mice. *Transgenic Res* 10, 545-553.

Webber, E. M., Bruix, J., Pierce, R. H., and Fausto, N. (1998). Tumor necrosis factor primes hepatocytes for DNA replication in the rat. *Hepatology* 28, 1226-1234.

Webber, E. M., Godowski, P. J., and Fausto, N. (1994). In vivo response of hepatocytes to growth factors requires an initial priming stimulus. *Hepatology* 19, 489-497.

World Health Organization (2014). Cancer. In.

Yahagi, N., Shimano, H., Matsuzaka, T., Sekiya, M., Najima, Y., Okazaki, S., Okazaki, H., Tamura, Y., Iizuka, Y., Inoue, N., *et al.* (2004). p53 involvement in the pathogenesis of fatty liver disease. *J Biol Chem* 279, 20571-20575.

Zorn, A. M. (2008). Liver development.

Chapter 4

An Inducible Model System for Spatial and Temporal Control of *Spy1* Expression

Introduction

A single transgenic mouse model allowing for constitutive overexpression of a protein of interest undoubtedly provides an excellent model in which to study altered expression levels on various tissue systems. The ability to induce expression and control it in a temporal and spatial manner however, opens up more avenues of exploration and allows for more specific questions to be answered (Gunther et al., 2002; Haruyama et al., 2009; Muller, 1999; Sun et al., 2007; Zhang et al., 2010; Zhu et al., 2002). The reverse tetracycline transactivator system, rtTA, was developed as a solution to some of the pitfalls associated with the tetracycline transactivator system (tTA), allowing for inducible expression of a transgene upon administration of doxycycline (Gossen et al., 1995). In the tTA system, the transgene of interest is on in the absence of doxycycline (Furth et al., 1994). For the transgene to be turned off, doxycycline is administered which presents problems when transgene activation is required again (Muller, 1999; Sun et al., 2007; Zhang et al., 2010). Removal of doxycycline allows for transgene expression, however, induction of the gene is dependent on removal of the substance from the organism's system, thus rapid induction of the transgene is not achievable. Using the rtTA system, transgene expression is induced upon delivery of doxycycline allowing for rapid induction of gene expression. Upon removal of doxycycline, gene levels have been shown to return to basal levels 24 hours after removal of doxycycline (Blakely et al., 2005; Gunther et al., 2002). Thus, the rtTA system has proven to be a more robust and effective system at inducing transgene expression during specified periods of development.

Mammary gland biology has utilized this system and developed the MMTV-rtTA system. This system has tighter control of transgene expression, is highly specific to the mammary gland as compared to other MMTV models and demonstrates more homogenous expression through the mammary gland (Gunther et al., 2002). Expression of the transgene can be seen as early as 6 hours after doxycycline induction and reach steady state levels by 48 hours (Gunther et al., 2002). Removal of doxycycline returns transgene expression to basal levels 24 hours after withdrawal

(Gunther et al., 2002). Additionally, levels of transgene expression can be titrated based on the dose of doxycycline administered (Gunther et al., 2002). Thus, this system provides a model to allow for specific spatial and temporal induction of a transgene while also allowing researchers to induce transgene expression at varying levels, something which cannot be achieved using classic transgenic model systems. The advantages of using an inducible system have been demonstrated using the MMTV-rtTA promoter driving c-Myc overexpression within the mammary gland (Blakely et al., 2005). Using this system, a 72 hour period during pregnancy was shown to be the key stage of development that impairs the ability of mice to successfully nurse their pups if high levels of c-Myc are expressed (Blakely et al., 2005). To further validate the inducible system, c-Myc expression was turned on and was found to recapitulate the phenotype observed in the MMTV-Myc mouse (Blakely et al., 2005). These findings further validate the use of the MMTV-rtTA model as a valuable tool in studying altered gene expression at specified times of mammary development.

We aim to utilize the MMTV-rtTA system to study the precise role of the cell cycle regulator Spy1 in various stages of mammary development. Spy1 levels have been shown to be tightly regulated during the course of development, with high levels corresponding to periods of proliferation and apoptosis, and low levels corresponding to periods of differentiation (Golipour et al., 2008). Overexpression of Spy1 via mammary fat pad transplantation leads to accelerated development as well as the development of mammary tumours (Golipour et al., 2008). The development of mammary tumours precludes studying the role of Spy1 in lactation. Previous data has shown that overexpression of Spy1 in an *in vitro* setting led to abnormal morphology of the cells when treated with differentiation stimuli, suggesting a key role for Spy1 during normal mammary differentiation (Golipour et al., 2008). An inducible model system would allow us to turn on Spy1 during key periods of mammary differentiation, such as during pregnancy and lactation, and to investigate the precise period of development critical for Spy1 downregulation.

Herein we describe the development of the Spy1-pTRE transgenic mouse. Crossing this newly developed transgenic mouse with the MMTV-rtTA mouse, we have demonstrated inducible expression of Spy1 within the mammary gland upon administration of doxycycline. Additionally, we have data supporting that long term Spy1 expression does not alter mammary development. This system will prove to be a valuable tool in the study of Spy1 in mammary gland development.

Materials and Methods

Construction and Generation of Spy1-pTRE Transgene

Site directed mutagenesis was conducted to generate an XbaI site in Flag-Spy1A-pLXSN (Porter et al., 2003). The pTRE-Tight caspase 3 (p12) : : n2 [TU#817] vector (Addgene 16084) was subsequently digested with EcoRI and XbaI to remove the caspase 3 insert and allow for ligation of the Flag-Spy1 coding sequence from the Flag-Spy1A-pLXSN vector into the pTRE-Tight backbone.

Generation and Maintenance of Spy1-pTRE Mice and Maintenance of MMTV-rtTA Mice

The Spy1-pTRE vector was digested with XhoI to remove the vector backbone and isolate the Spy1-pTRE transgene fragment. The resulting transgene fragment was sent to the London Regional Transgenic and Gene Targeting Facility where pronuclear injections were performed in B6CBAF1/J hybrid embryos. Identification of positive founders as well as subsequent maintenance of the colony was performed using PCR analysis. The PCR reaction conditions were as follows. A 25uL reaction containing 100ng of genomic DNA, 0.4uM forward primer [5' GTGTACGGTGGGAGGCCTATATAA 3'], 0.4uM reverse primer [5' GTCATAGCCAAAAGATACTTGTCTGC 3'] and 12.5uL of New England Biolabs Master Mix was prepared. PCR cycling conditions were as follows: 95°C for 2 minutes 30 seconds; 40 cycles of 95°C for 45 seconds, 60°C for 45 seconds and 72°C for 1 minute 30 seconds, followed by a final extension at 72°C for 10 minutes. Spy1-pTRE mice were maintained on the B6CBAF1/J background and were also backcrossed with FVB mice to generate Spy1-pTRE mice on an FVB background.

MMTV-rtTA mice were obtained from the lab of Dr. Roger Moorehead from the University of Guelph, and were maintained on an FVB background. PCR analysis was utilized for the identification of mice containing the MMTV-rtTA transgene. Briefly, 50ng of genomic tail DNA was added to a 25uL reaction (1x PCR buffer, 2mM MgSO₄, 0.2mM dNTP, 0.04U/uL UBI

Taq Polymerase, 0.4uM forward primer [5'TGCAGAGCC AGCCTTCTTAT 3'], 0.4uM reverse primer [5' CCTCGATGGTAGACC CGTAA 3']. PCR cycling conditions were as follows: 94°C for 5 minutes, 36 cycles of 94°C for 30 seconds, 58°C for 30 seconds and 72°C for 45 seconds, followed by a final extension of 72°C for 7 minutes.

Expression was induced by feeding mice food containing 2g/kg of doxycycline ad libitum (Harlan Laboratories). Mice were maintained following the Canadian Council on Animal Care Guidelines under the animal utilization protocol 10-16 approved by the University of Windsor.

Quantitative Real Time PCR Analysis

RNA was isolated from flash frozen tissue using the Qiagen RNeasy Plus Mini Kit as per manufacturer's instructions. cDNA was synthesized using Superscript II (Invitrogen), as per manufacturer's instructions. Real Time PCR was performed using Sybr Green detection (Applied Biosystems) on a Viiia7 Real Time PCR System (Life Technologies) and was analyzed using the Viiia7 Real Time PCR System software. Sequences for Flag-Spy1 and mouse GAPDH primers were as follows:

Flag Spy1 Forward: 5'TGACAAGAGGCACAATCAGATGT 3'

Flag Spy1 Reverse: 5' CAAATAGGACGCTTCAGAGTAATGG3'

Mouse GAPDH Forward: 5' GATGCCCCCATGTTTGTGAT 3'

Mouse GAPDH Reverse: 5' GTGGTCATGAGCCCTTCCA 3'

Whole Mount Analysis

Inguinal glands were collected and spread onto a positively charged slide. Slides were immersed in Clarke's Fluid (75% ethyl alcohol, 25% acetic acid) overnight. The following day, glands were placed in 70% ethyl alcohol for 30 minutes at room temperature and were subsequently left in Carmine Solution (0.2% carmine, 0.5% potassium sulfate) to stain ductal structures overnight. Glands were placed into de-staining solution (1% hydrogen chloride, 70%

ethyl alcohol) for 4 to 6 hours until the gland appeared to have been sufficiently de-stained. The glands were subsequently dehydrated in ascending concentrations of ethyl alcohol for 15 minutes each (70%, 95%, 100%) before being cleared in xylene overnight (or until glands were sufficiently cleared). Glands were mounted with Permount toluene solution (Fisher Scientific) and images were acquired using a Leica M205 FA stereo microscope (University of Windsor) and captured using LAS V4.3 software.

Histology and Immunostaining

Briefly, inguinal glands were fixed in 10% neutral buffered formalin and were subsequently dehydrated through a series of ascending ethanol concentrations, followed by clearing in xylene. Following clearing in xylene, the tissues were embedded in paraffin wax and sectioned into 5µm sections using the Leica RM2125RT. For immunohistochemistry, sections were first rehydrated in a series of descending ethanol concentrations, followed by heat mediated antigen retrieval with 10mM sodium citrate buffer pH 6.0. Next, endogenous peroxidase activity was blocked using 3% H₂O₂ diluted in methanol, and sections were subsequently blocked using MOM blocker (Biocare Medical; mouse secondary antibody) or 3% BSA-0.1% Tween-20 in 1x PBS (rabbit secondary antibody). Sections were incubated in primary antibody diluted in appropriate blocker overnight at 4°C. Following incubation in primary antibody, sections were washed with 1xPBS and were incubated for 1 hour in a humidified chamber in secondary antibody diluted in the appropriate blocker at 1:750. Sections were once again washed with 1xPBS and were treated with ABC reagent (Vectastain ABC Kit) as per manufacturer's instructions. Sections were subsequently stained with DAB reagent (DAB Peroxidase Substrate Kit, Vector Laboratories) as per manufacturer's instructions, and were counterstained with haematoxylin (Vector Laboratories). In a series of ascending ethanol concentrations, sections were dehydrated and coverslipped using Permount toluene solution (Fisher Scientific). Images were obtained using the LEICA DMI6000 inverted microscope with LAS 3.6 software.

Haematoxylin and eosin stained slides were rehydrated in a series of descending ethanol concentrations, and were then washed in distilled water. Sections were stained with haematoxylin (Vector Laboratories), and were rinsed in running tap water for up to 10 minutes. Sections were subsequently stained with eosin (Sigma Aldrich) and were dehydrated in a series of ascending ethanol concentrations before being coverslipped using Permount toluene solution (Fisher Scientific).

Results

Spy1-pTRE transgenic mouse model generation and model validation.

The Spy1-pTRE transgene was cloned as described in materials and methods. Briefly, the Flag-Spy1 human cDNA sequence was cloned into the pTRE-Tight vector, digested to remove vector backbone, and sent to the London Regional Transgenic and Gene Targeting Facility. Construction of this transgene will allow for inducible spatial and temporal expression of Spy1 under the control of the pTRE-Tight promoter (Figure 1A) upon administration of doxycycline. The resulting Spy1-pTRE mice are crossed with the MMTV-rtTA mouse model generating pups of four potential genotypes (Figure 1A). The MTB-Spy1 mouse will contain both the Spy1-pTRE transgene and MMTV-rtTA transgene. This double transgenic mouse will overexpress Spy1 specifically within the mammary gland upon administration of doxycycline. Pups resulting from the cross may also contain only one of the transgenes, or neither. These offspring are used as controls as administration of doxycycline will not result in Spy1 overexpression.

Spy1-pTRE founders were identified via PCR analysis and germline transmission from founder to offspring was also confirmed (Figure 1B). Once germline transmission of the transgene was confirmed, Spy1-pTRE mice were crossed with MMTV-rtTA mice to produce the MTB-Spy1 mice and appropriate controls. 5 week old MTB-Spy1 mice and their control littermates were administered doxycycline through their diet, and tissue from the inguinal glands was collected 72 hours after beginning the doxycycline diet. To confirm that Spy1 expression is indeed induced in this model, qRT-PCR analysis was performed (Figure 1C). The analysis showed that after doxycycline administration, there is a significant increase in Spy1 expression levels in the MTB-Spy1 mice as compared to their control littermates. Thus, this indicates that the Spy1-pTRE transgenic model system is a reliable tool to study the effects of inducible spatial and temporal overexpression of Spy1 on murine mammary gland development.

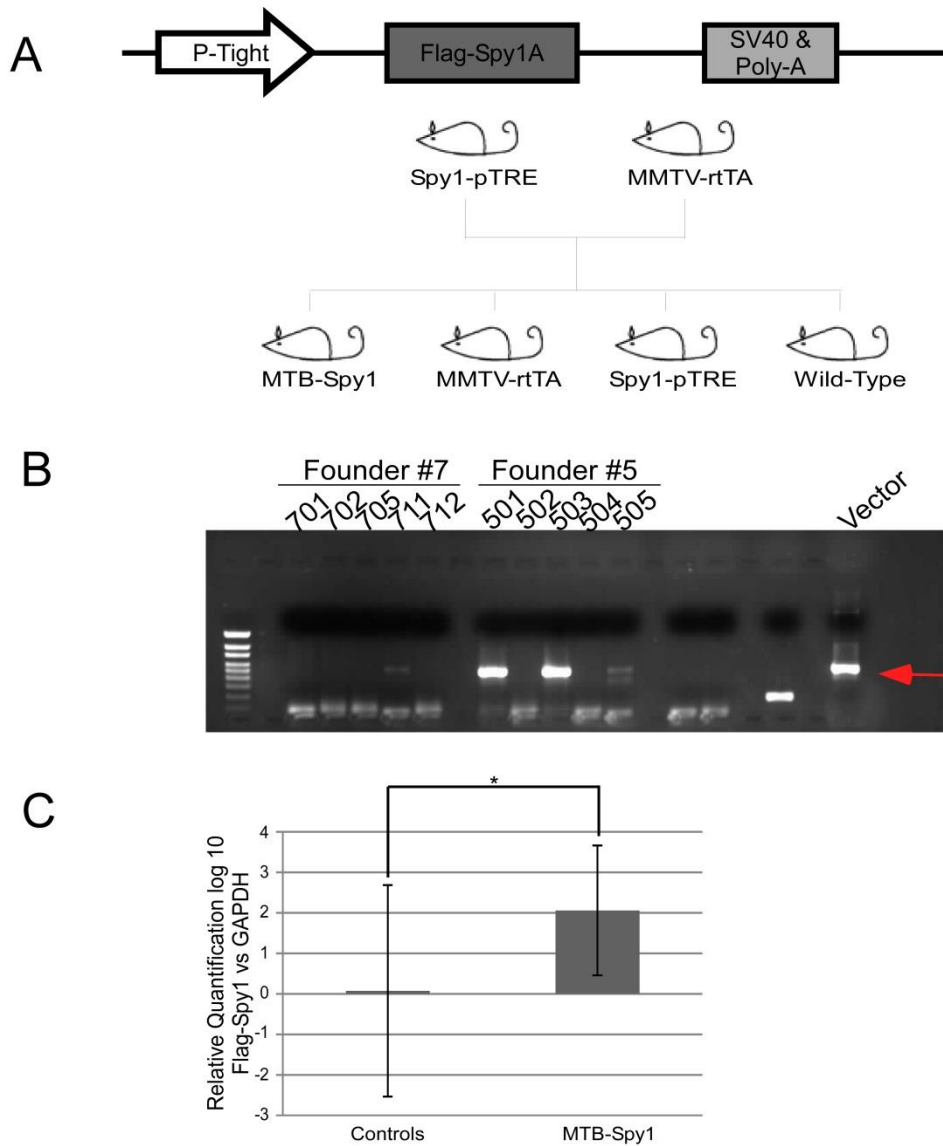


Figure 1: Generation of Spy1-pTRE transgenic mouse model. A) Schematic illustrating transgene design and proposed experimental breeding scheme with all genotypes indicated. **B)** Blot depicting PCR analysis for identification of Spy1-pTRE founder mice. **C)** qRT-PCR analysis of Spy1 mRNA levels in the inguinal mammary glands of female MTB-Spy1 and control mice treated with doxycycline for 72 hours with levels of Spy1 corrected for total GAPDH (MTB-Spy1 n=9, Controls n=7). Error bars represent SE; Students t-test *p=0.014577.

Prolonged expression of Spy1 does not alter gross mammary gland morphology.

To study the effects of long term overexpression of Spy1 on normal mammary gland development, MTB-Spy1 mice and control littermates of both genotypes were placed on a doxycycline diet for one year. Mice from all genotypes were also allowed to undergo multiple rounds of pregnancy as it is well known from other MMTV models that subsequent rounds of pregnancy can lead to tumour formation (Stewart et al., 1984). In the MMTV-Myc model, all mice develop mammary adenocarcinomas by the second or third pregnancy, highlighting the importance of studying long term overexpression in parous mice (Stewart et al., 1984). Inguinal glands were collected after 1 year, and qRT-PCR analysis was performed to determine if Spy1 levels were still elevated in MTB-Spy1 mice as compared to control (Figure 2A). Analysis revealed that significantly elevated levels of Spy1 were maintained in the MTB-Spy1 mice even after one year of induction. To test if elevated levels of Spy1 altered normal mammary development, whole mount and immunohistochemical analysis was performed (Figure 2B, C). No significant differences were noted in the gross morphology of MTB-Spy1 mammary glands as compared to control. Additionally, even with multiple rounds of pregnancy, elevated levels of Spy1 did not lead to tumourigenesis; therefore prolonged Spy1 overexpression does not affect the development of the mammary gland.

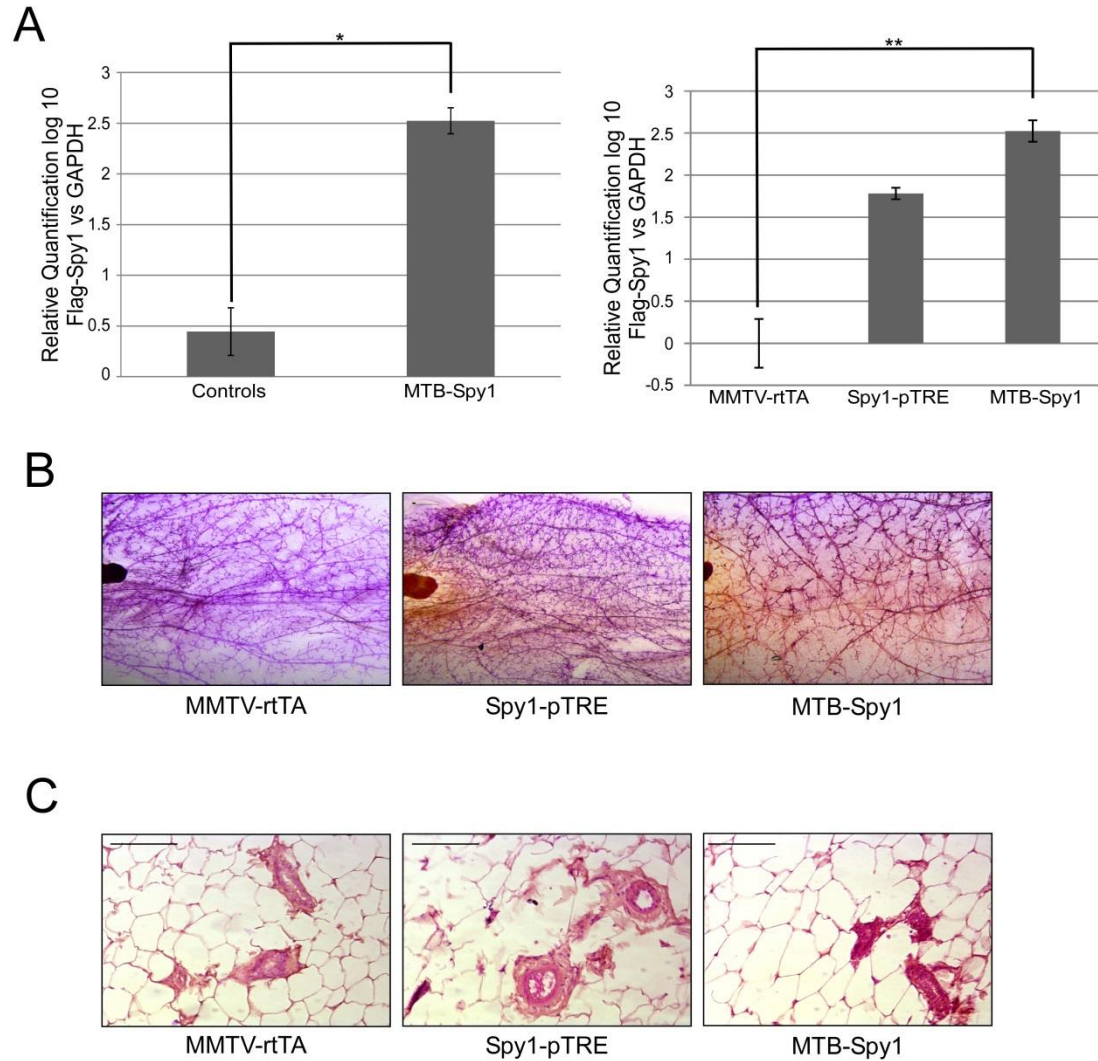


Figure 2: Long term exposure to doxycycline does not alter mammary development. **A)** qRT-PCR analysis of Spy1 mRNA levels in inguinal glands of control (MMTV-rtTA, Spy1-pTRE combined; n=4) and MTB-Spy1 (n=3) mice [or of MMTV-rtTA (n=3), Spy1-pTRE (n=1) and MTB-Spy1 (n=3) mice]. Levels of Spy1 corrected for total levels of GAPDH. **B)** Representative images of whole mounts of the inguinal glands of MMTV-rtTA, Spy1-pTRE and MTB-Spy1. **C)** Representative H&E stain of inguinal glands of MMTV-rtTA, Spy1-pTRE and MTB-Spy1 mice. Scale bar=0.1mm Error bars represent SE; Students t-test *p=0.044245 **p=0.015716.

Discussion

Inducible transgenic model systems allow for tighter control and regulation of protein expression, and open further avenues of study that a constitutive model does not allow (Sun et al., 2007; Zhu et al., 2002). The Spy1-pTRE mouse model was generated to permit a more detailed study of Spy1 overexpression on particular stages of mammary gland development. Crossing this mouse with the MMTV-rtTA mouse generated the MTB-Spy1 mouse. Using the MTB-Spy1 mouse, Spy1 expression can be turned on either long term, or during discrete windows of mammary gland development upon the administration of doxycycline. Upon withdrawal of doxycycline, Spy1 expression is returned to its normal levels during that phase of development.

Prior to experimentation with this model, it first had to be demonstrated that all three of the founder lines for the Spy1-pTRE mouse were capable of Spy1 overexpression once crossed with the MMTV-rtTA mouse and administered doxycycline. Indeed we show that within 72 hours of doxycycline administration, we see a significant increase in Spy1 expression in MTB-Spy1 mice. Further comparison with MTB-Spy1 control mice not on a doxycycline diet can be used to further prove expression is induced in the presence of doxycycline. Thus, this proves that this model effectively overexpresses Spy1 and will be an effective tool to study the effects of altered Spy1 levels during discrete stages of development.

The first step was to determine if prolonged elevation of Spy1 levels altered normal mammary gland development, and importantly, if it could induce spontaneous tumourigenesis. MTB-Spy1 mice and their control littermates were left on the doxycycline diet for a period of one year. During this time, cohorts of mice underwent multiple rounds of pregnancy. This experimental design is pivotal to our understanding as the MMTV promoter is hormonally driven and multiple rounds of pregnancy in an MMTV model can lead to tumourigenesis because increased levels of hormones during pregnancy further elevate levels of the protein of interest (Stewart et al., 1984). Although the mice were parous, none of the mice developed tumours during the course of the treatment. When expression levels of Spy1 were examined at the end of

the induction period, it was found that we do in fact see significantly higher levels of Spy1 in the MTB-Spy1 mice indicating that long-term exposure to doxycycline does allow for prolonged overexpression of Spy1 within the mammary gland. Although we did not see any tumour development, it was still possible that normal development of the gland could be affected. Whole mount and immunohistochemical analysis of the mammary gland was performed and no overt gross morphological differences were noted, indicating that the overexpression of Spy1 alone is not sufficient to induce developmental changes.

Previous data reported that the overexpression of Spy1 *in vivo* via mammary fat pad transplantation led to altered mammary development (Golipour et al., 2008), however, using the MTB-Spy1 model, prolonged overexpression of Spy1 does not lead to any alterations in mammary development. This discrepancy can be explained by two possibilities. First, the mammary fat pad transplantation experiment was performed in Balb/C mice and utilized the HC11 cell line which is known to have a mutated p53 (Merlo et al., 1993). It is known that Spy1 is capable of overcoming DNA damage induced checkpoints and apoptosis (Barnes et al., 2003; Gastwirt et al., 2006; McAndrew et al., 2009). It is quite possible that effects on normal development were seen in the mammary fat pad transplantation model due to the interaction between Spy1 and mutated p53, indicating that a second hit or alteration in protein levels is required for Spy1 to affect development. Second, the MTB-Spy1 mouse generated from the Spy1-pTRE and MMTV-rtTA cross is of a mixed background. The Spy1-pTRE mouse was generated on a B6CBAF1/J hybrid background, and the MMTV-rtTA mouse is maintained on an FVB background. The C57BL6/J mouse is known to be highly resistant to tumourigenesis and to the effects of MMTV, thus the FVB strain is more commonly used in the generation of MMTV mouse models (Beutner et al., 1996; Davie et al., 2007; Rollini et al., 1992). While the resulting MTB-Spy1 mouse would therefore be of a B6CBAF1/J-FVB hybrid, perhaps the influence of the C57BL6/J strain still does not allow for Spy1 to exert its effects on mammary development. To test this possibility, the Spy1-pTRE mouse is currently being backcrossed onto the FVB strain.

This will simplify breeding and will determine if the lack of phenotype is due to the influence of mouse strain. Further investigation into these possibilities must be undertaken to determine the precise effects of altered Spy1 levels on normal mammary development.

The Spy1-pTRE mouse model has been confirmed as a tool to induce specific overexpression of Spy1 upon administration of doxycycline. This model provides an advantage over traditional models as it allows for temporal and spatial control of induced expression. The Spy1-pTRE mouse model will allow us to answer more specific questions about mammary gland development, as well as enabling us to answer questions in other tissue systems, such as the brain, simply by choosing a different tissue specific promoter to drive expression of rtTA. Thus, this model will prove to be an excellent tool for future studies of the precise role of Spy1 in regulating normal development and in the initiation and onset of tumourigenesis.

Acknowledgements

We thank Drs Espanta Jalili and Dorota Lubanska for construction of the Spy1-pTRE transgene, the London Regional Transgenic and Gene Targeting Facility and Dr. Christopher Pin and Lindsay Drysdale for development of the Spy1-pTRE mouse model, and Dr. Roger Moorehead for providing the MMTV-rtTA mouse. We also thank Dr. Dorota Lubanska, Ingrid Qemo, Ellen Laurie and Nick Paquette for technical assistance. This study was funded by the Canadian Cancer Society/Canadian Breast Cancer Research Alliance (#02051). B.F. also acknowledges support from the University of Windsor, Ontario Graduate Scholarship Program and Canadian Breast Cancer Foundation.

References

- Barnes, E. A., Porter, L. A., Lenormand, J. L., Dellinger, R. W., and Donoghue, D. J. (2003). Human Spy1 promotes survival of mammalian cells following DNA damage. *Cancer Res* 63, 3701-3707.
- Beutner, U., McLellan, B., Kraus, E., and Huber, B. T. (1996). Lack of MMTV superantigen presentation in MHC class II-deficient mice. *Cell Immunol* 168, 141-147.
- Blakely, C. M., Sintasath, L., D'Cruz, C. M., Hahn, K. T., Dugan, K. D., Belka, G. K., and Chodosh, L. A. (2005). Developmental stage determines the effects of MYC in the mammary epithelium. *Development* 132, 1147-1160.
- Davie, S. A., Maglione, J. E., Manner, C. K., Young, D., Cardiff, R. D., MacLeod, C. L., and Ellies, L. G. (2007). Effects of FVB/NJ and C57Bl/6J strain backgrounds on mammary tumor phenotype in inducible nitric oxide synthase deficient mice. *Transgenic Res* 16, 193-201.
- Furth, P. A., St Onge, L., Boger, H., Gruss, P., Gossen, M., Kistner, A., Bujard, H., and Hennighausen, L. (1994). Temporal control of gene expression in transgenic mice by a tetracycline-responsive promoter. *Proc Natl Acad Sci U S A* 91, 9302-9306.
- Gastwirt, R. F., Slavin, D. A., McAndrew, C. W., and Donoghue, D. J. (2006). Spy1 expression prevents normal cellular responses to DNA damage: inhibition of apoptosis and checkpoint activation. *J Biol Chem* 281, 35425-35435.
- Golipour, A., Myers, D., Seagroves, T., Murphy, D., Evan, G. I., Donoghue, D. J., Moorehead, R. A., and Porter, L. A. (2008). The Spy1/RINGO family represents a novel mechanism regulating mammary growth and tumorigenesis. *Cancer Res* 68, 3591-3600.
- Gossen, M., Freundlieb, S., Bender, G., Muller, G., Hillen, W., and Bujard, H. (1995). Transcriptional activation by tetracyclines in mammalian cells. *Science* 268, 1766-1769.
- Gunther, E. J., Belka, G. K., Wertheim, G. B., Wang, J., Hartman, J. L., Boxer, R. B., and Chodosh, L. A. (2002). A novel doxycycline-inducible system for the transgenic analysis of mammary gland biology. *FASEB J* 16, 283-292.

Haruyama, N., Cho, A., and Kulkarni, A. B. (2009). Overview: engineering transgenic constructs and mice. *Curr Protoc Cell Biol Chapter 19*, Unit 19 10.

McAndrew, C. W., Gastwirt, R. F., and Donoghue, D. J. (2009). The atypical CDK activator Spy1 regulates the intrinsic DNA damage response and is dependent upon p53 to inhibit apoptosis. *Cell Cycle* 8, 66-75.

Merlo, G. R., Venesio, T., Taverna, D., Callahan, R., and Hynes, N. E. (1993). Growth suppression of normal mammary epithelial cells by wild-type p53. *Ann N Y Acad Sci* 698, 108-113.

Muller, U. (1999). Ten years of gene targeting: targeted mouse mutants, from vector design to phenotype analysis. *Mech Dev* 82, 3-21.

Porter, L. A., Kong-Beltran, M., and Donoghue, D. J. (2003). Spy1 interacts with p27Kip1 to allow G1/S progression. *Mol Biol Cell* 14, 3664-3674.

Rollini, P., Billotte, J., Kolb, E., and Diggelmann, H. (1992). Expression pattern of mouse mammary tumor virus in transgenic mice carrying exogenous proviruses of different origins. *J Virol* 66, 4580-4586.

Stewart, T. A., Pattengale, P. K., and Leder, P. (1984). Spontaneous mammary adenocarcinomas in transgenic mice that carry and express MTV/myc fusion genes. *Cell* 38, 627-637.

Sun, Y., Chen, X., and Xiao, D. (2007). Tetracycline-inducible expression systems: new strategies and practices in the transgenic mouse modeling. *Acta Biochim Biophys Sin (Shanghai)* 39, 235-246.

Zhang, Q., Triplett, A. A., Harms, D. W., Lin, W. C., Creamer, B. A., Rizzino, A., and Wagner, K. U. (2010). Temporally and spatially controlled expression of transgenes in embryonic and adult tissues. *Transgenic Res* 19, 499-509.

Zhu, Z., Zheng, T., Lee, C. G., Homer, R. J., and Elias, J. A. (2002). Tetracycline-controlled transcriptional regulation systems: advances and application in transgenic animal modeling. *Semin Cell Dev Biol* 13, 121-128.

Chapter 5

Development of a Gene Targeted Spy1 Model System

Introduction

The advent of technology to render an endogenous gene inactive has greatly enhanced our understanding of the normal functioning of hundreds of genes, which has facilitated the treatment of a wide variety of human diseases (Bouabe and Okkenhaug; Capecchi, 2005). A downfall of this strategy is embryonic lethality. Losing the function of many gene products early in development will lead to failure of the embryo to thrive (Hakem et al., 1996; Hall et al., 2009). While this can be beneficial in understanding the role of the gene in early stages of development, it hinders our ability to study its function in other biological processes and diseases that develop later in life. To overcome this pitfall, a strategy that allows for control over the timing and tissue specificity of gene ablation was developed. The Cre/loxP system was first discovered in P1 bacteriophage, and it has now been successfully employed in the field of gene targeting to allow for conditional gene knockout (Nagy, 2000; Sauer, 1998; Wagner et al., 1997). This system involves the use of a transgenic animal which expresses Cre recombinase under the control of a tissue specific promoter, and a gene targeted animal which contains loxP sites flanking a functionally essential portion of the gene of interest (Hamilton and Abremski, 1984; Muller, 1999; Nagy, 2000; Voziyanov et al., 1999). The presence of the loxP sites will not affect gene function thereby circumventing the issue of gene lethality. When these two mice are crossed together, tissue specific expression of Cre recombinase will lead to removal of the essential part of the gene leading to gene knockout. Understanding the basic function of a gene during normal development facilitates our understanding of human disease development, progression and ultimately, treatment. Thus the Cre/loxP system facilitates and enhances the study of the essentiality of hundreds of genes, and has proven to be a valuable tool time and time again.

The study of cell cycle regulation has been enhanced through the use of gene targeted approaches. Cell cycle regulators, such as cyclin dependant kinases (CDKs) and cyclins, play a key role in regulating cell proliferation and it was thought that ablation of gene function would result in embryonic lethality. This however, was not the case for all genes. Gene knockouts of

CDK2, cyclin E, and CDK4 among others resulted in viable mice, and while these mice may have had developmental defects such as sterility, it demonstrated that these genes were not essential for viability of the organism (Berthet et al., 2003; Ciemerych and Sicinski, 2005; Geng et al., 2003; Mendez, 2003; Rane et al., 1999). Knockouts of CDK1 however, resulted in embryonic lethality, highlighting the importance of this CDK in the normal development of the organism (Santamaria et al., 2007). One cell cycle regulator that has to date not been studied in a gene targeted system, is the atypical cyclin-like protein Spy1. Spy1 can bind and activate CDK2 in absence of the classical phosphorylation events, and can also directly bind to the CDK inhibitor p27 leading to further activation of CDK2 (Cheng et al., 2005a; Karaïskou et al., 2001; McAndrew et al., 2007; Porter et al., 2002; Porter et al., 2003). Overexpression of Spy1 shortens G1 phase of the cell cycle and increases cellular proliferation, while depletion of Spy1 levels greatly reduces the rate of cell proliferation and slows movement into M phase of the cell cycle, thus demonstrating that Spy1 is an important part of the cell cycle machinery (Porter et al., 2002). To further highlight the importance of Spy1 in normal cell cycle progression, Spy1 was initially discovered in *Xenopus* oocytes, which are arrested at the G2/M transition during normal development (Lenormand et al., 1999). It was discovered that injection of Spy1 into these oocytes leads to rapid maturation of the oocyte and progression through the G2/M transition (Ferby et al., 1999; Lenormand et al., 1999). It was also noted that expression of Spy1 was upregulated after stimulation with progesterone, the hormone responsible for progression of *Xenopus* oocytes through meiosis (Ferby et al., 1999; Lenormand et al., 1999). Ablation of Spy1 significantly delayed oocyte maturation upon progesterone stimulation (Ferby et al., 1999; Lenormand et al., 1999). Taken together, these results suggest that Spy1 may be required for oocyte maturation and could therefore play an essential role in normal embryonic development.

While the studies in *Xenopus* oocytes have demonstrated the importance of Spy1 in oocyte maturation, it remained to be determined if this role was conserved in mouse oocytes. Indeed, injection of Spy1 mRNA into mouse oocytes arrested in prophase I resulted in germinal

vesicle breakdown (GVBD), an essential step in resumption of meiosis (Terret et al., 2001). Additionally, injection of Spy1 mRNA in early stage mouse embryos causes cleavage arrest and inhibits polar body extrusion suggesting that it could act in M phase to inhibit the meiotic cell cycle (Terret et al., 2001).

Based on our knowledge of the key role Spy1 plays in regulating normal cell proliferation and oocyte maturation, one could hypothesize that a complete gene knockout of Spy1 could render the embryo non-viable and lead to embryonic lethality, circumventing the study of the essentiality of Spy1 in other tissue systems such as the mammary gland. To avoid the issue of embryonic lethality, a conditional gene targeting approach has been employed to allow for the conditional deletion of Spy1 in a tissue specific manner. Utilizing the Cre/loxP system, we sought to generate a floxed mouse harbouring loxP insertions around the area of the Spy1 gene responsible for its function, the Speedy-RINGO box. The Speedy-RINGO box is required for the binding of Spy1 to CDKs, therefore, abolishing the ability of Spy1 to bind to CDK2 will render the gene non-functional (Cheng et al., 2005a; Cheng et al., 2005b; Porter et al., 2002). Herein we describe the gene targeting approach taken to generate the first conditional gene targeted mouse for the Spy1 gene.

Materials and Methods

Plasmids

The targeting vector for *Spy1* was generated by Vega Biolab, and BAC clones bMQ256e05 and bMQ185H8 were purchased from GeneService Sanger. Exon 4 of *Spy1* was flanked on either side by loxP sites placed in the intronic region of the gene. A neomycin cassette was inserted in the targeted region adjacent to the 5' loxP site in the opposing orientation to the gene. A BamHI site was also introduced in the targeted region to aid in screening for correctly targeted clones.

Probes for southern blot analysis of the 5' and 3' ends as well as for Neo incorporation, were isolated from the appropriate mouse genomic DNA, or targeting vector respectively. The isolated probe fragments were cloned into the pCR TOPO 2.1 Vector using the TOPO-TA Cloning Kit (Invitrogen) as per manufacturer's instructions. Following generation of the vectors, probes can be readily isolated by digestion of the vector with EcoRI to isolate the probe fragments for [α -³²P]-dCTP labeling.

Gene Targeting

Electroporation of the targeting vector was performed by the London Regional Transgenic and Gene Targeting Facility in R1 ES cells. Targeted clones were identified by southern blot analysis as described below. Clones that were identified to have been correctly targeted were injected into blastocysts to generate chimeric mice.

Southern Blot Analysis

10ug of genomic DNA in a 30uL reaction volume was digested overnight at 37°C with BamHI, PstI or NdeI for 5', 3' or Neo screening respectively. The following morning, an additional 1uL of the appropriate enzyme was added and the reaction was allowed to continue for an additional 4 hours at 37°C. A 0.8% agarose gel was prepared without ethidium bromide and

samples were run at 30 volts for 10 hours. Following the gel run, the gel was stained with ethidium bromide in 1X TAE and imaged next to a UV ruler to measure migration of the ladder. The gel was then washed twice with wash buffer 1 (1.5M sodium chloride, 0.5M sodium hydroxide) for 30 minutes each followed by a 5 minute wash with distilled water. The gel was then washed twice with wash buffer 2 (1M ammonium acetate, 0.02M sodium hydroxide) 30 minutes each. Overnight capillary action transfer using paper towels was then set up using nitrocellulose membrane (Fisher Scientific; GE Nitrocellulose Membrane Nitropure 0.45µM). Transfer buffer has the same composition as wash buffer 2. The following morning, the membrane was left to dry on the bench for 1 hour before baking under pressure at 80°C. For probe labelling, the appropriate probe was gel extracted using the Sigma GenElute Gel Extraction Kit (Sigma Aldrich) as per manufacturer's instructions, following digestion of the appropriate vector with EcoRI to isolate the probe fragment. Once the probe was successfully extracted, the membrane was placed in hybridization buffer (4X SET, 10X Denhardt's, 0.1% sodium pyrophosphate, 25mM Na₃PO₄, 0.2% SDS) for 1 to 2 hours at 65°C. The extracted probe was labeled with [α -³²P]-dCTP using the Promega Prime-a-Gene Labeling System (Promega) as per manufacturer's instructions. Probe was purified to remove unincorporated nucleotides using a Sephadex G50 purification column. Purified probe was heated at 95°C for 5 minutes and added to 5mL of hybridization buffer heated to 65°C. Membrane was hybridized overnight at 65°C. The following day, the membrane was washed 3 times 10 minutes at room temperature with low stringency wash buffer (2xSSC, 0.1% SDS), followed by 3 10 minute washes at 65°C with high stringency wash buffer (0.2X SSC, 0.1% SDS). Membrane was set up for a minimum of 3 nights exposure with Super Sensitive Phosphor Screen (Perkin Elmer), and was subsequently imaged using the Cyclone Plus Phosphor Imager (Perkin Elmer).

Genotyping Procedure

Samples were screened for 3' end loxP incorporation by PCR analysis. PCR was conducted as follows: a 25uL reaction (1x PCR buffer, 2mM MgSO₄, 0.2mM dNTP, 0.04U/uL UBI Taq Polymerase, 0.4uM forward primer [5' GATTCA AGTGGATTA ACTCTGGGGACC 3'], 0.4uM reverse primer [5'GACAGAGAAAGTGTGTGTGTTGGAGG 3'] was prepared, and PCR cycling conditions were 95°C for 10 minutes followed by 40 cycles of 95°C for 1 minute, 60°C for 2 minutes and 72°C for 1 minute followed by a final elongation at 72°C for 10 minutes.

Results

Spy1 conditional knockout targeting vector design.

To examine the importance of *Spy1* in development of the mammary gland, we sought to generate a conditional knockout mouse via gene targeting of exon 4. LoxP sites were introduced flanking exon 4 as illustrated in the targeting vector design in Figure 1A. Successful generation of the targeting vector was verified using restriction enzymes illustrated on the targeting vector verification map (Figure 1B). To detect successful homologous recombination, southern blot analysis was utilized. Probes were designed outside of the arms of homology and were tested for specificity by probing previously digested ES cell DNA with both the 5' and 3' probes. Probes were deemed to be specific for the *Spy1* sequence as seen in the representative images in Figure 1C.

To further validate events of successful homologous recombination, a southern blot screening strategy to ensure the Neo selection marker was in the correct location in the gene was designed (Figure 2A). The generated Neo probe was also tested for specificity to determine if it would be suitable for screening (Figure 2B). This was accomplished by testing specificity of the probe with ES cell DNA that had been previously digested with BamHI, which should yield a 1.5kb band once the Neo probe binds. Identification of the 1.5kb fragment indicates that the Neo probe is indeed specific for its intended sequence.

To prepare for screening of the *Spy1* floxed mice, primers were designed flanking the loxP site located 3' of exon 4 (Figure 2C). Designing primers in this location allows for detection of the wild-type allele (lower band), the floxed allele (upper band) or the presence of both the wild-type and floxed allele within the same mouse (Figure 2D).

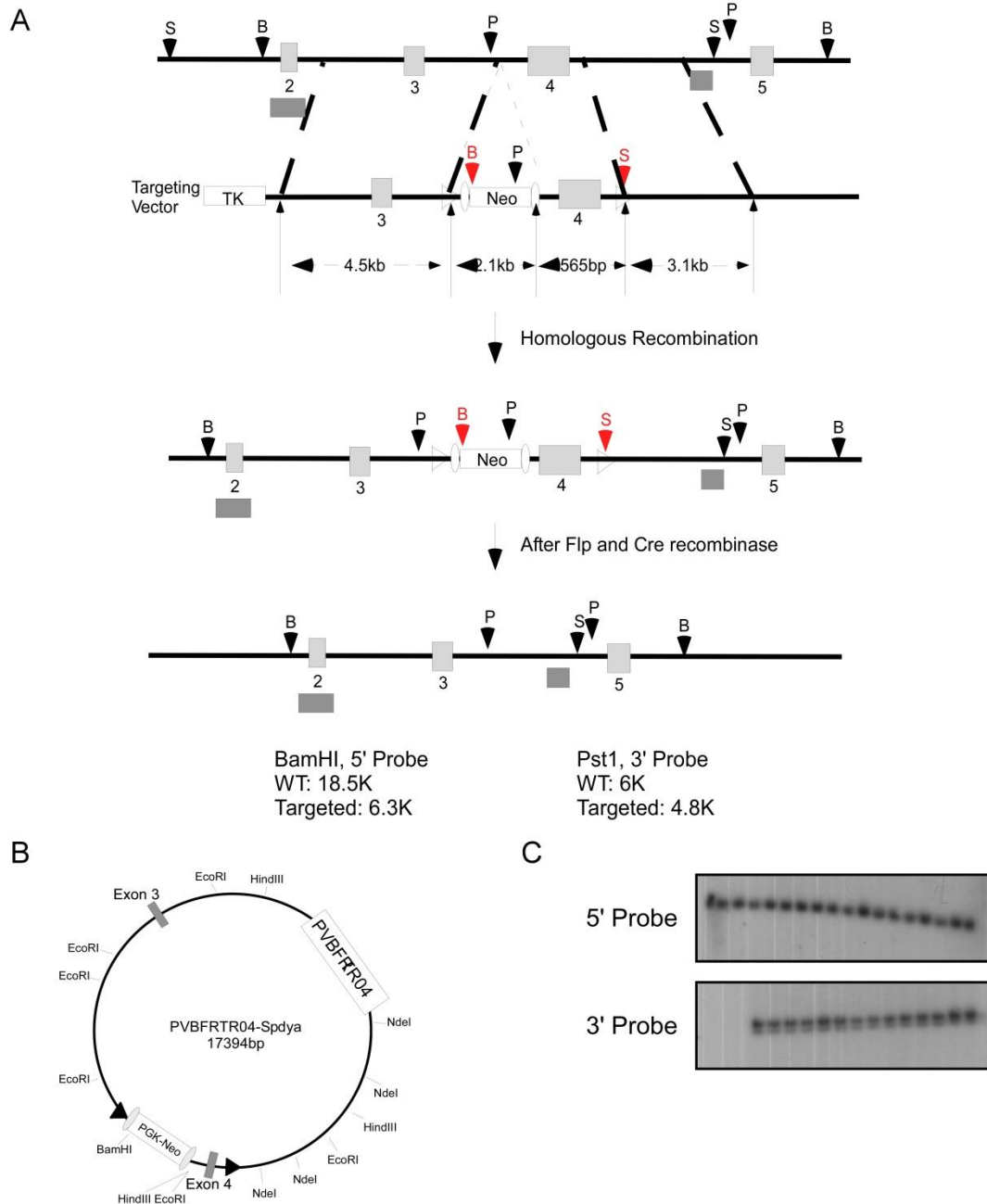


Figure 1: *Spdy1* conditional knockout mouse targeting vector design. **A)** Genomic structure of *SpdyA* and targeting vector design illustrating location of loxP sites flanking exon 4 and insertion of Neo selection cassette. Map also illustrates location of restriction enzyme sites where B is BamHI, P is PstI and S is SacI. LoxP and Frt sites are indicated by the triangles and ovals respectively, and light grey boxes indicate exons where dark grey boxes indicated location of probes for southern blot analysis. **B)** Verification map of the *SpdyA* targeting vector. Location of restriction enzymes to use for vector verification are indicated on map. **C)** Southern blot to indicate specificity of 5' and 3' probes to be used in screening of ES cell clones for homologous recombination. Each lane represents an individual ES cell clone that was previously digested with HindIII from a previous southern blot screen.

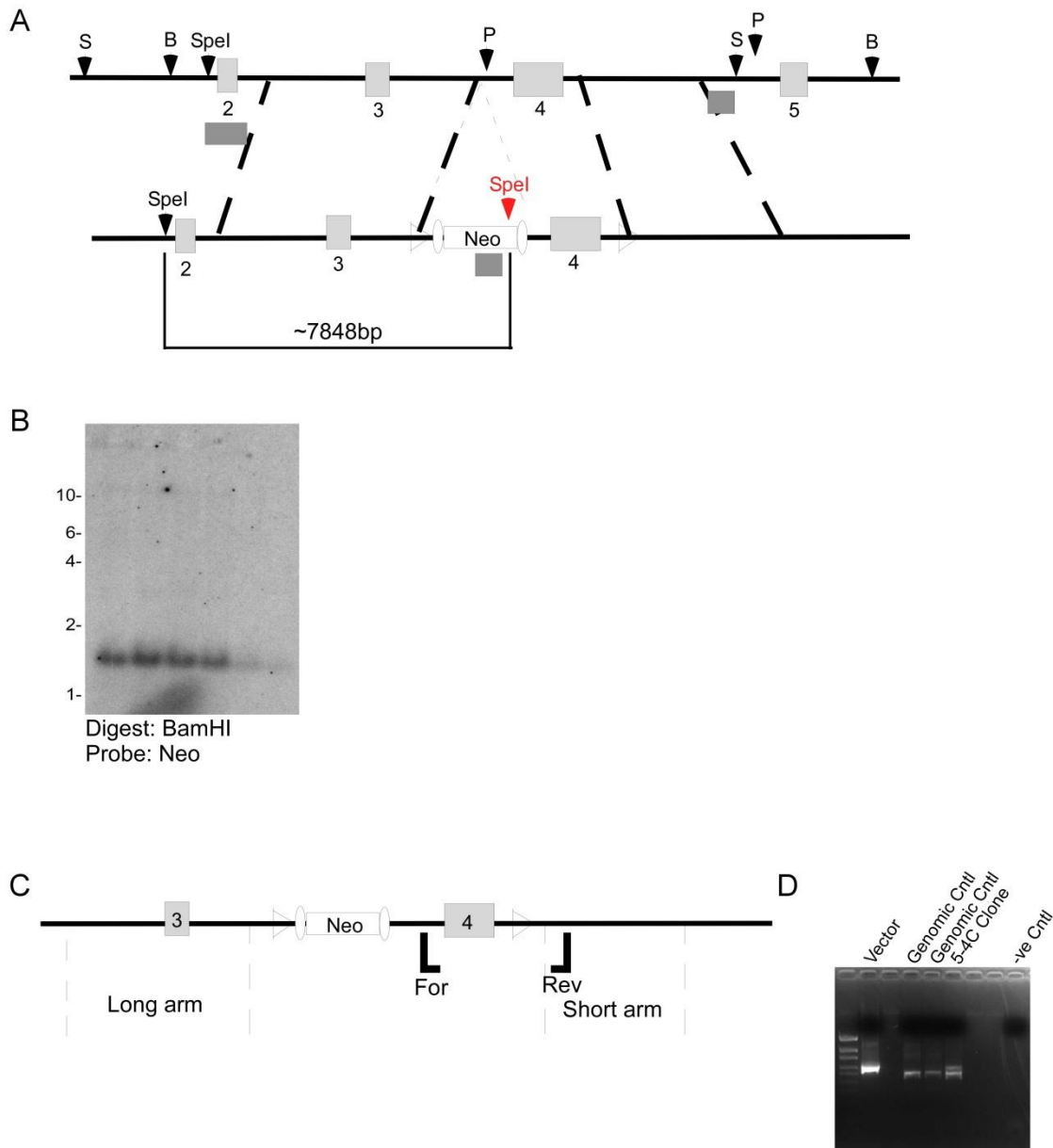


Figure 2: Screening strategy for Neo incorporation and PCR analysis. A) Genomic structure of Spyl and targeting vector illustrating location of probe within Neo sequence (dark grey box) and location of SpeI restriction enzyme cut sites to be used in Neo incorporation screening. **B)** Southern blot of ES cell clones that had been previously digested with BamHI. Screening with the Neo probe will give a band of 1.5kb when digested with BamHI. Each lane represents an individual clone. **C)** Location of forward (for) and reverse (rev) primers to be used for PCR analysis to screen for floxed allele. **D)** PCR indicating ability to successfully detect the wild type (lower band) and floxed allele (upper band) as indicated by the presence of 2 bands in the 5-4C Clone.

Identification of ES cell clone demonstrating successful homologous recombination.

A total of 222 clones were generated from electroporation of the Spyl targeting vector into R1 ES cells. All clones were initially screened using the 5' probe through a BamHI digest. Out of the initial clones generated, 16 were identified as potentially having successful homologous recombination by the presence of both the wild-type band at 18.5kb and the targeted band at 6.3kb. These clones were then digested with PstI to enable screening with the 3' probe to check for proper homologous recombination on the 3' end. One clone, 5-4C, was shown to be successfully targeted on the 3' end through the presence of the wild-type band at 6kb and the targeted band at 4.8kb (Figure 3A). Based on the results from the initial southern blot screens, 5-4C was deemed to have undergone successful homologous recombination and the resulting ES cells from this clone were injected into 3.5 day old C57BL/6 blastocysts. Prior to injection, clone 5-4C was re-grown for injection. DNA from the resulting population that was injected into the blastocyst was received and screened once again for validation of successful homologous recombination using all three of the designed probes for southern blot analysis (5', 3' and Neo). Results from this final screen were surprising. Although clone 5-4C previously showed successful recombination at both ends, the final screen after injection showed only the presence of the wild-type allele and no floxed allele (Figure 3B). Additionally, use of the Neo probe showed that the Neo insert was not inserted in the correct location as the predicated size of the resulting fragment, 7.8kb, was not seen. Thus, this final analysis demonstrates that the chimeric mouse resulting from the blastocyst injections was not correctly targeted, although initial analysis showed the presence of both a wild-type and floxed allele on both the 5' and 3' ends of the targeted area.

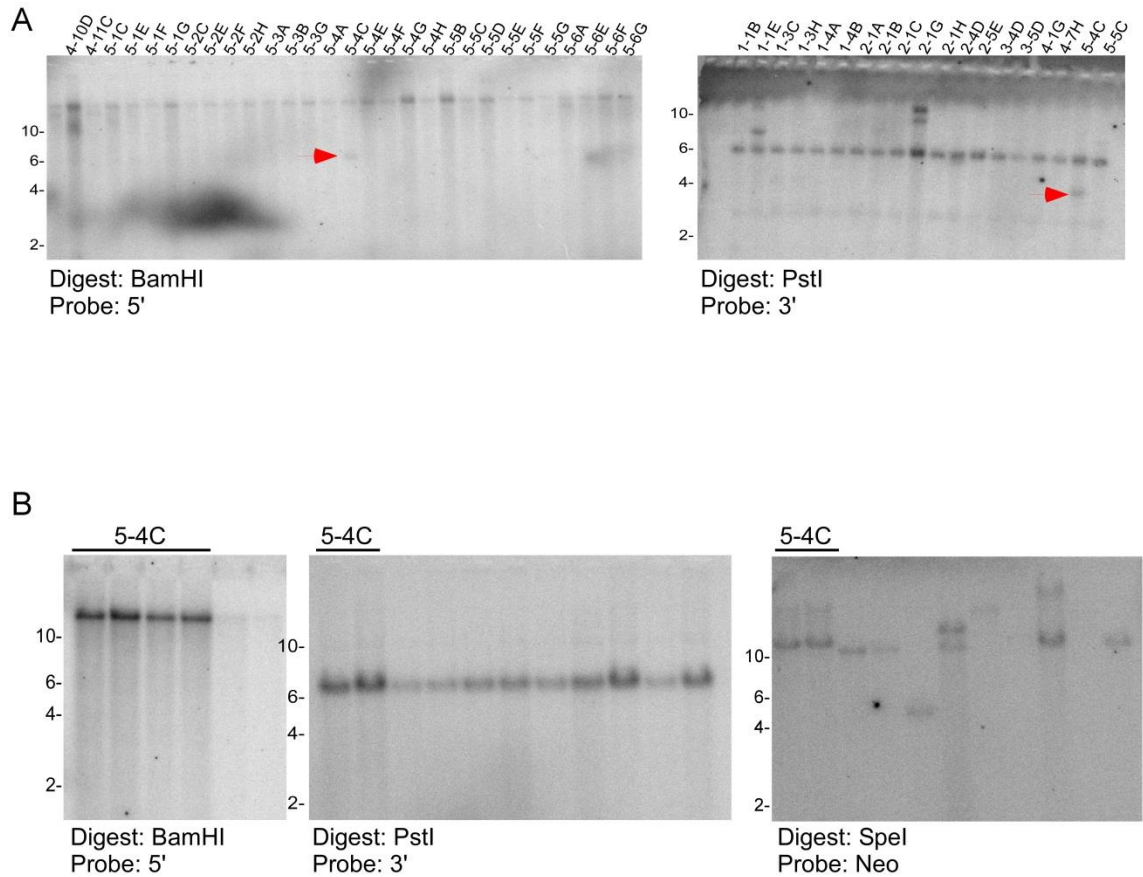


Figure 3: Southern blot analysis of ES cell clones. A) Southern blot analysis of select ES cell clones from initial electroporation. Restriction enzyme and probe used in blot is found below each image. Each lane represents an individual ES cell clone. Red arrow indicates location of targeted allele. **B)** Southern blot analysis of selected clone 5-4C (lanes indicated on blot). Remainder of lanes are additional ES cell clones used as controls. Probes used in each hybridization, and restriction enzyme used to digest genomic DNA is indicated below each blot.

Discussion

The use of gene targeted animal models has helped to revolutionize our understanding of the basic functions of many genes. Herein, we described an approach to conditionally knockout the novel cell cycle regulator, Spy1. Spy1 was originally identified in a screen for *Xenopus* cDNA that would confer resistance to UV radiation in a rad1 deficient strain of *S.pombe* (Lenormand et al., 1999). It was found that Spy1 was present as maternal mRNA in *Xenopus* oocytes, and injection of Spy1 RNA into *Xenopus* oocytes allowed for rapid progression through G2/M phase of the cell cycle and oocyte maturation (Lenormand et al., 1999). Based on these findings, a full knockout was not pursued as it was believed that the full knockout may be embryonic lethal, or would cause phenotypes that would prevent the study of the loss of Spy1 on normal mammary gland development, which is a system in which we sought to study the essentiality of Spy1. Additionally, use of a conditional approach would allow for targeted spatial and temporal expression of Cre recombinase in select tissues or cell populations, generating a model in which the study of the essentiality of Spy1 in various systems could be studied without interference of potential phenotypes in other systems.

The design of the Spy1 targeting vector presented some challenges. First, the Spy1 gene has multiple start sites. To ensure full knockout is achieved upon Cre recombination, the targeted location must be chosen carefully to ensure no functional protein remains. For this reason, exon 4 was targeted as this exon contains in it a large portion of the Speedy-RINGO box which is essential for its binding to CDK2 (Cheng et al., 2005a; Cheng et al., 2005b; Porter et al., 2002). Removal of the Speedy-RINGO box would ultimately render the Spy1 protein non-functional. Additionally, the only remaining protein would be a portion of the N-terminus which contains phosphorylation sites that target Spy1 for degradation. Thus any protein generated would ultimately be non-functional due to the lack of the Speedy-RINGO box, and targeted for degradation. In addition to the challenges presented by the Spy1 gene itself, further challenges were presented by the presence of a gene encoding for non-coding RNA, Trmt61b. While this

gene at present is not known to be translated, affecting the sequence of this gene could in and of itself manifest as a phenotypic change in the development of the generated mouse. To ensure this does not happen, the area targeted by the loxP sites is in an intronic region of the *Trmt61b* gene diminishing the possibility of disruption to this non-coding RNA.

Once the targeting vector design was completed, the next critical step was ensuring the screening strategy via southern blot analysis was specific and would be able to detect both the wild-type and targeted alleles effectively. The strategy for screening the 3' end of the targeting vector also presented challenges in that a large portion of this end of the *Spy1* gene shows homology to a region of chromosome 1. All three probes designed for southern blot screening of the resulting ES cell clones were tested and were shown to be specific and sufficient for detection of the wild-type alleles indicating they would also be able to detect the targeted allele in the case of successful homologous recombination.

Initial screening of the electroporated ES cells yielded one potential successfully targeted clone, clone 5-4C. Having one successfully targeted clone demonstrates that the targeting efficiency of the designed targeting vector was quite low. Additionally, having only one clone to proceed with blastocyst injections is inherently risky as problems with growing up the clone, aneuploidy or being unable to re-confirm the genotype means there is no fall back clone on which to go back to. In this case, clone 5-4C was injected into C57BL/6 blastocysts and upon southern blot analysis of the injected clone, it was found that the targeted allele was no longer present. Only the wild-type allele was detected during the re-confirmation of clone 5-4C, indicating that this clone was in fact not properly targeted and only contains part of the targeting vector inserted randomly within the genome.

A number of possibilities exist to explain as to how correct targeting of a clone could initially be seen and then upon re-confirmation is no longer present. The simplest explanation is simply human error. Perhaps when the clone was picked from the plate to be re-grown for injections, the wrong well was chosen. Given the large number of clones that are initially

produced and screened, this very well could be a reasonable explanation for the result seen during the re-confirmation of the clone. Another possibility could be due to a heterogeneous population of ES cells within the clone. If wild-type cells were present in the clone and did not initially grow, when the clone was grown back up, it is possible these wild-type cells had by this point acquired resistance to Neomycin and overtook the culture. Additionally, the culture of ES cells is quite difficult and it could be that the targeted cells differentiated and were ultimately lost (Tremml et al., 2008). Due to the large number of possibilities to explain the loss of the targeted allele, it was decided that the original targeting vector be re-examined and improved upon to improve the chances of successful homologous recombination to improve targeting efficiency.

During the original design of the targeting vector, there was a noted discrepancy in the published sequence of the *Spy1* gene and the length of the 5' homologous arm. The published sequence is based on the C57BL/6 mouse strain while the strain of mouse being targeted is a strain of 129. The targeting vector lacked a 1.5kb sequence as predicated based on the published C57BL/6 sequence. Attempts to isolate this sequence from a second BAC clone failed, and based on the predicated size of the wild-type fragment, it was determined that the 129 strain of mouse does indeed lack this 1.5kb sequence. This shows the inherent variability between strains of mice and highlights the importance of knowing the full sequence of the strain being targeted. To further improve targeting efficiency, the CRISPR/Cas system will be employed. The CRISPR/Cas system makes use a system utilized by bacteria and archaea to seek out and eliminate any invading viruses or plasmids (Sander and Joung, 2014; Yang et al., 2014). In this system, a guide RNA (gRNA) targets the Cas9 endonuclease to a specific site within the genome to generate a double stranded break (Sander and Joung, 2014; Yang et al., 2014). Once a double strand break is produced, a knockout, knock-in, conditional allele or mutation may be introduced at the site of the break and incorporated into the genome via DNA repair mechanisms such as homologous recombination (Fujii et al.; Sander and Joung, 2014; Shen et al.; Wang et al.; Yang et al., 2014; Yang et al.). To generate a targeted allele, Cas9 mRNA, two gRNAs and single

stranded DNA containing the loxP site surrounded by arms of homology specific to the site of double stranded break are injected (Sander and Joung, 2014; Yang et al., 2014; Yang et al.). This system provides many advantages over the classic method of genome modification in generating gene targeted mice as the timeline of completion is much quicker and multiple genes can be targeted at one time (Wang et al.; Yang et al.). To utilize this new system, the full sequence of the *Spy1* gene in the 129 strain of mouse where targeting is to occur must be known. After analysing the targeting vector closely, a 200bp insert was noted directly after the 3' Frt site flanking the Neo insertion cassette. This 200bp insert is located very close to exon 4 meaning that it could affect the splicing of *Spy1* and ultimately affect its function even prior to Cre recombination. It remains to be determined however, if this 200bp insert is a by-product of the vector itself, or if this is sequence specific to the 129 strain and not found in the C57BL/6 strain. To proceed with CRISPR/Cas, the *Spy1* sequence of the area in question in the R1 ES cells being used in targeting will be sequenced to determine the full sequence of the *Spy1* gene in this strain of mice.

If the sequence in question is indeed incorrect and will cause problems with proper gene targeting, then the targeting vector design will need to be re-evaluated and a new strategy may need to be developed and new targeting vector designed. Given the amount of time this may take, alternate approaches to study the essentiality of *Spy1* in various systems, such as the mammary gland, are being evaluated. The generation of transgenic model systems is a much less time consuming endeavour. Once cloning of the transgenic vector is completed, pronuclear injections can be performed and screening for potential founders could occur in as early as 6 weeks from the time of injection (Haruyama et al., 2009). Once founders are identified, they can immediately be bred to expand the colony and analysis can begin much quicker than if gene targeting were to be used. Transgenic model systems employing the use of shRNA are commonly used with much success (Dow et al.). Using this approach, a transgenic vector containing the sequence for sh*Spy1* will be generated. The transgenic vector will utilize the pTRE-Tight promoter thereby allowing for inducible temporal and spatial expression of sh*Spy1* upon administration of doxycycline.

Transgenic mice expressing the reverse tetracycline transactivator, rtTA, under the control of various promoters are readily available for use. Development of the pTRE-shSpy1 mouse model will provide a system in which the essentiality of Spy1 can be studied. This system will not provide complete knockout of Spy1, but instead, knockdown of Spy1 levels; thus it remains possible that with small amounts of functional Spy1 present different phenotypes may be seen with knockdown as compared to a full knockout. However, given the time required for the generation of the conditional knockout mouse, the pTRE-shSpy1 transgenic mouse will become a valuable tool.

The generation of a targeting vector to allow for the generation of the first Spy1 conditional knockout mouse presented many challenges. While there have been setbacks in this process, the value of generating this model far outweighs any challenges. It is now clear that further elucidating the sequence of Spy within the 129 strain is key to generating a functional Spy1 conditional knockout. An shSpy1 transgenic mouse will provide a valuable tool in which to study the essentiality of Spy1 in development while the finer details of the gene targeting project are mapped out. Generating an *in vivo* system to study loss of Spy1 function will be key to fully elucidating the precise role Spy1 plays in regulating developmental processes.

Acknowledgements

We thank Vega Biolab for construction of the targeting vector, Dr. Christopher Pin and Linsay Drysdale from the London Regional Transgenic and Gene Targeting Facility for generation of the *Spy1* floxed mouse and technical assistance, and Dr. Fred Dick for assistance in design and execution of this project. Special thanks to Paul Stafford and Daniel Passos from the University of Western Ontario for technical assistance. B.F. acknowledges support from the University of Windsor, the Ontario Graduate Scholarship Program and Canadian Breast Cancer Foundation.

References

- Berthet, C., Aleem, E., Coppola, V., Tessarollo, L., and Kaldis, P. (2003). Cdk2 knockout mice are viable. *Curr Biol* 13, 1775-1785.
- Bouabe, H., and Okkenhaug, K. Gene targeting in mice: a review. *Methods Mol Biol* 1064, 315-336.
- Capecchi, M. R. (2005). Gene targeting in mice: functional analysis of the mammalian genome for the twenty-first century. *Nat Rev Genet* 6, 507-512.
- Cheng, A., Gerry, S., Kaldis, P., and Solomon, M. J. (2005a). Biochemical characterization of Cdk2-Speedy/Ringo A2. *BMC Biochem* 6, 19.
- Cheng, A., Xiong, W., Ferrell, J. E., Jr., and Solomon, M. J. (2005b). Identification and comparative analysis of multiple mammalian Speedy/Ringo proteins. *Cell Cycle* 4, 155-165.
- Ciemerych, M. A., and Sicinski, P. (2005). Cell cycle in mouse development. *Oncogene* 24, 2877-2898.
- Dow, L. E., Premsrirut, P. K., Zuber, J., Fellmann, C., McJunkin, K., Miething, C., Park, Y., Dickins, R. A., Hannon, G. J., and Lowe, S. W. A pipeline for the generation of shRNA transgenic mice. *Nat Protoc* 7, 374-393.
- Ferby, I., Blazquez, M., Palmer, A., Eritja, R., and Nebreda, A. R. (1999). A novel p34(cdc2)-binding and activating protein that is necessary and sufficient to trigger G(2)/M progression in *Xenopus* oocytes. *Genes Dev* 13, 2177-2189.
- Fujii, W., Onuma, A., Sugiura, K., and Naito, K. One-step generation of phenotype-expressing triple-knockout mice with heritable mutated alleles by the CRISPR/Cas9 system. *J Reprod Dev* 60, 324-327.
- Geng, Y., Yu, Q., Sicinska, E., Das, M., Schneider, J. E., Bhattacharya, S., Rideout, W. M., Bronson, R. T., Gardner, H., and Sicinski, P. (2003). Cyclin E ablation in the mouse. *Cell* 114, 431-443.

Hakem, R., de la Pompa, J. L., Sirard, C., Mo, R., Woo, M., Hakem, A., Wakeham, A., Potter, J., Reitmair, A., Billia, F., *et al.* (1996). The tumor suppressor gene *Brcal* is required for embryonic cellular proliferation in the mouse. *Cell* 85, 1009-1023.

Hall, B., Limaye, A., and Kulkarni, A. B. (2009). Overview: generation of gene knockout mice. *Curr Protoc Cell Biol Chapter 19*, Unit 19 12 19 12 11-17.

Hamilton, D. L., and Abremski, K. (1984). Site-specific recombination by the bacteriophage P1 lox-Cre system. Cre-mediated synapsis of two lox sites. *J Mol Biol* 178, 481-486.

Haruyama, N., Cho, A., and Kulkarni, A. B. (2009). Overview: engineering transgenic constructs and mice. *Curr Protoc Cell Biol Chapter 19*, Unit 19 10.

Karaiskou, A., Perez, L. H., Ferby, I., Ozon, R., Jesus, C., and Nebreda, A. R. (2001). Differential regulation of Cdc2 and Cdk2 by RINGO and cyclins. *J Biol Chem* 276, 36028-36034.

Lenormand, J. L., Dellinger, R. W., Knudsen, K. E., Subramani, S., and Donoghue, D. J. (1999). Speedy: a novel cell cycle regulator of the G2/M transition. *Embo J* 18, 1869-1877.

McAndrew, C. W., Gastwirt, R. F., Meyer, A. N., Porter, L. A., and Donoghue, D. J. (2007). Spyl enhances phosphorylation and degradation of the cell cycle inhibitor p27. *Cell Cycle* 6, 1937-1945.

Mendez, J. (2003). Cell proliferation without cyclin E-CDK2. *Cell* 114, 398-399.

Muller, U. (1999). Ten years of gene targeting: targeted mouse mutants, from vector design to phenotype analysis. *Mech Dev* 82, 3-21.

Nagy, A. (2000). Cre recombinase: the universal reagent for genome tailoring. *Genesis* 26, 99-109.

Porter, L. A., Dellinger, R. W., Tynan, J. A., Barnes, E. A., Kong, M., Lenormand, J. L., and Donoghue, D. J. (2002). Human Speedy: a novel cell cycle regulator that enhances proliferation through activation of Cdk2. *J Cell Biol* 157, 357-366.

Porter, L. A., Kong-Beltran, M., and Donoghue, D. J. (2003). Spy1 interacts with p27Kip1 to allow G1/S progression. *Mol Biol Cell* *14*, 3664-3674.

Rane, S. G., Dubus, P., Mettus, R. V., Galbreath, E. J., Boden, G., Reddy, E. P., and Barbacid, M. (1999). Loss of Cdk4 expression causes insulin-deficient diabetes and Cdk4 activation results in beta-islet cell hyperplasia. *Nat Genet* *22*, 44-52.

Sander, J. D., and Joung, J. K. (2014). CRISPR-Cas systems for editing, regulating and targeting genomes. *Nat Biotechnol* *32*, 347-355.

Santamaria, D., Barriere, C., Cerqueira, A., Hunt, S., Tardy, C., Newton, K., Caceres, J. F., Dubus, P., Malumbres, M., and Barbacid, M. (2007). Cdk1 is sufficient to drive the mammalian cell cycle. *Nature* *448*, 811-815.

Sauer, B. (1998). Inducible gene targeting in mice using the Cre/lox system. *Methods* *14*, 381-392.

Shen, B., Zhang, J., Wu, H., Wang, J., Ma, K., Li, Z., Zhang, X., Zhang, P., and Huang, X. Generation of gene-modified mice via Cas9/RNA-mediated gene targeting. *Cell Res* *23*, 720-723.

Terret, M. E., Ferby, I., Nebreda, A. R., and Verlhac, M. H. (2001). RINGO efficiently triggers meiosis resumption in mouse oocytes and induces cell cycle arrest in embryos. *Biol Cell* *93*, 89-97.

Tremml, G., Singer, M., and Malavarca, R. (2008). Culture of mouse embryonic stem cells. *Curr Protoc Stem Cell Biol* *Chapter 1*, Unit 1C 4.

Voziyanov, Y., Pathania, S., and Jayaram, M. (1999). A general model for site-specific recombination by the integrase family recombinases. *Nucleic Acids Res* *27*, 930-941.

Wagner, K. U., Wall, R. J., St-Onge, L., Gruss, P., Wynshaw-Boris, A., Garrett, L., Li, M., Furth, P. A., and Hennighausen, L. (1997). Cre-mediated gene deletion in the mammary gland. *Nucleic Acids Res* *25*, 4323-4330.

Wang, H., Yang, H., Shivalila, C. S., Dawlaty, M. M., Cheng, A. W., Zhang, F., and Jaenisch, R. One-step generation of mice carrying mutations in multiple genes by CRISPR/Cas-mediated genome engineering. *Cell* *153*, 910-918.

Yang, H., Wang, H., and Jaenisch, R. (2014). Generating genetically modified mice using CRISPR/Cas-mediated genome engineering. *Nat Protoc* *9*, 1956-1968.

Yang, H., Wang, H., Shivalila, C. S., Cheng, A. W., Shi, L., and Jaenisch, R. One-step generation of mice carrying reporter and conditional alleles by CRISPR/Cas-mediated genome engineering. *Cell* *154*, 1370-1379.

Chapter 6

General Discussion and Future Directions

Discussion and Future Directions

This thesis describes the generation of the first transgenic model systems to drive expression of Spy1 in a temporally and spatially controlled manner. The advent of technologies to generate transgenic and gene targeted models has revolutionized our understanding of the basic molecular mechanisms which regulate developmental processes and ultimately progression to carcinogenesis. No such models had previously existed for Spy1, therefore limiting research to *in vitro* studies and transplantation of manipulated cells back into an *in vivo* setting. While these techniques are commonly used in the literature and have proven to be reliable, the use of mouse models inherently provides many advantages over other study systems. Inducing changes in protein expression levels in a normal environment eliminates potential effects due to immortalization of cells. Maintenance of an environment reflective of normal conditions also prevents loss of extracellular signals from the local environment that typically affects the cellular processes, playing important roles in influencing cell fate and cell cycle decisions.

Two transgenic model systems were generated. The MMTV-Spy1 mouse was designed to target overexpression of Spy1 specifically to the mammary gland. Using the MMTV promoter, we were able to study the effects of aberrant Spy1 expression on mammary development and tumorigenesis. MMTV-Spy1 mice displayed normal mammary development and did not develop spontaneous tumours, even after multiple rounds of pregnancy. Lack of an overt developmental phenotype could simply be due to the strain of choice in generating this model. MMTV-Spy1 mice were generated on a B6CBAF1/J background which are resistant to mammary tumorigenesis (Beutner et al., 1996; Davie et al., 2007). The C57BL6/J strain is well documented to be highly resistant to many forms of tumorigenesis. In addition, this strain is known to be resistant to MMTV infection potentially due to differences in major histocompatibility complexes which can lead to immune mediated resistance (Beutner et al., 1996; Davie et al., 2007). It is plausible then that if backcrossed onto a susceptible strain of mouse commonly used in the development of MMTV transgenic models, we may see an overt

difference in mammary development and the onset of mammary tumorigenesis. The MMTV-Spy1 mouse has been backcrossed ten generations onto an FVB background. Although preliminary analysis shows only subtle differences similar to results seen on the B6CBAF1/J background, it remains to be seen if over time and after repeated cycles of pregnancy, these mice develop gross morphological changes and spontaneous mammary tumours.

Importantly, the highly resistant B6CBAF1/J MMTV-Spy1 mice showed increased susceptibility to tumour formation when challenged with the carcinogen DMBA. Spy1 expressing mice display a significant increase in the number of overall tumours and mammary tumours formed over their control littermates when treated with DMBA. Since DMBA exerts its carcinogenic properties by causing damage to the DNA, and Spy1 is known to override cellular checkpoints and apoptotic pathways in response to DNA damage (Barnes et al., 2003; Das et al., 1989; Gastwirt et al., 2006; McAndrew et al., 2009; Melendez-Colon et al., 1999), we investigated whether the presence of exogenous levels of Spy1 elicited any effects on DNA damage response signaling. Levels of p53 were examined after treatment with DMBA and were found to be significantly elevated in MMTV-Spy1 mice. Additionally, a higher percentage of cells were γ H2AX positive. Increased levels of p53 could indicate a delayed or impaired DNA damage response in response to DMBA treatment due to elevated levels of Spy1 which are known to override DNA damage signaling checkpoints (Barnes et al., 2003; Gastwirt et al., 2006; McAndrew et al., 2009). To further corroborate this, an increase in γ H2AX indicates the presence of unrepaired damage. Levels of γ H2AX are proven to be a reliable marker of the amount of DNA damage a cell has sustained or accumulated, and an increase in γ H2AX has been demonstrated in various forms of cancer (Dickey et al., 2009). Taken together, increased levels of both p53 and γ H2AX indicate the DNA damage response is either delayed or inactive. The inability of the cell to repair damage would lead to accumulation of damage over time contributing to the onset of tumorigenesis.

Surprisingly, aged male MMTV-Spy1 mice displayed a significant increase in the number of spontaneous liver tumours. Previous reports have documented expression of MMTV driven transgenes in male reproductive organs and salivary glands, although expression in the liver has only been reported thus far in females (Callahan and Smith, 2000; Cardiff and Kenney, 2011; Wagner et al., 2001). We show a significant increase in Spy1 expression in aged male MMTV-Spy1 livers, which correlates with increased tumour formation and lipid accumulation in the liver. NASH is a fatty liver disease characterized by significant fat accumulation, inflammation, injury and fibrosis which has the potential to develop into full blown HCC (Dowman et al., 2010; Takahashi et al., 2012; The National Digestive Diseases Information Clearinghouse, 2014). We show that MMTV-Spy1 male livers display an increase in lipid formation, and a significant increase in nuclear size. Increased nuclear size could be due to either increased ploidy or senescence (Gonzalez-Reimers et al., 1987; Nakajima et al., 2010). Since elevated levels of Spy1 are known to increase rates of cellular proliferation (Porter et al., 2002), perhaps increased levels of Spy1 in the liver could lead to increased DNA replication and therefore increased DNA content. Assessing DNA content via flow cytometry through isolation of primary hepatocytes, or immunohistochemical analysis using the Feulgen stain would allow us to elucidate if the increase in nuclear size is due to increased DNA content. An increased number of senescent cells could also explain the significant increase observed as nuclear size is known to correlate with senescence (Nakajima et al., 2010; Rodier and Campisi, 2011). Importantly, senescent cells are capable of promoting malignancy in certain cell systems highlighting the important role the presence of these cells play (Krtolica et al., 2001). Most importantly, elevated levels of p53 and its downstream target p21 were also noted in the livers of MMTV-Spy1 males. Levels of p53 have been shown to be increased in cases of NASH correlating with higher degrees of inflammation (Farrell et al., 2009; Panasiuk et al., 2006; Yahagi et al., 2004). An increase in p21, which leads to cell cycle arrest and is correlated with the presence of senescent cells, was also noted (Nakajima et al., 2010). Additionally, livers of MMTV-Spy1 mice also have elevated

levels of active caspase 3 indicating higher rates of apoptosis. Taken together, these results indicate activation of the DDR in response to increased rates of tissue injury and inflammation.

Both male and female MMTV-Spy1 mice have increased susceptibility to tumour formation in the liver and the mammary gland respectively. Interestingly, in both tissue types we see elevated levels of the tumour suppressor p53 indicating stress response activation. We have shown that under normal circumstances, an increase in p53 following damage acts to downregulate expression of Spy1, allowing for inhibition of the cell cycle and for the appropriate repair machinery to be activated. Our data suggests that after damage has been repaired, levels of Spy1 begin to increase, presumably to contribute to the activation of CDK2 allowing for re-entry into the cell cycle and subsequent cell cycle progression. In non-malignant cells, this would prevent the accumulation of deleterious mutations or alterations and prevent Spy1 from sustaining cell proliferation and survival. In cases of sustained elevation of Spy1 levels, this may in itself serve as a stressor, causing aberrant proliferation of the cell. Sensing abnormal rates of proliferation, levels of p53 increase to degrade Spy1 to slow down rates of cellular proliferation. If Spy1 levels remain elevated, it may become a battle between the stress response signaling of p53 and the ability of Spy1 to override these mechanisms to sustain enhanced cellular proliferation. Under conditions of DNA damage or injury, if p53 is unable to keep levels of Spy1 in check, Spy1 will continue to sustain elevated rates of proliferation and enhance cell survival in the presence of damage, ultimately leading to tumour initiation. In cases of p53 mutation or loss of p53 resulting in compromised activity, elevated levels of Spy1 go unchecked significantly increasing rates of proliferation and contributing to the onset of oncogenesis.

The ability of Spy1 to promote tumour initiation may then be dependent on its ability to overcome p53 mediated checkpoints. Thus, loss or inactivation of p53 may be a contributing factor in Spy1 tumour formation. To test this, the effects of overexpression of Spy1 and loss of p53 need to be tested in an *in vivo* setting. This can be accomplished utilizing a variety of experimental designs. First, knockdown of p53 could be induced in the mammary glands of

MMTV-Spy1 mice via intraductal injection of siRNA. Intraductal injections have proven to be an effective method of introducing drug or siRNA directly to the mammary epithelium (Krause et al., 2013). While this is an effective method, one disadvantage is that expression of the siRNA would not be stable meaning injections would need to be delivered on a regular basis to ensure stable knockdown of p53. A more effective method to test the effects of p53 knockdown on Spy1 driven tumour development would be to cross the MMTV-Spy1 mouse model with the existing p53 null mouse. The p53 knockout mouse is known to succumb to tumours such as lymphomas at a short latency period (Donehower et al., 1992; Jacks et al., 1994). To overcome this, the MMTV-Spy1 mouse could instead be crossed with the heterozygote p53 mouse meaning only one allele would be lost. While this would be a far superior method than the use of intraductal injections, it does pose some inherent problems. It is well documented that the MMTV promoter does not drive expression of the transgene in a homogenous manner (Rao et al., 2014; Wagner et al., 2001). This means that although knockdown of p53 would be observed in every cell of the mammary gland, some of these cells would not be overexpressing Spy1 leading to a mixed population of cells within the gland. To ensure that all cells contain both p53 knockdown and Spy1 overexpression, a different transgenic system would need to be generated. Instead of using the full p53 null mouse, the p53 floxed mouse could be used to introduce loss of p53 under the control of the MMTV promoter. A new transgenic mouse containing both Cre recombinase and Spy1 under the control of the MMTV promoter would be generated. Use of a bicistronic vector would allow for simultaneous expression of both Spy1 and Cre under the control of the MMTV promoter and would ensure all cells with Spy1 overexpression would also have loss of p53. The use of bicistronic vectors in transgenic mice using the MMTV promoter has already been successfully demonstrated and has proven to be a valuable model to test the expression or knockdown of multiple genes within the same cell (Rao et al., 2014; Ursini-Siegel et al., 2008). Crossing a bicistronic MMTV-Spy1-Cre mouse with the existing p53 floxed mouse would be a more superior method than simply crossing the MMTV-Spy1 mouse and p53 null mouse. Using

these models, the effects of reduced p53 activity on Spy1's ability to promote mammary tumourigenesis would be tested. Crosses could be done on either the B6CBAF1/J or FVBN/J background to determine if loss of p53 activity can lead to spontaneous tumour formation in a model expressing elevated levels of Spy1. If spontaneous mammary tumours do form, this would prove that the ability of Spy1 to promote mammary tumour formation is dependent on loss or mutation of p53. This would have a profound impact on our understanding of breast cancer characterized by loss of p53. Patients with Li-Fraumeni syndrome have an increased predisposition to the development of breast cancer caused by inheritable germline mutations in p53 (Akashi and Koeffler, 1998). If Spy1 is capable of promoting tumour initiation after loss of p53 function, it could prove to be an attractive therapeutic target specifically in this subset of patients.

The effects of loss of p53 function in the development of HCC could also be tested utilizing the MMTV-Spy1 mouse. Hydrodynamic tail vein injections have been demonstrated to successfully deliver plasmid DNA and siRNA within the mouse, with concentrated expression in the liver (Liu et al., 1999). Expression can be sustained with repeated injections to test the effects of p53 knockdown on the development of NASH and HCC in the MMTV-Spy1 mouse model. Using this approach, we would be able to determine if loss of p53 accelerates the development of tumours in this mouse as currently spontaneous tumours are not noted until mice have reached one year of age. It is plausible that loss of p53 function could accelerate this phenotype leading to early disease and tumour onset.

To more specifically address the effects of Spy1 in liver disease and tumour formation, the Spy1-pTRE mouse that I have generated could be crossed with an existing transgenic mouse that drives expression of a transgene under the control of the albumin promoter specifically in hepatocytes, the Alb-rtTA mouse (Liu-Chittenden et al., 2012). The Spy1-pTRE mouse provides an inducible system that could be used for the study of elevated Spy1 levels in a variety of tissue systems. Here we have described its use in the mammary gland by validating the model through

crosses with the MMTV-rtTA mouse. Additionally, this mouse can be crossed with the Nestin-rtTA mouse to study the effects of Spy1 expression in subsets of populations within the brain known to express Spy1. This is especially important given the role Spy1 is known to play in driving brain tumour initiating cell populations in gliomas (Lubanska et al., 2014). To further elucidate the role Spy1 plays in the development of NASH and HCC, we could drive expression of Spy1 specifically within hepatocytes at various stages in development through the administration of doxycycline. This would allow us to directly test the effects of aberrant Spy1 expression on liver development and would lead to higher levels of Spy1 than are seen in the MMTV-Spy1 male livers as this would be driven in a liver specific manner, and not simply due to leakiness or altered activation of the MMTV promoter. Using this system would allow us to better elucidate the role of Spy1 in tumour initiation and combined with hydrodynamic tail vein injection to knockdown p53, we would be able to determine the precise relationship between p53 signaling and activity and Spy1 mediated tumorigenesis.

Our data supports that Spy1 plays an essential role in mediating tumour initiation in cases of aberrant or loss of p53 activity, and thus presents itself as a key player in promoting oncogenesis. The essentiality of Spy1 in this process needs to be examined to elucidate the complete molecular mechanism responsible for mediating these events. To this end, we have described an approach for the generation of a gene targeted mouse that will allow for conditional knockout of Spy1 in a tissue specific manner. Using this mouse, in conjunction with the MMTV-Cre mouse, we will be able to determine the essentiality of Spy1 both in normal development of the mammary gland and in tumour initiation. Treatment of the Spy1 knockout mouse with DMBA will allow us to monitor the onset of tumour formation to determine if loss of Spy1 leads to increased tumour latency and decreased tumour formation. If this is the case, this would indicate that Spy1 plays an essential role in promoting tumour formation and could thus be an early indicator of propensity to develop breast cancer, making it an attractive diagnostic marker. Similar types of studies could be conducted using the Alb-Cre mouse to knockout Spy1

specifically within the liver. Using this approach we would be able to determine if Spy1 itself leads to the onset of NAFLD and ultimately NASH. Generating a model in which the effect of loss of Spy1 on development and tumorigenesis can be studied is an essential step in fully elucidating the full molecular mechanism of these processes.

Using two different study systems, we have shown that elevated levels of Spy1 enhance susceptibility to tumorigenesis. In both cases, increased levels of p53 were also found indicating that overexpression of Spy1 could potentially act as a stressor, eliciting a stress response within the cell. In response to stress, p53 is upregulated to try to prevent unrestrained cell proliferation and survival of cells in the presence of damage. Increased p53 ultimately leads to a decline in Spy1 levels in normal circumstances. With sustained elevation of Spy1, p53 may be unable to reduce Spy1 to the physiological levels required to sustain normal rates of proliferation, and cellular proliferation goes unchecked. If loss of p53 occurs, or activity is diminished, Spy1 is capable of promoting proliferation in its absence and leads to uncontrolled cell proliferation and survival in the presence of DNA damage. Over time, this will lead to the accumulation of deleterious mutations and promote the initiation of tumorigenesis. Thus, understanding the complex relationship between Spy1 and p53 mediated signaling is essential in understanding the factors contributing to tumorigenesis. Further exploring and understanding this relationship will open new avenues in the treatment of these diseases and will ultimately provide new therapeutic targets and novel therapies in the treatment of oncogenesis.

References

- Akashi, M., and Koeffler, H. P. (1998). Li-Fraumeni syndrome and the role of the p53 tumor suppressor gene in cancer susceptibility. *Clin Obstet Gynecol* *41*, 172-199.
- Barnes, E. A., Porter, L. A., Lenormand, J. L., Dellinger, R. W., and Donoghue, D. J. (2003). Human Spyl promotes survival of mammalian cells following DNA damage. *Cancer Res* *63*, 3701-3707.
- Beutner, U., McLellan, B., Kraus, E., and Huber, B. T. (1996). Lack of MMTV superantigen presentation in MHC class II-deficient mice. *Cell Immunol* *168*, 141-147.
- Callahan, R., and Smith, G. H. (2000). MMTV-induced mammary tumorigenesis: gene discovery, progression to malignancy and cellular pathways. *Oncogene* *19*, 992-1001.
- Cardiff, R. D., and Kenney, N. (2011). A compendium of the mouse mammary tumor biologist: from the initial observations in the house mouse to the development of genetically engineered mice. *Cold Spring Harb Perspect Biol* *3*.
- Das, S. K., Delp, C. R., Bandyopadhyay, A. M., Mathiesen, M., Baird, W. M., and Banerjee, M. R. (1989). Fate of 7,12-dimethylbenz(a)anthracene in the mouse mammary gland during initiation and promotion stages of carcinogenesis in vitro. *Cancer Res* *49*, 920-924.
- Davie, S. A., Maglione, J. E., Manner, C. K., Young, D., Cardiff, R. D., MacLeod, C. L., and Ellies, L. G. (2007). Effects of FVB/NJ and C57Bl/6J strain backgrounds on mammary tumor phenotype in inducible nitric oxide synthase deficient mice. *Transgenic Res* *16*, 193-201.
- Dickey, J. S., Redon, C. E., Nakamura, A. J., Baird, B. J., Sedelnikova, O. A., and Bonner, W. M. (2009). H2AX: functional roles and potential applications. *Chromosoma* *118*, 683-692.
- Donehower, L. A., Harvey, M., Slagle, B. L., McArthur, M. J., Montgomery, C. A., Jr., Butel, J. S., and Bradley, A. (1992). Mice deficient for p53 are developmentally normal but susceptible to spontaneous tumours. *Nature* *356*, 215-221.
- Dowman, J. K., Tomlinson, J. W., and Newsome, P. N. (2010). Pathogenesis of non-alcoholic fatty liver disease. *QJM* *103*, 71-83.

Farrell, G. C., Larter, C. Z., Hou, J. Y., Zhang, R. H., Yeh, M. M., Williams, J., dela Pena, A., Francisco, R., Osvath, S. R., Brooling, J., *et al.* (2009). Apoptosis in experimental NASH is associated with p53 activation and TRAIL receptor expression. *J Gastroenterol Hepatol* 24, 443-452.

Gastwirt, R. F., Slavin, D. A., McAndrew, C. W., and Donoghue, D. J. (2006). Spy1 expression prevents normal cellular responses to DNA damage: inhibition of apoptosis and checkpoint activation. *J Biol Chem* 281, 35425-35435.

Gonzalez-Reimers, C. E., Santolaria-Fernandez, F. J., Castaneyra-Perdomo, A., Jorge-Hernandez, J. A., Martin-Herrera, A., and Hernandez-Nieto, L. (1987). Hepatocyte and nuclear areas in alcoholic liver cirrhosis: their relationship with the size of the nodules and the degree of fibrosis. *Drug Alcohol Depend* 19, 357-362.

Jacks, T., Remington, L., Williams, B. O., Schmitt, E. M., Halachmi, S., Bronson, R. T., and Weinberg, R. A. (1994). Tumor spectrum analysis in p53-mutant mice. *Curr Biol* 4, 1-7.

Krause, S., Brock, A., and Ingber, D. E. (2013). Intraductal injection for localized drug delivery to the mouse mammary gland. *J Vis Exp*.

Krtolica, A., Parrinello, S., Lockett, S., Desprez, P. Y., and Campisi, J. (2001). Senescent fibroblasts promote epithelial cell growth and tumorigenesis: a link between cancer and aging. *Proc Natl Acad Sci U S A* 98, 12072-12077.

Liu-Chittenden, Y., Huang, B., Shim, J. S., Chen, Q., Lee, S. J., Anders, R. A., Liu, J. O., and Pan, D. (2012). Genetic and pharmacological disruption of the TEAD-YAP complex suppresses the oncogenic activity of YAP. *Genes Dev* 26, 1300-1305.

Liu, F., Song, Y., and Liu, D. (1999). Hydrodynamics-based transfection in animals by systemic administration of plasmid DNA. *Gene Ther* 6, 1258-1266.

Lubanska, D., Market-Velker, B. A., deCarvalho, A. C., Mikkelsen, T., Fidalgo da Silva, E., and Porter, L. A. (2014). The cyclin-like protein Spy1 regulates growth and division characteristics of the CD133+ population in human glioma. *Cancer Cell* 25, 64-76.

McAndrew, C. W., Gastwirt, R. F., and Donoghue, D. J. (2009). The atypical CDK activator Spy1 regulates the intrinsic DNA damage response and is dependent upon p53 to inhibit apoptosis. *Cell Cycle* 8, 66-75.

Melendez-Colon, V. J., Luch, A., Seidel, A., and Baird, W. M. (1999). Cancer initiation by polycyclic aromatic hydrocarbons results from formation of stable DNA adducts rather than apurinic sites. *Carcinogenesis* 20, 1885-1891.

Nakajima, T., Nakashima, T., Okada, Y., Jo, M., Nishikawa, T., Mitsumoto, Y., Katagishi, T., Kimura, H., Itoh, Y., Kagawa, K., and Yoshikawa, T. (2010). Nuclear size measurement is a simple method for the assessment of hepatocellular aging in non-alcoholic fatty liver disease: Comparison with telomere-specific quantitative FISH and p21 immunohistochemistry. *Pathol Int* 60, 175-183.

Panasiuk, A., Dzieciol, J., Panasiuk, B., and Prokopowicz, D. (2006). Expression of p53, Bax and Bcl-2 proteins in hepatocytes in non-alcoholic fatty liver disease. *World J Gastroenterol* 12, 6198-6202.

Porter, L. A., Dellinger, R. W., Tynan, J. A., Barnes, E. A., Kong, M., Lenormand, J. L., and Donoghue, D. J. (2002). Human Speedy: a novel cell cycle regulator that enhances proliferation through activation of Cdk2. *J Cell Biol* 157, 357-366.

Rao, T., Ranger, J. J., Smith, H. W., Lam, S. H., Chodosh, L., and Muller, W. J. (2014). Inducible and coupled expression of the polyomavirus middle T antigen and Cre recombinase in transgenic mice: an in vivo model for synthetic viability in mammary tumour progression. *Breast Cancer Res* 16, R11.

Rodier, F., and Campisi, J. (2011). Four faces of cellular senescence. *J Cell Biol* 192, 547-556.

Takahashi, Y., Soejima, Y., and Fukusato, T. (2012). Animal models of nonalcoholic fatty liver disease/nonalcoholic steatohepatitis. *World J Gastroenterol* 18, 2300-2308.

The National Digestive Diseases Information Clearinghouse (2014). Nonalcoholic Steatohepatitis. In.

Ursini-Siegel, J., Hardy, W. R., Zuo, D., Lam, S. H., Sanguin-Gendreau, V., Cardiff, R. D., Pawson, T., and Muller, W. J. (2008). ShcA signalling is essential for tumour progression in mouse models of human breast cancer. *EMBO J* 27, 910-920.

Wagner, K. U., McAllister, K., Ward, T., Davis, B., Wiseman, R., and Hennighausen, L. (2001). Spatial and temporal expression of the Cre gene under the control of the MMTV-LTR in different lines of transgenic mice. *Transgenic Res* 10, 545-553.

Yahagi, N., Shimano, H., Matsuzaka, T., Sekiya, M., Najima, Y., Okazaki, S., Okazaki, H., Tamura, Y., Iizuka, Y., Inoue, N., *et al.* (2004). p53 involvement in the pathogenesis of fatty liver disease. *J Biol Chem* 279, 20571-20575.

Appendix A- List of Primers

qRT-PCR Primers

Flag-Spy1

- Forward: 5'TGACAAGAGGCACAATCAGATGT 3'
- Reverse: 5' CAAATAGGACGCTTCAGAGTAATGG3'

Human GAPDH

- Forward: 5' GCACCGTCAAGGCTGAGAAC 3'
- Reverse: 5' GGATCTCGCTCCTGGAAGATG 3'

Human p53

- Forward: 5' CCTGAGGTTGGCTCTGACTGTAC 3'
- Reverse: 5' TGGAGTCTTCCAGTGTGATGATG 3'

Human Spy1

- Forward: 5' TTGTGAGGAGGTTATGGCCATT 3'
- Reverse: 5' GCAGCTGAACTTCATCTCTGTTGTAG 3'

Mouse Albumin

- Forward: 5' CTAAACCGATGGGCGATCTCACT 3'
- Reverse: 5' CCCACTAGCCTCTGGCAAAT 3'
- Primers sequence obtained from "Mammalian hepatocyte differentiation requires transcription factor HNF-4 α "

Mouse GAPDH

- Forward: 5' GATGCCCCCATGTTTGTGAT 3'
- Reverse: 5' GTGGTCATGAGCCCTTCCA 3'

Mouse Nestin

- Forward: 5' GGCTTCTCTTGGATTCCTGACCC 3'
- Reverse: 5' TGGGCTGAGGACAGGGAGCAC 3'

Mouse p21

- Forward: 5' GCCTGACAGATTTCTATCACTCCAA 3'
- Reverse: 5' AGAGTGAGGGCTAAGGCCGA 3'

Mouse p53

- Forward: 5' CACAGCGTGGTGGTACCTTATG 3'
- Reverse: 5' GGTCCCACTGGAGTCTTCCA 3'

Genotyping Primers

MMTV-rtTA Genotyping

- Forward: 5' TGCAGAGCC AGCCTTCTTAT 3'
- Reverse: 5' CCTCGATGGTAGACC CGTAA 3'

MMTV-Spy1 Genotyping

- Forward: 5' CCAAGGCTTAAGTAAGTTTTTGG 3'
- Reverse: 5' GGGCATAAGCACAGATAAAACACT 3'

Spy1-pTRE Genotyping

- Forward: 5' GTGTACGGTGGGAGGCCTATATAA 3'
- Reverse: 5' GTCATAGCCAAAAGATACTTGTCTGC 3'

Probe Generation for Southern Blot Analysis

3'Probe

- Forward: 5'
GCATGTACCGGTAGGAATGGAATTTAGTTGGTGGTAAAACACTTGCC 3'
- Reverse: 5' GCGCGCGTTTTAAACTGTGTAAATTCCTAGACAGAAACACCTAC 3'

5'Probe

- Forward: 5'
GCATGTACCGGTCAACACCCGCCCGCCCCCCCCACACATATGCACATCAATTTG 3'
- Reverse: 5'
GGCGCGCGTTTTAAACGAGCCTGATTTTACATGAATAGTGACAGTAGGTGGTG
3'

Neo Probe

- Forward: 5' GCCACACCCAGCCGGCCACAGTCGATGAATCCAGAAAAGC 3'
- Reverse: 5' GTCAAGACCGACCTGTCCGGTGCCCTGAATGAACTGCAG 3'

Appendix B: Detailed Protocols

I. Southern Blot Protocol

- 1) Digest 10ug of DNA overnight at 37C
 - 30uL reaction volume total
 - o 3uL of buffer
 - o 1uL of appropriate enzyme
 - o 26uL of H₂O + DNA
- 2) Following morning, add an additional 1uL of the appropriate enzyme and continue digesting at 37C (for ~3-4hrs)
- 3) Prepare 0.8% agarose gel with NO ethidium bromide added
 - Make 400mL of agarose for our big gel rigs
 - When gel has solidified, remove tape and leave combs in gel; place in running apparatus with combs still in gel and pour freshly made 1xTAE over gel; let gel sit in buffer for ~30min before removing combs
- 4) Run DNA on 0.8% agarose gel O/N → 30V for 10hrs
 - Leave 2 spaces between ladder and first sample
 - Combs have 38wells therefore can run 34 samples per comb if run 2 ladders
- 5) Place gel in glass baking dish and stain with EtBr in 1xTAE for ~15min while gently shaking
- 6) Image the gel beside a UV ruler in order to measure migration of the ladder
 - NOTE: to transfer gel into and out of glass baking dish use glass photo frame; slide glass plate under the gel to gently lift gel without ripping the wells
- 7) Rinse gel in buffer 1 (made fresh that morning) 2x 30min each (rinsed in glass baking dish)
- 8) Rinse with water for ~5min
- 9) Rinse gel in buffer 2 (made fresh that morning) 2x 30min each (rinsed in glass baking dish)
- 10) Assemble O/N capillary action transfer apparatus
 - Transfer buffer is buffer 2
 - Membrane is nitrocellulose (Fisher (GE) WP4HY00010- NitroPure supported nitrocellulose 0.45micron, 30cmx3m roll)
 - Gel size is 8"x8": paper towels, 3 sheets of filter paper and nitrocellulose paper should be cut to this exact size
 - Whatmann filter paper used in Western blot transfer is used as wick and filter paper; wicks should be cut wider than 8" (~9-10"); use entire length of filter paper sheet for wick
 - Large Tupperware container with lid on and glass picture frame glass piece are used as the base for the transfer platform (glass photo frame is used to provide level surface to place the gel; glass is placed on top of the lid of the Tupperware container)
 - 2 smaller Tupperware containers are used as the reservoirs on either side of the transfer platform
 - 3 wicks are wet with transfer buffer and placed on top of the platform with each end hanging into the reservoirs on either side submerged as much as possible
 - Use glass pipette to roll out air bubbles in wick

- Carefully place gel upside down onto the wick and try to keep wells intact (will need to mark them later)
 - o Try to place gel centred on wick
 - o Remove air bubbles using glass pipette
 - o Trim off ladder and excess gel using razor
 - Place nitrocellulose membrane on top of gel
 - o Once on gel can't be moved
 - o Trim excess off if membrane is too wide (gel will be slightly smaller once ladder is trimmed off)
 - o Roll out air bubbles
 - Have 3 pieces of Whatmann filter paper cut to size; soak each one in transfer buffer and place one at a time on top of the membrane removing air bubbles after adding each one
 - To prevent buffer from bypassing the gel surround gel with plastic wrap
 - o Tear off piece of plastic wrap, roll it and cut to size if need be and place around all 4 edges of gel
 - o Usually stack 2 pieces on top of one another
 - Need ~10cm stack of paper towels cut to size
 - o Place stack of paper towels on top of filter paper; ensure it is centred
 - Put dry glass frame plate on top of paper towels
 - Place weight on top of glass plate
 - o No heavier than 500g
 - o Ensure it is centred so stack of paper towels will not fall over
 - Make sure reservoirs are filled with transfer buffer
 - Transfer O/N
- 11) Disassemble transfer apparatus
- Stack of paper towels should be almost entirely wet and gel should be flat
 - Remove gel and nitrocellulose together and mark wells with pencil on the membrane
- 12) Dry the membrane for 1hr on benchtop between 2 pieces of Whatman paper
- 13) Bake membrane between 2 pieces of Whatman paper, then all wrapped in aluminum foil at 80C 20-25mg Hg for 2hrs
- Membrane should be slightly brown at edges and should no longer smell of the transfer buffer
 - Cut one of the corners of the membrane to orient later
 - ***NOTE: after membrane has been baked, membrane can safely be stored until needed for hybridization; doesn't need to happen immediately after DNA has been fixed to membrane
- 14) Pre-hyb membrane for 2hrs at 65C
- Hybridization buffer should be heated at 55C before hand
- 15) While membrane is in pre-hyb; label probe with α P32 dCTP (Perkin Elmer BLU513Z * rest of catalog number is dependent on quantity ordered; 6000Ci/mmol)
- Probes are digested with appropriate enzyme to gel extract probe from vector (digest 2ug of vector to ensure sufficient yield and high enough quality DNA)
 - Gel extract using Sigma Gel Extraction Kit following protocol from kit

- Label probe using Promega Prime-a-Gene Labeling System (U1100) following protocol BUT double rxn
 - o Labeling 5x buffer 20uL
 - o Mixture of unlabeled dNTPS (dATP, dTTP, dGTP) 4uL
 - o Nuclease free BSA 4uL
 - o α P32 dCTP 6000Ci/mmol (100uCi) 5uL
 - o DNA polymerase 1 large fragment-Klenow 2uL
 - o DNA 50ng
 - o H2O up to 100uL (H2O + DNA=65uL)
 - Denature DNA sample by heating at 95-100C for 2minutes; rapidly chill the tube on ice
 - Assemble reaction (add P32 last in hot lab; rest of reaction is assembled in main lab since not hot)
 - Incubate reaction at room temperature for 60minutes

16) Purify the probe

- Take 3mL syringe and remove plunger; place syringe in 15mL tube
- Place glass wool up to 1mL mark → do not pack tightly
- Sephadex G50 beads prepared in advance → no measurement, just pour some of the Sephadex G50 powder into 50mL tube and add TE buffer; shouldn't be too viscous, solution will be cloudy
- Add Sephadex G50 beads (GE Healthcare Sephadex G50 fine 100ug 17-0042-01) on top of glass wool up to ~1.5mL mark (add so that above that mark since need to spin down); add to centre of syringe
- Spin at 1000rpm for 1min; check to make sure bead layer is at correct level, no cracks and is level; if not, add more beads and spin again
- Once probe is labeled add to centre of column (100uL max/column)
 - o Before adding, cut lid off of 1.5mL tube and place in 15mL tube then put syringe with prepared column back into 15mL tube so that the flow through is collected in the 1.5mL tube
- Spin 1000rpm for 1min and collect flow through
- Since our scintillation counter is not accurate, Geiger both the purified probe and the column (which contains unincorporated nucleotides) to ensure labeling was successful

17) Add entire 100uL of purified probe to 5mL of hybridization buffer and incubate O/N at 65C

18) Wash the membrane 3x for 10min each at room temperature in low stringency wash buffer

19) Wash the membrane 3x for 10 min each at 65C in high stringency wash buffer

20) Place membrane in film cassette wrapped in plastic wrap so that phosphor screen doesn't get wet; set up exposure with phosphor screen at room temperature; min 3 nights exposure

Wash Buffer 1-1L

87.66g NaCl
 20g NaOH

Wash Buffer 2-2L

154.16g $\text{NH}_4\text{CH}_3\text{COO}$
 1.6g NaOH

Hybridization Buffer-500mL

200mL 10X Set (4x final)
 100mL 50X Denhardts (10X final)
 5mL 10% sodium pyrophosphate (0.1% final)
 37.9mL 0.33M Na_3PO_4 pH 6.9 (0.025M final)
 5mL 10% SDS (0.2% final)
 151.1mL H_2O

Low Stringency (cold) Buffer- 200mL

20mL 20X SSC
 1mL 20% SDS
 179mL H_2O

High Stringency (hot) Buffer-200mL

2mL 20X SSC
 1mL 20% SDS
 197mL H_2O

50X Denhardt's Solution- 500mL

5g Ficoll 400
 5g PVP
 5g BSA Pentax Fraction V

Bring up to 500mL with H_2O , and filter through 0.45 μm syringe using 60mL syringe and freeze at -20 $^\circ\text{C}$ in 45mL aliquots

10X SET- 1L

87.66g NaCl (1.5M)
 24.3g Tris Base (0.2M)
 20mL 0.5M EDTA (0.01M)
 pH to 7.8 with HCl and fill to 1L with H_2O

0.33M Na_3PO_4 - 100mL

5.47g Na_3PO_4
 pH to 6.9 with HCl and fill up to 1L with Na_3PO_4

Reagents:

Company	Item Name	Catalog Number
Fisher Scientific	GE Nitrocellulose Membrane Nitropure 0.45uM 30cmx3m roll	WP4HY00010
Sigma Aldrich	Glass Wool	18421-500G
GE Healthcare Sciences	Sephadex G50 Fine 100ug	17-0042-01
Fisher Scientific	Hybridization Tubes	13-247-150
Promega	Prime-a-Gene Labeling System	U1100
Sigma	GenElute Gel Extraction Kit	NA1111-1KT
Perkin Elmer	dCTP P32 6000Ci/mmol 20mCi/mL	BLU513Z (remainder of catalog number is dependent on amount of radiation ordered.

Appendix C: Direct Interactions with p27 and Cdk2 Regulate Spy1-Induced Mammary Tumorigenesis

Direct Interactions with both p27 and Cdk2 Regulate Spy1-Mediated Proliferation *in vivo* and *in vitro*

Mohammad Al Sorkhy, Bre-Anne Fifield and Lisa A. Porter *

University of Windsor, Dept. of Biological Sciences

Windsor, ON N9B 3P4

* Corresponding author:

Phone: (519) 253-3000 x4775

Fax: (519) 571-3609

lporter@uwindsor.ca

Abstract

Background

Cell growth and proliferation are tightly controlled by the cyclic regulation of the cyclin dependent kinases (Cdks). Cdks are positively regulated through interactions with regulatory cyclin partners as well as being negatively regulated through interactions with Cdk inhibitors. More recently, families of cyclin-like proteins have emerged with unique abilities to regulate the Cdks. One of these proteins, Spy1A1 (SPDYA; herein referred to as Spy1), has demonstrated a pivotal ability to directly bind and regulate both the Cdks as well as at least one Cdk inhibitor, p27^{Kip1}. Spy1 accelerates somatic cell growth and proliferation and has been implicated in a number of human cancers including the breast, brain and liver. The physiological role for direct interactions between Spy1 and the distinct binding partners Cdk2 and p27 have not been addressed.

Methods

Herein we isolate key residues mediating the direct interaction with p27 and use mutants of Spy1 unable to interact specifically with either Cdk2 or p27 to study the effects on cell growth and tumorigenesis.

Results

Disrupting the direct interaction with either Spy1 binding partner decreased endogenous activity of Cdk2, as well as Spy1-mediated proliferation. However, only the direct interaction with p27 was essential for Spy1-mediated effects on p27 stability. *In vivo* neither mutation prevented tumorigenesis, although preventing interactions with both p27 and Cdk2 slowed the rate of Spy1-mediated tumorigenesis and decreased overall tumour volumes.

Conclusion

These data support the conclusion that direct interactions with both p27 and Cdk2 contribute to Spy1-mediated effects on cell growth. Hence, it is important to elucidate the dynamics of these interactions and to consider these data when assessing functional outcomes.

Introduction

Cell cycle regulation is an intricately controlled process that plays a critical role in all cell fate decisions. The catalytic cyclin dependent kinases (Cdks) are dependent on the production and destruction of their regulatory subunits, the cyclin family of proteins. Cyclin-Cdk complexes undergo a series of well established post-translational modifications to assume a fully activated state [1,2]. The G1/S cyclin-Cdk complexes are also negatively regulated through interactions with the Cip/Kip family of Cdk inhibitors (CKI) which includes p27, p21 and p57. It is crucial that Cdk regulation be tightly controlled to prevent the onset of tumorigenesis; in many forms of cancer elevated Cdk2 kinase activity and decreasing levels of p27 correlate positively with tumorigenic potential and negatively with patient prognosis [3,4]. The central requirement for activated Cdks implicates these kinases as potential therapeutic targets, and indeed this approach has shown tremendous potential in pre-clinical tumorigenesis models [5,6]. However with the exception of hematological malignancies, Cdk inhibitor therapy has been largely disappointing in the clinic [7,8]. Targeting metastatic ER+/HER2- have shown promise for select Cdk inhibitors recently, but it is clear that thorough characterization of the active Cyclin-Cdk partners in select patient populations will be necessary to optimize targeting [8,9] One factor that needs to be considered when stratifying patient populations is the presence of ‘cyclin-like’ proteins capable of activating the Cdks using very unique mechanisms [10,11]. Cdks bound to the Speedy/RINGO class of cyclin-like proteins are not dependent on post-translational modifications for activation, and they are less sensitive to inhibition by the Cdk inhibitors p21 and p27 [11,12].

One protein within the Speedy/RINGO class, Spy1A1 (SPDYA), herein referred to as Spy1, is capable of binding to, and activating, both Cdk1 and Cdk2 leading to increased rates of cell proliferation and inhibition of apoptosis when overexpressed [10,13,14]. The region regulating Spy1 interactions with Cdks are within the highly conserved S/R Box and several specific Spy1 residues have been identified to reduce binding affinity with Cdk2 *in vitro* [12].

Unlike any known cyclin proteins, Spy1 has also been shown to directly bind to the CKI p27, ultimately leading to p27 degradation [15]. Spy1-p27 and Cdk2 can immunoprecipitate together, supporting the rationale that they can form a trimeric complex, however Spy1 can also interact with each protein directly *in vitro* [11,16]. Data suggests that in a trimeric complex Spy1 preferentially binds p27 to prevent its inhibitory interactions with Cdk2, and that Cdk2 binding to Spy1 stabilizes this interaction and aids in the phosphorylation of p27 on T187, leading to p27 degradation [11,15].

Spy1 is elevated in the majority of breast carcinomas and Spy1 overexpression in the mouse mammary gland induces rapid and invasive tumorigenesis [17,18]. Defining the physiological role for direct interactions between Spy1-Cdk2 and Spy1-p27 in cell proliferation is an essential step toward resolving the mechanism by which Spy1 promotes mammary tumorigenesis.

This work isolates 4 key amino acids responsible for mediating the binding between Spy1 and p27. Using mutants of these sites we compare effects to a mutant form of Spy1 defective in binding to Cdk2. Our data demonstrates that abrogation of binding between Spy1 and p27 significantly inhibits degradation of the CKI and subsequently reduces the proliferative capacity of Spy1 *in vitro*. In opposition, abrogated direct binding to Cdk2 demonstrated little effect on Spy1-mediated degradation of p27 or proliferative effects in the presence of the CKI. Preventing interactions with either Cdk2 or p27 had comparable effects on endogenous activity of Cdk2 and contributed to the basal effects of Spy1 on proliferation. Importantly, direct Spy1 interactions with both p27 and Cdk2 play a role in mediating the rate of tumorigenic onset caused by Spy1. However, disrupting either interaction alone did not prevent tumour formation. These data stress that the prevalence and kinetics of these specific interactions *in vivo* will have significant effects on the functional outcomes of Spy1 expression. These details become very important when considering mechanisms of targeting Spy1, p27 or Cdks for drug therapy.

Methods

Ethics statement. BALB/c mice were maintained following the Canadian Council on Animal Care guidelines at the University of Windsor (protocol #06-19).

Cell culture. Human embryonic kidney cell line, HEK293 (ATCC) were maintained in DMEM medium (Sigma) supplemented with 10% (vol/vol) fetal bovine serum (Hyclone). HC11, a non-transformed, immortalized BALB/c mouse mammary epithelial cell line (provided by Dr. C. Shermanko; University of Calgary) were maintained in RPMI 1640 medium (Hyclone) containing 10% (vol/vol) fetal calf serum (Sigma), supplemented with 5 µg/ml insulin (Sigma), and 10 ng/ml EGF (Calbiochem). Both cell lines were maintained in 2 mM L-glutamine (Sigma), penicillin (Invitrogen), and streptomycin (Invitrogen), and were cultured in a 5% CO₂ environment. Cell counts were conducted with trypan blue exclusion and quantified using a BioRad TC10 Automated Cell Counter.

Plasmid and mutagenesis. Creation of Myc-Spy1 in PCS3 was described previously [10]. Spy1-PEIZ was generated by moving Flag-Spy1 from Spy1-PJT0013 [11] through EcoR1 and Xba1 restriction sites into the lentiviral PEIZ vector (provided by Dr. B. Welm, University of Utah). Spy1-D90, Spy1-R170 and Spy1-R170-PEIZ were created in Myc-Spy1-PCS3 using Quik Change PCR Multi Site-Directed Mutagenesis (SDM). Spy1-R170 mutation was made using primers

A315 5'-
GTAAAGGGACCAGCTCTGGGATGCAATTGACTATGCGGCTATTGTAAGCAGG-
3' and # A316 5'-
CCTGCTTACAATAGCCGCATAGTCAATTGCATCCCAGAGCTGGTCCCTTAAC-3'

;Spy1-D90 was made using primers #A123 5'-
GATTTCTTGTGGATGGCATGCTGCTGTAAAATTGC-3' and #A124 5'-
GTAAAGGGACCACTGGGATGSAAGACTATGCGGCTATTGTAAGCAGG 3', Spy1-R170-

PEIZ lentivirus plasmid was created by engineering an EcoR1 site upstream of Spy1 in Spy1-PCS3 using primers #A532 5'-CTTGATTAGGTGACACTATAGAATTCAAGCTTGTCTTTTTG-3' and #A533 5'-CAAAAAGAACAAGTAGCTTGAATTCTATAGTGTCACCTAAATCAAG-3'. Spy1-R170 was moved to PEIZ lentivirus vector via the EcoR1 and XbaI sites. Successful cloning in all cases was determined by DNA sequencing (Robarts Sequencing Facility; Univ. of Western Ontario).

Immunoblotting (IB) and immunoprecipitation (IP). Cells were harvested and lysed in 0.1% NP-40 lysis buffer (0.1% NP-40, 20mM Tris pH 7.5, 5mM 0.5M EDTA, 100mM NaCl in RO water) containing protease inhibitors (100 ug/mL PMSF, 5 ug/mL aprotinin, 2 ug/mL leupeptin) for 30 min on ice. Bradford Reagent was used to determine the protein concentration following the manufacturer's instruction (Sigma). Aliquots of lysates containing 20-30 µg protein were subjected to electrophoresis on denaturing SDS-10% polyacrylamide gels and transferred to PVDF-Plus 0.45 micron transfer membranes (Osmonics Inc.) for 2 hr at 30 V using a wet transfer method. Blots were blocked for 2 hr in TBST containing 3% non-fat dry milk (blocker) at room temperature, primary antibodies were reconstituted in blocker and incubated overnight at 4°C, secondary antibodies were used at a 1:10,000 dilution in blocker for 1 hr at room temperature. Blots were washed three times with TBST following incubation with both the primary and secondary antibodies. Washes were 6 min each following the primary antibody and 10 min each following the secondary antibody. Chemiluminescent Peroxidase Substrate was used for visualization following the manufacturer's instruction (Pierce). Chemiluminescence was quantified on an Alpha Innotech HD2 (Fisher) using AlphaEase FC software.

For IP equal amounts of protein were incubated with primary antisera as indicated overnight at 4°C, followed by the addition of 10 ul protein A–Sepharose (Sigma) and incubated at 4°C with gentle rotation for an additional 2 hr. These complexes were then washed three times with 0.1% NP-40 lysis buffer and resolved by 10% SDS-PAGE.

Transfections and infections. Cells were transfected overnight using polyethylenimine (PEI) branched reagent Sigma (408727), 10 µg of DNA was mixed with 50 µL of 150 mM NaCl and 30 µg PEI for 10 min then added to a 10 cm tissue culture plate.

Lentiviral infections were carried out using a modified protocol from Welm et. al [19]. In brief; PEI transfection of Lenti-XTM 293 producer cell lines (Cat. No. 632180, Clontech, CA) was conducted as described above, 16 hr post-transfection, media containing viral particles was concentrated, titred and stored at -80°C. Cells were screened for ZS-Green using flow cytometry. HC11 infections were optimized using 2×10^5 cells/well in a 6-well plate to determine the multiplicity of infection (MOI). HC11 cells were seeded with media lacking antibiotics for 18 hr, media was removed and transfection media lacking antibiotics and serum added. Viral particles were added in a final concentration of 8×10^5 transfection units (TU = MOI * cell number), and polybrene was added to a final concentration of 10 µg/ml. Mixture was incubated for 4 hr, followed by a media change to growth media lacking antibiotic.

Antibodies. The generation of Spy1 antibody was previously described [10]. Myc antibodies both mouse (9E10) and rabbit (C19), HA (Y11 and F7) and p27 (F8) were purchased from Santa Cruz. Actin antibody (MAB150R) was purchased from Calbiochem. HRP conjugated secondary mouse antibody (A9917) and rabbit antibody (A0545) were purchased from Sigma.

Pulse chase. 16 hr post-transfection with indicated constructs, serum free media was replaced with Cys-Met free media (D0422; Sigma) supplemented with dialyzed FBS (F0392; Sigma) for 1 hr. S^{35} was added to a final concentration of 500 µCi for 4 hr followed by 4 washes with 1X PBS and supplementation with growth media containing 2 mM Cys-Met. Cells were lysed at indicated time points, ran on an SDS-PAGE gel. Incorporated sulfur was visualized using a Cyclone storage phosphor system and quantified using OptiQuant software (Perkin Elmer).

Kinase assays. Cells were transfected, cultured in 10% FBS and lysed in 0.1% NP-40 lysis buffer. 18 hr post-transfection IP was carried out as described above and precipitates were washed four times prior to the addition of 50 μ l of kinase buffer (50 mM Tris-HCl pH 7.5, 10 mM MgCl₂, 1 mM DTT, 20 mM EGTA, 50 mM ATP, 10 μ Ci of [γ -³²P]ATP) and 74 μ g/ml H1 histone (Boehringer Mannheim). Reactions were incubated for 10 min at 30°C, sample buffer was added to stop the reaction and 50 μ l of each sample were analyzed by 10% SDS-PAGE. Incorporated phosphorylation was visualized using a Cyclone storage phosphor system and quantified using OptiQuant software (Perkin Elmer). IPs were subsequently probed on the same membrane.

Fat pad transplants. HC11 cells infected and selected for the relevant lentiviral constructs were injected into the cleared fat pad of the fourth mammary glands in 22-day old mice (250,000 cells per gland) as previously described [17]. Tumor incidence was monitored every 2 to 4 days beginning one week after surgery by palpitation of the gland. Glands were allowed to grow for 2 to 4 weeks following surgery. Tumour measurements were recorded using manual calipers and tumour volume was calculated as length (mm) x width (mm) x height (mm). Collected glands were either paraffin embedded for immunohistochemistry or flash frozen for protein, genomic or mRNA analysis.

Results

Resolving key Spy1 residues mediating binding with p27.

Using a panel of Spy1 deletion mutants previously described [20] we began to narrow down the region within the Spy1 protein that was necessary for p27 binding. Previously, it was determined that truncation of Spy1 at aa 215 retained the ability to bind p27, while truncation at aa 160 in Spy1 disrupted binding to p27 [15] (Fig. 1A; indicated beneath panel). We further tested these results using deletion mutants (DM) of Spy1 where the indicated regions were deleted (Fig. 1A). DMA represents a protein devoid of aa 1-57, DMB is devoid of aa 57-83,

DMC lacks aa 83-145, DMG lacks aa 147-239 and DMZ lacks aa 241-286. We first determined whether any of these Spy1 deletion mutants would result in abrogation of binding to p27. 293 cells were transfected with wild-type (WT) Spy1 or versions of the Spy1 protein harboring the specified deletions (DMA-DMZ) (Fig. 1B). Cells were lysed and equal amounts of protein immunoprecipitated with Myc antibody and analyzed by western blot. DMG failed to bind to p27, demonstrating that aa 145-239 are required for the binding between Spy1 and p27. This was not surprising given the large size of the deletion within DMG, as well as the previous results suggesting the essentiality of this region for binding [15]. Although p27 interacts in different ways with known partners, it was previously determined that p27 binding interactions favor positively charged amino acids on the binding partner [21,22,23]. Alignment of the potential p27-binding region within Spy1 from a number of different organisms noted a region of high similarity containing a string of 4 highly conserved positive amino acids (Fig. 1C). Previous binding interactions were found to depend on arginine interactions and were disrupted using arginine to alanine substitutions [22,23]. Hence, we generated a mutant of Spy1 containing alanine substitutions for arginines 170 and 174 (Spy1-R170) as well as a mutant containing alanine substitutions for arginines 179 and 180 (Spy1-R179) (Fig. 1D).

Spy1-R170 and -179 do not bind to p27.

To test the necessity of these conserved arginine residues for binding to p27, Myc-tagged Spy1-WT, Spy1-R170, or Spy1-R179 were transfected in combination with HA-tagged p27 in the presence of MG132 (Fig. 2A). IP/IB studies demonstrate that Spy1-R170 and Spy1-R179 mutants both reduce binding to p27 as compared to Spy1-WT binding (Fig. 2A). Reciprocally, IP with Myc antibody isolated p27 when Spy1-WT was overexpressed but not the mutant Spy1 constructs (Fig. 2B). It is notable that Cdk2 continued to bind to Spy1 in the presence of both p27-binding mutations (Fig. 2B), which is consistent with previous results demonstrating that Cdk2 binds more efficiently to Spy1 in the presence of overexpressed p27 protein [11]. We also examined the

interaction between endogenous p27 and Spy1-WT or mutant constructs. Following IP for the Myc-tagged Spy1 proteins, endogenous p27 protein was detected as part of a complex with Spy1-WT but not with either of the Spy1 non-binding mutants (Fig. 2C). Collectively, these results demonstrate that mutation of Spy1 at either arginines 170/174 or 179/180 abrogates binding interactions with the CKI p27. These mutants will provide a valuable tool in assessing the specific role for Spy1-p27 interactions in functional experiments.

Effect of Spy1 mutants on p27 degradation.

Direct binding of Spy1 protein to p27 enhances p27 degradation and subsequently activates Cdk2 kinase activity [11,15]. Importantly, Spy1 also directly binds to Cdk2 to activate kinase activity and it is known that Cdk2 phosphorylation of p27 on T187 promotes p27 degradation [24]. To determine whether the direct binding of Spy1 to p27 and/or Cdk2 is critical for Spy1-mediated degradation of p27, we utilized 293 cells transfected with either the Spy1-p27 non-binding mutants (Spy1-R170 and Spy1-R179) or the Spy1 mutant previously demonstrated to disrupt interactions with Cdk2 (Spy1-D90) [12]. Lysates were monitored by IB (Fig. 3A; left panel) and results over 3 separate experiments were quantified by densitometry (Fig. 3A; right panel). Cells transfected with Spy1-WT and Spy1-D90 resulted in a significant reduction in overall p27 protein levels as compared to cells overexpressing an empty vector control or the Spy1-p27 non-binding mutants. To further confirm these results we used radioactive sulfur (S^{35}) incorporation in a pulse chase assay, IP for p27, followed by IB and phosphor-image analysis to determine relative stability of p27 protein levels over 3 separate experiments (Fig. 3B). IgG was used as a control for the IP and lysates were used for control over transfections. Quantification of this data demonstrates that Spy1-WT and Spy1-D90 significantly reduce the stability of p27 protein levels over the empty vector control; however the Spy1-R170/R179 mutants were unable to significantly impact p27 turnover. These data demonstrate that the direct binding between Spy1 and p27 is essential for Spy1-mediated effects on p27 protein turnover. To determine the relative

effects of direct interactions with Cdk2 or p27 on Cdk2 kinase activity, a histone kinase assay was performed (Fig. 3C). Phosphor-quantification normalized to the Cdk2 IP demonstrated that preventing interactions with either p27 or Cdk2 reduced kinase activity to that of control, showing that each of these interactions is essential for Spy1-mediated activation of Cdk2.

Spy1 is known to override cell cycle inhibition by p27 [11]. To examine the effect of the Spy1 mutants on p27-induced cell cycle arrest, cells were transfected with the indicated constructs in the presence of p27 and cell number after 24 hr was assessed by trypan blue exclusion (Fig. 4A). Cells transfected with the Spy1-p27 non-binding mutants showed a significant decrease in the total cell number as compared to Spy1-WT, being comparable to that of the empty vector control. Importantly, the Spy1-D90 resulted in a significant increase in the total number of cells over the empty vector control, with numbers comparable to that of Spy1-WT. These results demonstrate that the ability of Spy1 to override the inhibitory effects of p27 is dependent on the direct interaction with p27. Measuring cell proliferation in the absence of p27 overexpression demonstrated that both Cdk2 and p27 binding mutants decreased Spy1-proliferative effects, although neither mutant completely rescued the effect of Spy1 overexpression (Fig. 4B). These results support the conclusion that direct interactions with both Cdk2 and p27 contribute toward Spy1-mediated proliferative effects.

Spy1 direct binding to both p27 and Cdk2 are important for Spy1-mediated tumorigenesis in vivo.

It has previously been shown that overexpression of Spy1 *in vivo* leads to accelerated rates of mammary tumorigenesis [17]. To determine if this is dependent on Spy1's interaction with either Cdk2 or p27, fat pad transplantation was performed on the cleared inguinal mammary gland of Balb/C mice using Spy1-WT expression on one side of the mouse and Spy1 mutants defective for either Cdk2 binding (Spy1-D90) or p27 binding (Spy1-R170) on the opposite side. One week following surgery, approximately 50-65% of all Spy1-WT glands had visible tumors

while only 20% of all Spy1-D90 glands and 10% of all Spy1-R170 glands had visible tumors (Fig. 5A). At day 21 post-transplant ~80-90% of all transplanted glands had detectible tumors, with no difference in numbers between mutant or WT forms of Spy1. Mice were humanely sacrificed at day 28 post-surgery due to the size and invasiveness of the Spy1-WT glands and glands were removed and studied. There were significant differences in the overall tumor size observed with Spy1-WT glands being much larger and more invasive than both the Spy1-D90 and Spy1-R170 tumors (Fig. 5B). These data indicate that Spy1 direct interactions with both p27 and Cdk2 are important for Spy1-mediated tumorigenesis *in vivo*. It further suggests that inhibition of both of these functional pathways is required to significantly reduce tumorigenic effects over time.

Discussion

Spy1 is an atypical Cdk activator known to increase cell proliferation and inhibit apoptosis when overexpressed in mammalian cells [10]. In addition to directly binding and activating Cdks, Spy1 is a binding partner for the CKI p27 [11]. *In vitro* and *in vivo* experiments demonstrate that Spy1 directly binds and co-localizes with nuclear forms of p27, functioning to override p27-mediated cell cycle inhibition [11]. Like Cyclin E/Cdk2, Spy1 overexpression is also associated with an increase in phosphorylation of p27 at T187 leading to its proteasomal degradation and enhanced cell cycle progression [15]. Whether the effects on p27 degradation are mediated through the direct binding of Spy1 to Cdk2 or p27 was not previously known. To address this question we first created and characterized two p27 non-binding mutants (Spy1-R170 and Spy1-R179). These mutants were used along with a Cdk2 binding mutant (Spy1-D90) that has been previously described [16], in proliferation assays as well as in assays to assess p27 protein levels. We determined that direct binding of Spy1 to p27 was required to promote p27 degradation, as well as to override a p27-induced cell cycle arrest. The direct binding of Spy1 to both Cdk2 and p27 were required for Spy1-mediated activation of Cdk2 and overall effects on

cell proliferation. These data demonstrate that there are differences in the mechanism by which Spy1-p27 and Spy1-Cdk2 drive cell proliferation and Cdk2 kinase activity.

Role of Spy1-p27 binding in tumorigenesis.

Elevated expression of Spy1 is found in many forms of human cancer [18,25,26,27,28]. In this present study, we have demonstrated that abrogating direct interactions between Spy1 and either p27 or Cdk2 significantly decreases the rate of tumorigenesis and overall tumour size *in vivo*. Low levels of p27 protein has been implicated in many human cancers including breast [29] and is found to correlate with poor patient outcome [29]. Constitutive activation of Cdk2 has also been shown to result in mammary gland hyperplasia, fibrosis, and mammary tumors in a MMTV–cyclin D1–Cdk2 derived cell line [30]. Given that Cdk2 targets p27 for degradation [31], it is a valid hypothesis that these proteins are regulating each other; interestingly however, our data suggests that direct interactions with both p27 and Cdk2 are important in driving the tumorigenic activities of Spy1. Details on how these proteins function independently, as well as in a trimeric complex, is required to fully resolve the physiological and pathological roles of these interactions.

Acknowledgements

We thank Dr. C. Shermanko for providing the HC11 cell lines, Dr. B. Welm for providing lentivirus vector (PEIZ), Dr. D.J. Donoghue for supplying vectors and the Spy1 antibody and J. Maimaiti and N. Paquette for technical assistance.

Author Contributions

Experiments were conceived and designed by MAS, BF, LAP. Experiments were performed by MAS and BF. Data was analyzed by MAS, BF and LAP. Reagents/materials/tools provided by LAP. Manuscript was prepared by MAS, BF and LAP.

Figure legends

Figure 1. *Generation of Spy1 – p27 binding mutants.* (A) A schematic diagram of the Spy1 deletion mutants used for screening and their enzyme cut sites. The indicated regions are selectively deleted in each Spy1 mutant construct (ie. DMA lacks region A, DMB lacks region B, DMA lacks region C, DMG lacks region G, DMZ lacks region Z). Dotted line depicts the truncation mutant of Spy1 previously determined to retain the ability to bind p27 [15]. The solid line reflects the region previously shown to have lost the ability to bind p27. (B) 293 cells were transfected with Myc-Spy1-PCS3 (WT) or the different deletion mutants DMA-DMZ depicted above in the presence of HA-tagged p27 (HA-p27). Transfected cells were treated with MG132 (10 μ M) for 14 hrs prior to harvest, lysates were immunoprecipitated with Myc antibody and immunoblotted with HA antibody (upper panel) and Myc antibody (lower panel). This is one representative experiment of 3. (C) Alignment of a highly conserved amino acid sequence within the predicted p27 binding region from several species. Conserved positively charged residues to be mutated are noted with a box. Amino acid #s are indicated after the species in brackets. (D) Region G of Spy1 depicting the Arg. (R) residues which were mutated to Alanine (A) to create Spy1-R170 and Spy1-R179 mutations.

Figure 2. *R170 and R179 mutants of Spy1 abrogate binding to p27.* 293 cells were transfected with constructs indicated above the panels and treated with MG132 prior to lysis. Equal amounts of protein was subject to IP/IB as indicated below each panel (upper panels). For each experiment cell lysates were also run and blotted to demonstrate transfection efficiencies (lower panels). (A) Overexpression of all constructs and IP for HA-tagged p27. (B) Overexpression of all constructs and IP for Myc-tagged Spy1 constructs. (C) Transfection of Spy1-WT or mutant constructs and analysis using endogenous p27. Cells were maintained in 2% serum containing media for 14 hr following transfection to elevate endogenous p27 levels. All experiments reflect one representative experiment of 3.

Figure 3. *R170 and R179 mutants inhibit p27 down regulation.* 293 cells were transfected with HA-tagged p27 in the presence or absence of Myc-tagged empty-vector (PCS3), Spy1-WT, Spy1-R170, Spy1-R179 or Spy1-D90. (A) Lysates were blotted with HA (upper panel), Spy1 (middle panel) and Actin (lower panel) antibodies. Left panel is one representative blot of 3. Right panel reflects densitometry of p27 levels normalized to actin over 3 separate experiments. Error bars represent SEM. * $p < 0.05$. (B) Pulse chase assay was conducted, followed by IP for HA-tagged p27 and S35 incorporation measured by phosphor image analysis. Immunoblot using IgG antibody was used as a control. Left panel is one representative experiment of 3. Right panel represents quantification using OptiQuant software over 3 separate experiments. Error bars represent SEM, * $p < 0.05$. (C) Cdk2 IP from transfected lysates. Histone assay was conducted. Left panel is one representative phosphorimage of 2. Right panel represents average phosphor measurements over 2 experiments. Error bars represent SEM.

Figure 4. 293 cells were transfected with Myc-tagged empty-vector (PCS3), Spy1-WT, Spy1-R170, Spy1-R179 or Spy1-D90 in the presence (A) or absence (B) of HA-p27. Cell numbers were assessed using trypan blue exclusion and quantification over 3 separate experiments. Error bars represent SEM. ** $p < 0.01$; * $p < 0.05$. Right panels represent one representative blot of 3.

Figure 5.

Cleared mammary fat pads were transplanted with cells expressing Spy1-WT (WT) on the left and either Spy1-R170 (R170) or Spy1-D90 (D90) on the right. (A) Graphic depiction of the percent of mice remaining free from palpable tumours at time points following transplantation. Treatments occurred in groups of 3 using 3 separate colonies of infected cells. Total sample size = 45. Mann-Whitney, and Wilcoxon Matched Pairs Tests were performed (** $p < 0.01$; * $p < 0.05$). (B) Mice were humanely sacrificed at the indicated time points and glands showing visible tumors were isolated and measurements of height, length and width of the tumors were recorded.

Total average tumour volume over 45 mice transplanted with either R170 or D90 (right gland) and Spy1-WT (left gland) from three separate infections are depicted. ** $p < 0.002$; * $p < 0.05$.

References

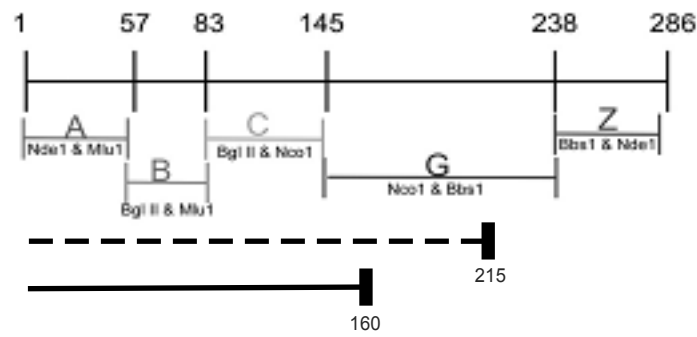
1. De Bondt HL, Rosenblatt J, Jancarik J, Jones HD, Morgan DO, et al. (1993) Crystal structure of cyclin-dependent kinase 2. *Nature* 363: 595-602.
2. Nurse PM (2002) Nobel Lecture. Cyclin dependent kinases and cell cycle control. *Biosci Rep* 22: 487-499.
3. Said TK, Medina D (1995) Cell cyclins and cyclin-dependent kinase activities in mouse mammary tumor development. *Carcinogenesis* 16: 823-830.
4. Alkarain A, Jordan R, Slingerland J (2004) p27 deregulation in breast cancer: prognostic significance and implications for therapy. *J Mammary Gland Biol Neoplasia* 9: 67-80.
5. Nair BC, Vallabhaneni S, Tekmal RR, Vadlamudi RK (2011) Roscovitine confers tumor suppressive effect on therapy-resistant breast tumor cells. *Breast Cancer Res* 13: R80.
6. Appleyard MV, O'Neill MA, Murray KE, Paulin FE, Bray SE, et al. (2009) Seliciclib (CYC202, R-roscovitine) enhances the antitumor effect of doxorubicin in vivo in a breast cancer xenograft model. *Int J Cancer* 124: 465-472.
7. Dickson MA, Schwartz GK (2009) Development of cell-cycle inhibitors for cancer therapy. *Curr Oncol* 16: 36-43.
8. Malumbres M, Pevarello P, Barbacid M, Bischoff JR (2008) CDK inhibitors in cancer therapy: what is next? *Trends Pharmacol Sci* 29: 16-21.
9. Guha M (2013) Blockbuster dreams for Pfizer's CDK inhibitor. *Nat Biotechnol* 31: 187.
10. Porter LA, Dellinger RW, Tynan JA, Barnes EA, Kong M, et al. (2002) Human Speedy: a novel cell cycle regulator that enhances proliferation through activation of Cdk2. *J Cell Biol* 157: 357-366.
11. Porter LA, Kong-Beltran M, Donoghue DJ (2003) Spy1 interacts with p27Kip1 to allow G1/S progression. *Mol Biol Cell* 14: 3664-3674.
12. Cheng A, Gerry S, Kaldis P, Solomon MJ (2005) Biochemical characterization of Cdk2-Speedy/Ringo A2. *BMC Biochem* 6: 19.
13. Barnes EA, Porter LA, Lenormand JL, Dellinger RW, Donoghue DJ (2003) Human Spy1 promotes survival of mammalian cells following DNA damage. *Cancer Res* 63: 3701-3707.

14. Gastwirt RF, Slavin DA, McAndrew CW, Donoghue DJ (2006) Spy1 expression prevents normal cellular responses to DNA damage: inhibition of apoptosis and checkpoint activation. *J Biol Chem* 281: 35425-35435.
15. McAndrew CW, Gastwirt RF, Meyer AN, Porter LA, Donoghue DJ (2007) Spy1 enhances phosphorylation and degradation of the cell cycle inhibitor p27. *Cell Cycle* 6: 1937-1945.
16. Cheng A, Xiong W, Ferrell JE, Jr., Solomon MJ (2005) Identification and comparative analysis of multiple mammalian Speedy/Ringo proteins. *Cell Cycle* 4: 155-165.
17. Golipour A, Myers D, Seagroves T, Murphy D, Evan GI, et al. (2008) The Spy1/RINGO family represents a novel mechanism regulating mammary growth and tumorigenesis. *Cancer Res* 68: 3591-3600.
18. Al Sorkhy M, Ferraiuolo RM, Jalili E, Malysa A, Fratiloiu AR, et al. (2012) The cyclin-like protein Spy1/RINGO promotes mammary transformation and is elevated in human breast cancer. *BMC Cancer* 12: 45.
19. Welm BE, Dijkgraaf GJ, Bledau AS, Welm AL, Werb Z (2008) Lentiviral transduction of mammary stem cells for analysis of gene function during development and cancer. *Cell Stem Cell* 2: 90-102.
20. Al Sorkhy M, Craig R, Market B, Ard R, Porter LA (2009) The cyclin-dependent kinase activator, Spy1A, is targeted for degradation by the ubiquitin ligase NEDD4. *J Biol Chem* 284: 2617-2627.
21. Wang W, Ungermannova D, Chen L, Liu X (2004) Molecular and biochemical characterization of the Skp2-Cks1 binding interface. *J Biol Chem* 279: 51362-51369.
22. Ungermannova D, Gao Y, Liu X (2005) Ubiquitination of p27Kip1 requires physical interaction with cyclin E and probable phosphate recognition by SKP2. *J Biol Chem* 280: 30301-30309.
23. Sitry D, Seeliger MA, Ko TK, Ganoth D, Breward SE, et al. (2002) Three different binding sites of Cks1 are required for p27-ubiquitin ligation. *J Biol Chem* 277: 42233-42240.
24. Montagnoli A, Fiore F, Eytan E, Carrano AC, Draetta GF, et al. (1999) Ubiquitination of p27 is regulated by Cdk-dependent phosphorylation and trimeric complex formation. *Genes Dev* 13: 1181-1189.
25. Zucchi I, Mento E, Kuznetsov VA, Scotti M, Valsecchi V, et al. (2004) Gene expression profiles of epithelial cells microscopically isolated from a breast-invasive ductal carcinoma and a nodal metastasis. *Proc Natl Acad Sci U S A* 101: 18147-18152.
26. Ke Q, Ji J, Cheng C, Zhang Y, Lu M, et al. (2009) Expression and prognostic role of Spy1 as a novel cell cycle protein in hepatocellular carcinoma. *Exp Mol Pathol* 87: 167-172.

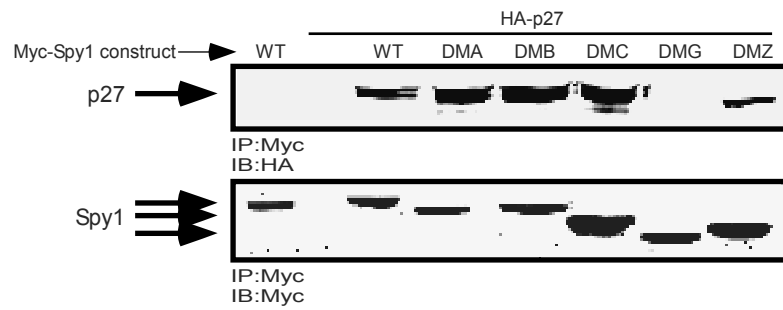
27. Hang Q, Fei M, Hou S, Ni Q, Lu C, et al. (2012) Expression of Spy1 protein in human Non-Hodgkin's Lymphomas is correlated with phosphorylation of p27(Kip1) on Thr187 and cell proliferation. *Med Oncol*.
28. Zhang L, Shen A, Ke Q, Zhao W, Yan M, et al. (2012) Spy1 is frequently overexpressed in malignant gliomas and critically regulates the proliferation of glioma cells. *J Mol Neurosci* 47: 485-494.
29. Slingerland J, Pagano M (2000) Regulation of the cdk inhibitor p27 and its deregulation in cancer. *J Cell Physiol* 183: 10-17.
30. Corsino P, Davis B, Law M, Chytil A, Forrester E, et al. (2007) Tumors initiated by constitutive Cdk2 activation exhibit transforming growth factor beta resistance and acquire paracrine mitogenic stimulation during progression. *Cancer Res* 67: 3135-3144.
31. Vlach J, Hennecke S, Amati B (1997) Phosphorylation-dependent degradation of the cyclin-dependent kinase inhibitor p27. *Embo J* 16: 5334-5344.

Figure 1

A



B



C

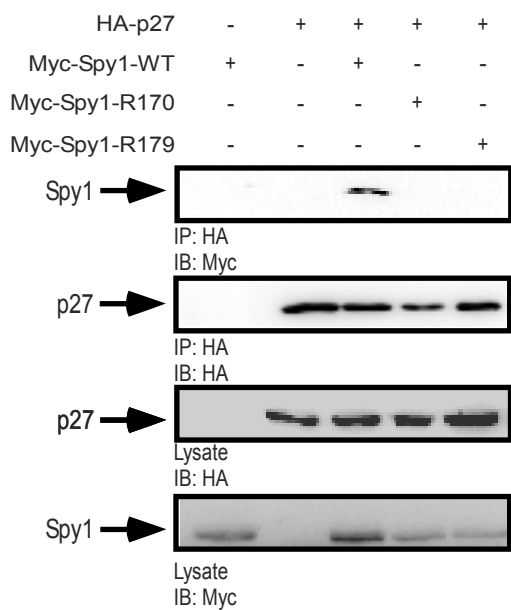
																			Total % Homology						
HumanA1 (160-184)	F	L	K	L	R	D	Q	L	W	D	R	D	Y	R	A	I	V	S	R	R	C	C	E	E	100
HumanA2 (160-184)	F	L	K	L	R	D	Q	L	W	D	R	D	Y	R	A	I	V	S	R	R	C	C	E	E	100
Pig (160-184)	F	L	K	L	R	D	Q	L	W	D	R	D	Y	R	A	I	V	S	R	R	C	C	E	E	90
Bovine (160-184)	F	L	K	L	R	D	Q	L	W	D	R	D	Y	R	A	I	V	S	R	R	C	C	E	E	89
Mouse (159-183)	F	L	R	L	R	D	Q	L	W	D	R	D	Y	R	A	I	V	S	R	R	C	C	E	E	85
Xenopus (150-174)	F	L	K	L	R	D	D	F	W	A	K	N	Y	R	A	V	V	S	R	R	C	C	E	E	50
Zebrafish (163-177)	F	L	K	Q	R	D	Q	L	W	A	R	E	Y	R	A	A	V	S	R	R	C	C	E	E	65
Schistosoma mansoni (171-195)	F	S	R	Q	K	E	A	L	W	A	R	G	Y	R	A	V	V	S	Y	R	C	C	K	E	45

D

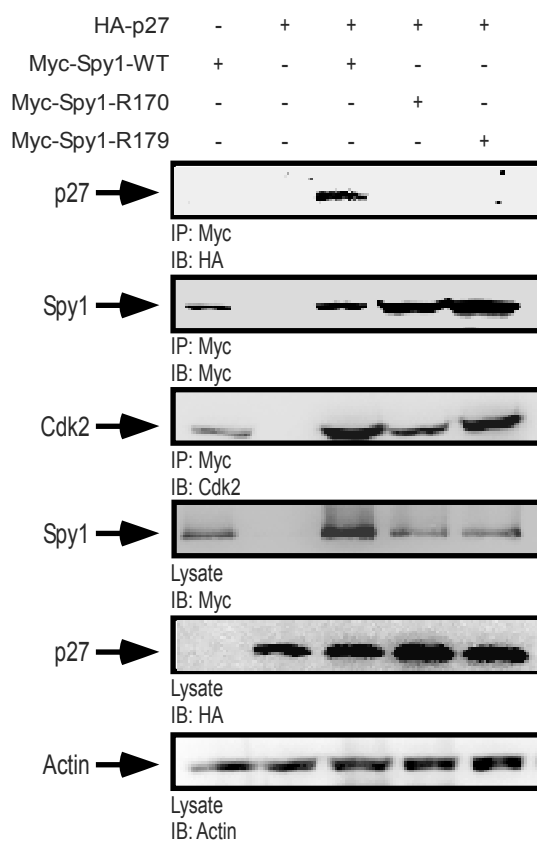
R170
R179
A
A
AA
 LKLRDQLWDRIDYRAIVSRRCCEEVMAIAPTHYIWQRERSVHHSGAVR

Figure 2

A



B



C

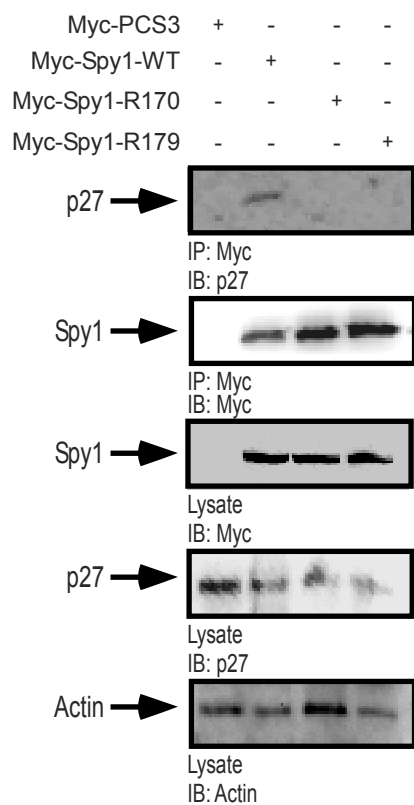


Figure 3

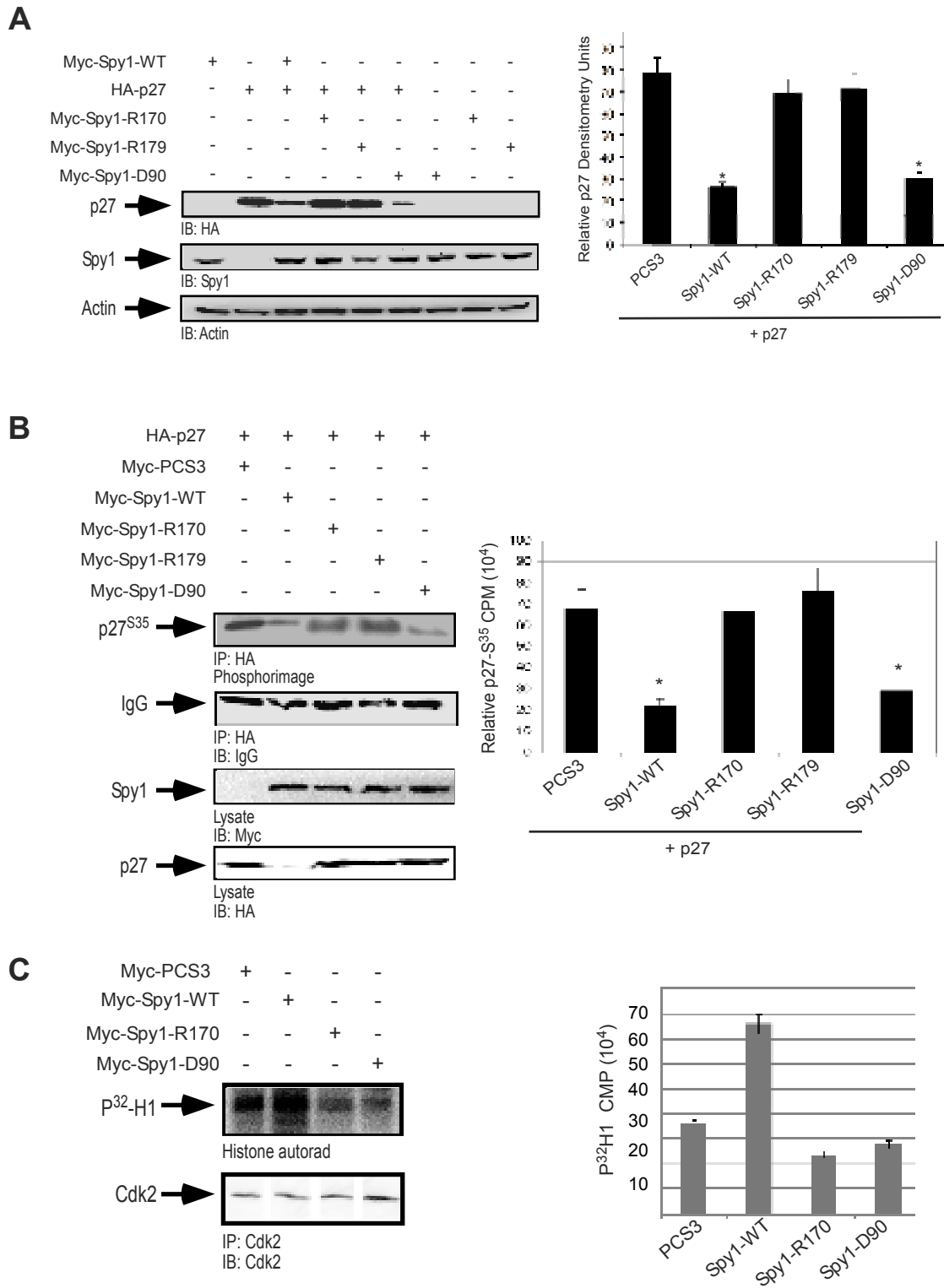


Figure 4

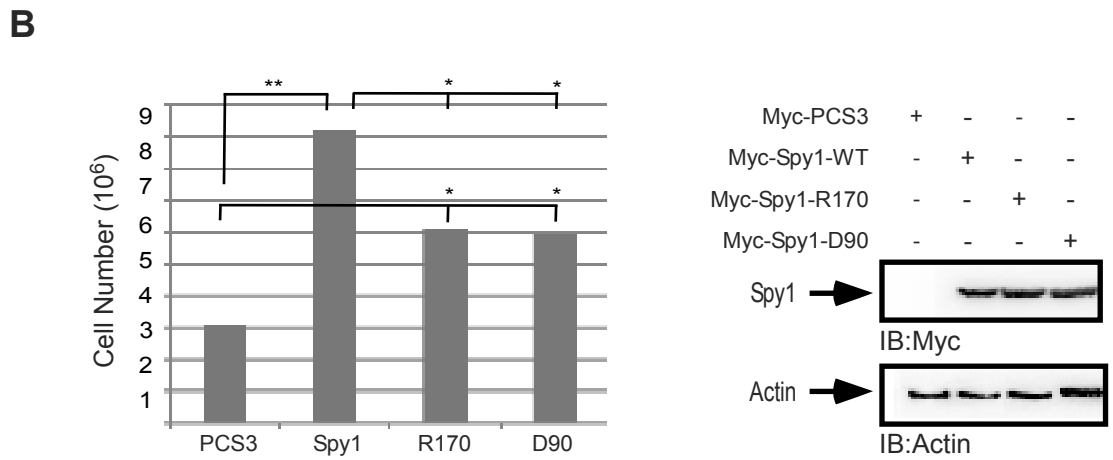
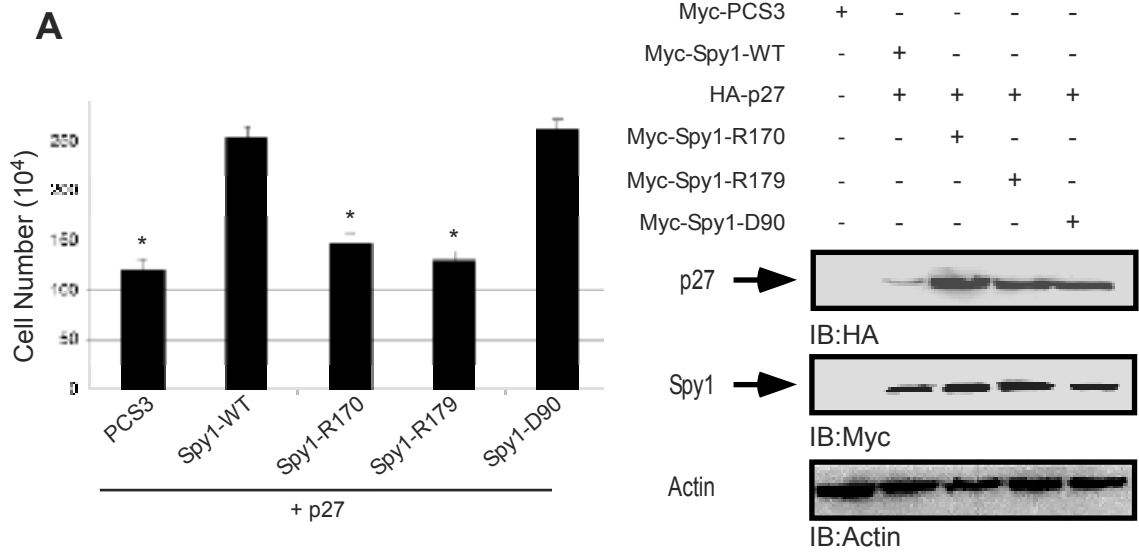
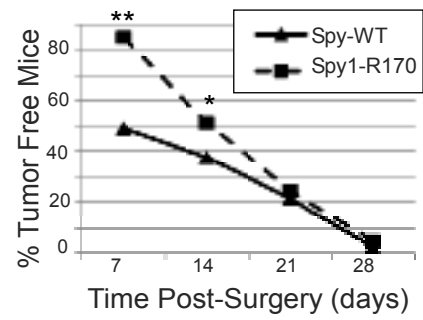
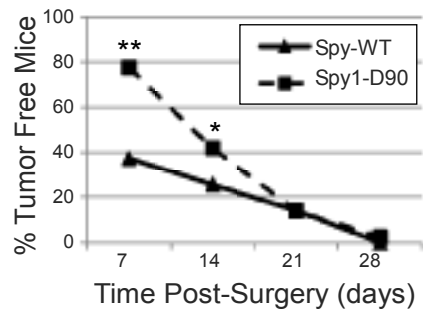


Figure 5

A



B

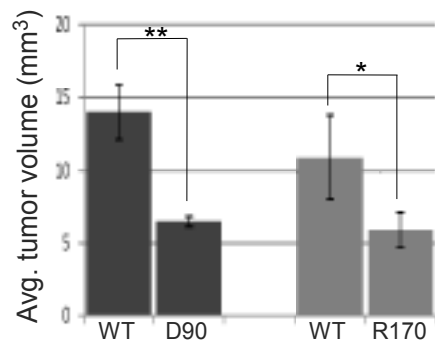


Figure S1

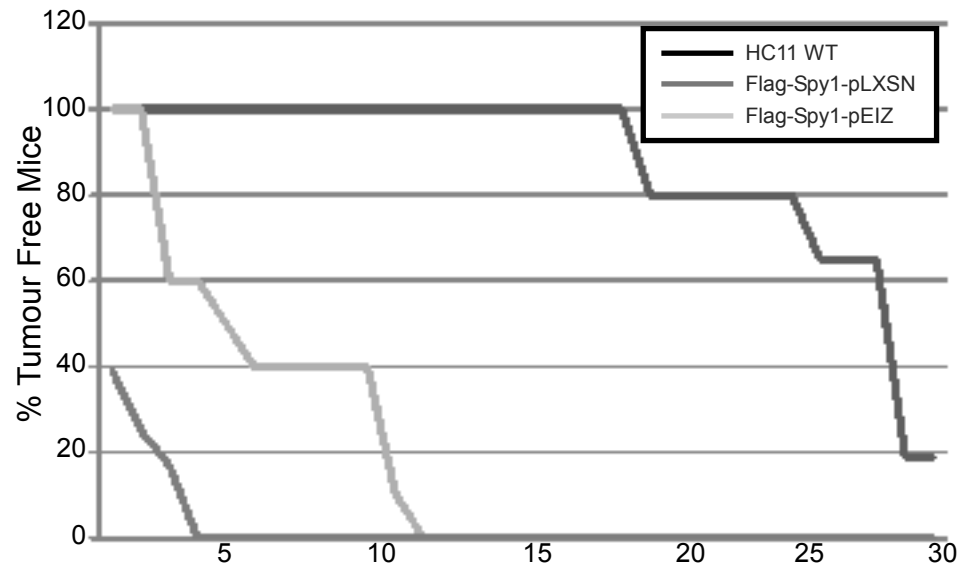
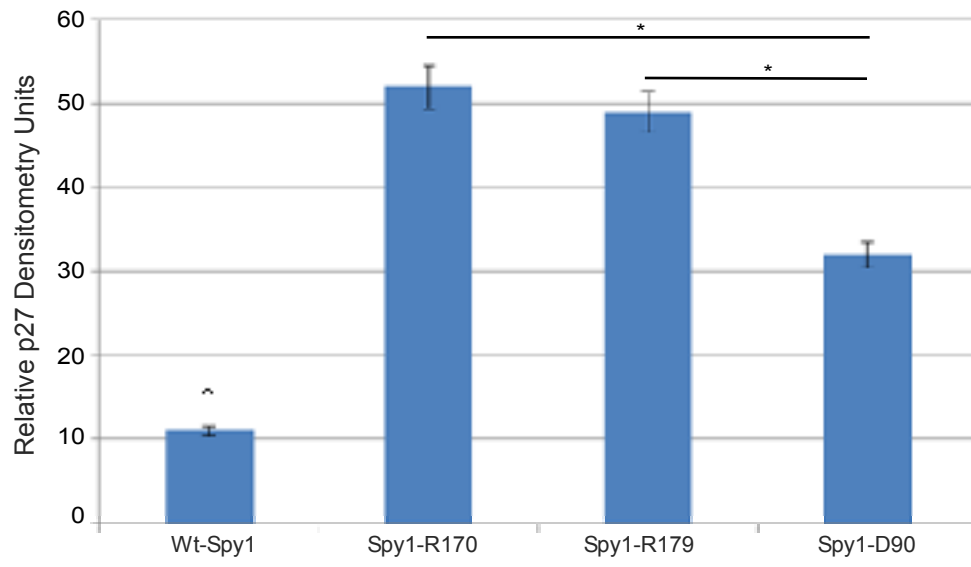


Figure S2



Appendix D- Permissions

To Whom It May Concern

Dear Sir\Mam

Please accept this letter as my authorization for Ms. **Bre-Anne Fifield** to use our co-authored publication entitled “Direct Interactions with both p27 and Cdk2 Regulate Spy1-Mediated Proliferation in vivo and in vitro” in her theses as an appendix. Please do not hesitate to contact me if you require further clarification.

Sincerely,

Mohammad Al Alsorkhy, PhD

Assistant Professor of Cell

Biology KSAU-HS

KSA

Vita Auctoris

NAME: Bre-Anne Fifield

PLACE OF BIRTH: Windsor, ON

YEAR OF BIRTH: 1987

EDUCATION: University of Windsor, B.Sc (H). in Biological Sciences, Windsor, ON, 2009

University of Windsor, Ph.D in Biological Sciences, Windsor, ON, 2014